# Functional Dental Morphology of Insectivorous Microchiropterans: Spatial Modelling and Functional Analysis of Tooth Form and the Influence of Tooth Wear and Dietary Properties

A thesis submitted for the degree of Doctor of Philosophy

Alistair R. Evans, B.Sc. (Honours)

School of Biological Sciences

Monash University

Australia

May 2003

Frontispiece: Reconstruction of the upper second molar of Gould's Wattled Bat *Chalinolobus gouldii*.

# **Table of Contents**

LIST OF TABLES	7
List of Figures	9
LIST OF PLATES	11
Abstract	13
GENERAL DECLARATION	15
Acknowledgements	17
Chapter 1. Introduction	19
1.1. Functional Morphology	19
1.2. Recent Approaches in Functional Dental Morphology	20
1.3. Engineering and Tooth Function	21
1.4. Dilambdodont and Tribosphenic Tooth Function	24
1.5. Tooth Wear	25
1.6. Insectivore Dietary Properties	26
1.7. Microchiropterans	26
1.8. Three-dimensional Tooth Modelling	27
1.9. Structure of Thesis	27
CHAPTER 2. THE TOOTH OF PERFECTION: FUNCTIONAL AND SPATIAL CONSTRAI	NTS ON
MAMMALIAN TOOTH SHAPE	33
2.1. Introduction	33
2.2. Materials and Methods	34
2.2.1. Definitions	34
2.2.2. Modelling tooth shapes	37
2.3. Results	39
2.3.1. Functional parameters	39
2.3.2. 'Anatomical' constraints	41
2.4. Discussion	42
2.4.1. Functional merits of model tools	42
2.4.2. Relationships between model shapes and real tooth shapes	43
2.4.3. Dietary properties	45
2.4.4. Interactions of constraints	46
2.4.5. Tooth modelling	47
2.5. Conclusions	47

CHAPTE	ER 3. SPATIAL AND FUNCTIONAL MODELLING OF CARNIVORE AND INSECTIVORE	
Molar	IFORM TEETH	53
3.1.	Introduction	53
3.1.	1. Occlusal geometry	55
3.2.	Methods	55
3.2.	1. Models	57
3.3.	Results	58
3.4.	Discussion	69
3.4.	1. Influence of protocone on tooth shape	69
3.4.	2. Comparisons of models and real teeth	70
3.4.	3. Autocclusion	72
3.4.	4. Therian molar modelling	74
3.4.	5. Tooth modelling	75
3.5.	Conclusions	76
Снарте	er 4. Confocal Imaging, Visualisation and 3-D Surface Measurement of	ī
SMALL	Mammalian Teeth	79
4.1.	Introduction	79
4.2.	Materials and Methods	80
4.2.	1. Moulding	80
4.2.	2. Casting	81
4.2.	3. Imaging	81
4.2.	4. Visual representation	84
4.2	5. Measurement	84
4.3.	Results	86
4.3	1. Imaging	86
4.3	2. Visual representation	86
4.3	3. Measurements	86
4.4.	Discussion	86
Снарте	er 5. Connecting Morphology, Function and Tooth Wear in	
Micro	CHIROPTERANS	91
5.1.	Introduction	91
5.2.	Functional Parameters	93
5.3.	Materials and Methods	94
5.3.	1. Tooth wear	94
5.3	2 Functional parameters	95

5.3.3.	Statistical methods	98
5.4. Resu	ılts	99
5.4.1.	Functional parameters	99
5.4.2.	PCA and NMDS	.102
5.5. Disc	eussion	.113
5.5.1.	Functional parameters	.113
5.5.2.	Crest size	.115
5.5.3.	Shape and function maintenance during wear	.116
5.5.4.	Functional relationships of attrition and abrasion of crests	.117
5.6. Con	clusions	.119
CHAPTER 6.	THE MATERIAL PROPERTIES OF INSECTS IN RELATION TO INSECTIVORY:	
CUTICLE THI	CKNESS AS AN INDICATOR OF INSECT 'HARDNESS' AND 'INTRACTABILITY'	.121
6.1. Intro	oduction	.121
6.1.1.	'Hardness'	.122
6.1.2.	Materials and structures	.124
6.1.3.	Cuticle structural properties	.127
6.2. Met	hods	.129
6.2.1.	Biomechanical properties of cuticle	.129
6.2.2.	Cuticle thickness in bat faeces	.130
6.3. Resu	ılts	.131
6.4. Disc	eussion	.138
6.4.1.	Cuticle thickness as a measure of biomechanical properties	.138
6.4.2.	Biomechanical properties of beetles and moths	.141
6.4.3.	Insect biomechanical properties	.142
6.5. Con	clusions	.145
CHAPTER 7.	DENTAL SPECIALISATION IN INSECTIVOROUS MICROCHIROPTERANS	
Consuming	'Intractable' and 'Tractable' Invertebrates	.147
7.1. Intro	oduction	. 147
7.2. Met	hods	. 149
7.2.1.	Study species	.149
7.2.2.	Functional parameters	.150
7.2.3.	Statistical methods and size correction	.150
7.3. Resu	ılts	.151
7.4. Disc	eussion	.163
7.4 1	Three hypotheses	.163

7.4	2.2. Biomechanical properties and tooth form in previous studies	168
7.4	3. Additional differences in tooth form	171
7.5.	Conclusions	172
Снарт	er 8. The Scaling of Tooth Sharpness	175
8.1.	Introduction	175
8.2.	Functional Scaling of Tooth Sharpness	175
8.3.	Processes that Influence Tooth Sharpness	177
8.4.	Empirical Data on Tooth Sharpness	180
Снарт	er 9. Discussion	187
9.1.	Comparative Function of Protoconoid Tooth Forms	187
9.2.	Comparative Function in Protoconoid and Carnassial Tooth Forms	190
9.3.	Effect of Size and Diet on Gross Morphology	193
9.4.	Thesis Conclusions	196
9.5.	References	198
PLATES	S	215
A DDENII	DICES	221

# **List of Tables**

Table 2.1. Shape and functional parameters for points and blades	37
Table 2.2. The important functional advantages of the protoconoid	43
Table 4.1. Measurements from scans of upper second molar of three specimens of	
Chalinolobus gouldii	86
Table 4.2. Relationship between resolution, number of scans accumulated at each z	
height and the time taken to scan	88
Table 5.1. Functional parameters relating to cusps for paracone and metacone for three	
wear states in C. gouldii	. 103
Table 5.2. Functional parameters relating to upper molar ectoloph crests for three wear	
states in C. gouldii	.104
Table 5.3. Cusp occlusion relief and fragment clearance for paracone and metacone	
basins and trigon groove for three wear states in C. gouldii	. 105
Table 6.1. Results of regression analyses for logged values of cuticle thickness vs	
punch strength, specific punch strength, work to punch and specific work to punch	
according to insect and sclerotisation	.132
Table 6.2. Species means of median and maximum thickness of cuticle fragments in	
the faeces of microbats, and number of fragments/mg	.133
Table 6.3. Published reports of diets for species in Table 6.2 that were investigated	
using the cuticle thickness measurement technique	.134
Table 7.1. Diets of the intractable (I) and tractable (T) feeding species examined in this	
study	.153
Table 7.2. Functional parameters relating to cusps for paracone and metacone for six	
species of intractable and tractable feeding bats	. 155
Table 7.3. Functional parameters relating to upper molar ectoloph crests for six species	
of intractable and tractable feeding bats	.156
Table 7.4. Cusp occlusion relief and fragment clearance for paracone and metacone	
basins and trigon groove for six intractable or tractable feeding species	.157
Table 7.5. Results of statistical comparisons of functional parameters within three	
microchiropteran families	.158
Table 8.1. Two isometric animals, A and B, of length <i>l</i> and 2 <i>l</i> , respectively, and their	
proportions for features that relate to tooth function.	.176
Table 9.1. Comparison of functional features in upper protoconoid-based tooth forms	.190

Table 9.2. Comparison of features that function in carnassial and protoconoid-based	
tooth forms	193

# **List of Figures**

Fig. 1.1. a) Dimensions of a single-point cutting tool; b) one type of chip breaker on a	
cutting tool designed to help clearance of fragments	29
Fig. 2.1. Tool design features.	36
Fig. 2.2. Single-bladed tool shapes and shape and functional parameters	38
Fig. 2.3. Double-bladed tool shapes and shape and functional parameters.	40
Fig. 2.4. Anatomical criteria for tool design	42
Fig. 2.5. Comparisons between the models and real mammalian tooth forms	44
Fig. 2.6. Putative relationships between tooth functional characteristics	46
Fig. 3.1. a) The 'reversed triangles' model of molar occlusion. b) The Crompton and	
Sita-Lumsden (1970) model of therian molar function	60
Fig. 3.2. Simple single-bladed models used as starting points for modelling	
mammalian teeth	61
Fig. 3.3. Simple double-bladed models used as starting points for modelling	
mammalian teeth	62
Fig. 3.4. Crest shapes that are possible for occluding upper and lower teeth with blades	
when the lower moves along a linear occlusal vector	63
Fig. 3.5. Modified models of mammalian tooth forms	64
Fig. 3.6. The effect of wear and crest shape on the alignment of occluding notches	65
Fig. 3.7. Improved model of dilambdodont molars	66
Fig. 3.8. Three-dimensional reconstruction of model shown in Crompton and Sita-	
Lumsden (1970)	68
Fig. 4.1. Two views of the standard glass specimen for moulding, casting and imaging	81
Fig. 4.2. Surface scans of standard glass specimen.	82
Fig. 4.3. Relationship between number of scans and surface noise in scan for two	
different surface noise-reduction methods	82
Fig. 4.4. Surface data representations of upper second molar of Chalinolobus gouldii	83
Fig. 4.5. Virtual reality modelling language reconstructions of upper second molar of	
Chalinolobus gouldii	84
Fig. 4.6. Virtual reality modelling language reconstructions of occlusion of upper and	
lower molar rows in Chalinolobus gouldii	85
Fig. 5.1. Rake angle, relief angle, wear land and edge sharpness of a crest viewed end-	
on	106

Fig. 5.2. 3-D reconstruction of <i>Chalinolobus gouldii</i> upper second molar	107
Fig. 5.3. Occlusal and anterior views of the right upper second molar of <i>Chalinolobus</i>	
gouldii showing three wear states	108
Fig. 5.4. Cusp sharpness for the first 400 $\mu m$ from the tip of the paracone and	
metacone of upper molars for three wear states in Chalinolobus gouldii	109
Fig. 5.5. Changes in cusp occlusion relief behind the mesostyle for three wear states in	
Chalinolobus gouldii	110
Fig. 5.6. a) PCA (Factor 1 vs Factor 2) and b) 2-D NMDS plots for all functional	
parameters for three wear states in 20 individuals of Chalinolobus gouldii	111
Fig. 5.7. a) The effect on the relief behind a crest of relative wear on the rake and relief	
surfaces. b) Relief angle is maintained after wear on rake surface for a linear relief	
surface but increases if relief surface is convexly curved	112
Fig. 6.1. Cuticle thickness (μm) vs punch strength (a), specific punch strength (b),	
work to punch (c) and specific work to punch (d) from punch tests of fresh cuticle	
according to insect type and level of sclerotisation.	135
Fig. 6.2. Cuticle thickness (μm) vs punch strength (a), specific punch strength (b),	
work to punch (c) and specific work to punch (d) from punch tests of fresh cuticle	
according to the region of the body from which the sample was taken	136
Fig. 6.3. Insect body mass (mg) vs minimum, median and maximum thickness ( $\mu m$ ) of	
cuticle fragments used in punch testing.	137
Fig. 7.1. Shaded relief reconstructions of upper second molars of six microchiropteran	
species	160
Fig. 7.2. PCA (Factor 1 vs Factor 2) plot for all functional parameters for three	
intractable and three tractable feeding species of microchiropterans.	161
Fig. 7.3. Eight functional parameters are depicted schematically for a cusp/crest	
structure, such as the paracone with pre- and postparacristae, and comparison of	
the expected tooth shapes for the three hypotheses in the text	162
Fig. 8.1. Possible scaling regimes for tooth sharpness vs body mass	184
Fig. 8.2. Wear and enamel distribution in protoconoid, carnassial and lophodont forms.	185
Fig. 8.3. Edge sharpnesses of a wide range of body masses and dietary types	186

# **List of Plates**

Plate 1. (Top) Three-dimensional reconstruction of the protoconoid, a fundamental	
double-bladed tool. (Bottom) Comparisons between the models and real	
mammalian tooth forms.	216
Plate 2. Three-dimensional reconstruction of the improved dilambdodont model	218
Plate 3. Front cover of <i>Journal of Microscopy</i> , November 2001	220

#### **Abstract**

The relationship between tooth form and function is a long-standing issue in the realm of functional morphology. However, in contrast to many other aspects of functional morphology, where many concepts and methods from engineering have been embraced, functional dental morphology has in many ways lagged behind in the application of these principles. The complexity and poor understanding of engineering applications such as tool function and fracture mechanics, which can be seen as analogous to the function of teeth and the fracture of food, have meant that techniques that allow the prediction of dental function from morphology have been lacking. This thesis seeks to address this deficit by the comprehensive application of several aspects of engineering to the issue of how teeth work, specifically, how the shape of an insectivore's teeth can be related to function.

The first major step in understanding dental function was to use engineering principles of machine tools to directly relate shape characteristics of teeth to how they will function. The result is a set of shape parameters, any alteration in which can be used to predict the relative change in the amount of force or energy that would be required for a tooth to function. These functional parameters are: tip sharpness and edge sharpness for cusps; rake, relief and approach angles, food capture and fragment clearance for crests.

Using these shape parameters as the dimensions of a multidimensional morphospace that includes all possible tooth shapes, only a very limited number will allow proper occlusion of the cusps and crests and have advantageous characteristics for all of the functional parameters listed above. From a search of this morphospace, the very few tooth shapes that do meet these criteria are remarkably similar to several tooth forms or structures that occur in extinct and extant mammals. These shapes can be considered 'ideal' in that they are very close to the morphology predicted to be the best functional shape. It appears, then, that these tooth forms are ideal functional shapes and are relatively unconstrained by the development and evolutionary history of mammals.

These ideal forms were then used to construct virtual three-dimensional model teeth that very closely emulate the shape and function of real tooth forms such as zalambdodont, insectivore premolars, dilambdodont and tribosphenic.

New fluorescent confocal imaging techniques for three-dimensional reconstruction of small teeth were developed and used to measure the important functional characteristics of microbat teeth. The use of Virtual Reality Modelling Language (VRML) allows the three-dimensional reconstruction of tooth occlusion of mammalian teeth for the first time,

representing a significant improvement on the use of occlusal diagrams to understand tooth occlusion. Measurements of the functional parameters from the digital tooth reconstructions demonstrate significant quantitative differences in morphological characters that predict a change in tooth function with wear, which has not been achieved with alternative approaches.

The concept of 'hardness' has long been used to describe the biomechanical properties of many groups of animals. However, due to the lack of a consistent definition, and the multitude of uses to which the term has been put, the use of the term 'intractability' has been advocated in this thesis to represent the extent to which the structural strength, stiffness and toughness are increased in a foodstuff. The thickness of the cuticle of an insect was found to be a good measure of the intractability of cuticle. The tremendous advantage of the use of cuticle thickness as a measure of the biomechanical properties of invertebrates means that the properties of a living insectivore can be directly quantified according to the thickness of the cuticle in its faeces. The quantitative measurement of intractability obtained through this technique can be used in correlations with adaptations of the masticatory apparatus, including tooth and skull morphology. This is a major advance on previous measures of the biomechanical properties of insectivore diets, and may represent the best technique of any dietary group in assessing the properties of its diet.

Comparisons between microbats that specialise on intractable or tractable insects illustrate some functional differences between tooth shape that arguably relate more to the risk of tooth fracture and increased wear rather than differences in the biomechanical properties of the diet. This conclusion challenges current views of insectivore tooth form and function.

Data gathered on the sharpness of microbat teeth was used to reassess the theoretical and empirical aspects of the scaling of tooth sharpness with body size. For large animals, it appears that the effect of tooth wear has the greatest influence on tooth sharpness, but the influence of development may be more important in smaller mammals.

Finally, aspects of general tooth morphology are addressed. Mammals of all sizes that consume tough foods will require crests for the forced crack propagation (cutting) of dietary items. It is suggested that cusps represent an adaptation to the concentration of forces, and therefore would be more prevalent in tooth forms of smaller animals with a smaller absolute bite force. This would predict that cusps are not required in larger animals, with larger bite forces, and their tooth forms should be dominated by crests. This is generally borne out in many groups of mammals.

#### **General Declaration**

In accordance with Monash University Doctorate Regulation 17/Doctor of Philosophy the following declarations are made:

I hereby declare that this thesis contains no material that has been accepted for the award of any other degree or diploma at any university or equivalent institution and that, to the best of my knowledge and belief, this thesis contains no material previously published or written by another person, except where due reference is made in the text of the thesis.

This thesis includes two original papers published in peer-reviewed journals. The core theme of the thesis is the functional dental morphology of microchiropteran insectivores. The ideas, development and writing up of all the papers in the thesis were the principal responsibility of myself, Alistair R. Evans, working within the School of Biological Sciences under the supervision of Professor Gordon Sanson.

The inclusion of co-authors reflects the fact that the work came from active collaboration between researchers and acknowledges input into team-based research.

In the case of Chapters 2 and 4 my contribution to the work involved the following:

Thesis chapter	<b>Publication title</b>	<b>Publication</b> status	Nature and extent of candidate's contribution
2	The tooth of perfection: functional and spatial constraints on mammalian tooth shape	Published	Conception and execution Contribution: 90%
4	Confocal imaging, visualization and 3-D surface measurement of small mammalian teeth.	Published	Partial conception and full execution Contribution: 80%

Signed:				
	Alistair R Evans			

#### Acknowledgements

I must express my deepest debt of gratitude to my supervisor Professor Gordon Sanson for inspiration throughout my entire undergraduate and postgraduate degrees. You never expect teeth to become such a large part of your life, but Gordon has introduced me to the world of the immense intricacies and incredible complexity of tooth form in its myriad guises, and for that I am forever thankful.

Thanks to the other members of the tooth lab who have helped me along the way at various points: Deb Archer, Nuvan Aranwela, Murray Logan, Peter Fell and Gen Perkins. Martin Burd, Alan Lill and Ralph Mac Nally were kind enough to read and comment on various drafts of some chapters.

Thanks to Lindy Lumsden for introducing me to the dark world of bats in trapping expeditions and the loan of insect traps. If you think the teeth are interesting you should see the rest of the animal...

Thanks to Mikael Fortelius and Jukka Jernvall for helpful discussions on odontocentric matters and their hospitality during my short trip to Finland. Thanks to Mikael for comments on the discussion of tooth sharpness in Chapter 8. Thanks also to Tracy Popowics and John Hunter for stimulating and at times rather heated discussions on the topic of scaling of tooth sharpness and the findings of Popowics and Fortelius (1997); the account that I give here will not necessarily be agreed upon by all.

Thanks to the people who allowed and enabled loans of bat skulls from their institution: Lina Frigo and Mark Darragh, Melbourne Museum; Sandy Ingleby and Tish Ennis, Australian Museum; Chris Norris and Bob Randall, American Museum of Natural History; Jim Patton and Chris Conroy, Museum of Vertebrate Zoology; Michael Carlton and Linda Gordon, National Museum of Natural History.

Ian Harper was a tremendous help in adapting confocal microscopy to the big microchiropteran teeth, and thanks to Gunta Jaudzems for assistance with various microscopy-related problems. Thanks to Lesley Kool for advice and help in casting and moulding of these little teeth. It really all depends on what you're used to as to what is big and what is little

Thanks to my co-editors of *The Victorian Naturalist*, Merilyn Grey and Anne Morton, and past editors Ed and Pat Grey, for their insights into the world of editing, publishing and dealing with authors. Thanks to Virgil Hubregste and Merilyn for proof-reading.

Thanks to my family for their understanding and support for these many years. And most of all, thanks to my wonderful wife Gudrun, who has managed to put up with much more tooth talk than I'm sure she ever imagined; her incredible patience and understanding have greatly helped me through the gestation of this work and made it possible.

# **Chapter 1. Introduction**

#### 1.1. Functional Morphology

The awareness of the influence of morphology on function has progressed substantially over the last few decades such that the mechanics of many biological systems are fairly well understood. Many systems, including terrestrial locomotion, flight, swimming, acoustics and certain aspects of feeding, have been successfully analysed using conventional mechanics and engineering concepts of force vectors, mechanical advantage, energetics and fluid dynamics (e.g. Alexander 1983, 1992; Bels *et al.* 1994). These techniques have allowed rigorous functional analyses and the construction of useful hypotheses from sound theoretical foundations. The use of these methods has profoundly increased the level of understanding of the factors involved in function in these systems. Questions of interest, such as the comparison of locomotion in bipeds and quadrupeds (McGeer 1992) and the flight mechanics of birds and bats (Norberg 1990), have been successfully addressed.

Like many aspects of morphology, the study of relationships between form and function of the dentition has a long history, extending back to Empedokles and Aristotle (Russell 1916; Kay 1975). It was recognised that the tooth forms of particular animals such as lions and horses appeared to match their diet extremely well. Despite what in many respects appears to be an obvious correlation, the exact reasons and the extent to which diet and dentition are matched are still issues of great significance and in many cases are unresolved.

Advances in understanding the function of the dentition has not been as rapid or successful as other morphological systems. Studies of the dentition have rarely examined function from a mechanical point of view, which is one aspect in which functional dental morphology falls behind most of functional morphology. In many respects, questions relating to systems like terrestrial locomotion and flight deal with structures and processes that more closely resemble engineering problems that are more amenable to analysis compared to investigating dental function. This thesis will examine the question of tooth form and function in insectivorous microchiropterans by the extensive application of engineering concepts.

## 1.2. Recent Approaches in Functional Dental Morphology

There was a great resurgence of interest in tooth function starting from the late 1960s. This was encouraged by new fossil finds and interpretations (Crompton 1971; Crompton and Sita-Lumsden 1970) along with technical and methodological innovations such as cinefluorography to examine mastication and oral transport in mammals (Crompton and Hiiemae 1970; Kallen and Gans 1972) and scanning electron microscopy for analysis of dental microwear (Gordon 1982; Rensberger 1978; Ryan 1979; Teaford 1988; Walker *et al.* 1978). Conceptual advances have been just as important, including the use of wear facets in reconstructing occlusal dynamics of teeth (Butler 1952; Mills 1966). This new work was built on the foundations of earlier important work in dental function and evolution (Butler 1941; Gregory 1920; Osborn 1888; Patterson 1956).

An important step in understanding the relations between tooth shape and function was made with Osborn and Lumsden's (1978) work. This paper identified some specific aspects of tooth shape that affected function. One aspect that was not explicit in that work, however, was expounded by Rosenberger and Kinzey (1976) and Lucas (1979), who argued that the biomechanical properties of foods are the primary determinants of the functional shape. This reasoning was expanded by Lucas and Luke (1984) who considered the major tooth forms that would function best for a variety of food types, characterised by their biomechanical properties. Blades are best for tough foods (where cracks must be continually driven through the food), and a mortar and pestle for brittle (with self-sustaining crack propagation) and most probably juicy foods. However, one of the most important aspects of Osborn and Lumsden's (1978) analysis, the identification of specific tooth shape characteristics that could be used to assess tooth function, was lacking in the later papers. In addition, the group of specific interest in this thesis, insectivores, was largely ignored in this body of work.

The main line of inquiry that has attempted to relate specific aspects of tooth shape to function and diet is due to Richard Kay and his co-workers and followers (Kay 1975, 1978, 1984; Kay and Covert 1984; Kay and Hylander 1978; Kay *et al.* 1978; Anthony and Kay 1993; Benefit and McCrossin 1990; Covert 1986; Dumont *et al.* 2000; Kirk and Simons 2001; Meldrum and Kay 1997; Strait 1991, 1993a, 2001; Ungar and Kay 1995; Williams and Covert 1994) examining primates. These studies have used 'shear quotient' or 'shear ratio', a measure of relative crest length (by a criterion of subtraction or standardised to tooth length or area or body mass), as a functional measure of tooth shape. The length of individual crests (such as the cristid obliqua) or the sum of several crests (crests 1-6 of Kay and Hiiemae 1974) have been used.

Shear ratio-type measures are not used in this thesis because they do not take into account the effect of cusp and crest shape on function. They are more indicative of the size of the crests rather than the comparative function, which will be as greatly affected by the non-occluding tooth surfaces as the occluding cusps and crest edges.

Strait (1991, 1993c) employed shear ratio to examine tooth form in insectivorous mammals, where it was found that hard feeders had lower shear ratios than soft feeders. This finding was predicted by Strait (1991, 1993c), but the reasoning behind this expectation has been challenged (Evans and Sanson 1998).

There have been many other studies that have incorporated useful functional analyses of teeth, or identified, expanded and/or measured some of the shape characteristics that will influence tooth function (Abler 1992; Bryant and Russell 1995; Evans and Sanson 1998; Frazzetta 1988; Freeman and Weins 1997; Lucas 1982; Mellett 1981, 1985; Popowics and Fortelius 1997; Rensberger 1973, 1975, 1986, 2000; Sanson 1980; Seligsohn 1977). Some of these in particular (e.g. Rensberger 1973; Seligsohn 1977) have made very substantial contributions to the understanding of dental form, but in large part their methods and approaches have not been followed or applied any further. Other important developments have been made, particularly in associating enamel microstructure with evolution and diet (Koenigswald and Clemens 1992; Koenigswald *et al.* 1987; Rensberger and Koenigswald 1980; Rensberger and Pfretzschner 1992), but these are not specifically addressed in this thesis.

Despite the significant conceptual and informational advances, few studies have attempted a complete analysis of tooth shape to compile a comprehensive list of shape variables that will affect function, and even fewer have measured these variables in teeth. These steps are necessary to achieve a holistic understanding of tooth function, not just in the theoretical sense but also in terms of the practical applications that exist in organisms.

## 1.3. Engineering and Tooth Function

The approach adopted in this thesis is that the form of the tooth largely dictates the function and occlusion of the tooth (for a food of given biomechanical properties). An understanding of how the shape and arrangement of cusps and the edges and associated surfaces of crests affect function is critical to the reconstruction of function for a given tooth form. The biomechanical properties of the diet will have a functional, and therefore selective, influence on the tooth form. In view of a considerable overlap in many of the questions that engineers and biologists tackle, the search for correlations between shape, function and biomechanical properties of teeth and food should start with investigating the

ways in which engineering analysis will improve understanding of tooth form and function

Many of the issues explored in this thesis have been addressed by mechanical and materials engineers to some extent (Gordon 1976, 1978). The advantages of engineering are manifold: engineers deal with a designed structure of greater simplicity in terms of materials and structure compared to biological systems; there is a greater understanding of the basis of the materials and structures; and they are more able to perform tightly controlled experiments. The phenomenal success of engineering is apparent in every aspect of modern life. These do not guarantee a perfect answer in engineering, but the major advances in materials engineering in the last few decades are indicative of the advantages of the current approaches.

From a mechanical perspective, there are two factors that have the most influence on the success with which a tooth will fracture food and reduce it to small fragments if necessary. First, the shape of a tooth will largely dictate how the stresses and strains are applied to the food. This requires the identification of specific aspects of tooth shape that influence function. Second, how the food responds to the applied stress and strain depends on its material and structural properties. This is the recognition of the influence of biomechanical properties of the diet on the function of teeth. In engineering, the first has been considered to some extent in the design and use of machine tools, e.g. lathe tools, that are designed to fracture materials. The second is the realm of materials engineering and fracture mechanics.

In mechanical engineering, the function and design of machining tools have many parallels to the bladed structures of teeth (Oberg *et al.* 2000; Ostwald and Muñoz 1997; Nee 1998; Pollack 1976). A single-point machining tool has cutting edges with its faces set at particular angles to the direction of movement and the workpiece (e.g. rake and relief angles; Fig. 1.1). Also, it may have features to clear material away from the edge of the tool to prevent clogging, such as a chip breaker, which is a notch or groove in the tip of the tool (Fig. 1.1).

The other side of the equation is represented by materials engineering, which examines the causes and consequences of stresses on materials and the mechanisms of failure and fracture (Atkins and Mai 1985; Ashby and Jones 1996; Askeland and Phulé 2003). Materials engineering uses concepts such as stress, strain, strength, stiffness, ductility and toughness to describe and quantify these effects. The objective of the dentition is to fracture food while not being fractured itself, so the material properties of both tooth and food are relevant.

However, the application of engineering principles to biological questions is complicated for many reasons. The principal reason is the great differences between the disciplines of engineering and biology in the aims of study and the methods that must be used. Engineers want to design structures that work; biologists want to understand working structures that they had no input in designing. One of the keys to successful engineering is a comprehensive understanding of all interactions of components within a structure before assembly, which is normally achieved by extensive testing of the components, including materials and component structures. Not only are biologists not privy to the results of pretesting, but this is not how biological structures were designed and built. Biological structures were not planned and constructed from the ground up – in large part they are haphazard adaptations of pre-existing structures to new uses, the products of the blind watchmaker (Dawkins 1986). Despite the lack of foresight, organismic design has the advantages of structural control at the atomic level and immense periods of time for extensive testing of designs. The history of biological study is replete with examples of how the resulting highly complex structures are extremely well adapted to their function (Alexander 1983; Vincent 1990; Wainwright et al. 1976).

Functional morphology is essentially the reverse engineering of biological structures, with all the mystery of why the structures exist, what their habitual function is, and how their function can be predicted from the morphology. The contrast between engineering and biology shows the greater requirement for prediction of function from form in biology compared to engineering.

This difference is apparent in the limits to which current engineering cannot confidently address biological questions. For instance, machine tool engineering practice is largely dependent on experimental results rather than a general theory of the function of the shape of machining tools. There has been surprisingly little analysis on the quantification of knife shape and function for cutting ductile materials (Frazzetta 1988; Abler 1992).

Likewise in materials engineering, there is inadequate knowledge of the processes of fracture, particularly the fracture of biological materials, for the prediction of how different structures will fail (Atkins and Mai 1985). This is largely due to the composite and intricate nature of the materials and structures of organisms, so that their mode of failure and fracture are highly complex. Engineers are mostly only interested in initial failure or fracture of a structure, and so the majority of the work reflects this. However, when considering the fracture of food by teeth, progressive and sustained fracture of structures and substructures is required. Some subdisciplines of materials engineering have

sought to deal with this issue (e.g. Lowrison 1974), and have been applied in the biological realm (Lucas and Luke 1983a, b), but they frequently deal with relatively homogeneous structures with properties incongruent with biological structures.

Some aspects of traditional engineering theory have been successfully applied to teeth, such as beam theory (Van Valkenburgh and Ruff 1987; Farlow *et al.* 1991), but these have limited use in their ability to model and predict the function of more complex teeth. One very promising technique for understanding the influence of tooth shape and biomechanical properties on function is the use of finite element stress analysis (FESA). It is only now emerging from its embryonic stage of development, and results have begun to reveal much about stress distribution in teeth and foods (Crompton *et al.* 1998; Macho and Spears 1999; Rensberger 1995; Spears 1997; Spears and Crompton 1996; Spears and Macho 1998; Spears *et al.* 1993; Yettram *et al.* 1976).

The arguably lack of success of functional dental morphology compared to other areas of functional morphology can be seen to be due to the difficulty of both the examination of the complex structures and the application of the principles established in engineering to the biological sphere. Also, though with less relevance today, there is the reluctance of the biologist to cross the language barrier and employ the knowledge of the engineer.

The conceptual and operational tools developed in engineering can give great insight into aspects that should be considered when examining biological function. But we should be cautious of the degree to which engineering principles can be usefully transferred to biology. Ironically, engineering concepts may be more applicable to biomaterials than engineering materials in some cases, as the properties of the latter may be considered to be affected by the distribution of flaws, whereas the former may be perfect materials to which the theory is more suited (Atkins and Mai 1985).

This thesis aims to establish the relevance and usefulness of engineering principles to functional dental morphology, particularly in terms of insectivorous dentitions, and set out aspects of tooth shape that can be used in the prediction of tooth function.

# 1.4. Dilambdodont and Tribosphenic Tooth Function

Functional analysis of dilambdodont and tribosphenic molars, found in microbats, shrews, moles and tree shrews, has largely lagged behind that of primates, with a more derived tribosphenic or quadritubercular form, and herbivores. The first two tooth forms are often considered primitive in the sense of being not as well adapted as the more recently-evolved forms. This perhaps has influenced interpretation of these forms, where

insectivore teeth are most often considered as inferior to the herbivore dentition for herbivory, and carnivore dentition for carnivory rather than focussing on the special adaptations required for insectivory. An important aim of this thesis is to reveal the superb adaptations of the insectivore tooth form to an invertebrate diet. The great similarities in the molar structure of dilambdodont when compared to zalambdodont (the molar form of solenodons, tenrecs and golden moles) and tribosphenic (primitive mammals and some marsupials) tooth forms mean that a firm functional foundation of the dilambdodont form will have application in these other forms.

The superb work of Percy Butler has shown insight into many aspects of insectivore dentition (Butler 1937, 1939, 1941, 1961, 1972, 1982, 1990, 1995, 2001). It established many important features of the relations between premolars and molars in development and evolution, and determined or confirmed cusp homologies along the tooth row and among mammal groups. Other important work on the dentition and occlusion in insectivorous mammals includes that undertaken by Mills (1966), as well as the work on the tribosphenic form of *Didelphis* (Crompton and Hiiemae 1970; Crompton and Sita-Lumsden 1970; Crompton *et al.* 1994; Stern *et al.* 1989). Comparisons of the molar effectiveness of different insectivore forms was compared by Sheine and Kay (1977) and (Moore and Sanson 1995).

#### 1.5. Tooth Wear

Recognition of the value of tooth wear for the reconstruction of tooth use is now well established through the application of techniques such as wear facet analysis and microwear. However, on the whole, the effect of wear on the function of the tooth has still been neglected. Studies of herbivores have revealed the influence of wear on tooth function (Lanyon and Sanson 1986; Logan and Sanson 2002; McArthur and Sanson 1988; Skogland 1988), which are based on qualitative wear states of the molars. It would be greatly preferable to use tooth features for which *a priori* predictions can be made regarding how changes in shape with wear will affect function. For many tooth forms, particularly those of insectivores, it has been assumed that increased wear will impede function (e.g. Verts *et al.* 1999a), but no quantitative predictions or measurements have been made of worn insectivore teeth to examine this presumption. Canine height is most frequently used as a measure of tooth wear; this may correlate with postcanine wear but does not make any specific prediction about the function of canine or postcanine teeth. Any measures of tooth function, including those used in this thesis, are only valuable if they have predictive value for worn teeth as well as unworn teeth.

## **1.6.** Insectivore Dietary Properties

Explicit in Lucas's (1979) view of tooth function is the necessity for information on the biomechanical properties and the modes of fracture of foods. However, very little work has been done in describing the properties of the insectivore diet. Descriptions of the invertebrates, particularly insects, as food only extended as far as concluding that some may be hard and brittle, and some soft and ductile (Lucas 1979; Lucas and Luke 1984).

The extent of knowledge of the biomechanical properties of insects and their constituent components has gradually increased (Hepburn and Chandler 1976; Hepburn and Joffe 1976; Hillerton 1984; Strait and Vincent 1998; Vincent 1992a), but is still fairly limited considering the immense range of material and structural adaptations that exist in such a large and important group of animals.

Classifications of insects as dietary items have used 'hardness', either according to a qualitative scale (Freeman 1981a) or by generalisations of hard insects as strong, tough, stiff and brittle compared to soft insects (weak, fragile, pliant and ductile; Strait 1993c). However, these characterisations are limited in their usefulness or have not been quantitatively tested. This thesis aims to establish sounder principles and methods of characterising the biomechanical properties of insects with the purpose of understanding the influence of insectivore dietary properties on tooth form.

# 1.7. Microchiropterans

Despite comprising approximately one fifth of mammalian species, investigations into most aspects of bats, including nutritional ecology, were scarce until the last few decades. This can be explained by the difficulty in gathering data on their foraging habits due to their crepuscular flight and aerial feeding. A significant amount of work on the comparative and functional morphology of this group is due to Patricia Freeman's series of studies on Chiroptera (Freeman 1979, 1981a, b, 1984, 1988, 1992, 1995, 1998, 2000; Freeman and Weins 1997). This work, along with comparable investigations in other groups, stimulated a great deal of other studies relating morphology of chiropteran skull and teeth to diet (Barlow *et al.* 1997; Czarnecki and Kallen 1980; Dumont 1995, 1997, 1999; Fenton *et al.* 1998c; Jacobs 1996; Reduker 1983; Rodríguez-Durán *et al.* 1993).

Examination of the diet of microchiropterans has revealed that some species appear to specialise on certain insect groups, such as beetles or moths (Black 1974; Ross 1967; Vaughan 1977; Warner 1985; Whitaker and Black 1976). Freeman (1979, 1981a) found that feeding on 'hard' invertebrates such as beetles correlated with robustness of jaws, areas for jaw muscle attachments, and the size of molars. Other patterns have since been

found that relate to the biomechanical properties of the insectivore's diet (Dumont 1995; Strait 1993b, c). However, differentiation between specialist insectivores with regard to the fine morphology of the molars has not been demonstrated.

# 1.8. Three-dimensional Tooth Modelling

A significant challenge in the comprehension of tooth form and function is the three-dimensional shape and occlusion through time of the complex morphologies of teeth. In the past this has not been possible, and reconstructions (at least published ones) are generally through line drawings, which cannot hope to sufficiently indicate the relations between teeth. Representation of the tooth in three dimensions is preferable, and various forms of imaging or scanning technology have made this possible (Boyde and Fortelius 1991; Reed 1997; Ungar and Williamson 2000; Zuccotti *et al.* 1998).

Two important aspects of this can be considered. First, three-dimensional analysis is required to understand more completely the fundamental aspects of tooth shape and the principles of morphology for occluding upper and lower teeth. Second, measurement of functional characteristics of teeth in three-dimensional space requires a full representation of teeth. Revolutions in computer and imaging technology have resulted in microscopes and computing software and hardware that can carry out these onerous tasks. Fluorescence laser confocal microscopy is able to build a three-dimensional model of an object, including small mammalian teeth. Any measurement that can be carried out by conventional calipers or protractors can be made on the teeth reconstructions, as well as surface areas, volumes and curvature, which would have been either impossible or laborious with previous methods. Virtual reality modelling language (VRML) allows the construction of three-dimensional computer models of any shape, along with real-time movement of objects. Simplified models of VRML teeth can be used to investigate principles of tooth shape and occlusion, and VRML reconstructions of upper and lower mammalian teeth can be occluded in virtual space to scrutinise the occlusion of mammalian molars in the full three dimensions for the first time.

#### 1.9. Structure of Thesis

The main objective of this thesis is to demonstrate that the types of rigorous functional analyses carried out in other morphological systems are possible in dental systems. To achieve this, it sets out to attain a greater understanding of the influence of insectivore tooth shape on function through use of tool engineering and understanding of occlusal geometry. The result should be a more predictive relationship between the

important aspects of wear and the biomechanical properties of foods on the quantitative function of insectivore teeth.

Chapter 2 establishes the functional characteristics of cusps and crests that can be gleaned from engineering principles or previous dental studies. These are used in the exploration of all possible tools (morphospace) to find those tools that best meet functional criteria. The final shapes from this exploration are used in Chapter 3 to construct threedimensional functional models of carnivore and insectivore molars and premolars. Chapter 4 describes the use of fluorescent confocal microscopy to generate three-dimensional reconstructions of microchiropteran teeth. These models can be used for the measurement of the functional parameters established earlier, and the reconstruction of occlusal dynamics of upper and lower molars. A comprehensive study of the molar form of a single microchiropteran species forms the basis of Chapter 5, which also examines the effect on function due to tooth wear. Chapter 6 explores the ways in which insects have been characterised as a dietary item, and specifically looks at the 'hardness' of invertebrates. It sets out to validate the use the of cuticle thickness as a measure of the biomechanical properties of invertebrates. Chapter 7 investigates the tooth form of 'hard-feeding' and 'soft-feeding' insectivorous microchiropterans in an effort to elucidate the influence of dietary properties on the tooth form of insectivores. A discussion on the scaling of tooth sharpness forms Chapter 8, setting out a theoretical model for the scaling of sharpness and incorporating data gathered in this thesis with published data. The thesis discussion (Chapter 9) looks more broadly at some of the issues raised throughout the thesis, such as the comparative function of tribosphenic-like and carnassial tooth forms and the influence of size and diet in mammals generally.

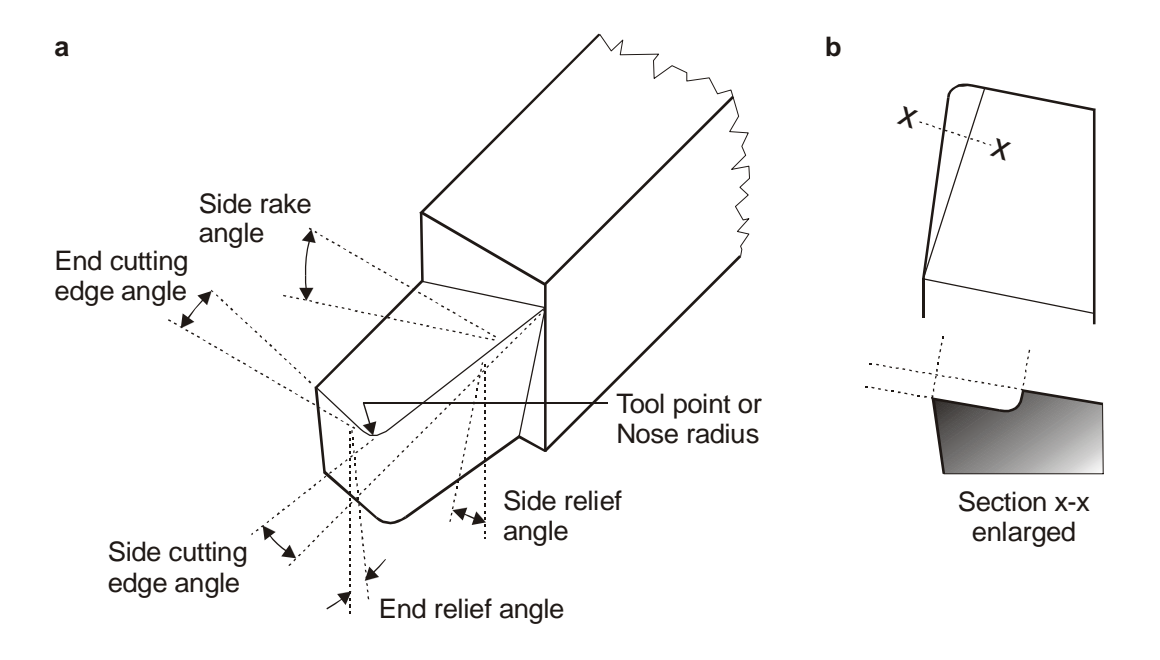


**Fig. 1.1.** a) Dimensions of a single-point cutting tool; b) one form of chip breaker on a cutting tool designed to help the clearance of fragments. (Redrawn from Oberg *et al.* 2000.)

# **Declaration for Thesis Chapter 2**

In the case of Chapter 2, contributions to the work involved the following:

Name	% contribution	Nature of contribution
Alistair R. Evans	90	Initiation, key ideas, development, data collection, interpretation, writing-up
Gordon D. Sanson	10	Advice and interpretation

#### **Declaration by Co-authors**

The undersigned hereby certify that:

- (1) they meet the criteria for authorship in that they have participated in the conception, execution, or interpretation, of at least that part of the publication in their field of expertise;
- (2) they take public responsibility for their part of the publication, except for the responsible author who accepts overall responsibility for the publication;
- (3) there are no other authors of the publication according to these criteria;
- (4) potential conflicts of interest have been disclosed to (a) granting bodies, (b) the editor or publisher of journals or other publications, and (c) the head of the responsible academic unit; and
- (5) the original data are stored at the following location and will be held for at least five years from the date indicated below:

J	Location: (	Clayton	Campus, So	chool of l	Biological <b>S</b>	Sciences, .	Monash t	Jniversity	٧

Signature 1:	 Date:	
Signature 2:	Date:	

# The tooth of perfection: functional and spatial constraints on mammalian tooth shape

ALISTAIR R. EVANS\* and GORDON D. SANSON

School of Biological Sciences, Clayton Campus, PO Box 18, Monash University, Victoria 3800, Australia

Received 22 April 2002; accepted for publication 19 September 2002

This paper addresses the question of how close mammalian teeth are to ideal functional forms. An 'ideal' form is a morphology predicted to be the best functional shape according to information of the relationships between shape and function. Deviations from an ideal form are likely to indicate the presence of developmental or genetic constraints on form. Model tools were constructed to conform to functional principles from engineering and dental studies. The final model shapes are very similar to several mammalian tooth forms (carnassial teeth and tribosphenic-like cusps), suggesting that these tooth forms very closely approach ideal functional forms. Further evidence that these tooth forms are close to ideal comes from the conservation over 140 million years, the independent derivation and/or the occurrence over a size range of several orders of magnitude of these basic tooth forms. One of the main functional shapes derived here is the 'protoconoid', a fundamental design for double-bladed tools that fits a large number of functional parameters. This shape occurs in tooth forms such as tribosphenic, dilambdodont and zalambdodont. This study extends our understanding of constraints on tooth shape in terms of geometry (how space influences tooth shape) and function (how teeth divide food). © 2003 The Linnean Society of London. *Biological Journal of the Linnean Society*, 2003, **78**, 173–191.

ADDITIONAL KEYWORDS: dentition – functional morphology – tooth modelling – carnassial – protoconoid – VRML reconstruction.

#### INTRODUCTION

At times, biological form appears to have reached perfection. Enzymes that act as perfect catalysts are found in a very wide range of organisms (where the reaction rate of such enzymes is limited by the diffusion of substrate molecules; Knowles & Albery, 1977). However, we presume that in the majority of cases, morphology does not achieve perfection due to the myriad constraints imposed on its form. Constraints have been generally grouped as formal, historical or functional (Gould, 1989). Formal refers to constraints due to geometry and the principles of physics, for example, only a limited number of physical shapes are permitted in the confines of three-dimensional space (Thompson, 1942; Stevens, 1974). Historical constraints embody the results of the particular conse-

quences of a taxon's history, and so such constraints are usually taxon-specific (Maynard Smith *et al.*, 1985). 'Developmental' constraints can be considered the expression of historical and formal constraints through ontogeny (Gould, 1989). Functional demands placed on morphology will also constrain shape. These can arise from many sources, and can often be in conflict (e.g. the inability to maximize both mechanical advantage of jaw muscles and gape; Lessa & Stein, 1992).

Mammalian dentition is an interesting sphere in which to investigate perfection and the influence of constraints on morphology. The function of teeth is largely dictated by their shape, and so formal and historical constraints on morphology may prevent a perfect functional form from coming into being. The importance of enhanced tooth function in the evolution of mammals has long been assumed, but how close mammalian teeth are to a perfect functional shape is not known, because criteria for judging perfect shape have never been formulated.

<sup>\*</sup>Corresponding author. E-mail: alistair.evans@sci.monash.edu.au

Maynard Smith  $et\ al.$  (1985) suggested the use of 'a priori adaptive predictions' to detect the presence of constraints on form. Where quantitative predictions of the form expected due to selection can be made, these can be compared to forms in nature. 'A fit with such predictions indicates an absence of relevant developmental constraints strong enough to counteract selection, whereas departure from prediction indicates their presence at least locally' (Maynard Smith  $et\ al.$ , 1985: 275). Although this was discussed in the context of developmental constraints, it could be extended to apply to any type of constraint, including functional.

The hypothesized shape can be considered an 'ideal' form: a morphology predicted to be the best functional shape according to knowledge of the relationships between shape and function. To construct an 'ideal' morphology, a priori constraints are applied to a form. These will usually include geometric constraints (limitations of three-dimensional space) and functional factors that relate shape to function. For the example of jaw mechanics mentioned above, the 'ideal' form for the position of adductor muscles in terms of mechanical advantage of the muscles would be as far from the fulcrum as possible.

To generate predicted functional forms, it is necessary to understand the relationships between shape and function. The present study concerns the function of teeth as tools for breaking down food (following Osborn & Lumsden, 1978; Lucas, 1979; Lucas, 1982; Lucas & Luke, 1984) and so requires knowledge of how tooth shape affects this function. Shape parameters that can be used to relate tooth shape to function were obtained from tools engineering and functional dental literature. Model teeth were constructed by incorporating the advantageous functional characteristics into basic starting tools to arrive at ideal shapes. The models show how these parameters interact in the form of an 'ideal' morphology that accommodates the functional constraints as well as possible, without the hindrance of developmental constraints.

Two additional geometric criteria imposed by an oral environment that may affect the tools' shape and function (serial repetition of tools and lateral movement) were also introduced to investigate the influence of these factors on tooth shape. Three-dimensional models were created in virtual computer space to fully account for the influence of geometric constraints. If the ideal and real tooth shapes are in close agreement, then we can conclude that other constraints do not substantially impede the fulfilment of the good functional features examined here.

Biological morphology is the result of complex interactions between physical principles and biological evolution at extremely diverse physical scales. Breaking apart and examining these interactions, using techniques such as the construction of 'ideal' morphologies that incorporate the factors constraining them, will give clues to underlying basic rules of form and function in biology, and a much greater insight into the functional aspects of that important mammalian attribute: complex tooth morphology.

#### MATERIAL AND METHODS

#### DEFINITIONS

This paper will consider the function of a tool in dividing 'tough' foods (that resist crack propagation; Strait & Vincent, 1998). Dietary items that can be considered to have high 'toughness' are found in very diverse taxa: from vertebrate muscle, tendons and skin, invertebrates (including much of the cuticle) to many plant structures (Lucas & Luke, 1984; Strait & Vincent, 1998). The model shapes will be derived without reference to particular food types (e.g. plant or animal material). Specific food types with additional properties may impose other functional demands that would further constrain ideal forms.

The function of a tool is to fracture the food, usually by being driven through it. This can be called 'forced crack propagation', or when performed by a blade, it is often termed 'cutting'. Mammalian teeth, particularly anterior ones, may be adapted for functioning in ways not related to dividing food (e.g. grooming or display), but only function relating to food division will be considered here.

In examining fundamental tooth shapes as topographic features, Lucas (1979) defined a 'point' as a surface with minute dimensions, and a 'blade' as a surface narrow in one dimension. Here, a 'point' will be defined as a location on a convex surface with high (local maximum) curvature in all directions on a twodimensional surface. A 'blade' is one with high curvature (essentially equal local maxima of curvature) in one dimension, with substantially lower curvature (i.e. close to flat) in the surface at approximately right angles to that direction. The end of a 'blade' may also be considered a 'point' in that there is no direction along the surface where the curvature is essentially zero (as is the case with a blade). 'Cusps' and 'crests', the biological analogues of the idealized shapes, have essentially the same topography as 'point' and 'blade', respectively, in terms of local maxima and minima of curvature. However, there is a diversity of biological shapes, and so to simplify the modelling process below, cusps and crests of real teeth will be modelled as points and blades, respectively.

Factors that are important in the function of points or blades, as discussed in either the biological or engineering literature, are outlined below, along with the reason why they are considered important. Despite many of these functional characteristics having been individually recognized before, they have not been assembled in a comprehensive analysis that defines ideal functional forms.

#### Point function

One of the major functions of a tool for dividing tough food is its ability to penetrate and drive through the food. Two major attributes of a pointed tool contribute to this function.

Tip sharpness. The stress required to initiate a crack will vary as the surface area of contact between the tool and the food. Tip sharpness is measured as the radius of curvature at the tip of a point, so a point with higher tip sharpness has a smaller radius of curvature (Evans & Sanson, 1998). A smaller radius of curvature will give a smaller area of contact (for a given elastic modulus of the food), and so produce a higher stress in the food (Lucas, 1982). Freeman & Weins (1997) and Evans & Sanson (1998) demonstrated that increased tip sharpness significantly decreased the force and energy required to penetrate foods.

Cusp sharpness. Once a point has initiated a crack in a tough food, it must be continually driven into the food to sustain propagation of the crack. The force and energy required will in part depend on the volume of the tool and the amount of food displaced. This can be quantified as 'cusp sharpness', which is inversely proportional to the volume of the point at increasing distances from the tip (Evans & Sanson, 1998). A point with higher cusp sharpness has a smaller cusp volume for a given distance from the tip. Increased cusp sharpness reduces the force and energy required for the tooth to drive through a tough food as fewer bonds in the material need to be broken or strained. Evans & Sanson (1998) demonstrated the functional importance of cusp sharpness, where decreased cusp sharpness increased the force and energy to drive a tooth through food.

#### Blade function

Criteria considered important to the function of a bladed tool are now defined. This list is as exhaustive as possible, and to our knowledge is more extensive than any other in the literature to date. Justifications for each of the criteria are given, based on engineering principles and previous dental modelling.

Edge sharpness. The edge sharpness of a blade is the radius of curvature of the blade edge. A blade with a smaller radius of curvature will have higher edge sharpness, analogous to the 'tip sharpness' of a point. Higher edge sharpness will decrease the area of contact and so increase stress in the food. The importance of edge sharpness was discussed by Frazzetta (1988) and Popowics & Fortelius (1997).

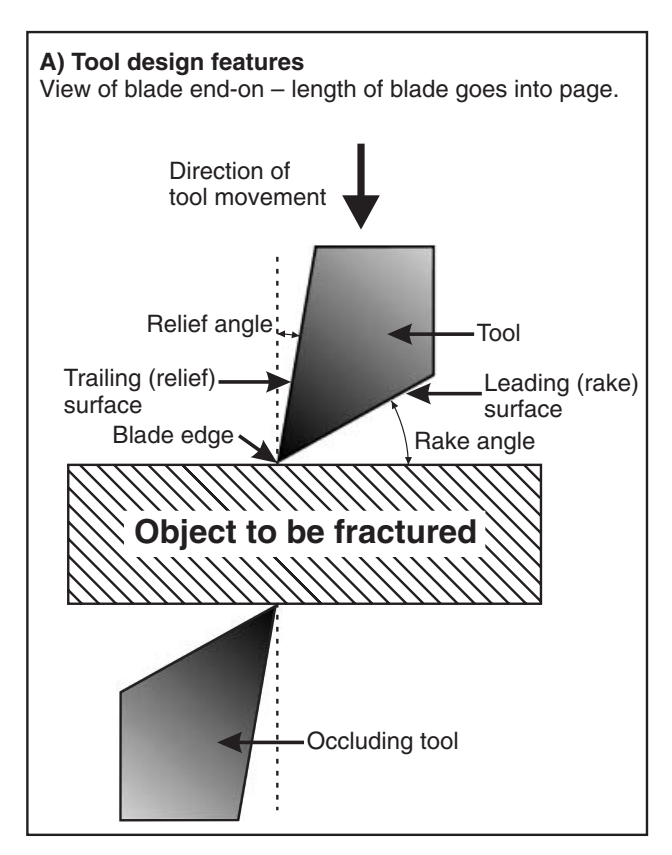
Rake angle. The angle between the leading (rake) surface of a tool and a line from the edge running perpendicular to the direction of tool movement is the rake angle (Fig. 1A). A blade with a positive rake angle (Fig. 1B) has its leading surface angled away from the material to be divided. Compared to a blade with negative rake, less force is required for such a blade to fracture food for a number of reasons. First, a negative rake blade generally must displace more material than one with positive rake, and so requires greater force and energy. Second, the surface area of contact between the food and a blade with negative rake will often be greater, and so a positive rake blade will result in higher stress for a given force. Third, the rake angle affects the force required to keep occluding blades together. When a rake surface contacts food, the blade will tend to be pushed in the direction perpendicular to the surface. Therefore, blades with a negative rake will be pushed apart when food is trapped between them, whereas a positive rake angle directs a blade towards its opposing blade.

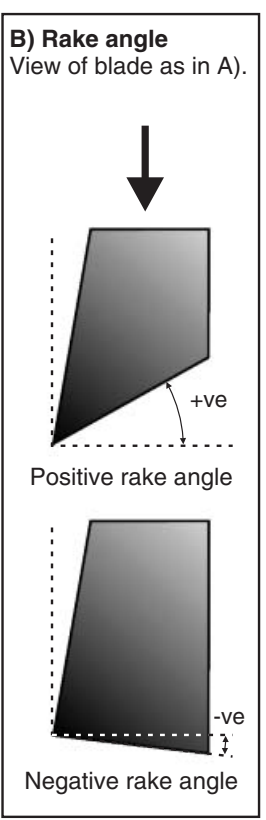
Osborn & Lumsden (1978) discussed the functional implications of rake angle. The rake angle of a blade has been shown to have a significant influence on the force and energy to divide food when dividing biological materials (in particular, leaves): a blade with a 30° rake angle required significantly less force than those of 15° or 0° (N. Aranwela, pers. comm.). Rake angle is a common variable in cutting tool engineering, and is a principal measure of the shape of machining tools (Pollack, 1976; Ostwald & Muñoz, 1997; Nee, 1998).

Relief angle. The angle between the direction of tooth movement and the trailing (relief) surface is the relief angle (Fig. 1A). Relief behind blades (also called 'clearance' in some engineering texts) reduces the effect of blades being forced apart by material caught between them, which would require greater force to maintain the proximity of crests. It also reduces friction due to blade—blade and blade—food contact due to food caught between the blades. Once sufficient relief is attained, no further benefit is achieved by increasing the angle, e.g. between 4° and 7° is best for sharp metal or glass sectioning blades shearing plant material for histology sections (Atkins & Vincent, 1984).

Relief angle has been noted by some workers in dental morphology (Osborn & Lumsden, 1978). It is common in the engineering literature, being another basic measure of machining tools (Pollack, 1976; Ostwald & Muñoz, 1997; Nee, 1998).

Approach angle. The approach angle of a blade is the angle between the long axis of the blade and a line perpendicular to the direction of movement (Fig. 1C). The mechanical advantage (MA) of a blade will depend on the approach angle ( $\alpha$ ) of the blade, where MA = 1/cos( $\alpha$ ) (Abler, 1992; Evans & Sanson, 1998), so that a





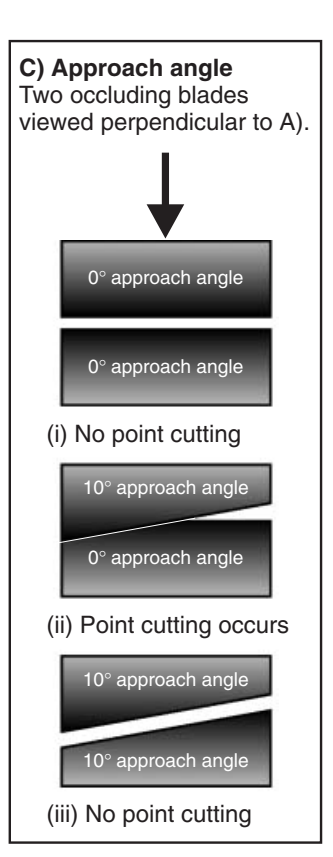


**Figure 1.** Tool design features. (A) Basic tool design features: leading surface, trailing surface, rake angle, relief angle. (B) Positive and negative rake angles. (C) Variation in the approach angle of two occluding blades and the effect on point cutting.

larger angle will have a greater mechanical advantage. The approach angle of blades will affect the 'point cutting' of the system, which occurs when the long axes of two occluding blades are not parallel, so that only one point (or two points if at least one blade is concave) meets at a time rather than the entire length (Fig. 1ii). Point cutting will decrease the amount of blade trailing surface area in contact at any one time (if there is no relief), which will increase pressure and decrease friction between the blades. Point cutting does not imply that the blade only fractures food at one point at a time, as fracture (or failure or deformation) of food will occur along the entire length of the blade in contact with food, but usually not simultaneously at all points. This is analogous to cutting thick rubber with a pair of scissors: the majority of the material is divided before the blades are close to one another (Abler, 1992).

Approach angle has been discussed by only a few authors in reference to teeth (Abler, 1992; Evans & Sanson, 1998), and point cutting by many others (e.g. Crompton & Sita-Lumsden, 1970; Seligsohn, 1977). The effect of approach angle on the required occlusal

force has been measured for sharp blades (Abler, 1992) and facsimile tooth crests (Worley & Sanson, 2000). In machining tools, it is called the inclination angle (Cubberly, 1989; Nee, 1998).

Food capture. Food is more likely to be completely divided if it is trapped between blade edges, preventing it from escaping off the ends of the blades and therefore being incompletely divided. Blades can be concave so that the ends meet first, enclosing the food before it is then fully divided. This is particularly relevant in foods with a very high Poisson's ratio (ratio of the strains perpendicular and parallel to the force; Lucas & Luke, 1984), which may be hard to trap between blades. A crest may be notched or curved (a sharp or rounded concavity, respectively). The functional advantages of capturing food have been recognized for many tooth forms (such as carnassial and tribosphenic; Van Valen, 1966; Savage, 1977; Freeman, 1979; Abler, 1992).

Fragment clearance. The function of blades will improve if the fractured material is directed away from the blades and off the rake surfaces. If material

is trapped on rake surfaces, this may prevent fracture of food caught between blades. Where there is insufficient space into which fractured material can flow, food may be compressed between opposing tooth structures and prevent the occlusion of crests. This becomes more relevant where blades on the same tool are closer together, resulting in a greater chance of food being caught between two opposing surfaces. In such circumstances, it is advantageous to create flow channels and exit structures to direct flow of food away from the blades and off the occlusal surface.

The movement and clearance of food has been given some attention in the dental literature: food movement was incorporated into Rensberger's (1973) models of herbivore teeth; Seligsohn (1977) discussed it in terms of food escapement; Sanson (1980) as sluiceways; and Frazzetta (1988) noted the clearance provided by 'gullets' between successive multiblade or serrated edges of teeth. In single point machining tools, an analogous process of chip clearance may be carried out by a change in inclination angle or by a chip breaker (a groove ground into the rake face of the tool that breaks chips into smaller pieces, allowing them to be thrown clear; Nee, 1998; Pollack, 1976).

### MODELLING TOOL SHAPES

Models of forced crack propagation tools can now be devised using the criteria outlined above. The objective is to examine the key principles related to shape and function of these tools, and the limits they place on possible tool shapes.

### Functional parameters

*Single-bladed tool.* The first system to be modelled is a tool with a single blade. The basic shape for such a

tool need only be a block that meets an opposing tool along one edge (the blade) of each block (Fig. 2A). Each blade is linear, with 0° rake, 0° relief, 0° approach angle and no capture, so the entire length of one blade meets the opposing blade at the same time. As a simplification, the tools move relative to each other in a vertical linear motion, so the blades move past one another rather like a guillotine. Each tool will occlude with another tool of the same shape to limit the number of possible tool combinations. It is assumed that fracture of the tools themselves is not possible, i.e. the tools have infinite strength. The influence of tool strength on shape is discussed later.

Our interest lies in variations of this basic tool shape. The inventory of all single-bladed tools with every conceivable variation in blade shape (the 'morphospace' for bladed tools) is too large for all shapes to be examined. Instead, we will define 'shape parameters', which are the 'dimensions' in which the shape of the tool can vary. For instance, one shape parameter is the radius of curvature at the tip of a point, and so a point tip can have a large or a small radius of curvature. The functional parameters relate the shape parameters to the function of the tool, so that the 'tip sharpness' of a point is the radius of curvature at the tip. The optimal state for each shape parameter (called the functional criterion) can be deduced from the functional parameters; in this instance, a small radius of curvature is advantageous for penetrating foods. The list of shape parameters, along with the corresponding functional parameters and criteria, is given in Table 1.

Most of the shape parameters can vary continuously, from either small to large, or positive to negative. Instead of examining the continuum, only two or three states for each of these are examined here, usually at the extremes of the continuum, e.g. for rake angle, negative, zero and positive angle; for relief

**Table 1.** Shape and functional parameters for points and blades. For each shape parameter, the possible states (e.g. small/medium/large) are listed, along with functional parameter that relates the shape to its function. The optimal state of each shape, according to the functional parameters, is also shown

Shape parameter	Possible states for shape parameters	Related functional parameter	Optimal shape state (functional criterion)
Radius of curvature of point tip	Small/medium/large radius	Tip sharpness	Small radius
Volume of point	Small/medium/large volume	Cusp sharpness	Small volume
Radius of curvature of blade edge	Small/medium/large radius	Edge sharpness	Small radius
Angle of leading surface of blade	Negative/zero/positive angle	Rake angle	Positive angle
Angle of trailing surface of blade	Zero/positive angle	Relief angle	Positive angle
Arrangement of blade edge	Zero/positive angle	Approach angle	Positive angle/point cutting present
	Relative heights of A, B and C: No capture/capture	Food capture	Capture present
General arrangement of rake surfaces	Trap food on rake surface/ clear food off rake surface	Fragment clearance	Clear food off rake surfaces

i) A=C>B

# A) Basic single-bladed tool B) Variation in three shape parameters Leading Leading surface Trailing surface Blade edge surface angle arrangement angle Blade **Trailing** В surface Direction of tool movement Positive LSA Positive TSA A=C>B Positive rake Relief present High AA PC present Capture present Negative LSA Zero TSA A>B>C Low AA Negative rake Relief absent PC present Capture absent C) Derived shapes Food capture area

**Figure 2.** Single-bladed tool shapes and shape and functional parameters. (A) The basic single-bladed tool has a single blade with 0° rake, 0° relief, 0° approach angle, and moves vertically. The blade on the tool is indicated. (B) Three of the shape parameters are altered: the angle of the leading and trailing surfaces and blade edge arrangement. (C) The derived shapes fulfil all eight functional criteria: tip, cusp and edge sharpnesses, rake, relief, capture, approach angle and fragment clearance. Each tool is shown singly and as it would occlude with another tool of the same shape. Abbreviations: A, B, C are apices A, B and C, respectively; LSA, leading surface angle; TSA, trailing surface angle; AA, approach angle; PC, point cutting.

ii) A>C>B

iii) A>B>C

angle, zero and positive angle. Blade edge arrangement cannot be considered in this way. Instead, the edge of the blade is defined by the positions of both ends (Apices A and C) and a middle point (Apex B) along the blade (Fig. 2B). The three apices lie in a vertical plane, ensuring that the edges of occluding blades meet.

Three-dimensional reconstructions of the tool models were created using Virtual Reality Modelling Language (VRML), a relatively simple programming language for three-dimensional computer modelling (e.g. Evans, Harper & Sanson, 2001). Model shapes were constructed using the 'IndexedFaceSet' command, where the three-dimensional coordinates of the tools are specified. A VRML browser such as 'CosmoPlayer 2.1' (Computer Associates International, Inc., Islandia, U.S.A) can be used to view the models and manipulate them in virtual threedimensional space to illustrate that proper occlusion occurs. All figures of the models (Figs 2-4) are from the VRML reconstructions. The purpose of VRML is to illustrate the 3-D morphology of the shapes and to test geometric hypotheses (i.e. that occlusion between blades occurs as predicted). It is not designed to specifically test the function of the tools in terms of force required to function, as this is assessed according to the functional parameters.

Starting with the basic tool described above, tools were created with all combinations of relative heights of Apices A, B and C (e.g. A = B = C, B > C = A, C > A > B). Each of these was assessed for point cutting and capture ability (the functional parameters related to blade edge arrangement). For the shapes that fulfil these two criteria, the remaining shape parameters were altered to correspond to the functional criteria. For instance, both rake and relief angles of the blades are modified from 0° (the state of the basic tool) to a positive angle. Some features do not need improvement from our basic shape (such as edge sharpness, as the edge has an infinitesimal radius) or may improve in parallel with change in others (such as approach angle, which can vary with capture). Figure 2B shows the effect on the shape of the tool when some of the shape parameters are altered individually.

Double-bladed tool. The model of a double-bladed tool used here has two blades set at an angle to each other, like a prism with an equilateral triangle at the base and top (Fig. 3A). Two of the edges on the top surface act as blades that occlude with blades of other tools. This design fits two blades in the space (or more precisely same tool length) of the previous one, with a greater combined blade length. Shapes other than the prism could be used (such as the cubic single-bladed tool, where two adjacent edges are blades), but the

particular choice of starting tool does not affect the final conclusions.

The morphospace for double-bladed tools is even larger than that of single-bladed tools. The junction of the two blades is Apex A, the other end is Apex C, and Apex B is in between. The tools made here will be symmetrical around Apex A. As for the single-bladed tool, all combinations of relative heights of A, B and C were constructed. The shape parameters of this tool are now altered according to the functional parameters. Figure 3B shows how several of the shape parameters can be individually modified on the double-bladed tool.

### 'Anatomical' constraints

In addition to the functional parameters used above, further criteria can be introduced that will influence the way that the tools can be used in real biological systems, that is, they are factors that may influence their shape and function in the mouths of animals. The objective is to see whether the shapes can accommodate these additional criteria, and to what degree they must be modified to do so.

First, we will create multiple functional copies of the tools, approximating many teeth in a jaw. The easiest way to do this is to arrange several of them serially, as if in a tooth row.

Second, we will introduce a degree of lateral movement, which is advantageous for several reasons. If a tooth in the mouth of an animal moves directly vertically, there may be a tendency for food to become trapped between the teeth or non-tooth structures (e.g. the jaw or palate), preventing the blades from coming into contact. Also, food may be forced into the gums of the opposing tooth row. The possibility of this occurring would be reduced by some amount of lateral movement of the opposing teeth, so that the vector of movement of the teeth (the occlusal vector) is now vertical with a lateral component. This is essentially extending the fragment clearance criterion to include prevention of food trapping between tooth and nontooth structures.

### RESULTS

### FUNCTIONAL PARAMETERS

Once the shape parameters of the tools have been altered according to the procedure above, the result is the subset of tool morphospace that fulfils the functional parameters. For each type of tool, several different designs may meet all of the functional criteria, as there may be multiple blade edge arrangements that allow for capture and point cutting.

### Single-bladed tool

The single-bladed tool shapes shown in Figure 2C fulfil the eight functional criteria. The three different tool

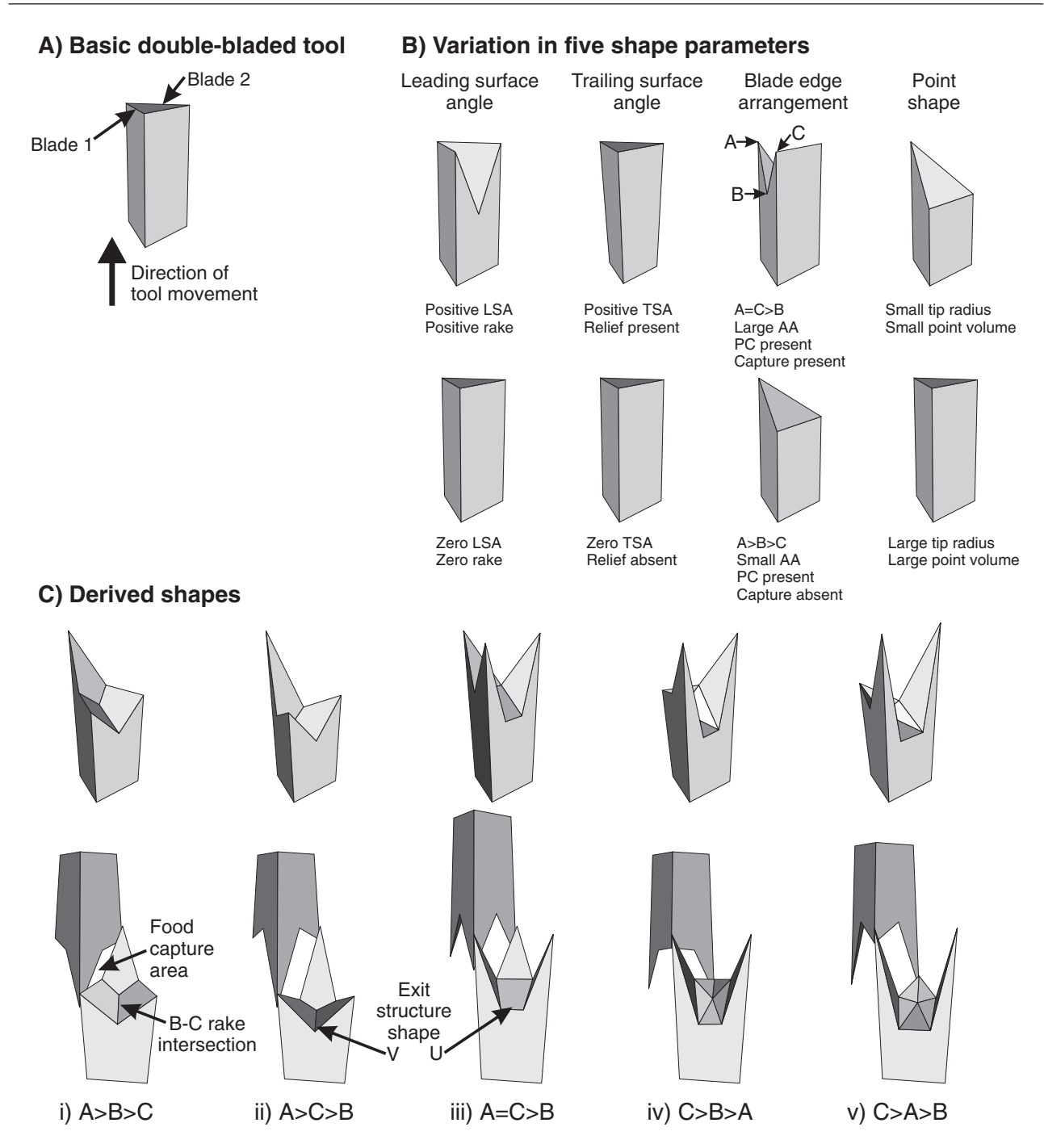


**Figure 3.** Double-bladed tool shapes and shape and functional parameters. (A) The basic double-bladed tool has two blades, each with 0° rake, 0° relief, 0° approach angle, and moves vertically. The two blades on the tool are indicated. (B) Five of the shape parameters are altered: the angles of the leading and trailing surfaces, blade edge arrangement and point shape (which includes both tip radius and cusp volume). (C) The derived shapes fulfil all eight functional criteria: tip, cusp and edge sharpnesses, rake, relief, capture, approach angle and fragment clearance. Each tool is shown singly and as it would occlude with another tool of the same shape. See Fig. 2 for abbreviations.

types in Figure 2 are: (i) the ends of blades are equal in height (A=C>B) and the tool is symmetrical; (ii) one end is the tallest apex, followed by the other end, with the notch the lowest (A>C>B); and (iii) the ends represent the maximum and minimum of the blade height, with the notch in between, but B is lower than the line A-C (A>B>C). These blades allow for capture (as they are 'notched' so that they enclose some area for food capture) and point cutting. All other possible shapes do not allow for capture when occluded with a tool of the same shape (e.g. B>A>C) or have zero approach angles for some length of the blade (e.g. A>B=C).

### Double-bladed tool

The general shapes that fit the functional criteria are shown in Figure 3C. The first three tools are: (i) primarily single-pointed, with the notch in each blade higher than the lateral points (A > B > C); (ii) one maximum point and two lower points, with the notch lower than lateral points (A > C > B); and (iii) a three-pointed design (A = C > B). These are essentially the double-bladed versions of our single-bladed tools, where the notch apex may be lower (C > B) or higher (B > C) than the lower end of the blade, but always lower than the line A–C. In these three tools, the highest points of each of the blades meet at the same point on the tool (A).

The other two derived shapes in Figure 3C (iv,v) differ topographically from the first three in that the junction of the blades (Apex A) is not the highest point of the tool. Good rake angles for these shapes can only be achieved by directing the rake surface deep into the body of the tool.

Once material has been divided, it must move off the rake surface to allow further fracture to occur (the 'fragment clearance' criterion). When two blades are placed on the same tool, this may be more difficult as the directions in which the material can flow are further limited. For the double-bladed tools, the third edge of the top triangle has become an 'exit structure' (Fig. 3C) out of which divided material must flow. In designing these tools, the junction between the rake surfaces of the B–C segments of the blades (B–C rake intersection; Fig. 3C) could have been made horizontal. However, to improve the flow off the rake surfaces, it has been sloped away from the blades into the exit structure.

The shape of the exit structure differs between these tools. A U-shaped exit structure was used for 3iii as a greater volume of material will probably be divided by this shape as shown by the greater capture area. For 3iv–v, the proximity of the rake surfaces of the two blades near Apex A may restrict flow, so a larger U-shaped exit area was provided.

### 'ANATOMICAL' CONSTRAINTS

### Serial arrangement

Single-bladed. This can easily be achieved for our single-bladed tools. The simplest arrangement is to place the tools in a line so that the blades are parallel to the row of tools (the tooth row). This creates a continuous cutting edge that is zig-zag in the vertical direction, giving the appearance of a serrated blade.

*Double-bladed*. The double-bladed tools can be arranged serially so that the blades form a continuous, jagged cutting edge, and each tool occludes with two others.

Overall, both of these tool types can be arranged serially without the need to modify their shapes.

### Lateral movement

Single-bladed. A moderate amount of lateral movement is easily accommodated into these designs. A great amount is probably not necessary to avoid compression of food with this tool design, as there is less of a problem with food being trapped on the rake surfaces. The main feature that must be altered is the orientation of the blades. For blades that move along a linear trajectory, the easiest arrangement is for the entire length of the blade (the three apices, including the notch defined by B) to be in a plane that includes the vector of tooth movement (i.e. occlusal vector is perpendicular to the normal of the plane). The vertically moving tools fit this pattern, as the occlusal vector is vertical and each blade lies in a vertical plane. Therefore, when blades are arranged to introduce some lateral movement, they must be in a plane that includes the occlusal vector. Also, for blades on two different tools to occlude, they must be orientated in the same plane (which is not guaranteed, as there are infinitely many planes with normals that are perpendicular to a given vector). When the blades are concavely shaped, food will be captured between the blades and there will be at most two point contacts between the occluding blades (Fig. 4i).

Double-bladed. The double-bladed tools can only move laterally in one direction, so that the original rake surface is still the leading surface of the tool. This means that Apex A of one tool moves vertically and laterally in the direction of Apex A of the opposing tool. If the tool moves in the other lateral direction (so that the relief face becomes the leading face, and A moves towards C of the opposing tool) then the tool will run into the junction between the two tools it occludes with.

Introducing lateral movement into the doublebladed system is slightly more complicated than the

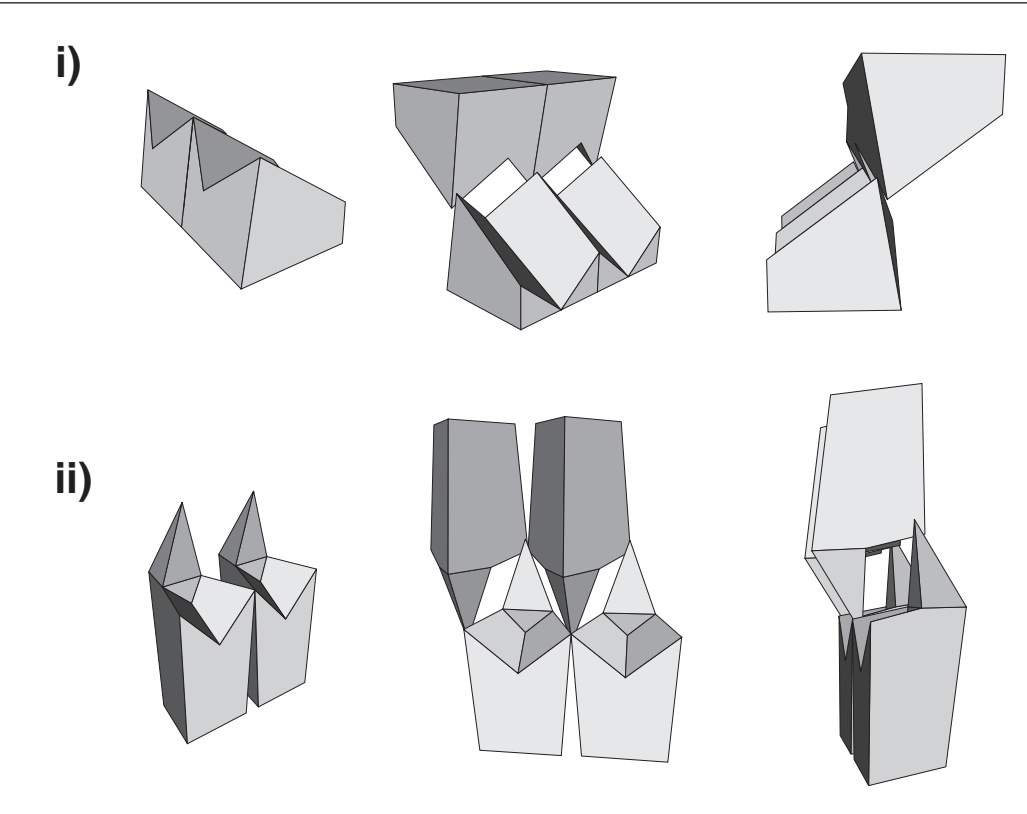


Figure 4. Anatomical criteria for tool design. Single-bladed (i) and double-bladed (ii) tools arranged serially and with lateral movement.

single-bladed, but the same principles apply. For two blades to occlude, they must be in the same plane that includes the occlusal vector. If there are multiple blades on a tool (e.g. two), the intersection between the two blade planes will be a line, and this line will be parallel to the occlusal vector.

For the one-pointed double-bladed shapes (3i,ii), shifting the tip of the main point (A) towards Apex C ensures that it is pointing closer to the direction of tooth movement. This will improve penetration by the main point, aid in the rearrangement of the blade planes so they include the occlusal vector, and improve the rake angle of the blades leading down from the main point (Fig. 4ii).

Lateral movement with a three-pointed tool (3iii) and the other two-bladed shapes (3iv,v) is more difficult. It is possible to reconfigure them so that the blades will contact throughout the stroke, but the degree of lateral movement will be more restricted when compared to the one-pointed shape.

VRML files for some of the single-bladed (4i) and double-bladed (4ii) tools are given in the Appendices. These include the three-dimensional coordinates of the shapes and the vectors of tooth movement, and allow the full three-dimensional shape and occlusion of the tools to be viewed.

### DISCUSSION

Considering all of the tools in the large eightdimensional tool morphospace examined here, there are only a few tool designs that are able to fulfil the constraints imposed by geometry and those dictated by the functional parameters. The shapes derived above will now be examined in more detail.

### FUNCTIONAL MERITS OF MODEL TOOLS

The shape parameters of the tools have been altered to conform to the functional criteria for point and blade function. This makes them highly effective tools for the fracture of food by forced crack propagation, as the force and energy required for them to divide food should be minimized or at least reduced compared to the starting tools. Once anatomical constraints are also incorporated into the designs (Fig. 4), the models are capable of being accommodated in the mouth of an animal, at least for the simple instances considered.

Despite the fact that all of these tools do fulfil our functional criteria, they are not functionally equivalent for several reasons. Some of the tools (2ii,iii, 3i,ii) have a single maximum point that will be the first to contact the food and initiate a crack; others have two

(2i, 3iv,v) or three (3iii). A one-pointed design may be more advantageous in terms of force (having only one initial point as opposed to three, and so produce three times the stress for a given force). However, crack initiation and propagation at a greater number of points may allow faster fracture of food.

The tools also differ in the extent to which they can fulfil the functional requirements. For the single-bladed tools, large approach angles and capture areas are easier to achieve for design 2i than for 2ii and 2iii. For the double-bladed tools, it is difficult to achieve a good rake angle for tools 3iv,v (especially at Apex A, where the rake surface must be directed deep into the body of the tool) compared to tools 3i–iii. Lateral movement is more restricted in shapes 3iii–v and further compromises the rake angles of 3iv,v. From this, it appears that the first two shapes (3i,ii) are the best designs for our criteria and most closely approach our 'ideal' functional tooth shape.

We will coin a new term for the final double-bladed tool with one maximum point: protoconoid, taken from 'proto' meaning 'first or primitive', 'con' from 'conus' meaning 'cone' and 'oid' meaning 'like'. This is not to be confused with protoconid, the main cusp on lower tribosphenic teeth. The protoconoid is not a single cusp or point, as the name may imply—it is a functional complex consisting of a specific arrangement of points, blades and the surrounding tooth surface. The term 'protoconoid' will be used to refer to both the vertically and laterally moving tools (3i,ii, 4ii), as they all possess common functional benefits, as listed in Table 2.

# RELATIONSHIPS BETWEEN MODEL SHAPES AND REAL TOOTH SHAPES

After specifically disregarding the shapes of real teeth in designing our model tools, it is now interesting to consider how similar the derived functional shapes are to shapes that occur in animal teeth. Comparison

Table 2. The important functional advantages of the protoconoid

- 1 Initial penetration by a single maximum point with high tip and cusp sharpness
- 2 Forced crack propagation along blades
- 3 High edge sharpness of blades
- 4 Blades with positive rake angle
- 5 Relief present behind blades
- 6 Ability to capture food between blades for fracture
- 7 Good approach angle and point cutting
- 8 The presence of an 'exit structure' to allow food fragments to flow off the rake surfaces of the blades
- 9 Many copies can be placed serially to form a tooth row
- 10 A degree of lateral movement is easily accommodated

between the teeth of animals and the models created here, based solely on a priori assessments of the factors that will affect the function of forced crack propagation tools, reveal many similarities and consistencies. Correspondence between shapes can be assessed in terms of topography of the teeth (the position and arrangement of cusps and crests) and how well they fit the functional criteria, which will be reflected in the fine details of tooth surface shape.

### General topography

There are many tooth shapes that are topographically equivalent to the single-bladed tools. The symmetrical single-bladed tool (2i; Fig. 5A) is comparable to a carnassial (Savage, 1977; Mellett, 1981; Van Valkenburgh, 1996), both having a single blade with a large notch and cusps at each end (Fig. 5C). The carnassial tooth form is a relatively common tooth shape found in several diverse carnivorous lineages, particularly carnivorans (formed by the fourth upper premolar and first lower molar:  $P^4/M_1$ ) and the extinct creodonts  $(M^{1-2}/M_{3-4}).$ 

The asymmetrical tools (2ii,iii; Fig. 5A) appear in many more settings, such as the premolars of animals with tribosphenic-like teeth and in carnivores (Fig. 5D; Freeman, 1981; Mills, 1966). The general form of these premolars is a single asymmetrical blade. The crests of all of these teeth have the middle apex of the crest (B) lower than a straight line connecting the ends (A and C), allowing capture of food between the blades.

The topography of the protoconoid designs (3i,ii, 4ii; Fig. 5B) greatly resembles many cusp-crest complexes of real tooth forms, such as zalambdodont (found in some insectivorans, e.g. tenrecs), dilambdodont (many microchiropterans and insectivorans, e.g. shrews and desmans) and tribosphenic molars (some primitive mammals and many insectivores, e.g. opossums) and several extinct groups (e.g. symmetrodonts and pantotheres) (Fig. 5E; Mills, 1966; Crompton, 1971; Freeman, 1981). The main cusp structures of these teeth (for upper tribosphenic molars, paracone and metacone, and lower molars, protoconid and to a lesser extent hypoconid) have a basic protoconoid shape. For all of these complexes, there is a single, tallest cusp that is the junction of two crests. Each crest is asymmetrical, with the ends of crests at unequal heights, and concave, allowing capture. Cusps are present at the lower end of each crest (e.g. parastyle, paraconid in tribosphenic molars).

### Functional parameters

The carnassial and tribosphenic tooth forms also have great similarities in the detailed shape of the tooth surface with the single- and double-bladed models. For instance, the crests of most carnassial and tri-

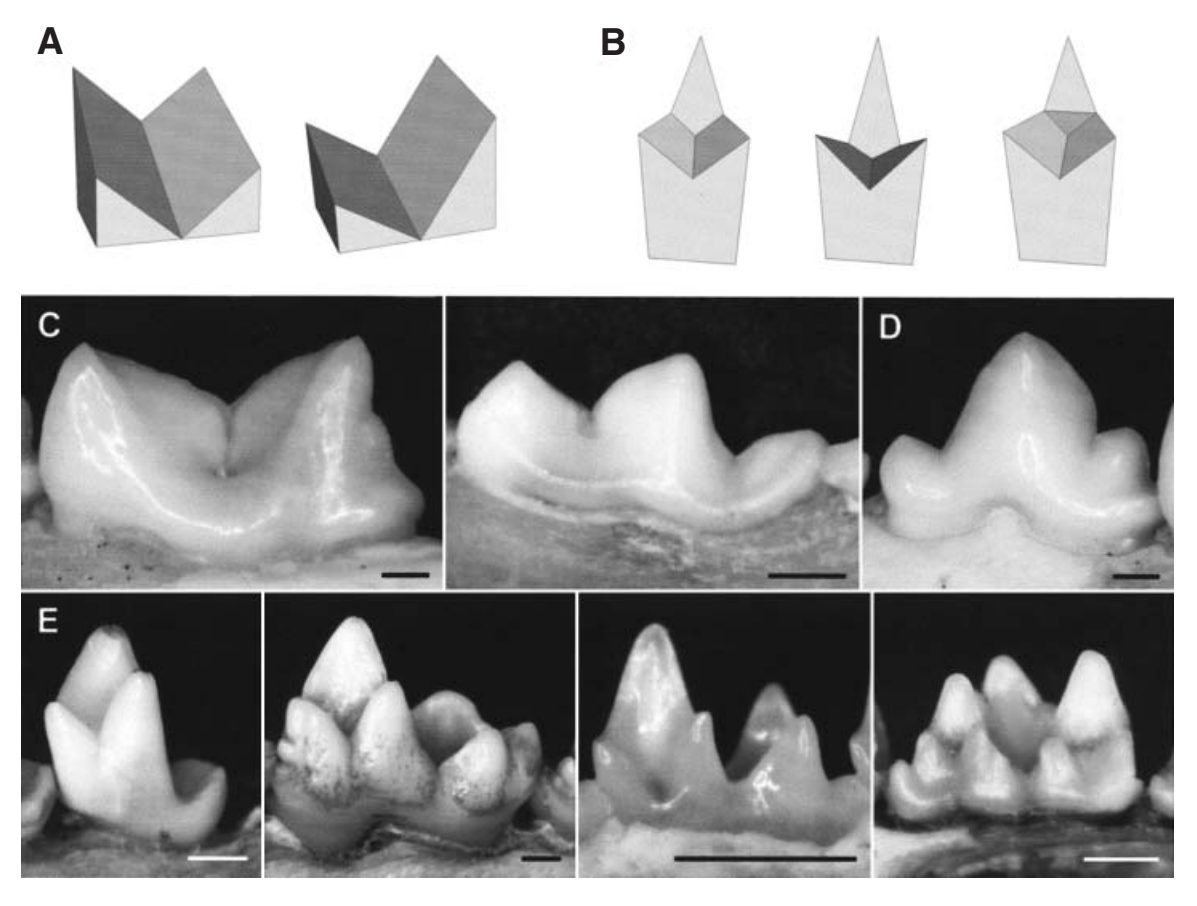


**Figure 5.** Comparisons between the models and real mammalian tooth forms. L–R. Model tools: (A) single-bladed tools, symmetrical (2i) and asymmetrical (2ii); (B) double-bladed tools (3i, 3ii, 4ii). Mammalian tooth forms: (C) lower carnassials of *Felis catus* (Carnivora: Felidae) and *Mustela frenata* (Carnivora: Mustelidae); (D) premolar of *F. catus*; (E) lower molars of *Tenrec ecaudatus* (Insectivora: Tenrecidae), *Didelphis virginiana* (Didelphimorphia: Didelphidae) and *Chalinolobus gouldii* (Chiroptera: Vespertilionidae), and upper molar of *Desmana moschata* (Insectivora: Talpidae). Scale bars = 1 mm.

bosphenic teeth have a positive rake angle and relief behind the crests (Evans, 2000; Osborn & Lumsden, 1978; Evans, in press; unpublished data). They allow for capture of food and point-cutting (Crompton & Sita-Lumsden, 1970; Seligsohn, 1977; Osborn & Lumsden, 1978; Lucas & Luke, 1984; Evans, 2000; Evans, in press; unpublished data) and have high edge sharpness (Evans, 2000; Freeman, 1992; Popowics & Fortelius, 1997; Evans, in press; unpublished data). Flow of food off rake surfaces is assisted, as the exit structure in tribosphenic cusps slopes away from the blades (Evans, in press; Seligsohn, 1977). In other words, these teeth largely conform to the functional criteria set out above.

### 'Ideal' forms and constraints

The similarity between real tooth shapes and the ideal functional forms can now be addressed. According to the functional and limited anatomical criteria from which they were constructed, the models are the best possible functional shapes. Their close similarity to animal tooth forms suggests that these teeth have the best shape for their function. Their shape, then, is not substantially limited by developmental constraints – the developmental processes of mammalian teeth allow the construction of essentially perfect functional shapes. Dental morphology has managed to escape whatever developmental constraints apply to it to achieve essentially optimal functional tooth designs, and these teeth are largely shaped by the geometric and functional demands placed upon them. It is interesting to note how often the tribosphenic tooth form is often considered 'unspecialised', apparently in the sense of 'unadapted' to a specific use. In truth, it can be seen how superbly adapted this tooth form is.

Dental evolution has surmounted additional functional demands not considered in this model that may be in conflict with a tooth's food-fracturing function, such as the biomechanical properties of the teeth themselves (Popowics, Rensberger & Herring, 2001).

For example, without being sufficiently strong and stiff, teeth would not be able to fracture most foods without themselves being broken or deformed (Lucas, 1979). The relative strength of the tool and food will influence tool shape. If a weaker material were used to construct the tools, it is likely that the following tool features would be altered: greater robustness of tooth features overall; decreased tip sharpness (rounding of cusp tips); decreased cusp sharpness (shorter, fatter cusps); decreased edge sharpness (rounding of blade edges); and decreased sharp angles in tooth features (e.g. notch in blades would not be as sharp, as the notch would act to concentrate forces and promote tooth fracture). The bulk of the minor differences between the models and teeth can be seen as being due to the influence of tooth strength, but these do not influence the qualitative shape of the tools and the conclusion that they fulfil the functional criteria set out above.

If a rigorous investigation of the effects of tool strength on shape were to be undertaken, a more complicated modelling process would be required that takes into account the stresses generated in both the food and tool when the tool is functioning and relate it to the stresses that each could withstand. This modelling would require more detailed specification of the forms of the tool and food, producing results of reduced generality. Instead, the models constructed here give qualitative shapes in terms of broad topography and functional parameters, allowing largescale trends to be discerned. Without additional complication, strength can be taken into account in a limited way, such as providing another reason to prefer shapes 3i,ii over 3iii-v, as the latter of these shapes tend to have taller, thinner cusps that risk fracture.

The lack of constraints on morphology can also be detected by convergences in form, which will be independent of the a priori predictions used to create the model (Maynard Smith et al., 1985). Tooth forms containing protoconoid-like shapes have persisted in mammals for over 140 million years, being present in early therians (Sigogneau-Russell, Hooker & Ensom, 2001) and extant insectivorans and microchiropterans. Likewise, the maintenance of morphology over a significant time span and wide range of scales could also indicate freedom from constraint. Carnassial forms have been independently derived in several carnivorous lineages (more than five times in fossil and modern carnivorans and twice in marsupials; Butler, 1946). Similar tooth forms are present in animals of widely varying body size, often over three orders of magnitude in body mass, e.g. dilambdodont or tribosphenic (2 g shrew to 2 kg opossum) and carnassial (50 g mustelids to 200 kg lion; body masses from Silva & Downing, 1995).

This final point indicates the likelihood of a very significant feature of these designs that enables them to function at such different sizes: the function must rely on some shape characteristics that are relatively scale-independent. Many of the functional features discussed here are size-independent (e.g. topographic features such as presence of cusps to aid penetration of food and crests for crack propagation; surface shape such as rake, relief and approach angles of crests). Conservation of these features would be expected over large (if not all) size ranges, resulting in the ideal solution being largely identical for all tooth sizes. This is very likely to be the case for the single- and double-bladed tool shapes derived here.

The maintenance of and convergence onto a few tooth forms, and their presence at differing scales, point to the conclusion that development has very little, if any, constraining influence with respect to these functional shapes. It appears that their developmental regime has allowed these functional shapes to be achieved very early in their evolutionary history.

### DIETARY PROPERTIES

The physical properties of a food should determine the 'ideal' tooth shape to divide it (Lucas, 1979). The diversity of mammalian diets includes strong bones, tough and viscoelastic meat, high- and low-fibre leaves, and fruits that are hard and strong or weak and juicy. The method of best dividing a food will differ with the type of food, as each food will impose its own functional demands. We would therefore expect a variety of ideal shapes to be found in mammals.

The protoconoid and carnassial shapes appear to be the best functional shapes for a food simply considered as 'tough'. Animals that possess these tooth forms are largely insectivorous or carnivorous (e.g. insectivorans, microchiropterans, canids and felids), which may indicate that invertebrates and vertebrate flesh can be treated as being largely similar in terms of the functional demands placed on tooth form.

A large number of mammalian molar forms is not derivable from the above modelling (e.g. molars of humans and herbivores such as rats, horses and kangaroos). It is likely that this can largely be attributed to the influence of additional constraints imposed by physical properties (e.g. high hardness or strength, brittleness or juiciness) that more greatly influence functional form than toughness for a given food type. The extent to which the food needs to be divided will also influence tooth form.

Although these other forms do not resemble the ideal shapes of this study, this does not indicate that these other forms are not in some sense functionally 'ideal'. The general shapes of ideal tooth forms for other dietary types have been speculated upon

(Osborn & Lumsden, 1978; Lucas, 1979; Lucas & Luke, 1984), but further detailed analysis is required to assess whether there are any major developmental constraints preventing the construction of this ideal form. However, the high degree of parallelism, convergence and size-independence exhibited by these forms suggests they may be 'ideal' for some diet, or as close as can be achieved given non-functional constraints.

### INTERACTIONS OF CONSTRAINTS

As well as the constraints on the shapes of teeth and tools discussed above (geometric considerations, functional and anatomical criteria), interactions between these factors also constrain tooth shape. Altering any criterion may interfere with the optimization of others, or some may be modified in parallel (e.g. approach angle and capture), so that each criterion can only be maximized to a certain extent, generally limited by geometry. Figure 6 is a putative map of the main inter-

actions between the functional criteria and a few other dimensions, showing which criteria are generally affected when others are altered. Three-dimensional blade length is simply the length of the blade in three dimensions (Fig. 6 inset). Functional blade length is the length of a cut made by a blade: the two-dimensional length of the blade projected onto a plane normal to the occlusal vector (PNOV).

An important case where geometry plays a role is where the packing of blades on a tool is increased, usually by the addition of other blades. There are compromises between the advantages of increased packing (a greater amount of food can be divided with one stroke; the breakage function of Lucas & Luke, 1983) and the ability to conform to the functional criteria. Compared to the single-bladed model, increased packing of blades in the double-bladed model means it is harder to fulfil the criteria. Trade-offs will occur, as the function of each blade is more likely to interfere with the function of a nearby blade. For certain blade configu-

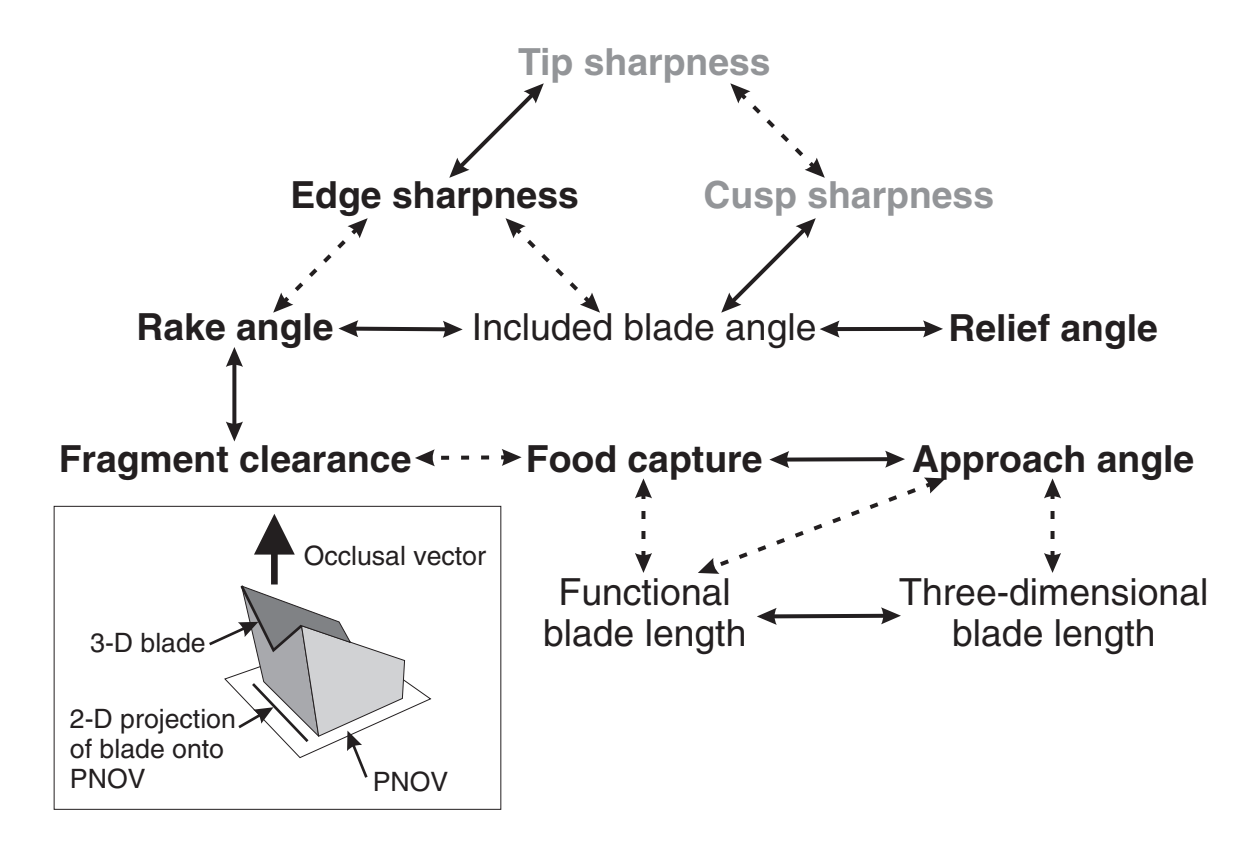


**Figure 6.** Putative relationships between tooth functional characteristics. Bold characters are the eight criteria considered in this paper, with grey characters affecting points and black characters affecting blades; non-bold characters are other factors that may be considered combinations or derivations of the eight criteria. Solid arrows signify a strong relationship: if one of these features is altered, it has a direct affect on the others; dashed arrows signify a weaker relationship, such as an indirect effect. This shows which other features would change in order to accommodate an alteration in that character. 'Included blade angle' equals (90° – rake angle – relief angle). The other characters are defined in the text.

rations, these interactions and constraints may be more apparent, so that the final tool shape is a compromise of many features. This is demonstrated by tools 3iv-v, where the configuration of the blade edges means that a good rake angle is difficult to achieve.

### TOOTH MODELLING

The purpose of this study was to reduce the complexities of mammalian teeth to distil the essential characteristics of a functioning tooth. These include the geometric arrangement of particular components and their ability to function in a given manner. The power of the present analysis lies in the model being fully explicit, where every feature is specifically determined by the functional parameters. Also, each factor that is incorporated is independently justifiable and can be considered and rejected separately, allowing the dissection of the relative importance of each feature. For instance, the effect of approach angle can be individually inspected to show its importance in tooth function, and removed from the model if deemed inappropriate.

This analysis is more detailed than earlier work that has considered the probable form of tooth structures for given dietary properties (Osborn & Lumsden, 1978; Lucas, 1979; Lucas, 1982; Lucas & Luke, 1984) in its consideration of shape factors that affect the function of teeth. This is presumably the reason for the greater degree to which the current model tools approach the shapes of mammalian teeth. The shapes derived here can be further examined through other types of analysis, such as computer modelling of forces (e.g. finite element analysis; Rensberger, 1995; Spears & Crompton, 1996; Spears & Macho, 1998) or empirical force-testing of alternative tool shapes (Abler, 1992; Evans & Sanson, 1998), to substantiate the results obtained - that the derived shapes are in some sense 'ideal' functional forms for dividing tough foods.

### CONCLUSIONS

This analysis does not merely predict that points and blades will be present in dentitions designed for fracturing tough foods, as earlier studies have largely done (e.g. Lucas & Luke, 1984); it extends the examination to predict the detailed form in which the entire functional tooth will be found (including shape of blade edge and surface surrounding blades and points). The models presented above appear to be the best to date in terms of predictive power and resemblance with tooth shapes that occur in mammals.

This paper also demonstrates the potency of the approach of Maynard Smith *et al.* (1985) for identifying constraints in morphology, which involves the use of a priori knowledge of function to generate ideal forms along with evidence from convergence and

maintenance of morphology throughout evolution. The method could be used much more frequently to detect the presence of constraints, and the proper identification of 'spandrels' (Gould & Lewontin, 1979; Pigliucci & Kaplan, 2000), in biological form.

Tooth modelling equips us with a method of simplifying and classifying the great diversity of tooth forms, such as variations of the basic carnassial or protoconoid forms. The evolution and degree of development of many features, such as single- or double-crested tooth shapes and the extent to which they conform to the functional criteria, may be tracked in fossil lineages, showing functional evolution of teeth in a new way. The possible paths of evolution can also be examined: for instance, there is only a limited number of basic arrangements of protoconoids possible, which will constrain the evolution of teeth even further.

This survey of tool morphospace confirms that there are only a limited number of shapes that conform to an 'ideal' functional morphology for teeth. This is also reflected in the high degree of conservation of many tooth forms. The causes are apparent: the limited options available in physics (in terms of function) and geometry (shape).

### ACKNOWLEDGEMENTS

Our thanks go to Gudrun Arnold, Deb Archer, Martin Burd, Nuvan Aranwela, Mikael Fortelius, Alan Lill, Ralph Mac Nally, Jukka Jernvall and Betsy Dumont for comments on the concepts presented here and earlier drafts of this paper, and John Rensberger and an anonymous reviewer for helpful and insightful advice.

### SUPPLEMENTARY MATERIAL

Full VRML reconstructions of all models constructed in this paper, from which Figures 2–4 have been drawn, are available from http://www.blackwell-publishing.com/products/journals/suppmat/BIJ/BIJ146/BIJ146sm.htm.

### REFERENCES

Abler WL. 1992. The serrated teeth of tyrannosaurid dinosaurs and biting structures in other animals. *Paleobiology* 18: 161–183.

**Atkins AG, Vincent JFV. 1984.** An instrumented microtome for improved histological sections and the measurement of fracture toughness. *Journal of Materials Science Letters* **3:** 310–312.

Butler PM. 1946. The evolution of carnassial dentitions in the Mammalia. Proceedings of the Zoological Society of London 116: 198–220.

Crompton AW. 1971. The origin of the tribosphenic molar. In: Kermack DM, Kermack KA, eds. *Early mammals*. London: Academic Press, 65–87.

- Crompton AW, Sita-Lumsden A. 1970. Functional significance of the therian molar pattern. *Nature* 227: 197–199.
- Cubberly WH, ed. 1989. Tool and manufacturing engineers handbook. Dearborn, MI: Society of Manufacturing Engineers.
- Evans AR. 2000. Applications of confocal microscopy to functional morphology: the effect of diet and wear on tooth sharpness and function in two microchiropterans *Chalinolobus gouldii* and *C. morio*. Abstracts of the 9th Australasian Bat Conference, Tocal, Australia, 25–28 April 2001. *Bat Research News* 41: 44.
- **Evans AR. in press.** Quantifying the relationship between form and function and the geometry of the wear process in bat molars. In: Akbar Z, McCracken GF, Kunz TH, eds. Functional and evolutionary ecology of bats: Proceedings of the 12th International Bat Research Conference. New York: Oxford University Press.
- Evans AR, Harper IS, Sanson GD. 2001. Confocal imaging, visualization and 3-D surface measurement of small mammalian teeth. *Journal of Microscopy* 204: 108–118.
- **Evans AR, Sanson GD. 1998.** The effect of tooth shape on the breakdown of insects. *Journal of Zoology* **246:** 391–400.
- Frazzetta TH. 1988. The mechanics of cutting and the form of shark teeth (Chondrichthyes, Elasmobranchii). Zoomorphology 108: 93–107.
- Freeman PW. 1979. Specialized insectivory: beetle-eating and moth-eating molossid bats. *Journal of Mammalogy* **60:** 467–479
- Freeman PW. 1981. A multivariate study of the family Molossidae (Mammalia, Chiroptera): morphology, ecology, evolution. Fieldiana Zoology 7: 1–173.
- Freeman PW. 1992. Canine teeth of bats (Microchiroptera): size, shape and role in crack propagation. Biological Journal of the Linnean Society 45: 97–115.
- Freeman PW, Weins WN. 1997. Puncturing ability of bat canine teeth: the tip. In: Yates TL, Gannon WL, Wilson DE, eds. *Life among the Muses: Papers in honor of James S Findley*. Albuquerque, NM: The Museum of Southwestern Biology, 225–232.
- **Gould SJ. 1989.** A developmental constraint in *Cerion*, with comments on the definition and interpretation of constraint in evolution. *Evolution* **43:** 516–539.
- **Gould SJ, Lewontin RC. 1979.** The spandrels of San Marco and the Panglossian paradigm: a critique of the adaptationist programme. *Proceedings of the Royal Society of London, Series B* **205:** 581–598.
- Knowles JR, Albery WJ. 1977. Perfection in enzyme catalysis: the energetics of triosephosphate isomerase. Accounts of Chemical Research 10: 105–111.
- **Lessa EP, Stein BR. 1992.** Morphological constraints in the digging apparatus of pocket gophers (Mammalia: Geomyidae). *Biological Journal of the Linnean Society* **47:** 439–453.
- Lucas PW. 1979. The dental-dietary adaptations of mammals. Neues Jahrbuch für Geologie und Paläontologie, Monatshefte 1979: 486–512.
- Lucas PW. 1982. Basic principles of tooth design. In: Kurtén B, ed. Teeth: form, function and evolution. New York: Columbia University Press, 154–162.

- Lucas PW, Luke DA. 1983. Methods for analysing the breakdown of food in human mastication. Archives of Oral Biology 28: 813–819.
- **Lucas PW, Luke DA. 1984.** Chewing it over: basic principles of food breakdown. In: Chivers DJ, Wood BA, Bilsborough A, eds. *Food acquisition and processing in primates*. New York: Plenum Press, 283–301.
- Maynard Smith J, Burian R, Kauffman S, Alberch P, Campbell J, Goodwin B, Lande R, Raup D, Wolpert L. 1985. Developmental constraints and evolution. *Quarterly Review of Biology* 60: 265–287.
- Mellett JS. 1981. Mammalian carnassial function and the 'Every effect'. Journal of Mammalogy 62: 164-166.
- Mills JRE. 1966. The functional occlusion of the teeth of Insectivora. Journal of the Linnean Society (Zoology) 46: 1–25.
- Nee JG. 1998. Fundamentals of tool design. Dearborn, MI: Society of Manufacturing Engineers.
- **Osborn JW, Lumsden AGS. 1978.** An alternative to 'thegosis' and a re-examination of the ways in which mammalian molars work. *Neues Jahrbuch für Geologie und Paläontologie Abhandlungen* **156:** 371–392.
- Ostwald PF, Muñoz J. 1997. Manufacturing processes and systems. New York: John Wiley & Sons.
- Pigliucci M, Kaplan J. 2000. The fall and rise of Dr Pangloss: adaptationism and the *Spandrels* paper 20 years later. *Trends in Ecology and Evolution* 15: 66-70.
- Pollack HW. 1976. Tool design. Reston, VA: Reston Publishing Co., Inc.
- **Popowics TE, Fortelius M. 1997.** On the cutting edge: tooth blade sharpness in herbivorous and faunivorous mammals. *Annales Zoologici Fennici* **34:** 73–88.
- Popowics TE, Rensberger JM, Herring SW. 2001. The fracture behaviour of human and pig molar cusps. *Archives of Oral Biology* **46**: 1–12.
- Rensberger JM. 1973. An occlusal model for mastication and dental wear in herbivorous mammals. *Journal of Paleontology* 47: 515–528.
- Rensberger JM. 1995. Determination of stresses in mammalian dental enamel and their relevance to the interpretation of feeding behaviours in extinct taxa. In: Thomason JJ, ed. Functional morphology in vertebrate paleontology. Cambridge: Cambridge University Press, 151–172.
- Sanson GD. 1980. The morphology and occlusion of the molariform cheek teeth in some Macropodinae (Marsupialia: Macropodidae). Australian Journal of Zoology 28: 341–365.
- Savage RJG. 1977. Evolution in carnivorous mammals. Palaeontology 20: 237–271.
- Seligsohn D. 1977. Analysis of species-specific molar adaptations in strepsirhine primates. In: Szalay FS, ed. *Contributions to primatology*, Vol. 11. Basel: S. Karger.
- Sigogneau-Russell D, Hooker JJ, Ensom PC. 2001. The oldest tribosphenic mammal from Laurasia (Purbeck Limestone Group, Berriasian, Cretaceous, UK) and its bearing on the 'dual origin' of Tribosphenida. Comptes Rendus de L'Academie des Sciences, Serie II, Sciences de la Terre et des Planètes 333: 141–147.
- Silva M, Downing JA. 1995. CRC handbook of mammalian body masses. Boca Raton, LA: CRC Press.

- Spears IR, Crompton RH. 1996. The mechanical significance of the occlusal geometry of great ape molars in food breakdown. *Journal of Human Evolution* 31: 517–535.
- **Spears IR, Macho GA. 1998.** Biomechanical behaviour of modern human molars: implications for interpreting the fossil record. *American Journal of Physical Anthropology* **106**: 467–482.
- Stevens PS. 1974. Patterns in nature. Boston, MA: Atlantic Monthly Press.
- Strait SG, Vincent JFV. 1998. Primate faunivores: physical properties of prey items. *International Journal of Primatol*ogy 19: 867–878.
- **Thompson D'AW. 1942.** On growth and form. Cambridge: Cambridge University Press.
- Van Valen L. 1966. Deltatheridia, a new order of mammals.

  Bulletin of the American Museum of Natural History 132: 1–
  126
- Van Valkenburgh B. 1996. Feeding behavior in free-ranging large African carnivores. *Journal of Mammalogy* 77: 240–254.
- Worley M, Sanson G. 2000. The effect of tooth wear on grass fracture in grazing kangaroos. In: Spatz H-C, Speck T, eds. *Proceedings of the Plant Biomechanics Meeting*. Freiburg-Badenweiler: Georg Thieme, 583–589.

### APPENDICES

These appendices contain instructions for generating the three-dimensional models of two ideal forms derived in this paper. Each file includes the 3-D coordinates for each corner of the shape (under the 'point' command) and the corners used to construct each face of the shape ('coordIndex'). The vectors of movement of the models are also given under the 'keyValue' of the 'PositionInterpolator' command. The code is entered in a simple text file with a .wrl extension. The file can be viewed using a VRML browser such as CosmoPlayer 2.1 for Windows (Computer Associates International, Inc., USA), available from http://www.ca.com/cosmo/. VRML browsers for Macintosh include Cortona VRML Client 1.1 (http:// www.parallelgraphics.com/products/cortonamac/) WorldView 2.0 (http://www.tucows.com/). CosmoPlayer and Cortona are plug-ins for web browsers (e.g. Netscape or Internet Explorer). Further instructions for viewing VRML files are given in Evans et al. (2001) and the Supplementary Material. VRML files for all models illustrated in this paper are available from A. Evans and in the Supplementary Material.

### APPENDIX 1

VRML code for single-bladed tool with serial arrangement and lateral movement, as shown in Figure 4i.

```
# VRML V2.0 utf8
# VRML model of single-bladed tool
# with serial arrangement and lateral movement
#
# Alistair Evans & Gordon Sanson, 2002,
# Monash University
```

```
# alistair.evans@sci.monash.edu.au
WorldInfo {}
NavigationInfo {
 type ["EXAMINE", "WALK"] }
Background { skyColor 1 1 1 }
Transform {
translation 14 0-10
 rotation 0 1 0 4
children [
  DirectionalLight {
   direction 0 0 1
   ambientIntensity 1 }] }
Viewpoint {
 description "View A"
 position 2.32 2.26 -2.39
orientation -0.07 0.97 0.23 2.51 }
Viewpoint {
description "View B"
position -2.87 \ 2.39 \ -2.85
orientation 0.08 0.98 0.18 3.95 }
Viewpoint {
description "View C"
position 0.33 1.31 5.55
 orientation 0.98 0.20 0.02 6.09 }
Transform {
children [
  DEF LowerTool Shape {
   geometry IndexedFaceSet {
    solid FALSE
    coordIndex [
     0, 1, 2, 3, -1,
     0, 1, 5, 4, -1,
     1, 2, 6, 9, 5, -1,
     2, 3, 7, 6, -1,
     0, 8, 4, -1,
     3, 7, 8, -1,
     4, 5, 9, 8, -1,
     6, 7, 8, 9, -1
    coord Coordinate {
     point [
      0\ 0\ 0,
      100.
      101,
      0 0 1,
      0.40,
      0.8\ 1\ 0,
      0.8 1 1,
      0 0.4 1.
      0 0 0.5,
      1 0.6 0.5] } }
   appearance DEF Appear Appearance {
    material Material {
     diffuseColor 1 1 1 } } ] }
Transform {
translation 0 0 1
children [USE LowerTool] }
DEF TopTrans Transform {
 translation 1.68 1.84 0
rotation 0 0 1 3.14159
children [
```

```
Transform {
                                                            WorldInfo {}
   rotation 0 1 0 0
                                                            NavigationInfo {
   children [
                                                             type ["EXAMINE", "WALK"] }
    DEF UpperTool Shape {
                                                            Background { skyColor 1 1 1 }
     geometry IndexedFaceSet {
                                                            Transform {
      solid FALSE
                                                             translation 14 0 -10
      coordIndex [
                                                             rotation 0 1 0 4
       0, 1, 2, 3, -1,
                                                             children [
       0, 1, 5, 4, -1,
                                                            DirectionalLight {
       1, 2, 6, 9, 5, -1,
                                                               direction 0 0 1
       2, 3, 7, 6, -1,
                                                               ambientIntensity 1 } ] }
       0, 8, 4, -1,
                                                            Viewpoint {
       3, 7, 8, -1,
                                                             description "View A"
       4, 5, 9, 8, -1,
                                                             position 5.02 2.99 -3.84
       6, 7, 8, 9, -1
                                                             orientation -0.07 0.99 0.15 2.32 }
      coord Coordinate {
                                                            Viewpoint {
       point [
                                                             description "View B"
        0\ 0\ 0,
                                                             position -0.88 2.65 -5.27
        1 0 0,
                                                             orientation 0 1 0.10 3.30 }
        1 0 1,
                                                            Viewpoint {
        0 0 1,
                                                             description "View C"
        0 0.4 0.
                                                             position -5.48 1.34 -0.73
        0.8 \, 1 \, 0.
                                                             orientation 0.02 1 0.03 4.52 }
        0.8 1 1,
        0 0.4 1,
                                                            Transform {
        0 0 0.5.
                                                             children [
        1 0.6 0.5]}}
                                                              DEF Proto1 Shape {
     appearance USE Appear } ] }
                                                               geometry IndexedFaceSet {
   Transform {
                                                                solid FALSE
    translation 0 0 1
                                                                coordIndex [
    rotation 0 1 0 0
                                                                 0, 1, 2, -1,
    children [USE UpperTool] } ] }
                                                                 0, 1, 4, 8, 3, -1,
                                                                 0, 2, 10, 6, 3, -1,
DEF TS TimeSensor {
                                                                 1, 2, 10, 7, 4, -1,
 loop TRUE
                                                                 5, 6, 10, -1,
 cycleInterval 4 }
                                                                 5, 7, 10, -1,
                                                                 5, 6, 7, -1,
DEF TopMovePI PositionInterpolator {
                                                                 6, 7, 9, -1,
keyValue [
                                                                 3, 6, 9, 8, -1,
   1.56 2.08 0,
                                                                 4, 7, 9, 8, -1
   2.04 1.12 0,
                                                                coord Coordinate {
   1.56 2.08 0]
                                                                 point [
key [0, 0.5, 1]}
                                                                  0.1 0 0.
                                                                  0.900,
                                                                  0.5 0 0.693,
ROUTE TopMovePI.value_changed
                                       TO
                                             TopTrans.
                                                                  0 1.2 0,
translation
                                                                  1 1.2 0,
ROUTE
          TS.fraction changed
                                       TopMovePI.set
                                                                  0.5 2 0.433,
fraction
                                                                  0.25 1.3 0.433,
                                                                  0.75 1.3 0.433,
                                                                  0.5 \ 0.8 \ 0,
                                                                  0.5054 1.1114 0.3163,
                     APPENDIX 2
                                                                  0.5\ 1.3\ 0.866]\}
VRML code for double-bladed tool with serial
                                                               appearance DEF Appear Appearance {
arrangement and lateral movement, as shown in
                                                                material Material {
Figure 4ii.
                                                                  diffuseColor 1 1 1 } } } } }
#VRML V2.0 utf8
                                                            DEF Transform Transform {
# VRML model of double-bladed tool
                                                             translation -1 0 0
# with serial arrangement and lateral movement
                                                             children [USE Proto1] }
# Alistair Evans & Gordon Sanson, 2002,
                                                            DEF TS TimeSensor {
# Monash University
                                                             loop TRUE
# alistair.evans@sci.monash.edu.au
                                                             cycleInterval 4 }
```

DEF TopTrans Transform {
 translation 0.5 3.08 0.519
 rotation 0 1 0 0
 children [
 DEF Transform\_2 Transform {
 rotation 1 0 0 3.141
 children [USE Proto1] }
 DEF Transform\_3 Transform {
 translation -1 0 0
 rotation 1 0 0 3.141
 children [USE Proto1] } ]

DEF TopMovePI PositionInterpolator {
 keyValue [
 0.5 3.26 0.39,
 0.5 2.54 0.909,
 0.5 3.26 0.39]
 key [0, 0.5, 1] }

ROUTE TS.fraction\_changed TO TopMovePI.set\_fraction
ROUTE TopMovePI.value\_changed TO TopTrans.
translation

# **Chapter 2 Addendum**

Plate 1 shows a full-colour reconstruction of the protoconoid with serial arrangement and lateral movement (Fig. 2.4ii), and a full-colour version of Fig. 2.5.

Appendix 1 contains VRML files for the major models constructed in Chapter 2.

The Electronic Appendix (see enclosed CD-ROM) contains VRML files illustrating colour reconstructions and animated occlusion for all models constructed in Chapter 2.

Appendix 3 contains a commentary on Chapter 2 published in Nature 422, 128.

Note: in the rest of this thesis, Tables 1-2 and Figures 1-6 of Chapter 2 are referred to as Tables 2.1-2.2 and Figs 2.1-2.6 respectively.

# Chapter 3. Spatial and Functional Modelling of Carnivore and Insectivore Molariform Teeth

# 3.1. Introduction

Teeth are attractive as study subjects for many and varied reasons, including their substantial contribution to the vertebrate fossil record and their intriguing developmental processes (Butler 1981; Fortelius 1985; Jernvall 1995). Another notable reason is the four-dimensional puzzles they present. Teeth have complex three-dimensional geometries that interlock with their occluding counterparts in a temporal sequence. Perhaps more importantly, the purpose of the geometry of the dentition is to perform several functions, the most significant of which is the efficient break-down of food (Lucas 1979).

Various aspects of tooth geometry and occlusion have been investigated including tribosphenic-like (Crompton and Sita-Lumsden 1970; Crompton *et al.* 1994; Kay and Hiiemae 1974), herbivore (Fortelius 1985; Greaves 1972) and carnivore molariform teeth (Bryant and Russell 1995; Mellett 1981, 1985). Certain geometric principles were established in these papers, but several of the predictions appear to have remained untested. Also, there does not seem to be a clear understanding of all geometric aspects of occlusion in many tooth forms. No comprehensive analysis of these principles has been carried out, nor any investigation of their implications. For example, we would like to know what dental shapes are feasible given certain geometric constraints; i.e. what are the limits to possible occlusal morphologies?

The tooth form of occluding 'primitive' therian teeth has been considered as a set of 'reversed triangles' (Fig. 3.1a; Crompton and Sita-Lumsden 1970; Crompton *et al.* 1994). This notion formed part of the 'trituberculy' theory of dental evolution (Gregory 1916; Osborn 1888, 1897), in which it was hypothesised that the ancestral dental shape of therians was of this form. However, many features of the geometry of occlusion and the full ramifications of the 'reversed triangle' design appear not to have been evaluated. Crompton and Sita-Lumsden (1970) modelled the two-bladed basic therian molar pattern as reversed triangles (each cusp is basically triangular and has two blades, the diagonal and transverse shearing edges, leading down from it; Fig. 3.1b). They concluded that it would be impossible for both of the blades on such a molar to be two-dimensional curves. If so, this would greatly limit the possible tooth and crest shapes, but the hypothesis has not been tested.

In order to deal with the complexity and diversity of mammalian tooth forms, it is necessary to elucidate some basic geometric principles of teeth. I suggest that there are two main competing geometric factors that influence dental morphology: the geometry of occlusion (ensuring proper alignment of tooth features such as crests) and the geometry of function (relating to shape that is advantageous for food fracture, thereby minimising force or energy for a tooth to fracture food). These can be considered separately by examining the features that influence occlusal geometry and those that relate to function. However, the ultimate goal is to understand how these interact in order to limit the forms that can be expressed, a minimum set of which actually occur in animals.

This paper will first explain the basic geometric principles of teeth, which have been expounded to some extent in the literature. We will investigate the important geometrical relations between occluding tooth components through the generation of hypotheses in the form of geometric models of teeth, regarding the form and manner of tooth function. Using these geometric principles, as well as aspects of shape that affect function, models of several tooth forms will be constructed, principally carnivore and insectivore molars and premolars. Mathematical geometry (e.g. planes and vectors) will be used for determination of certain occlusal events, and complete three-dimensional models of the teeth will illustrate occlusion of the entire tooth form. In this way, the influence of the different geometric factors on each other, and how they interact to create a final functional tooth form, can be examined.

The objective is to create models in which a) occlusion between upper and lower models occurs correctly (according to geometry outlined below); b) advantageous functional shape parameters are adhered to; c) the overall morphology of models is as similar as possible to real teeth; and d) the function of real teeth is emulated. This extends the work from the ideal shapes derived in Chapter 2 to more realistic approximations of mammalian teeth.

While testing the models will increase our understanding of the function and geometry of basic tooth patterns, it will also allow us to investigate the influence of particular components on the overall form and function of the upper and lower teeth. Any differences between models and real teeth may provide information about constraints on mammalian teeth (Chapter 2) and factors that may limit tooth design.

A major impediment to investigations of tooth geometry has been the difficulty in examining three-dimensional shapes and modes of occlusion, where previous models were often two-dimensional representations of three-dimensional models. This is explained in detail in Chapter 4. The use of three-dimensional computer reconstruction techniques

assists the investigation of these geometrical problems. Hypotheses about tooth geometry from earlier analyses will be examined by building 3-D reconstructions of the previous models.

# 3.1.1. Occlusal Geometry

Geometry of two simple blades occluding with each other will be considered first. Tooth occlusion will occur along a linear vector (the occlusal vector). The simplest case is for a blade to lie in a plane (and is therefore a two-dimensional curve); for two blades to align correctly, they must lie in the same plane in space (Fig. 3.2a), and the occlusal vector will be perpendicular to the normal of the plane (i.e. it will lie in the plane). The plane can be vertical (Fig. 3.2a) or at an angle to the vertical (Fig. 3.2b). The latter is the case for the model of carnassial teeth discussed by Mellett (1981), and both were used in the single-bladed models of Chapter 2.

An important derivation from this is the two-plane mode of occlusion (Crompton *et al.* 1994; Greaves 1972; Kay and Hiiemae 1974; Chapter 2). In this case there are two blades on each tool (Fig. 3.3a); each blade lies in a plane, and the occlusal vector is parallel to the intersection of the two planes (Fig. 3.3b,c). This can be extended to show how the two-plane mode would work with two phases of occlusion (fig. 3 in Fortelius 1985). The occlusal vector of teeth working in the two-plane mode of occlusion can be calculated from isolated teeth (Kay and Hiiemae 1974).

The more general case is that the shape of the two-dimensional projection along the occlusal vector is the same for two occluding blades or teeth. This includes multiple planes, curves, and a combination of the two with planes separated by curved joins (Fig. 3.4).

# 3.2. Methods

Models were designed to emulate the shape, movement and function of mammalian teeth. Specimens of several examples of the general tooth forms were examined. The general shape of upper and lower tooth components and manner of occlusion for each tooth form are described below. In some cases additional minor cusps and cingula (small enamel ledges or rims that surround part of the tooth) are also present, which often vary greatly between species, but to simplify the modelling process these are not considered here. The object is to model the generic characteristics of the tooth forms.

**Carnassials**: molars or premolars with a single long crest with a large, symmetrical V-shaped notch (Fig. 2.5c, p. 29; Plate 1), often with a more pronounced central notch (carnassial notch) which aids in dividing tough food at the end of a stroke (Abler 1992;

Van Valen 1969). The upper and lower crests are relatively similar in shape (Bryant and Russell 1995; Butler 1946; Mellett 1981, 1985; Van Valen 1966; Van Valkenburgh 1991). They occur in carnivorans (Carnivora), fossil creodonts (Hyaenodontia), and marsupials (e.g. Thylacoleonidae).

**Insectivore premolars**: the teeth have a single long notched crest, the ends of which are unequal in height, creating an asymmetrical notch. They may occlude with the crests of other premolars or of molars, and are partially molariform (Butler 1937, 1939; Freeman 1981b; Mills 1966; Slaughter 1970). The premolars modelled here are more akin to upper premolars that occlude with the first lower molar. They are found in insectivorans and microchiropterans.

**Zalambdodont molars**: the teeth comprise a single large cusp with two crests leading from it, forming a V-shaped 'ectoloph' viewed from above (Fig. 2.5e, p. 29; Plate 1). One crest of the ectoloph is often approximately transverse to the tooth row, and the crests of the upper and lower molars are generally similar (Butler 1937, 1941; McDowell 1958; Mills 1966). This tooth form is found in solenodons (Solenodontidae), tenrecs (Tenrecidae) and golden moles (Chrysochloridae). There is a basic topographic similarity to symmetrodonts (e.g. *Kuehnotherium*), pantotheres (e.g. *Amphitherium*, *Peramus*), *Zalambdalestes*, *Palaeoryctes* and the marsupials *Necrolestes* and *Notoryctes* (Carroll 1988).

Dilambdodont molars: the V-shaped ectoloph of the zalambdodont has been essentially duplicated on both the upper and lower molars (Butler 1941; Mills 1966). On the upper molar, the crests leading from these two large cusps form a W-shaped ectoloph, where all of the crests reach the buccal edge of the tooth (Fig. 2.5e, p. 29; Plate 1). A third major cusp is positioned laterally, dorsally and anteriorly on the upper tooth, and is often associated with one or two additional smaller cusps. On the lower tooth, the posterior cusp is lower than the anterior one and forms a basin which occludes with the upper lateral cusp (Fig. 2.5e, p. 29; Plate 1). During occlusion, the leading face of the lower posterior cusp meets the leading face of the upper lateral cusp (Kallen and Gans 1972; Mills 1966). These are found in shrews (Soricidae), moles (Talpidae), tree shrews (Tupaiidae), microbats (Microchiroptera), and extinct groups such as nyctitheriids (Carroll 1988), Palaeotherium, brontotheres. chalicotheres (Perissodactyla), Anoplotherium (Artiodactyla) Pantolambda (Pantodonta) (Butler 1982).

**Tribosphenic molars**: the tribosphenic form is similar to the dilambdodont form in having three main cusps on the upper tooth and two on the lower. The main difference from the dilambdodont form is that the ectoloph is not W-shaped – the two centre crests of

the ectoloph (collectively called the centrocrista) do not reach the buccal edge of the tooth (Butler 1982; Crompton and Hiiemae 1970; Mills 1966). The tooth form modelled here can also be considered dilambdodont (Butler 1941, 1996) or predilambdodont (Johanson 1996; Wroe *et al.* 2000). These are found in primitive mammals such as *Aegialodon*, *Pappotherium*, *Didelphodus* (Carroll 1988), marsupials (Didelphidae), and in a reversed form in the pseudotribosphenic molars of *Shuotherium*, where the basin in the lower tooth is anterior instead of posterior (Chow and Rich 1982).

For each tooth form, the surfaces of cusps and crests (and basins when present) were modelled as polygons in three-dimensional space where the vertices of each polygon were designated by x, y, z coordinates. The lower model moves with respect to the upper model according to the 'occlusal vector', the direction of tooth movement. Occluding crests were constructed according to the geometry described above to ensure proper alignment. The tooth structures were reconstructed in Virtual Reality Modelling Language (VRML; Chapter 2), which allows animation of 3-D structures to demonstrate occlusion.

The models of single- and double-bladed tools constructed in Chapter 2 were used as starting points. These simple shapes are excellent starting points for modelling teeth because they have been explicitly derived: their shape and the reasoning behind their construction are precisely known. They also possess many similarities to real tooth structures before additional modifications are made. These models conform to eight functional parameters that have been considered *a priori* to be important in the function of tools for dividing tough foods. The functional parameters are defensible in terms of machine tool engineering and dental function. These were described in detail in Chapter 2, and are: tip and cusp sharpness for points; edge sharpness, rake, relief and approach angles, food capture and fragment clearance for blades.

The simple models may represent entire mammalian teeth, or components of the teeth, so that each model tooth is constructed from one or more duplicates of the starting models. Successive changes were made to the models in order to more closely emulate real tooth forms. All changes were documented to make clear the modifications to these shapes that were necessary. Care was taken to adhere to the eight functional criteria as much as possible with each alteration of the models.

### **3.2.1.** Models

# **Carnassials**

The model of the carnassial was based on the symmetrical single-bladed tool with a single long blade with a V-shaped notch and a latero-vertical occlusal vector (Fig. 3.2b). In

order to approach more closely the carnassial tooth shape, the rake angle of the model was increased and a 'carnassial notch' was added. It allows a greater concentration of forces due to the increased approach angle and due to the reduced amount of material between the teeth once the central notches come into contact.

# **Insectivore Premolars**

The asymmetrical single-bladed model was used as the basis for the premolars of some insectivores (Fig. 3.2c). The rake angle was increased and the size of the smaller cusp decreased.

### **Zalambdodont Molars**

The starting point for the zalambdodont molar model was the basic protoconoid structure, which is a fundamental cusp-crest structure found in many tooth forms (Chapter 2). The base of the protoconoid is an equilateral triangle, and two of the top edges form blades, each of which has a V-shaped notch (Fig. 3.3). There are three main points on the protoconoid, which occur at the end of blades, and the point at the junction of the two blades is the tallest point on the model. The lower model moves with a latero-vertical occlusal vector. The upper and lower zalambdodont molars were modelled as 'right-angled' protoconoids, where the base of the protoconoid is a right-angled triangle with one blade perpendicular to the side of the model and the other oblique (Fig. 3.3d).

### **Dilambdodont Molars**

Each of the upper and lower dilambdodont molars was modelled as two 'right-angled' protoconoids in series. A third protoconoid was added on the lateral side of the upper model, and 'en echelon shear' occurs, where a blade from the lower model sequentially occludes with two or more blades of the upper (Crompton and Sita-Lumsden 1970), between the lower model and two protoconoids in the upper model.

# **Tribosphenic Molars**

The tribosphenic molar model was based on the basic dilambdodont model, the main difference being that the centre cusp of the ectoloph does not reach the buccal edge. In addition, the crests of the centrocrista are not concave in the same manner as the dilambdodont form (Butler 1996).

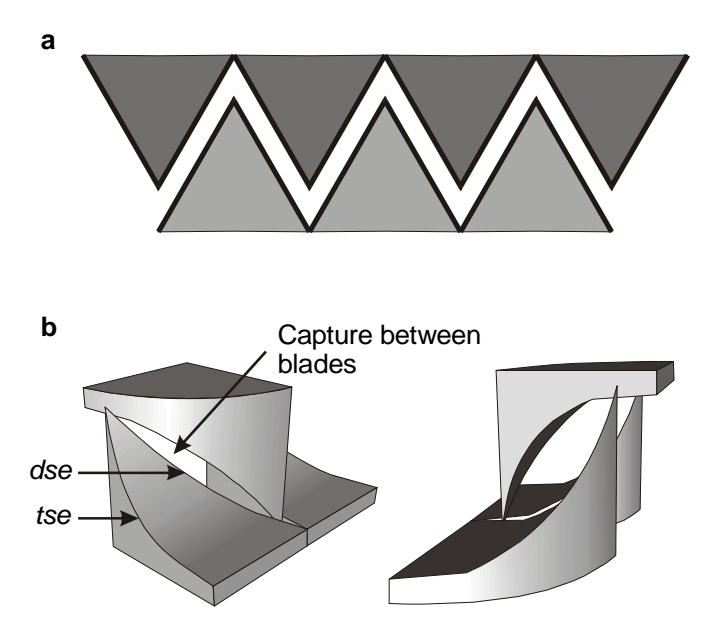
# 3.3. Results

The models of all tooth forms are shown in Fig. 3.5. The conventional dental nomenclature of these forms will be used to describe the models (Crompton 1971; Kay and Hiiemae 1974), and is illustrated in Fig. 3.7a. Appendix 2 and the Electronic Appendix

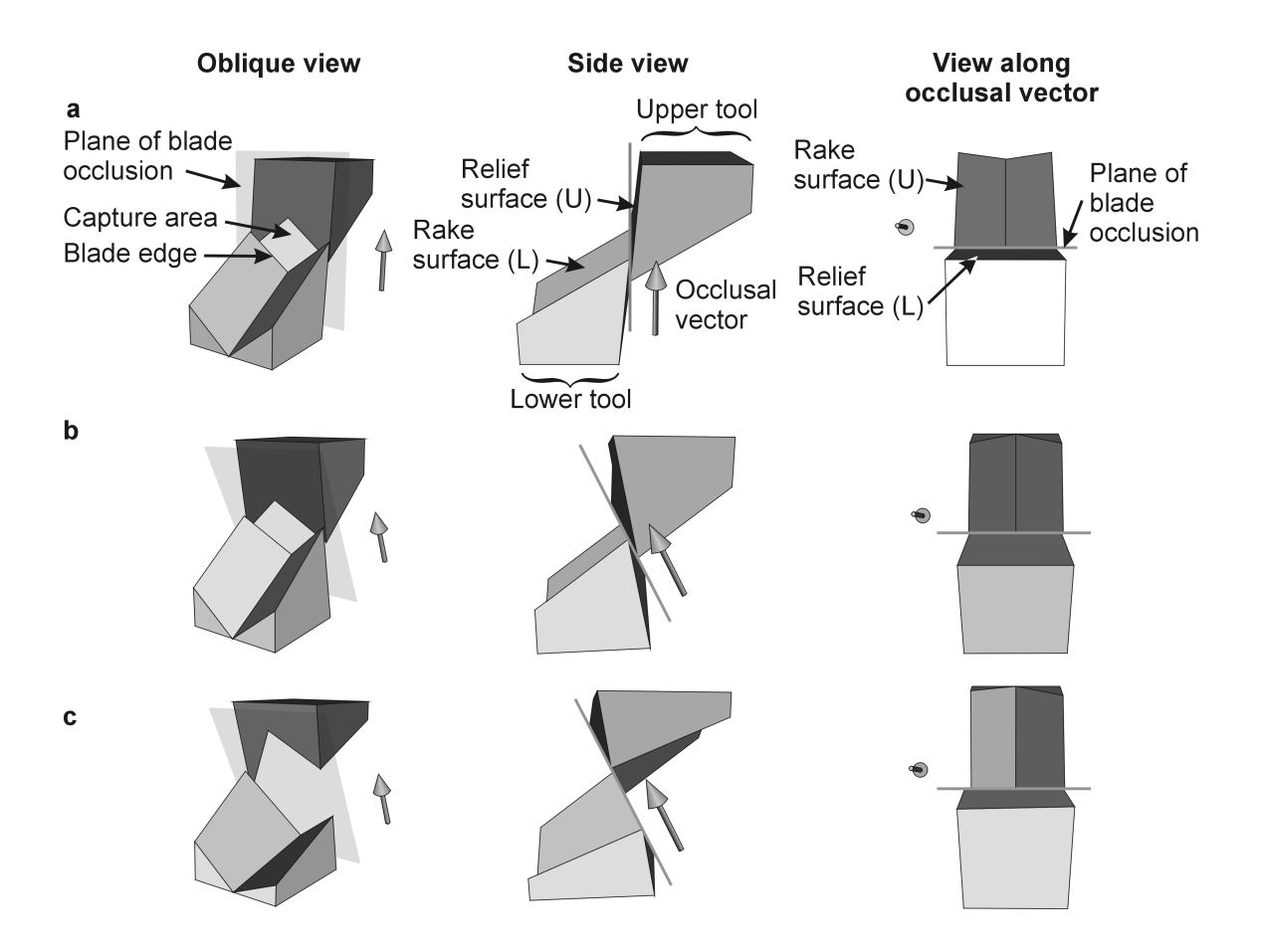
contain VRML files for all model teeth constructed in this Chapter, showing the three-dimensional shape and animated occlusion of the models.

As well as the two protoconoids in serial arrangement, the model of the upper dilambdodont tooth has a third protoconoid (with the protocone as the main cusp) in a lateral position (Fig. 3.5d). Two main functional changes result: on each tooth, two additional occluding blades and a flat 'crushing' basin are created. The crushing surfaces are the rake surfaces of the lower posterior (LPP) and the upper lateral (ULP) protoconoids. These are the talonid and the trigon basins respectively, and they meet at the end of the occlusal stroke. The posterior blade of the lower anterior protoconoid (LAP) occludes with two blades in the one stroke: with the anterior blade of the upper lateral protoconoid (UAP) and the anterior blade of the ULP. This *en echelon* shear is shown in Fig. 3.5d, where the plane of blade occlusion passes through the blades that occlude. Another blade is added to the lateral edge of the LPP (the previously non-occluding third edge) that occludes with the posterior blade of the ULP.

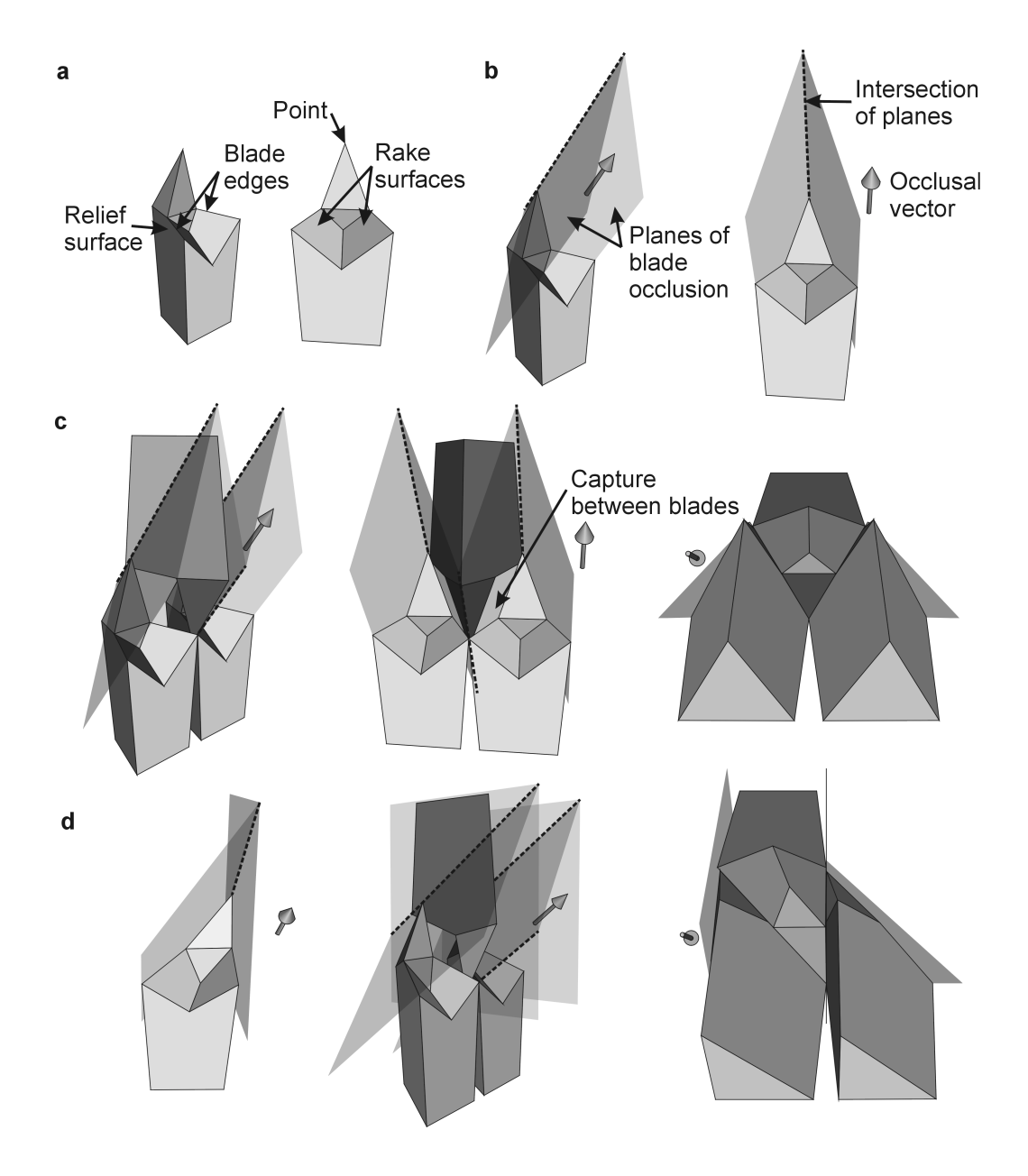
The main modification made in order to construct the tribosphenic model was the movement of the mesostyle from the buccal edge of the tooth, requiring lingual and dorsal movement of the hypoconid (Fig. 3.5e). The protoconoid structure in the upper molars is now further removed from the original shape. The full VRML files for all models constructed in this Chapter are included in Appendix 3.



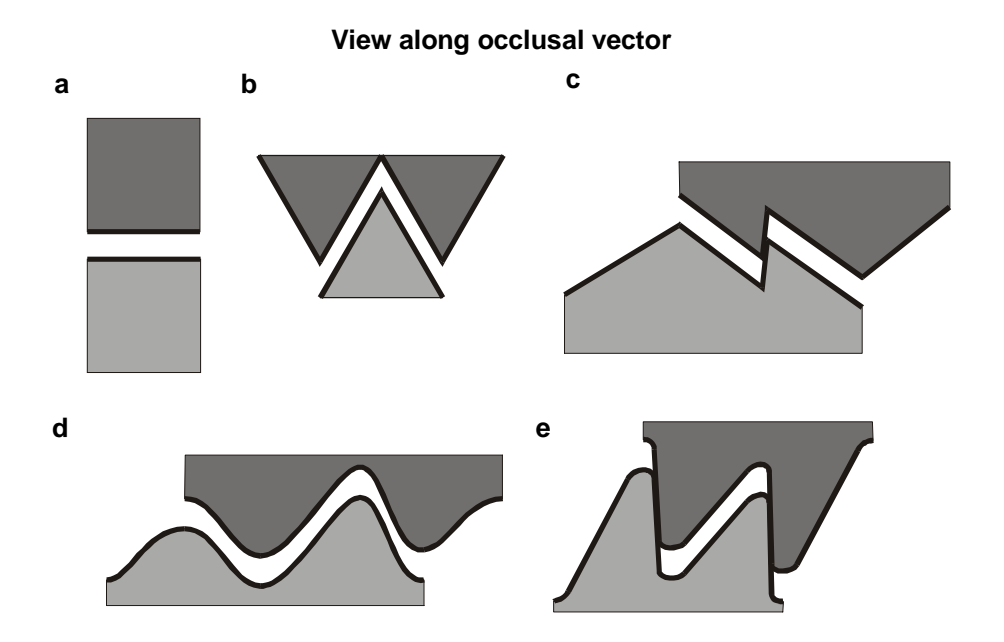
**Fig. 3.1.** a) The 'reversed triangles' model of molar occlusion, with upper (dark) and lower (light) molars in a triangular shape. b) The Crompton and Sita-Lumsden (1970) model of therian molar function; dse, diagonal shearing edge; tse, transverse shearing edge. Redrawn from Crompton and Sita-Lumsden (1970).



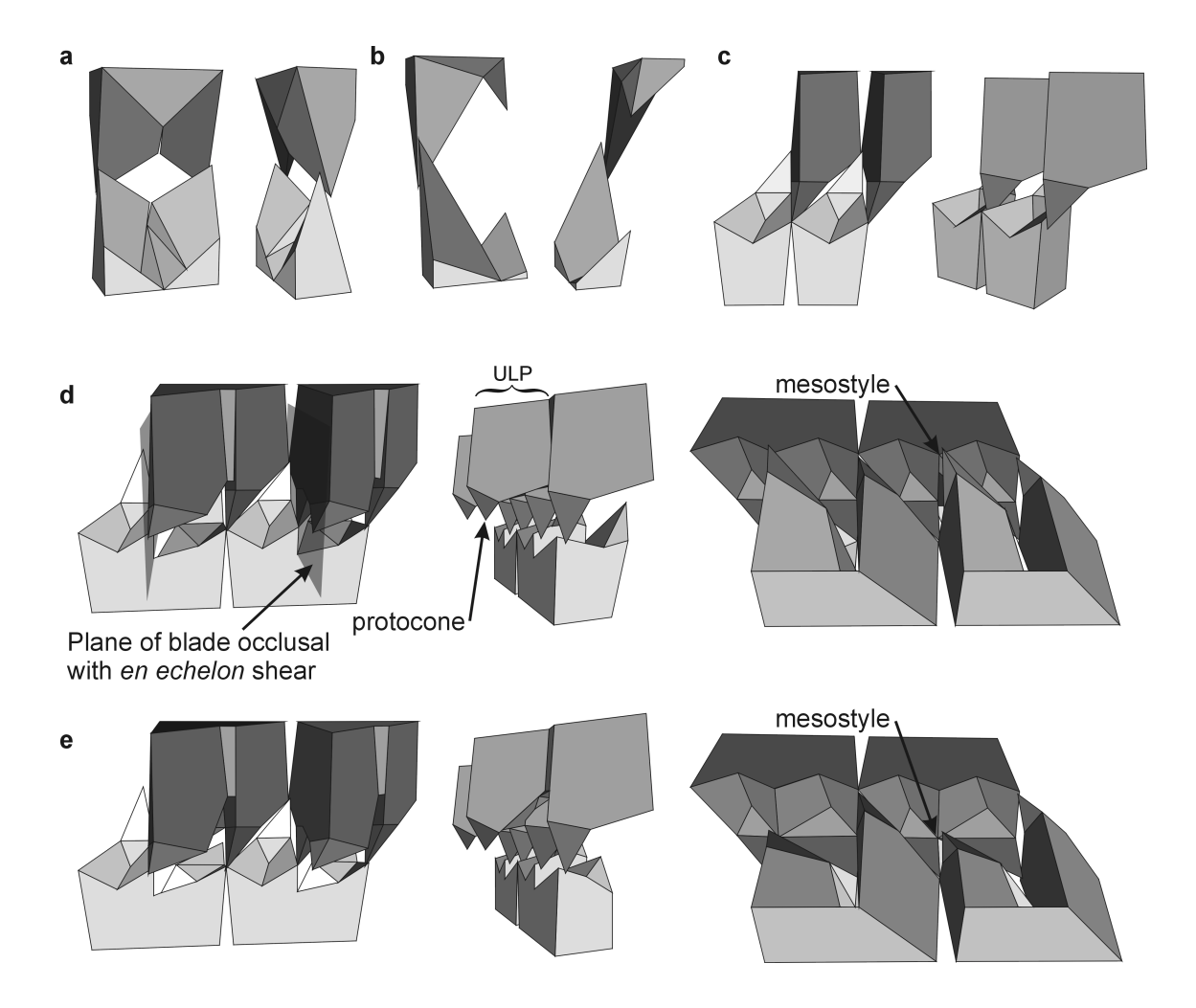
**Fig. 3.2.** Simple single-bladed models used as starting points for modelling mammalian teeth, illustrating occlusal geometrical principles: a) symmetrical with vertical movement; b) symmetrical with latero-vertical movement; c) asymmetrical with latero-vertical movement. The blade edge and rake and relief surfaces of the upper (U) and lower (L) models are indicated. The lower model moves according to the occlusal vector (solid arrow), and occluding blade edges always lie in the plane of blade occlusion (transparent grey plane). In all figures, upper model is dark, lower is light.



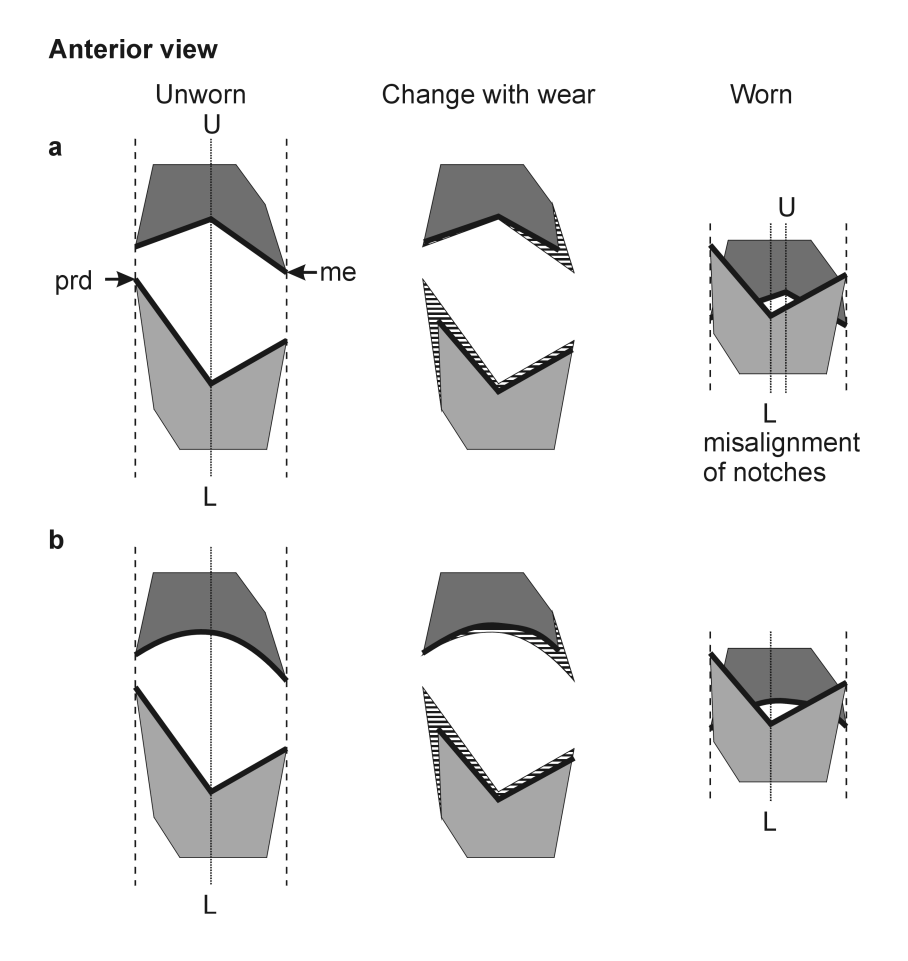
**Fig. 3.3.** Simple double-bladed models used as starting points for modelling mammalian teeth, illustrating occlusal geometrical principles: a) protoconoid with latero-vertical movement; b) showing blade planes; c) two lower and one upper protoconoid in occlusion; d) right-angled protoconoid. The intersection of planes of blade occlusion is indicated by a dashed line, which is parallel to the occlusal vector. Other conventions follow Fig. 3.2.



**Fig. 3.4.** Crest shapes that are possible for occluding upper (dark) and lower (light) teeth with blades (thick lines) when the lower moves along a linear occlusal vector. The shapes are viewed along the occlusal vector and are separated vertically on the page a small amount for clarity. a) single-bladed model; b) double-bladed model; c) planes in various orientations; d) curves; e) straight lines joined by curves where the cusps are located.

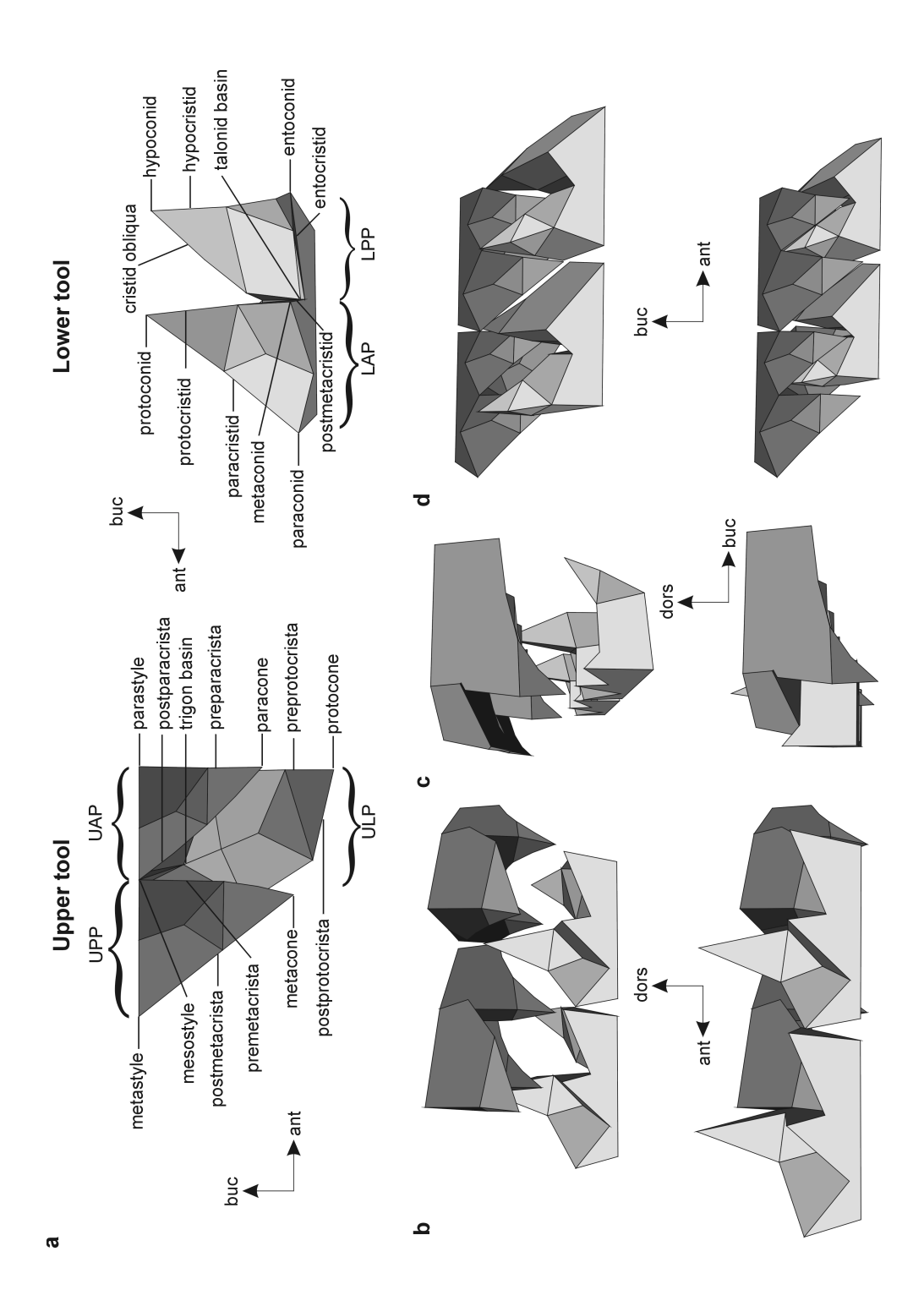


**Fig. 3.5.** Modified models of mammalian tooth forms: a) carnassial; b) insectivore premolar; c) zalambdodont; d) dilambdodont; e) tribosphenic. Planes of blade occlusion are shown in d) to illustrate *en echelon* shear. ULP, upper lateral protoconoid. The main difference in the dilambdodont and tribosphenic models is the distance of the mesostyle from the buccal edge of the model.



**Fig. 3.6.** The effect of wear and crest shape on the alignment of occluding notches. Each sequence (a and b) illustrates a particular arrangement of crests (thick lines) and notches on upper (dark) and lower (light) teeth in the unworn and worn states, and shows the change in shape after the removal of dental material by wear (horizontal hatching). a) Both the upper and lower crests are notched. Following wear, which mostly occurs on the end of the crest with the higher cusp (metacone (me) for the upper and protoconid (prd) for the lower), the notches no longer align in occlusion. However, when one of the crests is curved (b), the effects on the alignment of the notch are not as severe. Dashed lines show points at which the ends of crests occlude, dotted lines show the location of the upper (U) and lower (L) notches. Anterior view, with occlusal vector vertical.

**Fig. 3.7.** (**Opposite page**) Improved model of dilambdodont molars incorporating an anterior component to the previously dorsolingual movement, crescentic crests on the upper ectoloph crests and preprotocrista, and paracone smaller than the metacone, with consequently smaller talonid basin and shorter hypoconid. a) Nomenclature of upper and lower dilambdodont molars, and separate views of the upper and lower dilambdodont models. The centrocrista comprises the postparacrista and the premetacrista. Lingual (b), posterior (c) and buccal-occlusal (d) views of two upper and two lower model molars just after occlusion has started (top) and at centric occlusion (bottom), where the lower molar is at its dorsal maximum and the protocone is at the base of the talonid basin. ant, anterior; buc, buccal; dors, dorsal. UAP, upper anterior protoconoid; UPP, upper posterior protoconoid; ULP, upper lateral protoconoid; LAP, lower anterior protoconoid; LPP, lower posterior protoconoid.



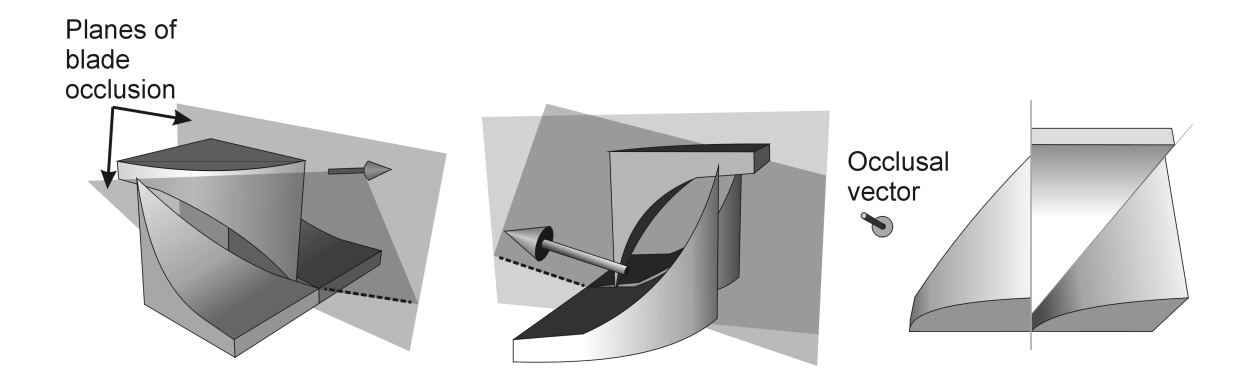


**Fig. 3.8.** Three-dimensional reconstruction of model shown in Crompton and Sita-Lumsden (1970), showing that both of the blades on the model are two-dimensional curves, as each lies in a plane.

## 3.4. Discussion

The models constructed above have significant similarities to the tooth forms on which they were modelled, and it is argued that they would function in the same manner as the original teeth due to the requirements of the geometries of occlusion and function being satisfied.

# **3.4.1.** Influence of Protocone on Tooth Shape

The models give us unprecedented ability to analyse the effect of the protocone on overall tooth shape. In effect, this identifies the changes that are required to create the dilambdodont and tribosphenic forms. In order to ensure proper functioning of the lateral protoconoid (ULP; protocone and associated crests) added to the two-protoconoid serial structure, several modifications were required:

- 1. The LPP main cusp (hypoconid) was reduced in height and/or moved buccally to prevent it colliding with the rake surface of the ULP;
- 2. Two crests were added to the lower models against which the crests of the ULP main cusp (protocone) occlude: the crest running from the posterior cusp of LAP (postmetacristid) and the crest on the exit structure of the LPP (entocristid);
- 3. The height of the anterior crest of the LPP (cristid obliqua) was reduced so that it no longer connected to the posterior cusp of the LAP (metaconid) and instead terminated near the base of the LAP main cusp (protoconid). This allowed the anterior crest of the ULP (preprotocrista) to shear against the posterior crests of the LAP (protocristid and postmetacristid);
- 4. The basin of the LPP (talonid basin) was deepened to form relief behind the new crests (postmetacristid and entocristid).

Increasing the number of blades in close proximity (e.g. through the addition of a protocone on the upper tooth) leads to modifications in the shape and function of the adjacent blades. Capture by several of the blades (e.g. cristid obliqua, postmetacristid) is reduced or removed. This is particularly true for the centrocrista crests of the upper tribosphenic molar, where food is captured by the combination of the two crests (postparacrista and premetacrista making up the centrocrista) rather than one. The rake angles of the crests associated with both the LPP (hypoconid) and the ULP (protocone) are decreased, and are therefore not as efficient. Fragment clearance from the LPP is impeded by the addition of a blade on the internal surface of the exit structure. This shows the influence of geometrical constraints on the number of blades that can be added while maintaining function of all previous and newly-added crests.

# 3.4.2. Comparisons of Models and Real Teeth

The models very closely mimic the shape and occlusion of mammalian tooth forms. However, there are a number of notable differences between each model and its corresponding tooth form. Some of these point to factors that constrain shape in mammalian teeth that are not considered in the models, but others reveal additional complexity in the function of mammalian dentitions.

### Robustness

Compared to the idealised perfect points of the model, the cusp tips of teeth are thicker and the embrasures into which they fit are wider. This is particularly true for the zalambdodont, dilambdodont and tribosphenic forms, where the cusp tips are often rounded in the antero-posterior direction. This is most probably related the requirement of increased strength at the tip of the cusps, where thicker teeth will be able to withstand greater stresses. The occluding embrasures must then be wider to accommodate the fatter cusps. Development may also constrain the tooth shapes, limiting the maximum pointedness of cusps that can be produced in ontogeny. Real teeth are often broader and rounder at the base of the cusps compared to the models, again probably related to increased strength and support.

Although the cusps and crests of dilambdodont and tribosphenic teeth do not have as high tip, cusp and edge sharpnesses as the models, they do represent an ingenious solution that maintains relatively high tip and edge sharpnesses while ensuring that proper occlusion occurs between crests and allowing additional reinforcement of the cusp. The pointed cusps of the models (Fig. 3.5d,e) would probably produce dangerously high stress concentrations that may fracture the cusp; however, rounding the entire cusp tip to strengthen it will reduce tip and edge sharpnesses. Instead, the cusp tips are rounded in the anteroposterior direction while being relatively flat on the buccal face. Such cusps have high tip and edge sharpness compared to a rounded cusp but allow occlusion between crests and would resist fracture to a greater extent.

# Cusp occlusion relief

In dilambdodont and tribosphenic molars, there is often significant relief behind the points on one tooth where another cusp occludes with it, which is termed cusp occlusion relief (described in further detail in Chapter 5). Relief is found behind occlusion points of cusps such as the protoconid (relief behind the parastyle/metastyle), hypoconid (mesostyle), protocone (postmetacristid/ entocristid junction lingual to the talonid basin) and to some extent the metacone (posterior cingulum on lower molar) and paracone (at the

most anterior point of the cristid obliqua). Only a small amount of cusp occlusion relief occurs in the models, usually due to the creation of relief behind the crests.

# Sizes of paracone and metacone

The upper models of dilambdodont and tribosphenic molars were constructed with the paracone and metacone the same size. In tribosphenic and more particularly dilambdodont teeth, the paracone is often smaller than the metacone, with the paracone closer to the buccal edge of the tooth and shorter in height. The size of the paracone affects the geometric relations between the upper and lower molars, particularly the width of the talonid basin.

When the hypoconid is lowered to accommodate the protocone in the dilambdodont model, it must also be moved laterally so that it still occludes with the mesostyle (due to the lateral movement of the teeth). If the metacone and paracone are the same size, the hypoconid must be moved a large distance laterally if the height is greatly decreased, resulting in a talonid basin that is substantially wider than the anterior (trigonid) basin. In the dilambdodont and tribosphenic models, the height of the hypoconid has not been substantially reduced. Moving the paracone closer to the buccal edge of the tooth, in effect reducing the size of the paracone, reduces the distance from the mesostyle to the paracone, so that the hypoconid does not need to be moved as far laterally for occlusion to occur.

# Shape of capture structure

The blades of the models constructed above have notched, i.e. V-shaped, capture structures. The few models of cusps or teeth that have been made previously have often implicitly or explicitly modelled the capture structure as a curved, 'crescentic' or U-shaped edge (Crompton and Sita-Lumsden 1970; Crompton *et al.* 1994; Lucas and Teaford 1994; Mellett 1981; Stern *et al.* 1989). It seems to have been assumed that a curved edge must function better because it occurs in nature. However, a V-shaped capture structure would be more efficient than a U-shaped one, as it would concentrate forces to a greater extent, particularly at the end of the stroke. An equal length of blade will shear past the opposing blade for each given distance the blades move closer together; in contrast, the U will result in a larger amount of crest coming together at the end of the stroke, reducing pressure at what is probably the most crucial point in the entire stroke. A notch will also have a higher approach angle at the end of the stroke.

The concavity in carnassial teeth is pointed (and further emphasised as the carnassial notch), as is the case for many crests in lower dilambdodont and tribosphenic teeth (e.g. microbats *Rhinolophus blasii* and *Plecotus townsendii*; marsupial *Didelphis* 

*marsupialis*). However, upper dilambdodont and tribosphenic teeth usually do not have notched ectoloph crests. This may be because a pointed notch may increase stress concentrations in the tooth at the tip of the notch, with a subsequent rise in the risk of the tooth fracturing at that point. An alternative is that it is related to the depth of tooth underneath the ectoloph crests, such that a deep, V-shaped notch would not fit.

# Effects of wear on occlusion

An important difference between real teeth and the models is that the former must accommodate wear. This becomes important when we consider how tooth shape and occlusion may be affected by wear. The function of notched crests will be optimal when the notches of opposing crests align in occlusion (Fig. 3.6a). If notches do not align, such as when their relative positions along the crests alter after wear, there may be regions in which the approach angles of opposing crests are close to parallel and the effectiveness of point cutting is reduced. This will greatly decrease the effectiveness of these crests at the end of the cutting stroke. A compromise would be to maximise efficiency in one occluding crest by making it notched, and minimise potential problems of misalignment by the opposing crest being curved (Fig. 3.6b).

# **Improvements to Models**

To illustrate how some of the differences between the models and real teeth influence the form of the models, a second model of the dilambdodont form was constructed (Fig. 3.7; Plate 2). This model incorporates an anterior component to the dorsolingual occlusal vector, as is the case with *in vivo* teeth; the transverse crest of the protoconoids is no longer directly perpendicular to the edge of the tooth; the paracone is smaller than the metacone, with a consequently smaller talonid basin and shorter hypoconid; additional cusp occlusion relief is added behind some points; and the upper ectoloph crests and preprotocrista are crescentic.

Additional modifications to the model could be introduced, such as movement of the lower teeth in an arc-like fashion, simulating the closing of a jaw, rather than the linear trajectory that was used. This would affect the size and orientation of the tooth components along the tooth row, depending on the distance from the condyle and its height above the tooth row, but is not likely to change the overall shape of the models to a great extent.

## 3.4.3. Autocclusion

A significant feature of teeth that must be considered is the means by which tooth components of upper and lower teeth are aligned and how their correct relationships are maintained. For instance, does the alignment of crests require additional dental or non-dental structures (such as guiding cusps or ridges) that do not function in food breakdown?

Mellett (1985) introduced the term 'autocclusal' to refer to occlusal alignment that is controlled by morphology rather than neurological processes. It was first applied in reference to the use of canines to aid in the alignment of the postcanine teeth, but we can extend this to include features that ensure proper alignment of teeth on the same tooth and other teeth in the tooth row. Some features of the autocclusal mechanism are obvious, such as the spacing of cusps in a tooth row to align with the corresponding embrasures in the opposing row, which can act in the same manner as the canines directing the movement of the lower jaw to ensure alignment of molars. Of greater interest is the maintenance of correct spatial relationships between other tooth features such as relief surfaces.

A simple consideration of blade occlusion may lead one to the conclusion that in order for blades to align there must be substantial contact between the relief (trailing) surfaces of two occluding crests, which would be indicative of no relief behind crests. Most previous models of teeth crests have displayed a lack of relief (Crompton and Sita-Lumsden 1970; Crompton et al. 1994; Lucas and Teaford 1994; Stern et al. 1989). For instance, it appears that Crompton et al. (1994) assume contact of the flat opposing relief surfaces, and therefore the absence of relief, is required for alignment of triangular cusps. However, crest relief is present in a large number of tooth forms (Chapters 5 and 7; unpublished data). Contrary to the models, contact between flat relief surfaces is not necessary to ensure proper occlusion. The models constructed here, and their underlying geometry, show that once proper occlusion has commenced (i.e., where the tallest protoconoid in the lower zalambdodont, dilambdodont and tribosphenic models has entered the embrasure between the two upper models, or the blades of the carnassial or premolars are in contact), autocclusal mechanisms will operate and mean that proper occlusion will follow, given a vertical or latero-vertical force applied to the lower teeth. Only the crest edges will contact (and possibly a small amount of relief surface, particularly in worn teeth), and the direction of tooth movement will be dictated by the arrangement of the crests. Therefore, relief is maintained in these teeth purely through the geometry of the tooth surface. This is the case for Mellett's (1981) model of carnassial function, where the arrangement of the blades automatically generates relief behind the blades.

Neurological requirements for alignment are therefore limited to the first (or possibly first few) contacts between upper and lower teeth (such as the protoconids of one or more molars entering the embrasure between upper molars, or contact between canines).

After this first contact, the alignment of crests dictates the movement of teeth. If a vertical force were applied by the masticatory musculature, the lower jaw would be directed laterally due to the arrangement of the blades, and contact between opposing blades would be maintained. A lateral component to the occluding vector could be introduced, but it cannot be any greater than that which would cause the blades to lose contact. In essence, this shows that these tooth forms are auto-aligning, and no additional morphological guides are necessary for correct alignment in these tooth forms.

The positive rake angles of most crests will also aid the alignment of teeth (Chapter 2). The rake surface of a crest will tend to be pushed perpendicular to the surface by food that contacts it, and so a positive rake will push a crest towards its opposing crests. In contrast, two occluding crests with negative rake will tend to be pushed apart by the food between them.

# 3.4.4. Therian Molar Modelling

A fully explicit model of a tribosphenic-like tooth is very effective in many respects, as has been demonstrated above. However, very few attempts at modelling a tribosphenic-type tooth have been reported in the literature, presumably due to the perceived complexity of the tooth structure and occlusion. In reality, this can be successfully analysed and the structure can be modelled without great difficulty, especially when approached as a modular design. A major impediment to previous work has been the difficulty in representing the dynamics of these structures using drawings alone, so this work has been aided by the use of computer reconstruction.

It seems that the only detailed attempt at modelling components of primitive therian or tribosphenic teeth is that of Crompton and Sita-Lumsden (1970). Their model of reversed triangles is similar to the blade arrangement of a right-angled protoconoid, with an oblique blade (diagonal shearing edge, dse; Fig. 3.1b) and perpendicular blade (transverse shearing edge, tse), each of which trap food between the opposing blades. They hypothesised that in order for both blades to maintain contact throughout a latero-vertical cutting stroke, the oblique blade must be a three-dimensional curve. In fact, as previously explained, the main requirement is that occluding blades are the same shape (either linear or curvilinear) when viewed along the linear occlusal vector (Fig. 3.4). The simplest case is for the blades to be linear, in which case they are two-dimensional curves (as is the case for all of the models in this paper), but it is possible for the blades to be any combination of curves in two or three dimensions. Crompton and Sita-Lumsden's (1970) model, then, is a subset of the larger class of models outlined in this paper.

The illustrations in Crompton and Sita-Lumsden (1970) were used to generate a three-dimensional reconstruction of their model. When this is done, their model is most easily interpreted as a cusp with two two-dimensional crests, since a plane can be fitted to each crest as it occurs in three-dimensional space (Fig. 3.8). This directly contradicts their conclusion on the limitations of tooth design. The conclusion regarding the shape of the dse comes from a mistaken belief that 'the intersection of a vertical convex surface and a concave surface' must be a three-dimensional curve (Crompton and Sita-Lumsden 1970:197), which, as shown by the reconstruction, is not necessarily the case.

Despite the large number of possible shapes that occluding crests can take, they are in fact fairly restricted. In carnassials and insectivore premolars, they are largely two-dimensional curves, and so lie in a plane. The crests of zalambdodont, dilambdodont and tribosphenic molars are most often two-dimensional for the majority of the crest, so that the notch of the crest lies within the plane. It is only at the ends of a crest that it becomes a three-dimensional curve – the rounded cusp tips and embrasures mean that the crest as a whole is a three-dimensional curve, and has the appearance of Fig. 3.4e.

# 3.4.5. Tooth Modelling

The possible applications of geometric modelling of teeth and tooth function are extremely diverse and offer great potential for understanding the interactions of tooth shape and function. Model teeth can be used to test other hypotheses relating to possible tooth geometries and examining correlated change in structure. For instance, dental models could disentangle which differences in tooth form between species are due to factors that have a major effect on tooth function and which are merely due to correlated geometry of upper and lower teeth, for example, the extent of anterior displacement of the protocone and the angle of the postmetacrista, which are variable among dilambdodont and tribosphenic tooth forms.

The greatest potential for tooth modelling may lie in examining hypotheses of dental occlusion in fossils. Probable 3-D dental morphologies can be reconstructed to a much higher level of complexity and accuracy than previously in cases where occluding teeth are unknown in the fossil record (e.g. *Shuotherium*; Chow and Rich 1982). In evolutionary studies, it can allow the construction of a functional series of teeth (e.g. early evolution of therian molars) showing how function is maintained during the evolutionary modification of tooth forms. This may indicate limitations on changes that can be made while tooth function is maintained, and consequent end points in the evolution of functional morphologies. The function of extinct, and even hypothetical, tooth forms can

be examined and compared to extant teeth in which the function is more extensively understood.

Very importantly, computer modelling of complex morphological structures allows the morphologist to extend any analysis beyond the page into the full four dimensions of teeth. This allows a significant improvement over the 'occlusal diagrams' that have been used for over one hundred years in an attempt to illustrate the occlusion between crests and cusps of opposing teeth. Dental models will be of great use in explaining the occlusion of teeth, helping both the teacher to illustrate, and the student to observe, the true occlusion of mammalian teeth.

# 3.5. Conclusions

The present models incorporate many more functional characteristics than previous models (such as rake and relief of blades) and their proper occlusion is demonstrated through computer reconstructions of their spatial relations. It is encouraging, then, that the final model shapes emulate mammalian tooth shapes much more closely than any previous models.

This shows that a consideration of the geometries of both occlusion and function can allow the examination of the multifarious elements that influence tooth shape, leading to a more sophisticated analysis of the complex morphologies of the mammalian dentition.

# **Declaration for Thesis Chapter 4**

In the case of Chapter 4, contributions to the work involved the following:

Name	% contribution	Nature of contribution
Alistair R. Evans	80	Initiation, key ideas, development, data collection, interpretation, writing-up
Ian S. Harper	15	Initiation and methods development
Gordon D. Sanson	5	Initiation, advice and interpretation

# **Declaration by Co-authors**

The undersigned hereby certify that:

- (1) they meet the criteria for authorship in that they have participated in the conception, execution, or interpretation, of at least that part of the publication in their field of expertise;
- (2) they take public responsibility for their part of the publication, except for the responsible author who accepts overall responsibility for the publication;
- (3) there are no other authors of the publication according to these criteria;
- (4) potential conflicts of interest have been disclosed to (a) granting bodies, (b) the editor or publisher of journals or other publications, and (c) the head of the responsible academic unit; and
- (5) the original data are stored at the following location and will be held for at least five years from the date indicated below:

# Location: Clayton Campus, School of Biological Sciences, Monash University

Signature 1:	 Date:	
Signature 2:	 Date:	
Signature 3:	 Date:	

# Confocal imaging, visualization and 3-D surface measurement of small mammalian teeth

A. R. EVANS\*, I. S. HARPER\*† & G. D. SANSON\*

\*Department of Biological Sciences and †Microscopy and Imaging Research Facility, Faculty of Medicine, Monash University 3800, Australia

**Key words.** Confocal microscopy, GIS, measurement accuracy, morphometrics, moulding and casting, surface noise measurement, VRML animation.

#### **Summary**

The difficulties traditionally faced by functional morphologists in representing and interpreting three-dimensional objects can now be mostly overcome using available laser and computer imaging technologies. A practical method for three-dimensional imaging of small mammalian teeth using confocal microscopy is reported. Moulding and casting of the teeth were first performed, followed by confocal fluorescence imaging. Accuracy and precision of the scanned structures were tested in morphometric studies by using a new technique to measure the noise in the scan of a three-dimensional surface, and linear and angular dimensions of the scans were compared with measurements made using traditional morphological tools. It is shown that measurements can be taken with less than 4% difference from the original object. Teeth of the microchiropteran bat Chalinolobus gouldii were scanned and measured to show the potential of the techniques. Methods for visualizing the small teeth in three-dimensional space, and animating the teeth in occlusion, show the power of this approach in aiding a three-dimensional understanding of the structure and function of teeth and other three-dimensional structures.

#### Introduction

The functional morphologist has often been limited to representing anatomy as a two-dimensional projection – a photograph or drawing on paper. Proportions and spatial arrangements of components can easily be distorted or obscured in the abstraction from three to two dimensions, and so interpretations of projected images obviously should be, and usually are, undertaken with care. Representation and measurement of the object in its original three

Correspondence: Alistair Evans. Tel.: + 61 39905 5655; fax: + 61 39905 5613; e-mail: alistair.evans@sci.monash.edu.au

dimensions is preferable. Therefore, an alternative approach is to digitize the object (represent the surface of the object by many discrete points in space) and manipulate the three-dimensional surface data in virtual space with appropriate software. The ability to carry out the preferred alternative, particularly for very small specimens that cannot easily be inspected and manipulated without aid, has become a possibility with the advent of laser and computer technology in the form of the laser scanning confocal microscope.

Three-dimensional morphological analysis of teeth is beginning to gain popularity as the technology becomes more available (Reed, 1997; Zuccotti et al., 1998; Ungar & Williamson, 2000), and the use of the confocal microscope for this work has begun on both microrelief (Boyde & Fortelius, 1991; Boyde & Jones, 1995) and macrorelief (Hunter & Jernvall, 1998; Evans et al., 1999; Jernvall & Selänne, 1999; Evans & Sanson, 2000) of tooth surfaces. The technology of confocal microscopy, where a laser point source and confocal optics are used to sample an object point by point in 3-D space, is generally directed towards optical sectioning and 3-D reconstruction of tissues, cells and organelles, but other novel applications continue to emerge. Thus, we and colleagues have found it possible rapidly and accurately to map the surface (topology) of small teeth in a fraction of the time previously taken using manual measurements with, for example, a Reflex microscope. However, there are some important issues that must be addressed to ensure accurate and consistent results using these methods. This paper describes techniques that give practical solutions to these problems.

The technique described here involves incorporating a fluorescent dye, namely eosin, into the cast of a tooth. Fluorescence confocal imaging is then used to gather the three-dimensional surface information of the tooth. Once information representing the surface of an object such as a tooth has been gathered, a greater range of measurements can be taken compared to the usual point-to-point

measures. Three-dimensional tooth shape can be measured, as well as areas and volumes, and the spatial relations between objects (i.e. how three-dimensional objects fit together) can be demonstrated. This means that the occlusion of the teeth can be visualized, which would normally be particularly difficult for small specimens when simply manipulating them by hand. Features highly relevant to tooth function can be identified and quantified, not just those features that are easy or convenient to measure, permitting the interpretation of the role of both the gross and finer-scale features in tooth function.

Confocal microscopy allows the reconstruction of surface topology from optical sections either by reflection or by fluorescence imaging. Reflection imaging of the teeth themselves, or gold sputter-coated replicas, would be ideal, but it was found that reflection imaging had a number of disadvantages. For original specimens, excessive reflection was observed at many positions over the surface, most likely due to enamel prisms or small sections of tooth surface perpendicular to the laser source causing significantly more reflection than the rest of the surface. This led to the misinterpretation of the surface position at these points of high reflection. Also, much less reflected light is obtained from a surface nearly parallel to the light direction (Cheng & Kriete, 1995), again making the interpretation of surface position inconsistent for the whole tooth. The advantage of fluorescence in this respect is that fluorescence photons can go in any direction, increasing the likelihood that light will be received by the objective. Internal reflection within the microscope is also often a problem: most commercial confocal microscopes for biology are not equipped with anti-reflection coatings or internal anti-reflection optics, and this renders them inadequate for imaging in reflection mode. Staining the surface of a cast with fluorescent eosin gave the strongest signal compared to the low amount of autofluorescence exhibited by real teeth and was more accurate than depositing a layer of eosin dissolved in oil on the surface.

While measurements on a digital model can be made with a high degree of precision (e.g. Valeri et al., 1998), it is necessary to show that the digital model accurately represents the original. In the processes of moulding and casting and in imaging, a number of sources of error are introduced. These include shrinkage and distortion in moulding and casting, and depiction of the surface in imaging. In order to test adequately the confocal method, a standard test specimen of glass with known linear dimensions and angles was constructed. It was then moulded and cast, and the casts measured independently with a Reflex microscope or profile projector to show how faithful the cast was to the original. The cast was then imaged, digitally reconstructed and measured.

The design of the glass specimen also allowed the testing of different methods of imaging to determine which had the least error or noise in the scan of a surface. In this paper, 'surface noise' shall be defined as the deviation of the digital surface from the true surface at each x, y point. As the top surface of the test specimen was a perfect plane, any deviations from the plane in the digital model represented surface noise and could easily be quantified.

To demonstrate the applicability of these techniques in a biological context, scans were made of teeth from three specimens of a bat, Chalinolobus gouldii, the molars of which are in the order of  $2 \times 2$  mm. Morphological measurements taken from the specimens using digital calipers, a common tool in morphometric studies, showed that the lengths of individual molars were very similar, and so in most studies would often be considered identical in terms of function. However, minute differences in tooth shape between individuals can be demonstrated and measured using confocal and computer technology, meaning that fine differences in function can now be discerned and quantified.

#### Materials and methods

#### Moulding

All specimens were cleaned with a small brush using 100% acetone, 100% ethanol and distilled water in succession, and allowed to air dry between each cleaning. Moulds were made of the upper half of a small glass specimen (about  $1.7 \times 1.7$  mm and 3 mm in height; Fig. 1) using silicone RTV 3110 (Dow Corning Corporation, Midland, U.S.A.). The glass specimen was first coated in a dilute soap solution, which then was allowed to dry, to prevent adhesion between the very smooth surface of the glass and the silicone.

The entire tooth rows of three specimens of Gould's wattled bat Chalinolobus gouldii (Vespertilionidae) (Museum Victoria specimens C3746 to C3748) were moulded and cast. Large undercuts on dental specimens, which may interfere with moulding (such as underneath the teeth, between the teeth and the bone) and which were not relevant to tooth function, were filled with modelling clay. Small teeth were moulded by using a pointed probe to apply very small amounts (a few mm<sup>3</sup>) of silicone to both sides of the tooth row. The silicone was gently pushed up the sides of the teeth, until the entire tooth surface and some surrounding bone were covered, while ensuring that no bubbles were present. A small basin made of modelling clay was filled with silicone and the tooth row covered with silicone was inverted and placed into the basin to set for 24 h at room temperature. The mould was gently removed using a flattened blunt probe inserted between the mould and specimen.

To ensure a robust cast that is easy to handle, the original mould was made into a larger mould with a greater volume by embedding it in a small tray (about  $25 \times 20 \times 10$  mm) made with Laboratory-Putty (Coltène, Whaledent, Mahwah,

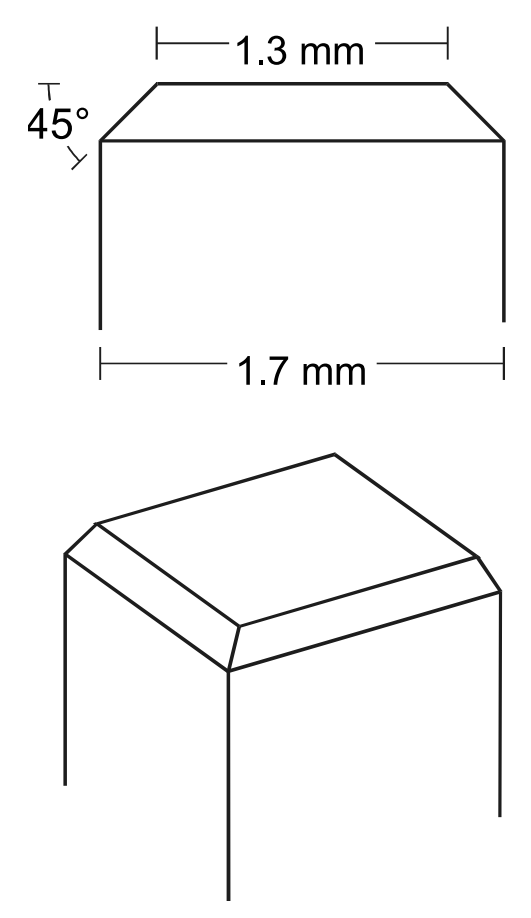


Fig. 1. Two views of the standard glass specimen for moulding, casting and imaging.

U.S.A.), with sides slanting outward to aid in later removal of the cast. The entire mould was then allowed to set.

#### Casting

The completed moulds were glued to microscope slides with silicone adhesive (CAF 3, Rhodorsil, Saint-Fons, France), and the slides placed into trays adapted for a hand centrifuge (Hettich Zentrifugen 1011I, Tuttlingen, Germany) which were designed to hold slides. The urethane EasyCast (British United Industries, Melbourne, Australia), which is opaque and stark white when cured, was used to make the casts. It was necessary to use a small paintbrush to eliminate most air bubbles introduced during mixing. More complex moulds (such as those of teeth) were then spun in the hand centrifuge 40 times at about 2000 rev min<sup>-1</sup>. The casts were removed from the mould at the appropriate demould time (25 min at 20 °C) and were then immediately dipped into a concentrated solution of eosin in acetone (2 g/100 mL). Eosin was used as it does not fade or bleach as rapidly as fluorescein, from which it is derived. Certainly other compounds will yield equally suitable results, but eosin was chosen simply for its resin-compatibility, photostability and wide emission spectrum, which together result in a strong, stable signal. Casts were found to be sensitive to photobleaching by sunlight and so were kept in the dark when not being scanned. Laser scanning, however, did not cause significant photobleaching.

#### **Imaging**

The casts were imaged using a laser scanning confocal microscope (Leica TCS\_NT, Leica, Sydney, Australia) with  $\times$  5 (0.12 NA) and  $\times$  10 (0.3 NA) dry objectives through rhodamine optics (excitation 568 nm and emission 590 long pass). The fields of view of these lenses are  $2\times 2$  mm and  $1\times 1$  mm, respectively. The pinhole was set at 1.00 optical unit, corresponding to a measured axial resolution of  $\pm$  35  $\mu$ m and  $\pm$  10  $\mu$ m, respectively. Care was taken not to oversaturate the detector when scanning. Optical slices were taken through the object in the x, y plane, where each slice was a square (e.g.  $256\times256$ ) pixel 8-bit image at medium scanning speed. Slices were taken at the same distance as the interval between pixels to make cubic voxels (volume pixels).

The Leica software 'PowerScan' was used to generate an 8-bit topological image from the stack of slices, where pixel intensity (grey level) represented height, by detecting the z height with the greatest fluorescence for each x, y point. The topological image was converted to x, y, z coordinates according to the fields of view in the x and y directions, and the z scan height. In the majority of these tests, the cubic voxels were 7.8  $\mu$ m long, generated in one of the following ways: for the  $\times$  5 lens, either a 256  $\times$  256 image was scanned at zoom 1 (field of view (FOV) of 2  $\times$  2 mm), or a 128  $\times$  128 image scanned at zoom 2 (FOV 1  $\times$  1 mm); for the  $\times$  10 lens, a 128  $\times$  128 image scanned at zoom 1 (FOV 1  $\times$  1 mm).

The two lenses were tested for the amount of surface noise in a scan. A varying amount of noise (random fluctuation in signal) is present at each pixel in a slice. As the height of the surface is judged according to the slice with the maximum signal, if noise at z height a is greater than signal at height b (the true position of the surface), then the position of the surface is misinterpreted as being at a rather than b. The surface noise at that point is then |a-b|. The surface noise level will also depend on the optical sectioning ability of the lens. With a small depth-offield (lenses with a higher numerical aperture), light from a limited range of z heights will be captured, with the surface detected in, for example, only one slice. Increased depth-offield (found with lower numerical apertures) means that light from the surface is captured from a greater number of z heights, and the surface is detected in many slices. As there will be random noise at each level, the slice where the signal + noise is greater than the signal + noise of every other

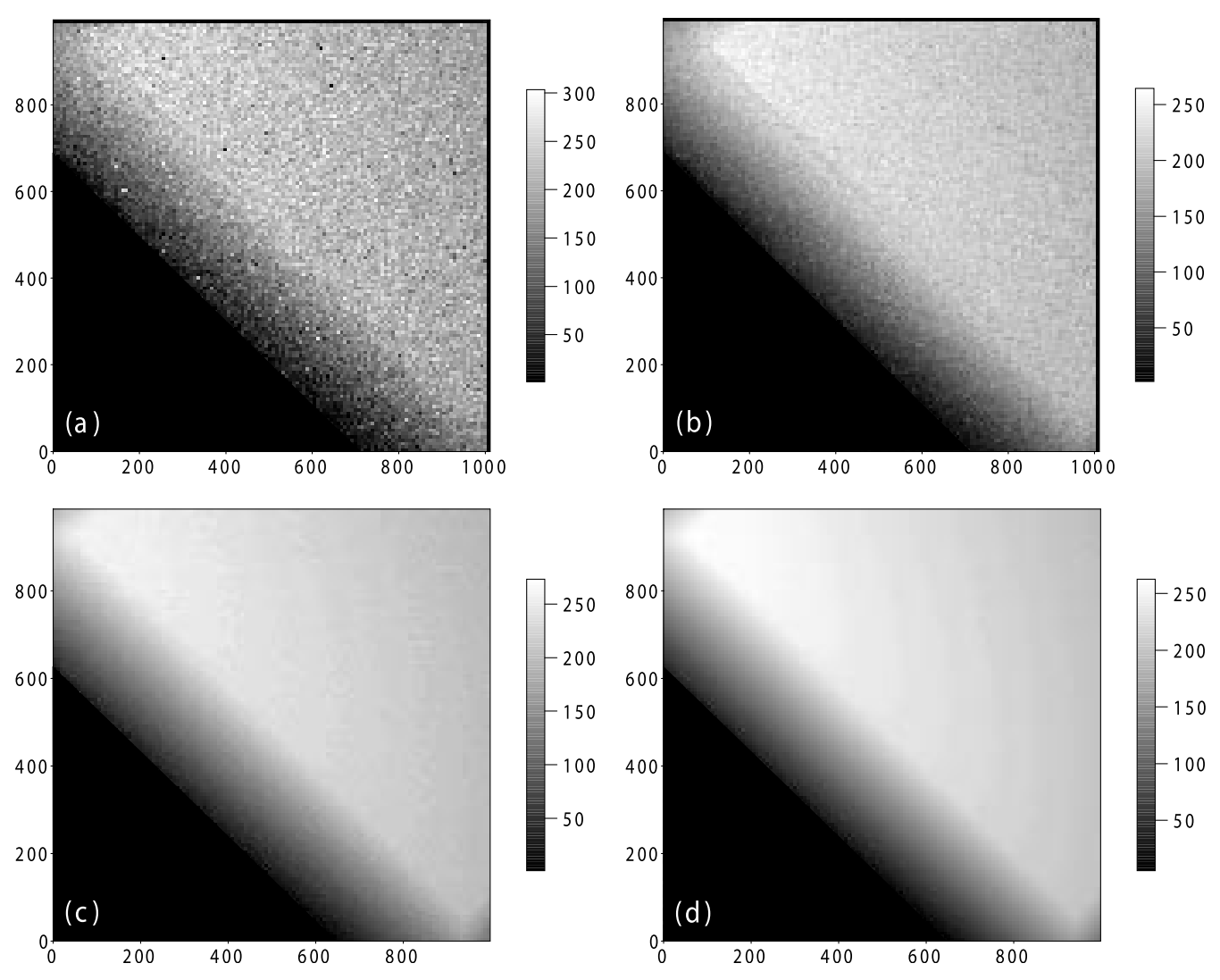


Fig. 2. Surface scans of standard glass specimen using (a)  $\times$  5 lens, Accumulation 1, one scan; (b)  $\times$  5, Accumulation 1, Average of 8 topological scans; (c)  $\times$  10, Accumulation 1, one scan; (d)  $\times$  10, Accumulation 1, Average 8. Dimensions in  $\mu m$ .

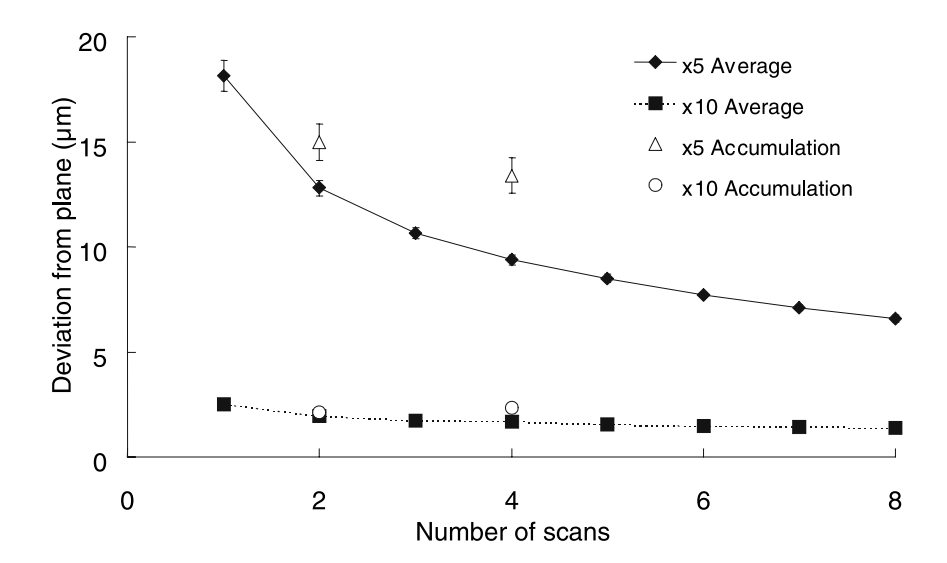


Fig. 3. Relationship between number of scans and surface noise in (mean ± SE of deviation from the plane in µm) for two different surface noisereduction methods: Accumulation and Average (number of casts scanned = 4).

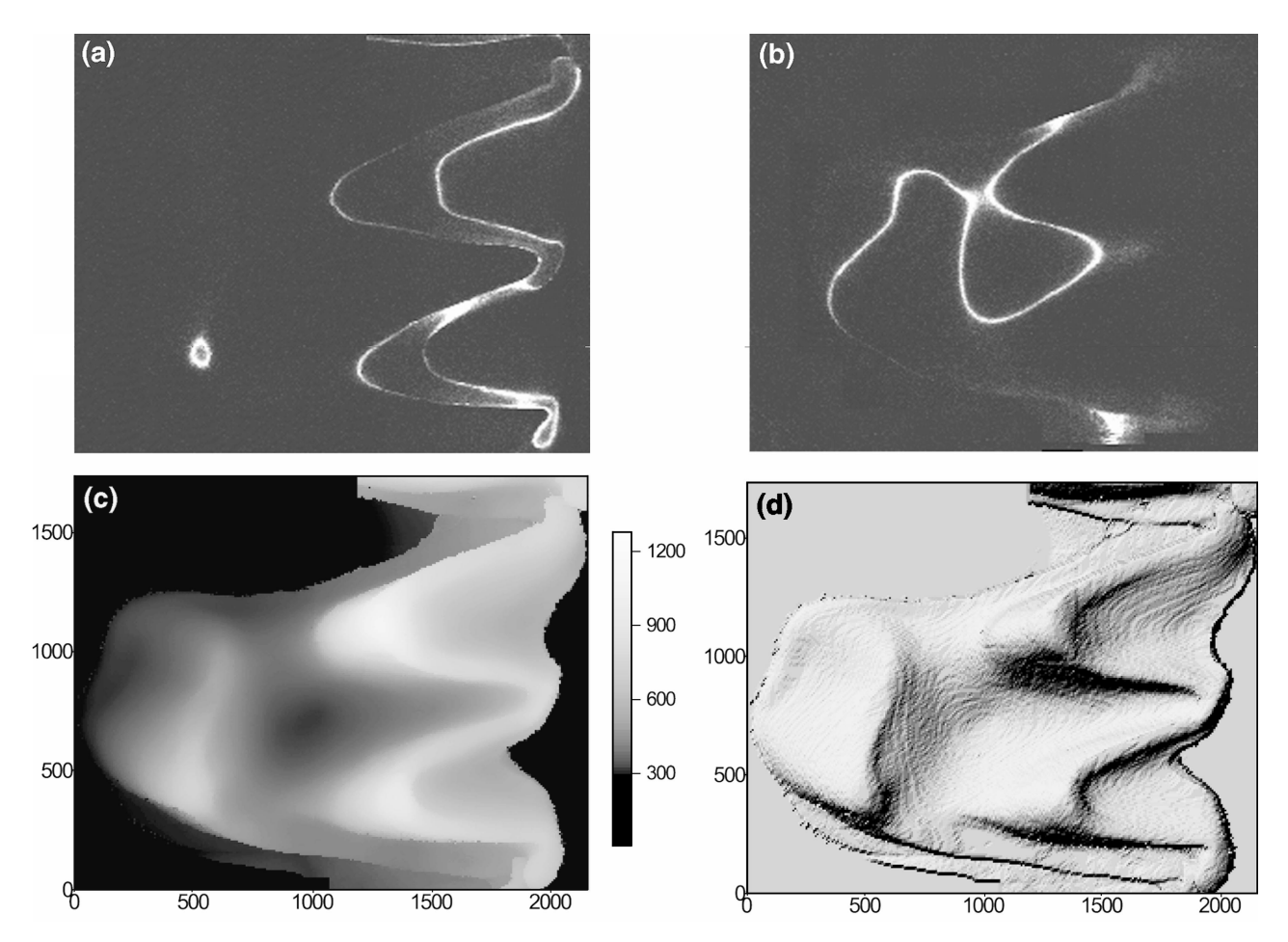


Fig. 4. Surface data representations of upper second molar of *Chalinolobus gouldii*: (a) and (b) optical slices through the tooth at different z heights, where white represents fluorescent surface; (c) topographic image, where grey level represents height; (d) shaded relief map, illustrating the tooth as a landform with light creating shadows on the surface. Dimensions in  $\mu$ m.

slice will be the position of the surface as interpreted by the computer. There is a greater potential for misinterpretation of the surface in this case, and so the average level of surface noise will be greater.

Surface noise in a scan for any given lens may be decreased in various ways. One method is to accumulate and average several images at each z height, and then create the topological image from the stack of accumulated image slices. Hence, topography created by an 'Accumulation 2' scan means that two images were averaged at each z height. Another method is to take the average of several topological images of the same area (where 'Average 2' means two topological images have been averaged). To test which of these two gives a better image (the one with the least surface noise), final 3-D data sets of the surface were made of a cast of the standard glass specimen using each of the methods. To measure the amount of surface noise, a plane (z = f(x,y) = ax + by + c) was fitted to all the points on the top surface (usually greater than 4000 points) and this plane was subtracted from the original data. This also takes into account differences in orientation between specimens, and hence the subtracted surface is only surface noise. The mean of the deviation of each point from the plane was then measured for an area of  $20 \times 20$  data points (making a standard 400 points for each scan).

Scans of the glass surface were carried out at 7.8  $\mu m$  cubic voxels for both  $\times$  5 and  $\times$  10 lenses. The same area of each cast was scanned eight times at Accumulation 1 (one scan) and twice each at Accumulations 2 and 4. Averages of two to eight scans were also generated. Surface noise was measured for each scan. Four casts, each from a different mould of the standard glass specimen, were scanned in this manner.

Urethane casts of the upper right second molar of three  $\it C. gouldii$  specimens were scanned using the  $\it \times$  10 lens at 128  $\it \times$  128 pixels (7.8  $\it \mu m$  cubic voxels) at Accumulation 2. The entire right upper and lower molar rows of one specimen were scanned using the  $\it \times$  5 lens at 128  $\it \times$  128 pixels (15.6  $\it \mu m$  voxels) at Accumulation 4. The tooth casts were positioned on modelling clay on a microscope slide so that as much of the occlusal surface was visible as possible,

i.e. there were no undercuts in the scan. Because the teeth were larger than the diameter of the field of view, several topographical images were taken and then manually tiled using Scion Image (Scion Corporation, Maryland, U.S.A.).

#### Visual representation

Once the topological image has been generated by the Leica 'PowerScan' software (in which height is represented by the grey level), this surface may be visualized as an extended focus image or as orthogonal views through the image stack, which is useful in assessing optical sectioning ability.

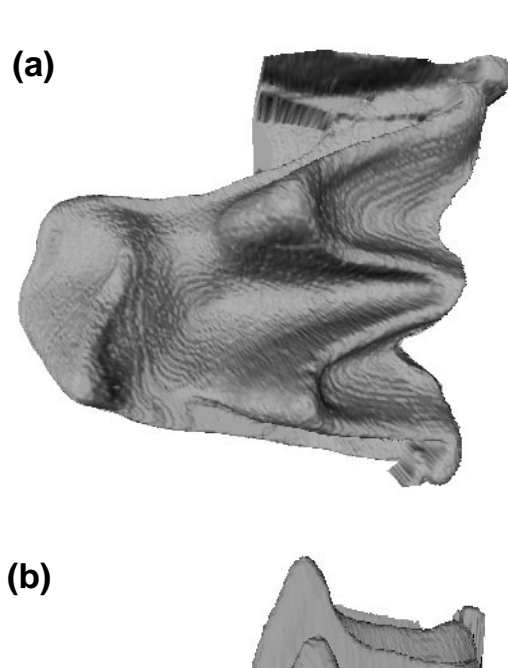
Another helpful tool is 'Virtual Reality Modelling Language' (VRML). VRML was originally developed for use on web pages as an alternative to 'Hypertext Markup Language' (HTML). It was designed for the simple construction of virtual objects and worlds. World builders and browsers such as 'Community Place Conductor 2.0' (Sony Corporation, Park Ridge, U.S.A.) and 'Cosmo Player 2.1' (Computer Associates International, Inc., Islandia, U.S.A.) can be used to construct and explore these worlds on the computer. It provides a simple way of representing objects in three dimensions, allowing the observer to view objects from any orientation and distance.

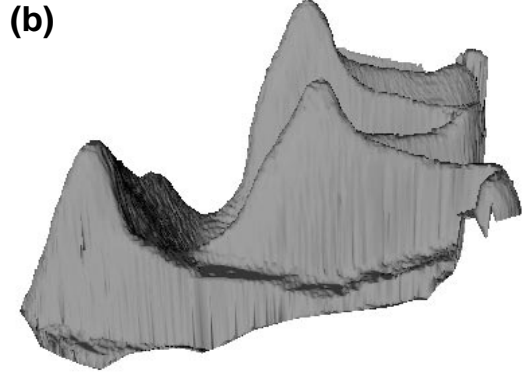
The command 'ElevationGrid' in VRML 97 allows the user to specify a uniform rectangular grid of varying height in the z = 0 plane. This is ideal for representing topological images from the confocal microscope, which are x, y matrices of zheights. When calibrated in the x, y and z directions, a VRML browser such as 'Cosmo Player 2.1' can generate a correctly proportioned representation of the tooth on the screen. which can be rotated in any direction, and a simulation of walking on the tooth surface can be produced. Two ElevationGrids can be generated in the same 'virtual world', and their positions in three-dimensional space at various time points can be specified using the 'TimeSensor' and 'PositionInterpolator' commands. The browser will interpolate the position of the moving teeth between the given time points, resulting in a smooth animation of teeth moving into and out of occlusion along a specified occlusal stroke. A full list and usage of VRML 97 commands can be found at http:// www.vrml.org/Specifications.

The other main software used was the geographical information systems (GIS) program Surfer (Win 32) V 6.04 (Golden Software, Inc., Golden, U.S.A.), which is used for geological surface mapping. This software allows the final surface to be viewed as a topographic image and a shaded relief image (simulating light falling on the surface), and also be used to obtain profiles of the surface.

#### Measurement

Independent measurements of the glass specimen were made using a Reflex Prior 52000 3-D motorized microscope





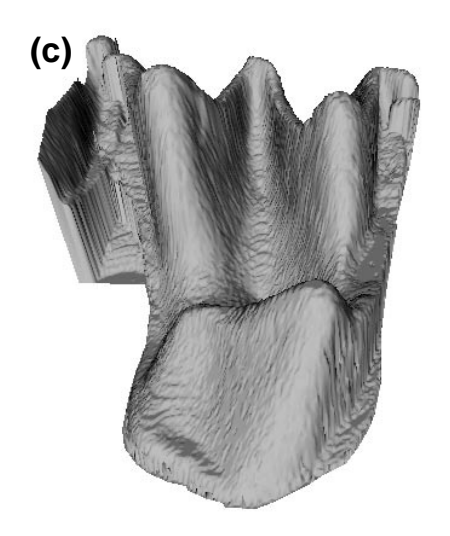


Fig. 5. Virtual reality modelling language reconstructions of upper second molar of Chalinolobus gouldii: (a) occlusal view; (b) anterior view; (c) lingual view.

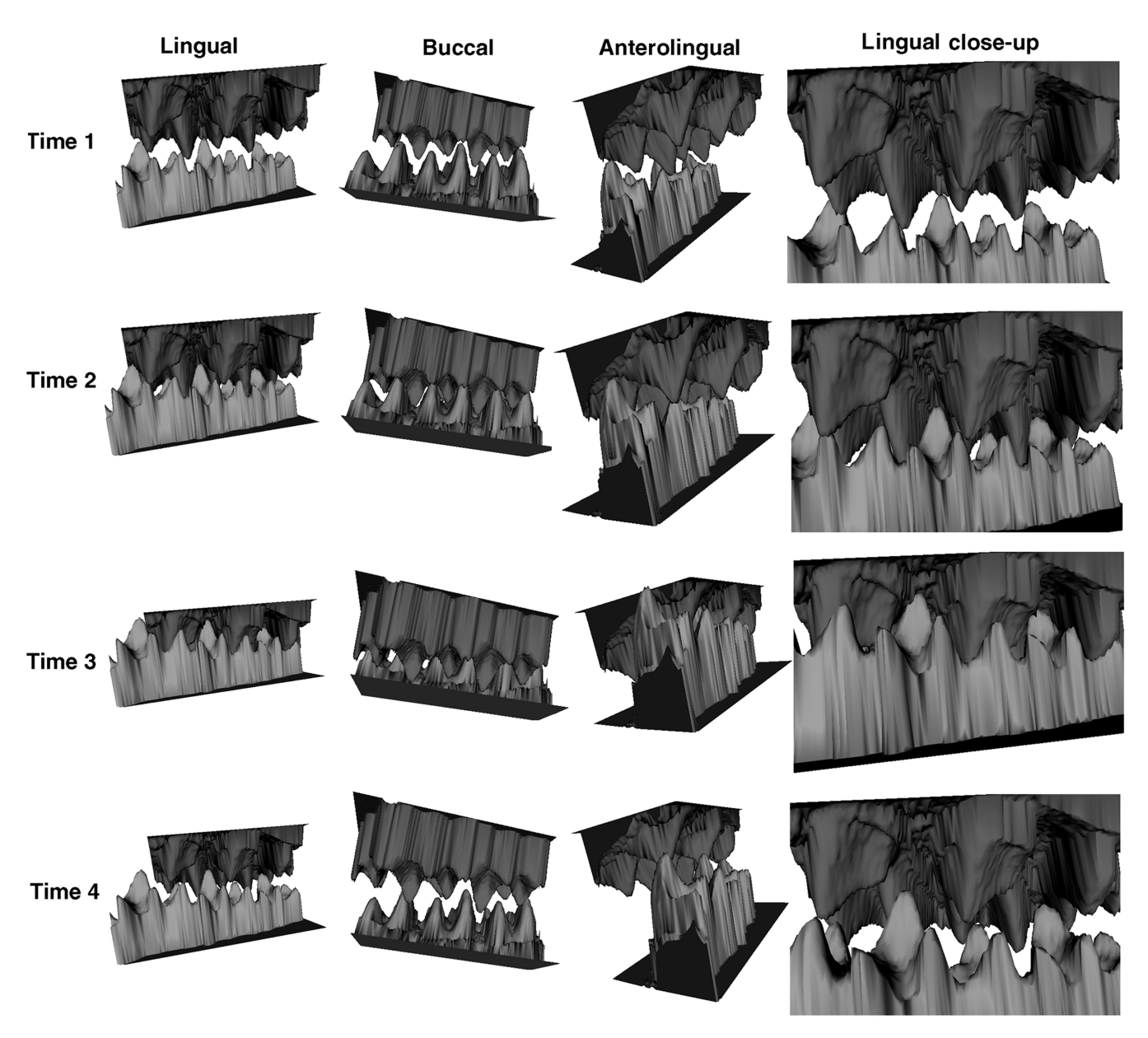


Fig. 6. Virtual reality modelling language reconstructions of occlusion of upper and lower molar rows in *Chalinolobus gouldii*. Four successive time points (Times 1–4) and four different views (lingual, buccal, anterolingual and a close-up from the lingual direction).

(Reflex Ltd, Somerset, U.K.), which can be used to capture manually the position of individual points in three dimensions. The length of one edge of the top face was measured using the Reflex. The angle between the top surface and the adjacent slanted face was found by measuring the specimen using a profile projector (Nikon Profile Projector V-20 A, Tokyo, Japan) at  $\times$  50 magnification. Reflex measurements were also made on each of the casts.

Measurements were made from the topographic scans of the glass specimen using Surfer. Surfer allows the user to digitize a point (obtain its 3-D coordinates) on the surface when viewing the image as a shaded relief map, in which the features of the object can more readily be recognized. The three-dimensional distance between the points can then easily be calculated. A plane was fitted to each of the top and side surfaces using all points on each surface, and the angle between these planes calculated.

Various measurements were made on the scans of *C. gouldii* teeth, including the surface areas and volumes of whole teeth and of particular features (such as cusps and basins), the three-dimensional length of crests, and angles between crests.

#### Results

#### **Imaging**

Topographic images of  $\times$  5 and  $\times$  10 scans of the glass specimen after averaging differing numbers of scans are shown in Fig. 2, where a decrease in surface noise can be seen after a number of scans is averaged. Figure 3 shows how the average deviation from a plane (i.e. surface noise) changes for differing numbers of scans using Average and Accumulation. The amount of surface noise in the scan decreased as an increasing number of scans was averaged. This is particularly obvious for the  $\times$  5 lens (mean  $\pm$  SE  $18.14 \pm 0.74 \,\mu\text{m}$  for one scan;  $6.59 \pm 0.18 \,\mu\text{m}$  for Average 8; n = 4). Surface noise did decrease to a small in the  $\times$  10 lens (2.53  $\pm$  0.17  $\mu$ m  $1.39 \pm 0.07 \,\mu m$  for one and Average 8 scans, respectively), but was always substantially less than that of the  $\times$  5 lens.

Scans of Accumulation 2 (14.98  $\pm$  0.87  $\mu$ m for  $\times$  5;  $2.12 \pm 0.14 \, \mu m$ for  $\times$  10) and Accumulation  $(13.38 \pm 0.84 \, \mu \text{m} \text{ for } \times 5; \ 2.34 \pm 0.06 \, \mu \text{m} \text{ for } \times 10)$ had less surface noise than a single scan (only one frame at each slice), but more than Average 2 for the same lens. This can in part be explained by the lower z resolution in Accumulation. For Average, the images were first converted to x, y, z data points and then averaged, and so the data were continuous in the z direction; for Accumulation, the z resolution was the sampling interval between stacks, and so the minimum deviation from the surface (apart from zero) was the interval between stacks.

#### Visual representation

Figures 4(a) and (b) show two optical slices through a tooth cast taken by fluorescence imaging. Two different visual representations of the same data are demonstrated in Figs 4(c) and (d): a topological image, where grey scale represents height; and a shaded relief map, where the surface is treated like a landscape over which light and shadow fall. All surface reconstructions presented in this paper are the raw data from the scans and have not been smoothed or interpolated. These modifications of the data may be useful for some studies and for simple visualization, but the raw data are used here to show that it is an accurate representation of the specimen. Views from different directions of a VRML reconstruction of the same tooth scan are shown in Fig. 5. Still frames from the animation of upper and lower teeth from several views at four separate times are shown in Fig. 6.

#### Measurements

The length of one edge of the glass specimen as measured by

the Reflex was  $1294.1 \pm 1.0 \mu m$ , and the angle between the top and side faces was  $44.46 \pm 0.05^{\circ}$  (10 replicate measurements for each). This length on all stained casts was  $1267.5 \pm 3.6 \mu m$  (10 replicate measurements on four casts; n = 4), showing a shrinkage of 2.1%. Measurements on unstained casts showed the casts were the same length, meaning that dipping a cast in acetone did not affect its dimensions.

Measurements of the digital surface showed a side length of  $1247.7 \pm 2.3 \mu m$ , a difference of 3.6% compared to the original specimen. The angle between the top and side surfaces was  $43.51 \pm 0.18^{\circ}$ , a difference of  $0.95^{\circ}$ .

A summary of some measurements taken from the bat tooth scans is shown in Table 1. Specimens generally increased in size (length and surface area measurements) in the following order: C3748, C3746, C3747.

#### Discussion

Confocal microscopy is useful for studying tooth surfaces. particularly molar and premolar tooth surfaces, as it can only be used for those macro surfaces that do not have undercuts. Full 3-D rendered models can be created of much smaller objects (e.g. whole cells or organelles), but cannot be done for larger objects using this method. There is a significant loss of signal intensity with increasing penetration into the specimen due to both absorption and scattering of the excitation beam on its way to the optical focus plane, and this applies also to the emitted light between the focus plane and detector (Cheng & Kriete, 1995). Additionally, any optical heterogeneity of the specimen will further degrade the signal, thus ensuring that undercut surfaces outside this level cannot be detected and reconstructed with any accuracy, regardless of the reconstruction software used. However, the entire surface of the molars of most animals, including the smallest, tribosphenic molars, can be imaged from at least one perspective without significant undercuts.

However, this does present a problem for more vertically extended teeth, such as canines, which often curve back on themselves. A full three-dimensional model of such teeth

**Table 1.** Measurements from scans of upper second molar of three specimens of Chalinolobus gouldii taken from the digital model using 'Surfer'.

Specimen	Tooth length (μm)	3-D length of crests (μm)	Tooth surface area (mm <sup>2</sup> )
C3746	1368.4	9305.5	6.16
C3747	1382.3	9433.8	6.32
C3748	1335.8	8810.9	5.98

can be constructed using the surface data from several views, but fitting together multiple views, and manipulation of the surface once it is constructed (which is usually in the form of polygons to represent the surface) is more complex. Another benefit is the higher resolution that can be obtained by confocal microscopy compared to many digital scanning devices currently available: e.g. the Surveyor 500 (Laser Design, Inc., Minneapolis, U.S.A.) used by Ungar & Williamson (2000) has a maximum resolution of 25.4  $\mu m$  in the three orthogonal directions. For a good representation of a small mammalian tooth, this is probably too large. Laser scanning confocal microscopy can reach resolutions of fractions of micrometres, but for an object the size of a tooth the resolution would be unnecessarily high, increasing data gathering and computational time.

The imaging method has been shown to be consistent over the various stages of data gathering – scans of the same cast and scans of casts from different moulds are all very similar. This gives us confidence that taking one scan from one cast of a mould should be representative of the original object, and so multiple moulds, casts and scans are not required, minimizing the time needed to gather data.

The published statistics on shrinkage for the materials used show an expected shrinkage of 0.2–0.4% for RTV 3110 and 1.0% for EasyCast. This means that for an object moulded and cast from both materials, shrinkage should be at most 2%. This is approximately the result that we obtained.

A number of different casting and moulding materials were tested for their use in fluorescence imaging of macro objects. Epoxy plastics were found to be inferior to the urethane in several respects. Epoxies are usually translucent and when the dye was incorporated into the cast a fluorescent signal from inside the cast was often detected and the position of the surface misinterpreted, especially at higher dye concentrations. At lower dye concentrations this was generally not a problem, but the surface noise was often higher than that for urethane, probably due to the signal being detected from a short distance inside the cast. The urethane used in this study is opaque, and hence the maximum fluorescence is detected from the surface only.

Epoxies can be highly corrosive to silicone moulding materials: only three or four casts may be made before the mould is significantly damaged, and even the first cast can show signs of deterioration (e.g. Araldite M (Ciba-Geigy, Melbourne, Australia) caused deterioration of RTV 3110 and CAF 3 moulds (A. R. Evans, personal observation); moulding and casting artefacts have been found by Gordon, 1984 and Teaford & Oyen, 1989). Many casts (> 20) can be made from silicone moulds when urethane is used. The main disadvantage of urethane compared to epoxy is the lower dimensional stability of urethane. Many epoxies have published shrinkages of 0.01% compared to 1% of urethane. It was considered, however, that the superior imaging of the

urethane casts would be of a greater advantage than a low shrinkage on a cast that may have defects due to the nature of the casting agent.

It is not known how the scanning accuracy (surface noise level) using other scanning and casting techniques compares with that reported here. Jernvall & Selänne (1999) report that three to six scans were averaged to achieve a final topographic image. Surface noise levels have not been published for 3-D scanning devices such as the Surveyor 500.

The difference in the amount of surface noise between the two lenses is extremely obvious, as would be predicted from their numerical aperture. The benefits of averaging multiple scans are also apparent, but the results here show that additional scanning does not always reduce noise. For example, very little surface noise reduction is gained from averaging more than two scans in the case of the  $\times$  10 lens. The scans of tooth casts with this lens were carried out using Accumulation 2 rather than Average 2 due to the necessity of tiling multiple images, as averaging tiled topological images would be tedious. There is a significant decrease in surface noise when using both averaging and accumulation with the  $\times$  5 lens. Accumulation 4 was used for scans of the entire tooth row made using this lens, which showed a large reduction in surface noise compared to Accumulation 1. The  $\times$  5 lens was used for tooth row scans due to the much larger field of view diameter to reduce the number of scans necessary to cover the area.

As the main application of this work is to analyse large numbers of teeth, an important consideration in deciding which lens to use is the scanning time. There is a trade-off between resolution (determined by the number of pixels), reduction of surface noise and time taken to scan. Measured scan times (Table 2) demonstrate that the time to scan one slice is simply related to the resolution and the number of scans accumulated. Scanning a *C. gouldii*  $M^2$  of  $2.2\times1.7$  mm using  $\times$  10 lens required five separate scans of 170 sections each to cover the area at voxel 7.8  $\mu m$  and took a total of 19 min 10 s. The scans of the entire molar tooth row at voxel 15.6  $\mu m$  with  $\times$  5 lens required three scans of about 115 slices (total of 15 : 30).

Scan times will also help to decide whether any improvement in the optical sectioning of the  $\times$  10 lens is offset by its smaller field of view. For the set-up used here, the same area and resolution is covered by  $\times$  5 lens at  $1.0~{\rm s~slice^{-1}}$  compared to  $4\times0.7~{\rm s~slice^{-1}}=2.8~{\rm s~slice^{-1}}$  for the  $\times$  10 lens, not including the time to reposition the object between scans. However, if the more important consideration is accuracy (reducing surface noise), then the  $\times$  10 lens would be better, given that an equivalent scan time gives a lower surface noise (Accumulation  $4,\times5,$  gives surface noise of  $13.38~{\rm \mu m}$  and takes  $4.1~{\rm s~slice^{-1}};$  Accumulation  $1,\times10,$  gives surface noise of  $2.53~{\rm \mu m}$  and takes  $2.8~{\rm s~slice^{-1}}$  for the same area).

Table 2. Relationship between resolution, number of scans accumulated at each z height and the time taken to scan. Results are the same for both  $\times$  5 and  $\times$  10 lenses.

$\begin{aligned} & Resolution \\ & (pixels \times pixels) \end{aligned}$	No. frames accumulated	Time to scan 100 slices (s)	Time per slice (s)	Time per scan (s)
128 × 128	1	68.75	0.69	0.69
$128 \times 128$	2	136.4	1.36	0.68
$128 \times 128$	4	271.6	2.72	0.68
$256 \times 256$	1	103.3	1.03	1.03
$256 \times 256$	2	204.1	2.04	1.02
256 × 256	4	406.7	4.07	1.02

Scans of whole teeth can then be made at the same resolution with lower surface noise using × 10 without a major increase in scanning time. These comparisons can be made for any microscope set-up once data on scan times and surface noise are obtained.

Using these methods, many measurements of the digitized teeth are currently possible (Table 1), including length, area and volume measurements. From these surface data, it is now possible to make measurements of surface sharpness (Evans & Sanson, 2000), which is important to tooth function (Freeman, 1992; Popowics & Fortelius, 1997; Evans & Sanson, 1998). Comparisons of these and other such measurements will be very important when dissecting out the differences in shape and therefore function in teeth of all forms.

Understanding the intricate arrangement of cusps and crests on a single tribosphenic tooth is very difficult, especially when only line drawings or photographs are available. The small size of the teeth also means that they must be viewed through a microscope. However, once digitized, the visualization can be carried out on the computer. A tooth represented in a VRML file (such as that shown in Fig. 5) can allow the viewer to fully grasp the three-dimensional shape of the tooth.

Reconstructing the occlusion of upper and lower tribosphenic teeth is also difficult and tedious for functional morphologists and students alike. In previous work on tooth function, the spatial relationships between tooth features could only be understood by embedding casts in resin at various stages of occlusion and then sectioning them (e.g. Crompton & Hijemae, 1970). The same representations can now be done on the computer by digital manipulation of the surface data of teeth, involving much less guesswork in orienting teeth and labour in making and sectioning casts.

From the reconstruction of tooth movement during the occlusal stroke, as seen in Fig. 6, the major events of tooth occlusion can be seen: the protoconid (the largest cusp on the lower molars) fits in the embrasure between the uppers; shearing occurs along the two crests leading down from the protoconid against crests on the upper teeth; and the lingual cusp on the upper tooth (protocone) fits into the talonid basin in the lower. Another consideration that is important but difficult to visualize when viewing two isolated teeth is that the lower tooth must move lingually during the occlusal stroke in order for these events to occur.

The advantages of digital reconstruction are very apparent, especially when considering small objects such as mammalian teeth. Conventional methods of visualizing how the upper and lower molars fit together for teeth less than 2 mm in length are extremely difficult and can be misleading. These advantages were seen to outweigh the slightly greater inaccuracy in measurements taken from the confocal compared to the Reflex microscope (a difference of less than 4%) - the benefits of the techniques greatly outweigh the costs (as similarly found in other studies comparing confocal and conventional microscopy accuracy, e.g. Delorme et al., 1998). Future digitizing techniques for small objects will easily overcome these drawbacks, and the methods of surface data manipulation described here will become an even greater part of the study of morphology than at present. All problems relating to the digitization of macro objects are not solved by confocal microscopy, as it is incapable of such reconstructions as a whole skull. However, the present study shows it to be very effective for small objects (millimetre size range), such as teeth.

#### Acknowledgements

Thanks to Lesley Kool, Department of Earth Sciences, Monash University, for advice on moulding and casting, and Lina Frigo, Mammalogy, Museum Victoria, for loan of specimens. Alistair Evans is supported by a Monash Graduate Scholarship.

#### Supplementary material

The following material is available from http://www.blackwell-science.com/products/journals/suppmat/JMS/ JMS939/JMS939sm.htm

Fig. S1. Animated view of optical slices stack through upper second molar of Chalinolobus gouldii.

Fig. S2. Virtual Reality Modelling Language reconstruction of upper second molar of Chalinolobus gouldii.

Fig. S3. Video of Virtual Reality Modelling Language reconstruction of occlusion of upper and lower molar rows of Chalinolobus gouldii.

Fig. S4. Animated Virtual Reality Modelling Language reconstruction of occlusion of upper and lower molar rows of Chalinolobus gouldii.

Figure S1 is an animated gif of successive slices through the tooth. Figure S2 is the VRML reconstruction where the tooth can be viewed from any direction. Figure S3 shows a colour video of tooth occlusion from one view: the animated

VRML file that can be viewed from all directions is shown in Figure S4.

#### References

- Boyde, A. & Fortelius, M. (1991) New confocal LM method for studying local relative microrelief with special reference to wear studies. *Scannina*. 13, 429–430.
- Boyde, A. & Jones, S.J. (1995) Mapping and measuring surfaces using reflection confocal microscopy. *Handbook of Biological Confocal Microscopy* (ed. by J. B. Pawley), pp. 255–266. Plenum Press, New York.
- Cheng, P.C. & Kriete, A. (1995) Image contrast in confocal light microscopy. *Handbook of Biological Confocal Microscopy* (ed. by J. B. Pawley), pp. 281–310. Plenum Press, New York.
- Crompton, A.W. & Hiiemae, K. (1970) Molar occlusion and mandibular movements during occlusion in the American opossum, *Didelphis marsupialis* L. Zool. J. Lin. Soc. 49, 21–47.
- Delorme, R., Benchaib, M., Bryon, P.A. & Souchier, C. (1998) Measurement accuracy in confocal microscopy. J. Microsc. 192, 151–162.
- Evans, A.R., Harper, I.S. & Sanson, G.D. (1999) Methods of digital measurement of tooth surface and occlusion. *Abstracts* 11th Int. Conf Confocal Microscopy, European Mol Biol. Laboratory (EMBL), Heidelberg, Germany, 11–15 April 1999, p. 23.
- Evans, A.R. & Sanson, G.D. (1998) The effect of tooth shape on the breakdown of insects. *J. Zool. (Lond.)*, **246**, 391–400.
- Evans, A.R. & Sanson, G.D. (2000) Applications of confocal microscopy to functional morphology: the effect of diet and wear on tooth sharpness and function in two microchiropterans *Chalinolobus gouldii* and *C. morio*. Proceedings of the 9th Australasian Bat Conference, Tocal, Australia, 25–28 April 2000. *Bat Res. News*, 41, 44.

- Freeman, P.W. (1992) Canine teeth of bats (Microchiroptera): size, shape and role in crack propagation. *Biol. J. Lin. Soc.* **45**, 97–115.
- Gordon, K.D. (1984) Pitting and bubbling artefacts in surface replicas made with silicone elastomers. *J. Microsc.* **134**, 183–188
- Hunter, J.P. & Jernvall, J. (1998) Decomposing early morphological diversity in ungulates: analysis of early Paleocene arctocyonid teeth. I. Vertebrate Paleontol. 18, 52A.
- Jernvall, J. & Selänne, L. (1999) Laser confocal microscopy and geographic information systems in the study of dental morphology. *Palaeontologia Electronica*, 2. http://palaeo-electronica.org.
- Popowics, T.E. & Fortelius, M. (1997) On the cutting edge: tooth blade sharpness in herbivorous and faunivorous mammals. *Ann. Zool. Fennici*, **34**, 73–88.
- Reed, D.N.O. (1997) Contour mapping as a new method for interpreting diet from tooth morphology. Am. J. Phys. Anthropol. Supplement, 24, 194.
- Teaford, M.F. & Oyen, O.J. (1989) Live primates and dental replication: new problems and new techniques. *Am. J. Phys. Anthropol.* **80**, 73–81.
- Ungar, P. & Williamson, M. (2000) Exploring the effects of toothwear on functional morphology: a preliminary study using dental topographic analysis. *Palaeontologia Electronica*, 3. http://palaeo-electronica.org/2000\_1/gorilla/issue1\_100.htm.
- Valeri, C.J., Cole, T.M. III, Lele, S. & Richtsmeier, J.T. (1998) Capturing data from three-dimensional surfaces using fuzzy landmarks. Am. J. Phys. Anthropol. 107, 113–124.
- Zuccotti, L.F., Williamson, M.D., Limp, W.F. & Ungar, P.S. (1998) Modeling primate occlusal topography using geographic information systems technology. *Am. J. Phys. Anthropol.* **107**, 137–142.

# **Chapter 4 Addendum**

Frontispiece shows a full-colour reconstruction of upper second molar of *Chalinolobus gouldii*.

Plate 3 shows the front cover of the *Journal of Microscopy* for November 2001.

The Electronic Appendix (see enclosed CD-ROM) contains VRML files of single tooth reconstructions and animated occlusion of tooth rows for images and reconstructions in Chapter 4.

Note: in the rest of this thesis, Tables 1-2 and Figs 1-6 of Chapter 4 are referred to as Tables 4.1-4.2 and Figs 4.1-4.6 respectively.

# **Chapter 5.** Connecting Morphology, Function and Tooth Wear in Microchiropterans

# 5.1. Introduction

Interest in the study of functional dental morphology is long-standing (e.g. Gregory 1920; Ryder 1878), particularly due to the predominance of fossils represented only by their dentition, and the desire to interpret them in order to learn about the animal's mode of living (e.g. Fortelius 1985; Kay 1984; Strait 1993c). Despite recent work demonstrating the importance of the dentition to the nutritional ecology of an animal (Lanyon and Sanson 1986; McArthur and Sanson 1988; Pérez-Barbería and Gordon 1998), much is still to be learned in relating morphology directly to the function of teeth.

Teeth can be examined as tools designed for the breakdown of food (Lucas 1979; Lucas and Luke 1984), and as for any tool, the shape of a tooth is a significant determinant of its function. This approach should greatly aid in the interpretation of the dentition's function, as an examination of tooth shape should reveal much about its function. However, very few studies have made use of dental measurements that can readily be interpreted in terms of function. To some extent, this is due to the difficulty of making such measurements using traditional morphometric techniques, but it is largely because a comprehensive understanding of the relationship between tooth shape and function has not been achieved. This study specifically deals with the function of microchiropteran molars (which can be considered dilambdodont; Freeman 1979), but the principles are equally applicable to other tribosphenic-like teeth (e.g. of opossums, shrews, desmans, tenrecs and some primates).

In endeavouring to assess tooth function by means of morphology, two types of dental measures can be recognised: those that primarily relate to the size of the feature being examined, and those that relate to its shape (Evans *in press* – see Appendix 3). Much previous analysis has relied on size measures: e.g. comparisons of relative crest lengths (Anthony and Kay 1993; Dumont *et al.* 2000; Kay 1975; Kay *et al.* 1978; Strait 1993c, 2001; Ungar and Kay 1995); ratios of dental parts (Kay 1975; Seligsohn 1977) or tooth types (Freeman 1984). For instance, studies of crest length explicitly equate the size (length) of crests with function. It is likely that increased crest length (e.g. where longer crests have been demonstrated in folivores and insectivores compared to frugivores; Anthony and Kay 1993; Kay 1975; Kay *et al.* 1978; Strait 1993a) influences the amount of food processed. However, the effect will be more complex, involving a number of

necessary trade-offs that will affect the overall efficacy of tooth function. This aspect has not been adequately addressed.

Very few investigations have tried to examine the quality of the crests – the fine details of the shape of crests and the surrounding surface – and how this affects function. When such shape characteristics have been examined, they have often related to the tooth surface as a whole (Ungar and Williamson 2000), and any specific effect on tooth function has not been identified. Arguably, most previous measures cannot be explicitly related to dental function or are principally correlates of more informative functional characteristics of teeth (see Chapter 2).

The deficit in the explanatory power of features like crest length is also apparent when trying to assess the consequences of tooth wear during an animal's lifetime. Changes in the shape of teeth will most often have an effect on their function. However, it is not usually recognised that wear does not necessarily change the shape of teeth. The teeth of most herbivores, such as selenodont molars (possessed by buffalo, antelope, etc.), are essentially non-functional in their newly-erupted form. A moderate degree of wear is required to transform the shape into its functional configuration (Luke and Lucas 1983). Once this has been achieved, the tooth is constructed so that its shape, and therefore function, is static for much of its life, despite the large amount of wear that will occur on the tooth (Rensberger 1988). A point is eventually reached in such high-crowned (hypsodont) tooth forms where the tooth stops growing and the functional form rapidly degrades.

The relationship between wear and shape for tribosphenic-like teeth has generally been neglected. The implicit assumption has been that wear adversely changes the functional shape of these teeth, so that the pre-formed occlusal morphology is fully functional and no wear is required for the tooth to function (Luke and Lucas 1983). However, no substantive data have been given in support of this proposition. Most studies of the function of these teeth have examined only unworn molars, in part because no reliable functional measures have been devised that allow comparison of unworn and worn teeth to test the above assumption. For instance, Ungar and Williamson (2000) correctly conclude that crest length is unlikely to be very informative when considering change in function with wear.

Retention of good functional shape can therefore be considered a principal imperative in tooth design. The dentition can be scrutinised for design features that prevent or minimise change due to wear. Such design features abound in herbivore teeth (such as

the vertical enamel pillars of enamel that form the cutting edges), but have generally not been identified in tribosphenic teeth.

This study will examine the upper molars of the microchiropteran *Chalinolobus gouldii* using nine functional parameters that have been developed in engineering or dental function studies. These functional parameters can be specifically related to function; for example, a change in the parameter can be used to predict an increase in force or energy for the tooth to function (Chapter 2). Several of these parameters have been recognised in the dental literature previously, but they have not been put into a comprehensive framework and the majority have not been measured on teeth. This will provide base-line data for the condition of these characters in unworn teeth and then allow investigation of changes with increasing wear. Because the functional parameters have predictive value, relative changes in the function from unworn to worn *C. gouldii* molars can be measured. As change in shape most likely means a change in function, design characteristics of these molars that reduce the effect of wear on shape change, and so maintain the shape and function of the teeth, will also be examined. The principles of function used in this Chapter are also applicable to the lower molars. The main objective was to develop tools for the interpretation of tooth function and the influence of wear.

## **5.2.** Functional Parameters

Arguably, the function of teeth can better be analysed by considering the function of components of the teeth separately rather than attempting a measure that purports to reveal the function of the entire tooth. Tribosphenic-like teeth can be seen as combinations of three basic tools: cusps, crests and basins. Cusps are advantageous for penetration of food, initiating a crack, and crests play a significant role in propagating the crack through the material. Basins are also involved with food fracture, but shape characteristics of basins are more difficult to interpret and will not be considered in this work. Strictly, these components are not independent of one another (e.g. cusps often occur at the ends of crests), but it is a useful distinction to make.

The functional parameters used in this work are characteristics of shape that can be related to the function of a tooth component. The function of the cusps and crests of microchiropteran molars will be analysed with reference to the following nine criteria of cusp and crest function: tip sharpness, cusp sharpness and cusp occlusion relief for cusps; edge sharpness, rake angle, crest relief, approach angle, capture area and fragment clearance for crests. Eight of these (excluding cusp occlusion relief, which was mentioned in Chapter 3) are described in detail in Chapter 2.

When dealing with worn teeth rather than the idealised shapes of Chapters 2 and 3, the measurement of relief becomes more complicated. Relief can be considered as the area enclosed between a line running from the tip of the crest parallel to the direction of tooth movement and the relief surface (Fig. 5.1). The relief angle is the angle of the relief surface of the crest relative to the vector of tooth movement. An area of no relief, usually produced by wear, is often apparent immediately behind the cutting edge, and is called the wear land.

Cusp occlusion relief is analogous to the relief of crests. In crested teeth, an opposing cusp often moves into a valley between two cusps or crests that are adjacent on the same tooth. When this occurs, friction between tooth surfaces due to food caught between the surfaces will push the teeth apart, increasing the force required. Relief behind the point at which the cusp occludes reduces friction and the tendency for occluding teeth to be separated.

# **5.3.** Materials and Methods

## 5.3.1. Tooth wear

Molars of 79 specimens (Australian Museum, Sydney and Museum Victoria, Melbourne) of the insectivorous microbat, Gould's Wattled Bat *Chalinolobus gouldii* (Vespertilionidae), were examined to survey the range and extent of molar wear. *Chalinolobus gouldii* has a body mass of about 7-20 g and forearm length of 36-44 mm (Churchill 1998). Widespread throughout Australia, it is an inhabitant of open forest, mallee, dense forest, tall shrubland and urban areas. It has been recorded feeding on a diverse range of insects, mostly beetles and moths, but also flies and orthopterans (Dixon 1995; Churchill 1998). Fig. 5.2 shows the gross morphology and nomenclature used throughout the text for the *C. gouldii* upper molar. The amount and exact location of wear is variable between individuals and between teeth of the same individuals; however, general trends in the wear sequence followed by most teeth can be determined. Occasional minor chipping of cusps and crests can occur at any stage of the wear sequence, and in general will not be considered in this discussion.

Specimens of *C. gouldii* were classified visually according to a scale from 1 (no wear) to 6 (very heavily worn) for the second molars. Fraction wear states (1.25 and 1.5) were used to signify only slight changes from the unworn condition, and so a wear state less than 2 signifies light wear. The wear states are divided into light wear (1-1.5), moderate wear (2-3) and heavy wear (4-6) so that the gross differences and changes in shape through wear can be examined between these three states. The three wear states,

described below, are illustrated in Fig. 5.3 indicating the main areas of wear and gross changes of tooth shape with wear.

## *Light Wear (1-1.5)*

Little wear (if any) is apparent along some of the crests as shiny attrition facets on the relief surfaces of the crests. There is little to no wear on the rake surfaces.

## Moderate Wear (2-3)

Abrasive wear on the rake surface is apparent, along with the attrition facets on relief faces. Approximately an eighth (wear state 2) to a half (wear state 3) of the rake surface is exposed dentine.

# Heavy Wear (4-6)

Substantial wear has occurred, and the entire rake faces of the paracone, metacone and protoconid may be exposed dentine. The height of the paracone and metacone are substantially reduced, and at wear state 6 the tooth is essentially flat.

# **5.3.2. Functional parameters**

Details of the methods for generating digital models of teeth are given in Chapter 4. Briefly, the upper molars of 20 C. gouldii specimens (ten with light wear; five with moderate wear; and five with heavy wear; specimens C3704, C3746, C3748, C3750, C4344, C4348, C4349, C5144, C13691, C16967, C18127, C18142, C18163, C19363, C19376, C19378, C22196, C23472, C23911, C26131; Melbourne Museum) were moulded and cast into urethane, which was then dyed with eosin, a fluorescent dye. The upper second molars were scanned with rhodamine optics using a Leica TCS confocal microscope. Scans were taken at two different resolutions: low resolution (8 µm cubic voxel, a three-dimensional 'volume element', so that an 8 µm cubic voxel has a length of 8 μm in three orthogonal directions) using a ×10 lens for entire teeth; and high resolution (1  $\mu$ m cubic voxel) using a ×40 dry lens. Teeth larger than the field of view of the ×10 lens (1 mm) were tiled to create a composite image of the entire object. The resulting topographical images were transformed to x, y, z coordinates and transferred into Surfer for Windows v. 6.04, a geological mapping program. Surface data was also converted to Virtual Reality Modelling Language (VRML) files using the ElevationGrid command to generate three-dimensional reconstructions of the tooth on the computer screen.

The nine functional parameters previously described were measured on confocal scans of the upper second molars. The measurement of most of these parameters was carried out in Surfer, along with a Visual Basic v. 6.0 program specially written that interfaces with Surfer for file and data manipulations. Tooth length was measured as the

three-dimensional distance from the most anterior point of the preparacrista to the most posterior point of the postmetacrista. In most instances, the functional parameters can be quantified from the confocal scans. However, for some this was not possible, so categorical differences in features were used according to observations made under a compound light microscope (×45).

The 'occlusal vector' is the vector of movement of the lower tooth relative to the upper tooth. It can be estimated as being parallel to the trigon groove, and so is the vector from a point at the buccal end of the trigon groove to a second point at the lingual end (just buccal to the trigon basin). VRML reconstructions of tooth occlusion showed that this is a good estimate of the trajectory of the lower tooth.

# **Cusps**

# Tip Sharpness

Tip sharpness was measured on high-resolution (1  $\mu$ m voxel) confocal scans of the tips of cusps, ensuring no undercuts. The topographical surfaces were smoothed three times using 9×9 kernel with centre weighting 4 in Surfer to reduce surface noise. The curvature of the smoothed surface was calculated using the Directional Derivative: Curvature option in Surfer, which calculates the curvature of the surface in a given direction, at 10° intervals for 180°. The maximum curvature at each x, y point for all directions was determined. The mean curvature (in  $\mu$ m<sup>-1</sup>) of a 20 × 20  $\mu$ m area at the tip of the cusp was calculated, and the reciprocal (radius of curvature in  $\mu$ m) is the tip sharpness of this cusp. Tip sharpness was only measured for the metacone.

# Cusp Sharpness

Cusp sharpness was measured on low-resolution (8  $\mu$ m voxel) confocal scans of whole teeth. A plane (termed the basal plane) was fitted to three points on the tooth: the bases of the trigon, paracone and metacone basins. The position of this plane will only be affected by extreme wear, as these features are usually the last to be worn. The basal plane was translated in the z direction so that it intersected the tip of the cusp (the highest point relative to the basal plane). The plane was translated downwards at intervals of 25  $\mu$ m in the direction parallel to the normal vector of the basal plane and the volume of the cusp above the plane was calculated. Cusp sharpness measurements were taken for the volume of the cusp at 25 and 100  $\mu$ m from the tip.

## Cusp Occlusion Relief

A profile of the tooth along the trigon groove was obtained using Surfer. The trajectory of the cusp that occludes with the mesostyle (i.e. the hypoconid) was estimated

as a line parallel to the occlusal vector starting at the mesostyle. The distance from each point of the profile from the hypoconid trajectory was measured, and the mean of these distances is the cusp occlusion relief. Cusp occlusion relief will be underestimated for some of the teeth due to minor undercutting of the surface lingual and dorsal to the mesostyle.

### **Crests**

# Edge Sharpness

Edge sharpness was measured on high-resolution (1  $\mu$ m voxel) confocal scans of the postmetacrista. Processing of surface data generally follows that for calculating tip sharpness. The topographical surfaces were smoothed three times, and Curvature analysis in Surfer was used to generate a map of the maximum curvature at each point. The curvature at all positions along the crest (approximately every 1  $\mu$ m) was calculated, and the edge sharpness is the reciprocal of the mean curvature of the crest. Edge sharpness was only measured for the postmetacrista.

#### Crest Rake

The RKP (rake perpendicular) plane was determined, which was perpendicular to both the occlusal vector and to the length of the crest. The profile of the rake surface is the intersection between the rake surface of the crest and the RKP plane positioned at the centre of the crest. A least-squares regression line was fitted to the first 100 µm of the profile using Microsoft® Excel 97, and the slope of this line gives the average rake angle for the first 100 µm of the rake surface. Means and standard deviations for angles cannot be calculated in the regular manner as they are on a circular scale, and so were calculated according to Zar (1999).

### Crest Relief

Three qualitative characters relating to relief were recorded by viewing specimens under a compound microscope at  $\times 45$  magnification: a) width of wear land; b) volume of space behind a crest; c) relative relief angle. The wear land is the area on the relief surface closest to the cutting edge that contacts the occluding crest. This is apparent as an attrition facet. The width of the wear land was classified as: L1, absent or very small (usually apparent as a thin strip on the relief surface along the crest, approximately 50-80  $\mu$ m in width); L2, moderate width ( $\sim 80-150~\mu$ m); or L3, very wide ( $\sim 150~\mu$ m). Volume of space behind a crest was estimated according to the relative height of the crest above the embrasure between teeth or the trigon groove: V1, small volume (crest height reduced by at least one half compared to unworn crest); V2, moderate volume (reduced by about one

quarter); V3, large volume (full height of unworn crest). The relief angle was classified as: A1,  $0^{\circ}$  relief angle (attrition facet covering most or all of relief surface); A2, small relief angle (approximately 1-10°); A3, large relief angle (relief angle noticeably larger than A2;  $\tau 10^{\circ}$ ). A wear land that covers the entire relief surface (some crests classified as L3) and  $0^{\circ}$  relief angle (A1) can be considered equivalent, as both represent no relief behind the crest.

# Approach Angle

The profile of each crest was smoothed, using the average of four points each side of a point, and a centre weighting of four. The angle between the line connecting each pair of adjacent points and the occlusal vector was calculated using trigonometry. The mean approach angle for a crest was calculated as the mean of the absolute values for the approach angle along its length. The mean of absolute values was used, as negative and positive approach angles are functionally equivalent.

# Food Capture

For each crest, the RKS (rake surface) plane was fitted to the tip of the closest mesial cusp (paracone or metacone) and the associated stylar cusps (e.g. parastyle and mesostyle for the paracone). The profile of the crest was projected onto the RKS plane along the occlusal vector: the intersection between the RKS plane and a line parallel to the occlusal vector passing through each point of the crest profile created a projection of the crest profile onto the rake surface plane. The area of the surface between the crest profile and the projected crest profile estimates the amount of food captured by the concavity in a crest

# Fragment Clearance

The size and extent of flow channels for directing food off rake surfaces was qualitatively assessed by examination under a compound microscope, as it was found to be too difficult to quantitatively measure by any other means. Fragment clearance was estimated for the paracone and metacone basins. The categories were: F1, bad fragment clearance (low crest height and absence of flow channels for directing food off the rake surface, i.e. when the rake surface is fairly flat, fragmented food would be forced against tooth surfaces rather than directed off the tooth); F2, medium fragment clearance (intermediate to F1 and F3); F3, good fragment clearance (tall cusps, with flow channels to direct food off the tooth surface).

## **5.3.3.** Statistical methods

Differences between the three wear states (light, moderate and heavy wear) for the quantitative features (tip, cusp and edge sharpnesses, rake and approach angles, and cusp

occlusion relief) were tested using Kruskal-Wallis tests in Systat for Windows v. 10.0 (SPSS, Inc.). Qualitative features (relief wear land, volume and angle, and fragment clearance) were tested with Pearson chi-square tests. Significance was determined using the exact distribution of the data using SPSS for Windows v. 10.0 (SPSS, Inc.). Significance level for all tests was p = 0.05.

Principal components analyses (PCAs) were carried out using Systat. Volume (mm³) and area (mm²) measures were reduced to linear measures by cube root and square root transformation respectively, and then all quantitative values were logged. Analyses were undertaken for functional parameters relating to the following five groups of variables: 1) the entire data set (including tooth length, which was included in all analyses); 2) paracone and related crests (tip and cusp sharpness of paracone; cusp occlusion relief of mesostyle; rake and approach angles, relief and capture area of pre- and postparacristae; fragment clearance of paracone basin); 3) metacone and related crests (as for paracone except for variables relating to metacone and pre- and postmetacristae); 4) interloph crests (parameters relating to postmetacrista and preparacrista); and 5) intraloph crests (parameters relating to premetacrista and postparacrista, and cusp occlusion relief of the mesostyle). Relief angle was omitted from the PCAs where there was no variation in relief angle over wear.

Non-metric multidimensional scaling (NMDS) was carried out using Primer 4.0 (Plymouth Marine Laboratory) using the same five groups as the PCA. Pairwise difference between the wear groups was tested using analysis of similarity (ANOSIM) and the influence of each factor on the dissimilarity between groups using similarity percentages (SIMPER). A significance level of 3% was used for the SIMPER analyses.

## 5.4. Results

# **5.4.1. Functional parameters**

# Cusps

# Tip Sharpness

Lightly worn cusp tips had significantly higher tip sharpness than worn specimens, indicated by the smaller radius of curvature of the cusp ( $25.6 \pm 2.6 \mu m$  vs  $50.3 \pm 8.0 \mu m$ ; mean  $\pm$  SE; Table 5.1).

## Cusp Sharpness

Cusp sharpness is approximately equal for the paracone and metacone of unworn teeth; on average it is slightly higher for the metacone (i.e. smaller volume; Table 5.1; Fig.

5.4). In general, the cusp sharpness of the main upper cusps decreases as the teeth wear, particularly for cusp sharpness to  $100~\mu m$ , so that cusp volume for a given distance from the tip increases. This is more apparent for the paracone, where the cusp sharpness decreases more substantially than for the metacone. However, there is variation in this general pattern. The majority of unworn cusps have high cusp sharpness. Most moderately worn cusps have only slightly lower cusp sharpness, but in a few individuals the cusps with moderate wear have even lower cusp sharpness than some highly worn cusps.

# Cusp Occlusion Relief

The relief behind the mesostyle for three wear states, represented by the space between the surface of the trigon groove and the path of the hypoconid, is shown in Fig. 5.5. Cusp occlusion relief is very high at low wear (average distance between trigon groove and path of hypoconid is  $129.71 \pm 11.45 \, \mu m$ ) and decreases significantly with increasing wear (high wear,  $33.20 \pm 5.96 \, \mu m$ ; p = 0.001; Table 5.3). At high wear, the mesostyle is worn away, leaving essentially no relief. In some specimens, wear at the lingual end of the trigon groove and in the trigon basin shows that the hypoconid contacts the upper tooth surface, signifying the lack of relief.

Cusp occlusion relief is also apparent at the points where the protoconid and the protocone occlude (the parastyle on the upper molar and the entocristid/postmetacristid junction on the lower molar respectively), but was not quantified in this study.

#### Crests

# Edge Sharpness

The results for edge sharpness measurements are shown in Table 5.2. Edge sharpness of the postmetacrista in the unworn state is  $14.4 \pm 2.1$  µm. After large amounts of wear, this increases significantly to  $24.4 \pm 3.0$  µm.

### Crest Rake

Several of the unworn crests have a small amount of negative rake for 10-50  $\mu$ m from the crest edge. When the rake angle for the first 100  $\mu$ m is calculated, all unworn ectoloph crests have a positive rake angle (Table 5.2).

After a small amount of wear, any small amount of negative rake originally present is removed. At higher wear states, the rake angle of all crests is highly negative and significantly different from the unworn state (all p < 0.01; Table 5.2). The most anterior crest (preparacrista) has the highest positive rake angle when unworn (31.81  $\pm$  2.89°), and the smallest negative rake angle when worn (-29.76  $\pm$  8.75°) compared to the other three

crests, but all of them have approximately the same change in angle between unworn and highly worn (~60°).

# Crest Relief

The crests of lightly worn molars have a small ridge on the relief surface along the crest edge. Attrition occurs first on this ridge creating the attrition facet that is seen on lightly-worn teeth. This attrition facet, or wear land, is approximately the same width for the length of the crest, and its presence maintains relief behind it. The crests are also relatively high above the associated valley, giving a large volume behind the crests.

As wear progresses, the raised ridge is removed and the attrition facet extends down the relief surface. In general, the wear land increases in width with wear, which was significant for three of the four crests (Table 5.2). The relief angle does not greatly increase with higher abrasion wear as the relief surface is fairly flat (see below). As the crest is worn and the distance from the crest to the adjacent valley decreases, the volume of space behind the crest into which food can flow decreases. On the relief surface of some crests is a small, shallow concavity (such as behind the postprotocrista) that would also contribute to relief of the crest, particularly at later wear stages. The overall effect of these parameters is that some relief is maintained but it is reduced compared to the unworn teeth.

# Approach Angle

The approach angle for ectoloph crests of unworn or lightly worn teeth is approximately equal, being between 36-43° (Table 5.2).

Approach angles generally increased with tooth wear. The change is highly significant for those crests that occlude with the crests of the protoconid (i.e. preparacrista and postmetacrista; p = 0.001), and also significant for the postparacrista (p = 0.014; Table 5.2).

## Food Capture

In unworn teeth, capture area is largest in the crests posterior to a cusp (postmetacrista and postparacrista; Table 5.2). There is significant change in the capture area from unworn to worn crests only in the postparacrista (p = 0.011; p > 0.05 for all other crests; Table 5.2).

## Fragment Clearance

In unworn teeth, the ectoloph crests are substantially higher than the adjacent paracone and metacone basins, and the rake surface is directed down into the basins, guiding divided food off the buccal edge of the tooth. Divided food that is on the buccal side of the ectoloph crests would flow off the rake surfaces across the basins. The height of

the paracone and metacone basins remains essentially constant but the depth of these flow structures is reduced with greater wear. In heavily worn specimens, the rake surface may be lower than the basin and so the fragments must be forced against the slope to be pushed off the rake surface and out towards the buccal side of the teeth. This has the effect of reducing the capacity to gather and direct food off the rake surfaces. Table 5.3 summarises the quantitative differences in clearance with wear. The reduction in fragment clearance occurs more quickly in the paracone than the metacone.

## 5.4.2. PCA and NMDS

There is a fairly high degree of separation among wear states along Factor 1 of the PCA plot using the entire data set (Fig. 5.6a). Many of the functional parameters were very highly correlated with Factor 1. Parameters with absolute correlations between 0.94 and 0.80 were: fragment clearance; approach angle for preparacrista and postmetacrista; relief volume; rake angle; paracone volume to  $100 \mu m$ ; capture area for postparacrista; and cusp occlusion relief. Tooth length had a correlation of 0.172 with Factor 1. Factor 2 was not highly correlated with any of the variables, with the third highest correlation being with tooth length (0.608). The plots using subsets of the data displayed similar patterns.

NMDS plots showed a clustering of individuals with similar wear states (light, moderate and heavy wear), which was very tight for the 10 lightly worn specimens in most plots (Fig. 5.6b). The moderate wear group was always found between the light and heavy wear groups. Stress for all 2-D plots was <0.10, and plots for subsets of the data were similar. ANOSIM for all variables found a significant difference between light-moderate, light-heavy and moderate-heavy (significance level <0.01%, <0.01% and 0.08% respectively). SIMPER analyses found that cusp occlusion relief contributed most to the differences between groups (average 10.61% for the three between-group comparisons), followed by rake angles of postparacrista (6.97%), postmetacrista (6.42%), premetacrista (6.30%) and preparacrista (6.24%), tip sharpness (5.70%), capture of postparacrista (4.69%) and edge sharpness (4.31%).

**Table 5.1.** Functional parameters relating to cusps (mean  $\pm$  SE) for paracone and metacone for three wear states in *C. gouldii*. n = 10 for light, n = 5 for moderate and heavy. me, metacone; pa, paracone. Significance level: \*\*\*  $p \le 0.001$ ; \*\* p < 0.01; \* p < 0.05; NS, not significant.

		Wear				
	Cusp	Light	Moderate	Heavy	p	
Tip sharpness (μm)	me	$25.6 \pm 2.6$	$47.5 \pm 10.6$	$50.3 \pm 8.0$	0.009	*
Cusp sharpness to	pa	$57.9 \pm 6.0$	$62.6 \pm 17.2$	$85.7 \pm 4.4$	0.056	NS
25 $\mu$ m (10 <sup>3</sup> $\mu$ m <sup>3</sup> )	me	$54.8 \pm 10.3$	$72.8 \pm 15.0$	$94.3 \pm 22.7$	0.353	NS
Cusp sharpness to	pa	1127.9 ± 82.7	$1464.7 \pm 288.9$	$1895.6 \pm 132.8$	0.018	*
$100~\mu m~(10^3~\mu m^3)$	me	$1084.6 \pm 118.0$	$1626.0 \pm 73.0$	$1670.6 \pm 280.7$	0.034	*

**Table 5.2.** Functional parameters relating to upper molar ectoloph crests (mean  $\pm$  SE, or median (minimum, maximum) for qualitative data) for three wear states in *C. gouldii*. n = 10 for light, n = 5 for moderate and heavy. Crests: prpac, preparacrista; popac, postparacrista; prmec, premetacrista; pomec, postmetacrista. Wear land: 1, small wear land; 2, moderate; 3, large. Volume of space behind crest: 1, small volume; 2, moderate; 3, large. Relief angle: 1, 0° relief angle; 2, small relief angle; 3, large. Significance level: \*\*\*  $p \le 0.001$ ; \*\* p < 0.01; \*\* p < 0.05; NS, not significant.

			Wear			
	Crest	Light	Moderate	Heavy	p	
Edge sharpness (μm)	pomec	$14.4 \pm 2.1$	$19.7 \pm 3.3$	$24.4 \pm 3.0$	0.016	*
Rake angle (°)	prpac	$31.81 \pm 2.89$	$-16.45 \pm 5.03$	$-29.76 \pm 8.75$	0.001	***
	popac	$20.95 \pm 4.79$	$-35.52 \pm 2.87$	$-41.95 \pm 6.53$	0.001	***
	prmec	$18.95 \pm 3.05$	$-11.76 \pm 10.78$	$-37.73 \pm 8.18$	0.005	**
	pomec	$14.61 \pm 5.35$	$5.06 \pm 13.06$	$-40.78 \pm 5.95$	0.009	**
Relief – wear land	prpac	1 (1, 2)	2 (2, 3)	1 (1, 2)	0.001	***
(qual)	popac	1 (1, 1)	2 (1, 3)	2 (1, 2)	0.086	NS
	prmec	1 (1, 2)	1 (1, 3)	2 (1, 3)	< 0.001	***
	pomec	1 (1, 1)	2 (1, 2)	2 (1, 3)	0.017	*
Relief – volume	prpac	3 (3, 3)	3 (2, 3)	2 (1, 2)	0.001	***
behind crest	popac	3 (3, 3)	3 (1, 3)	1 (1, 2)	0.008	***
(qual)	prmec	3 (3, 3)	3 (2, 3)	2 (1, 3)	0.004	***
	pomec	3 (3, 3)	3 (2, 3)	2 (1, 2)	< 0.001	***
Relief – angle	prpac	2 (2, 2)	2 (2, 2)	2 (2, 3)	1.000	NS
(qual)	popac	2 (2, 2)	2 (2, 2)	2 (2, 2)	1.000	NS
	prmec	2 (2, 2)	2 (2, 2)	2 (2, 2)	1.000	NS
	pomec	2 (2, 2)	2 (2, 2)	2 (2, 2)	0.499	NS
Approach angle (°)	prpac	$38.56 \pm 1.13$	$46.17 \pm 1.28$	$56.42 \pm 1.76$	0.001	***
	popac	$42.76 \pm 1.10$	$40.49 \pm 4.29$	$49.36 \pm 1.27$	0.014	*
	prmec	$36.12 \pm 1.19$	$40.40 \pm 4.52$	$39.04 \pm 3.36$	0.822	NS
	pomec	$37.78 \pm 0.76$	$40.35\pm0.98$	$50.02 \pm 1.51$	0.001	***
Capture area	prpac	$26.87 \pm 1.94$	$26.72 \pm 5.18$	$18.34 \pm 2.43$	0.084	NS
$(10^3~\mu m^2)$	popac	$67.37 \pm 5.03$	$73.11 \pm 8.85$	$31.65 \pm 4.60$	0.011	*
	prmec	$47.90 \pm 2.94$	$39.71 \pm 3.70$	$33.77 \pm 7.57$	0.153	NS
	pomec	$63.47 \pm 3.07$	$64.13 \pm 6.92$	$78.88 \pm 13.45$	0.597	NS

**Table 5.3.** Cusp occlusion relief (mean  $\pm$  SE) and fragment clearance (median, minimum and maximum in parentheses) for paracone and metacone basins and trigon groove for three wear states in *C. gouldii*. n = 10 for light, n = 5 for moderate and heavy. mesost, mesostyle; paba, paracone basin; meba, metacone basin. Significance level: \*\*\*  $p \le 0.001$ ; \*\* p < 0.05; NS, not significant.

			Wear			
	Feature	Light	Moderate	Heavy	_ p	
Cusp occlusion	mesost	$129.71 \pm 11.45$	$59.05 \pm 13.59$	$33.20 \pm 5.96$	0.001	***
relief (µm)						
Fragment	paba	3 (3, 3)	2 (2, 3)	1 (1, 1)	< 0.001	***
Clearance (qual)	meba	3 (3, 3)	3 (2, 3)	2 (1, 2)	0.001	***

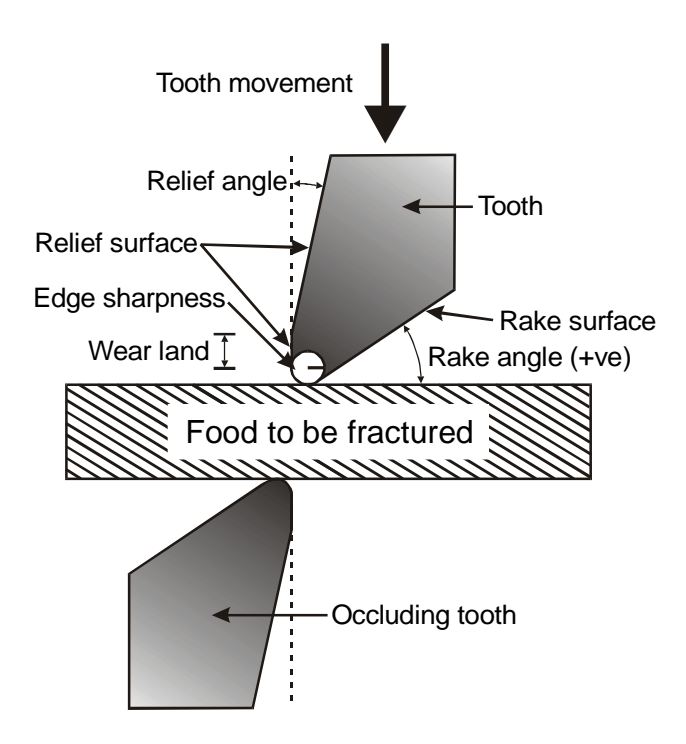


**Fig. 5.1.** Rake angle, relief angle, wear land and edge sharpness of a crest viewed end-on (length going into page). The circle radius indicating edge sharpness is enlarged for clarity, and is much smaller in real crests.

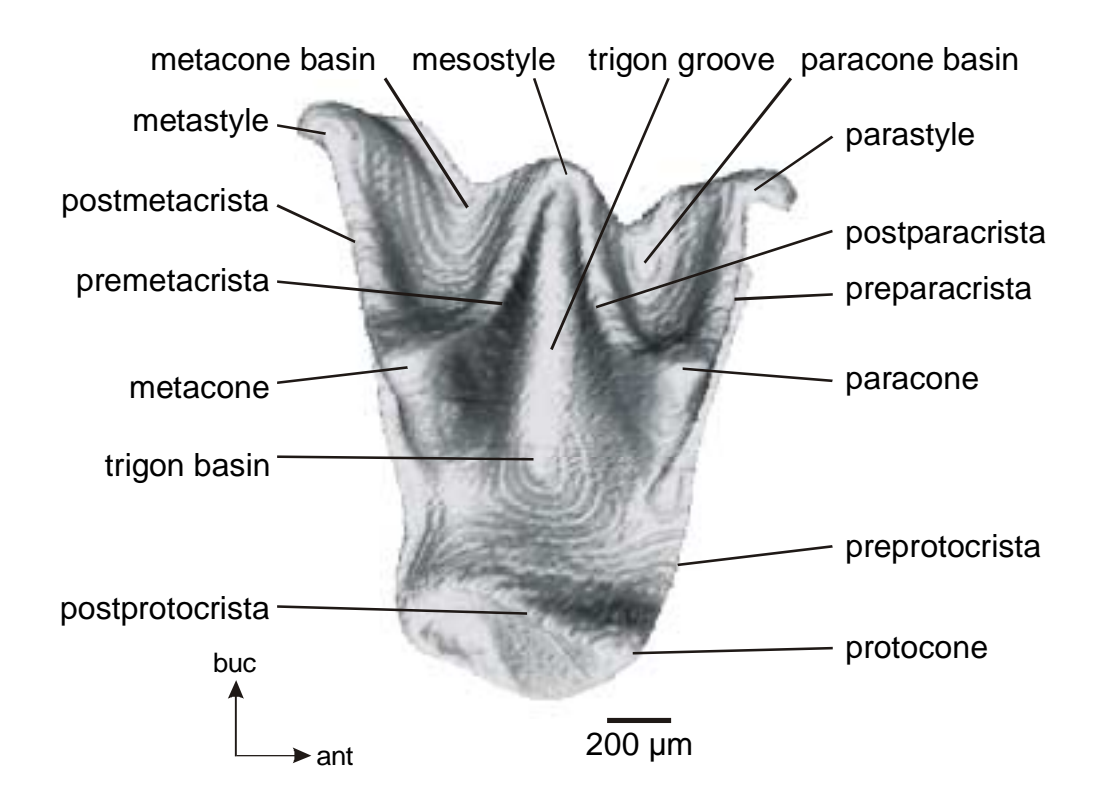


**Fig. 5.2.** 3-D reconstruction of *Chalinolobus gouldii* upper second molar (specimen C23911), illustrating terminology used throughout this thesis. Occlusal view. Abbreviations: ant, anterior; buc, buccal.

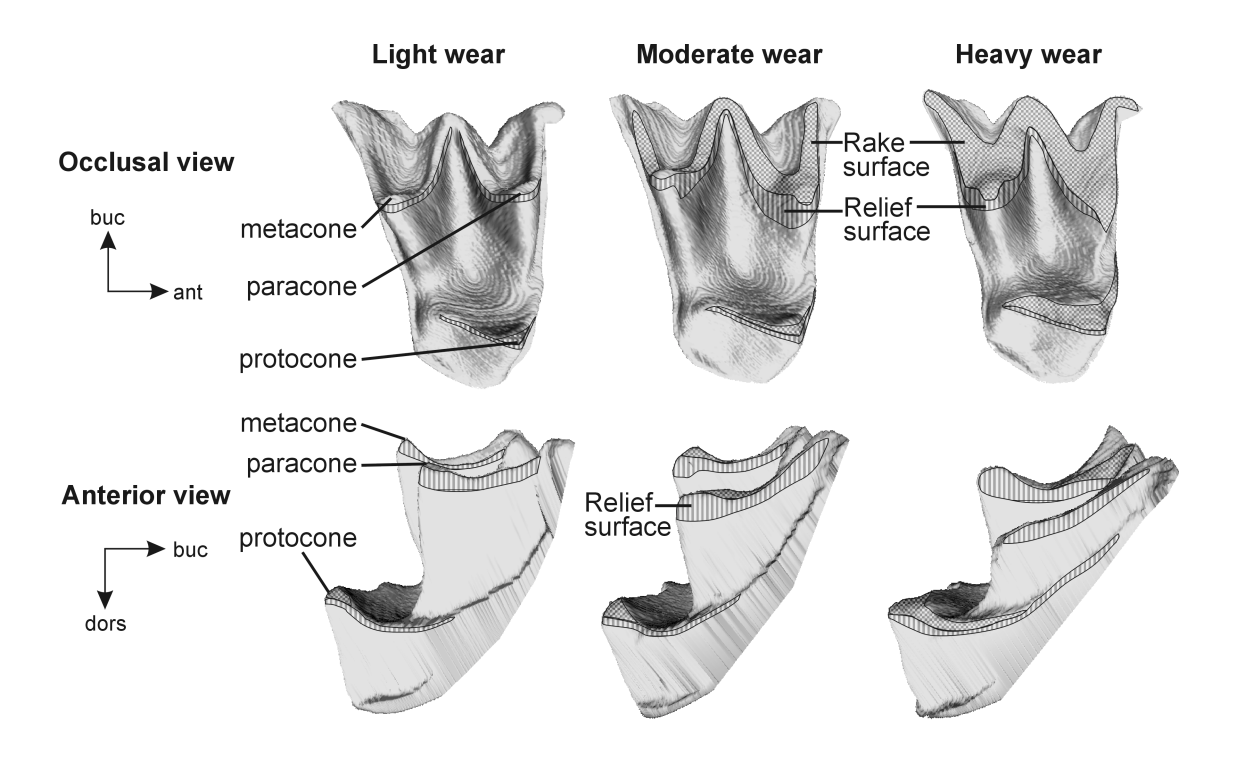


**Fig. 5.3.** Occlusal and anterior views of the right upper second molar of *Chalinolobus gouldii*. Three wear states are shown: light (C3704), moderate (C18142) and heavy wear (C3750). Wear on rake surface is shown by dotted area; wear on relief surface by vertical lines. Abbreviations: ant, anterior; buc, buccal; dors, dorsal.

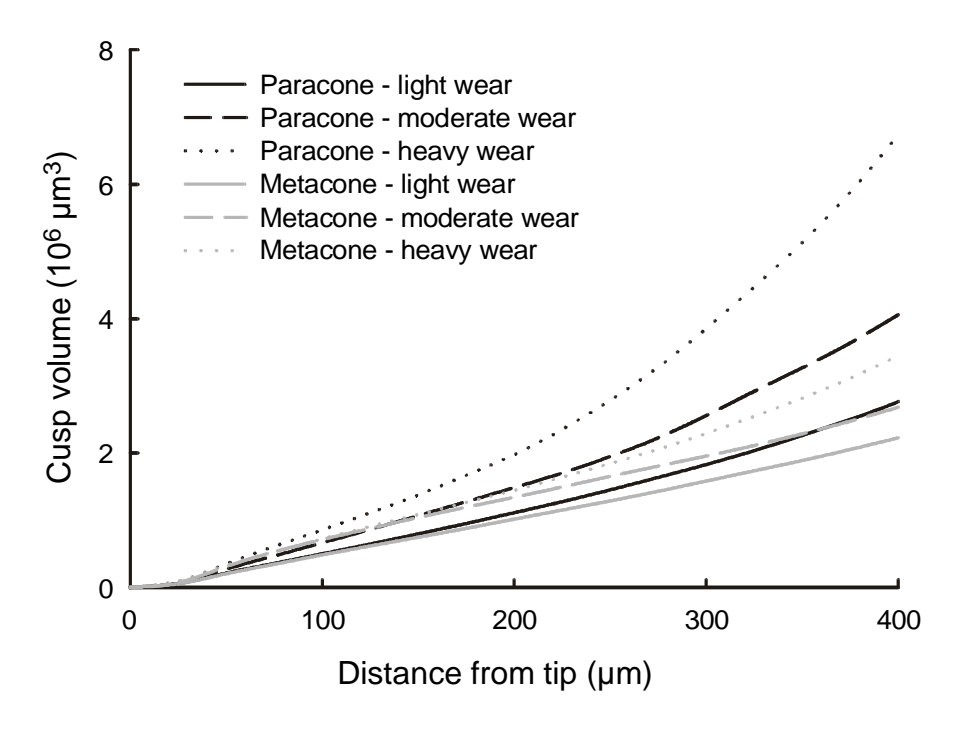


**Fig. 5.4.** Cusp sharpness for the first 400 μm from the tip of the paracone and metacone of upper molars for three wear states in *Chalinolobus gouldii*.

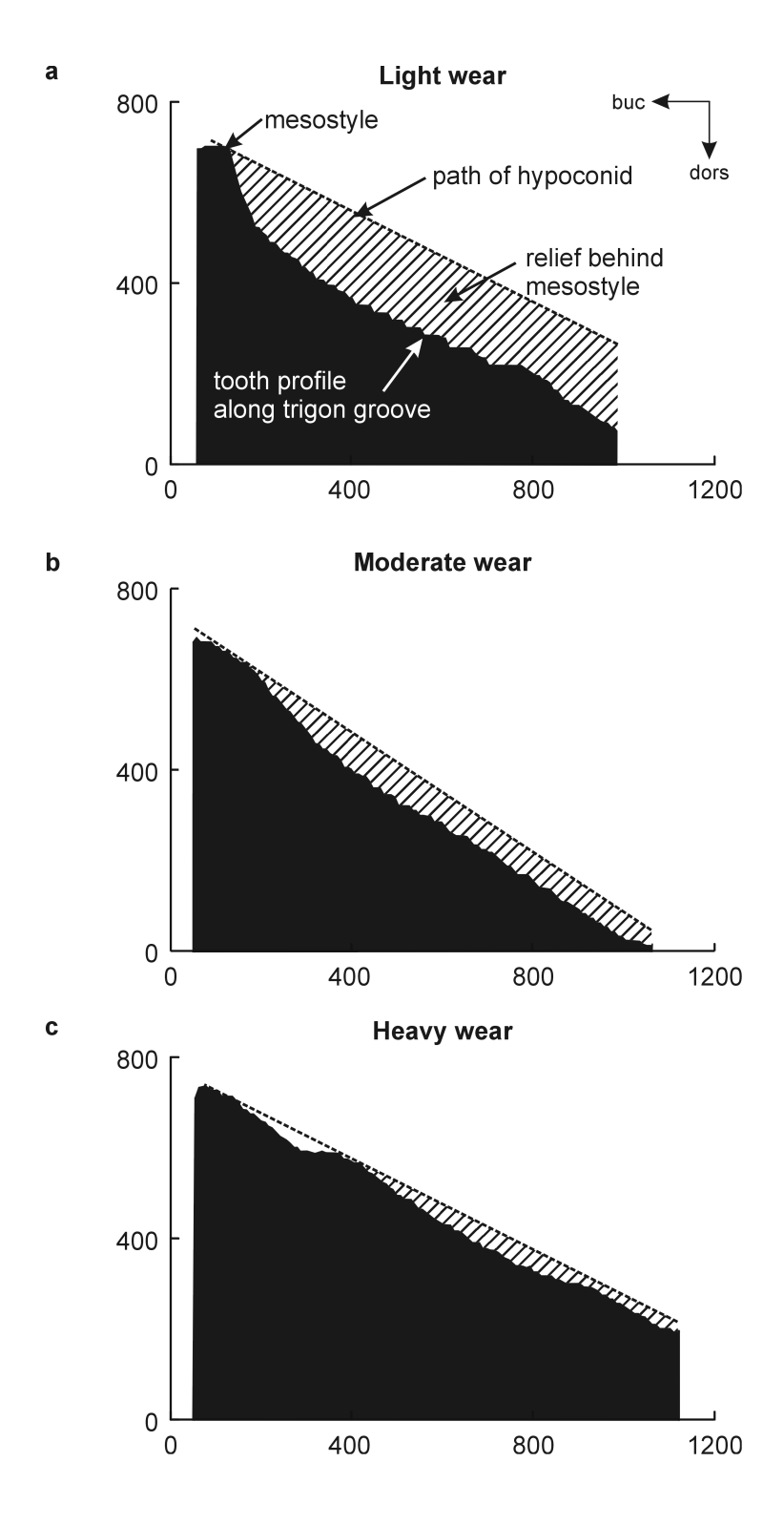


**Fig. 5.5.** Changes in cusp occlusion relief behind the mesostyle for three wear states in *Chalinolobus gouldii*. Black figure is profile of tooth surface along trigon groove; dashed line signifies path of occluding hypoconid (occlusal vector); hatching signifies relief behind mesostyle. a) Light, b) moderate and c) heavy wear. Axes measurements in μm.

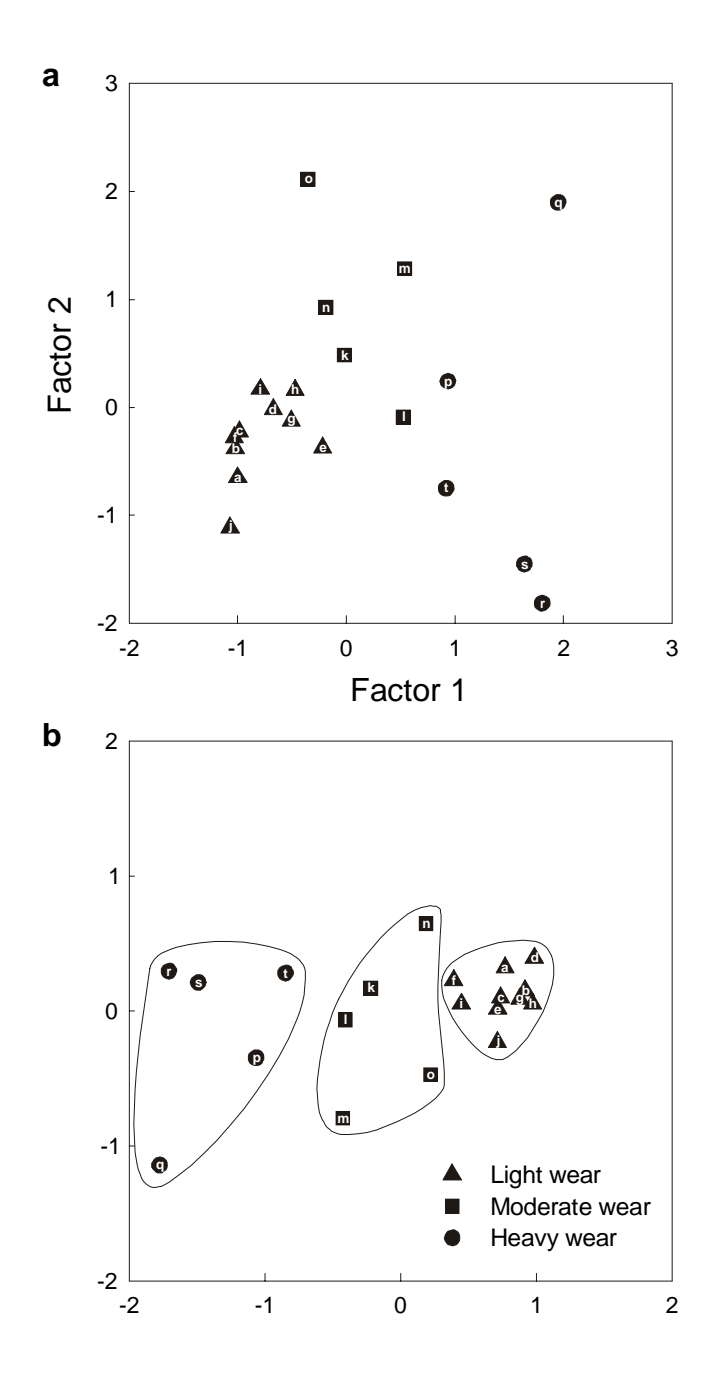


**Fig. 5.6.** a) PCA (Factor 1 vs Factor 2) and b) 2-D NMDS plots for all functional parameters for three wear states in 20 individuals of *Chalinolobus gouldii*. Letters indicate individual specimens: a-j, light wear; k-o, moderate; p-t, heavy.

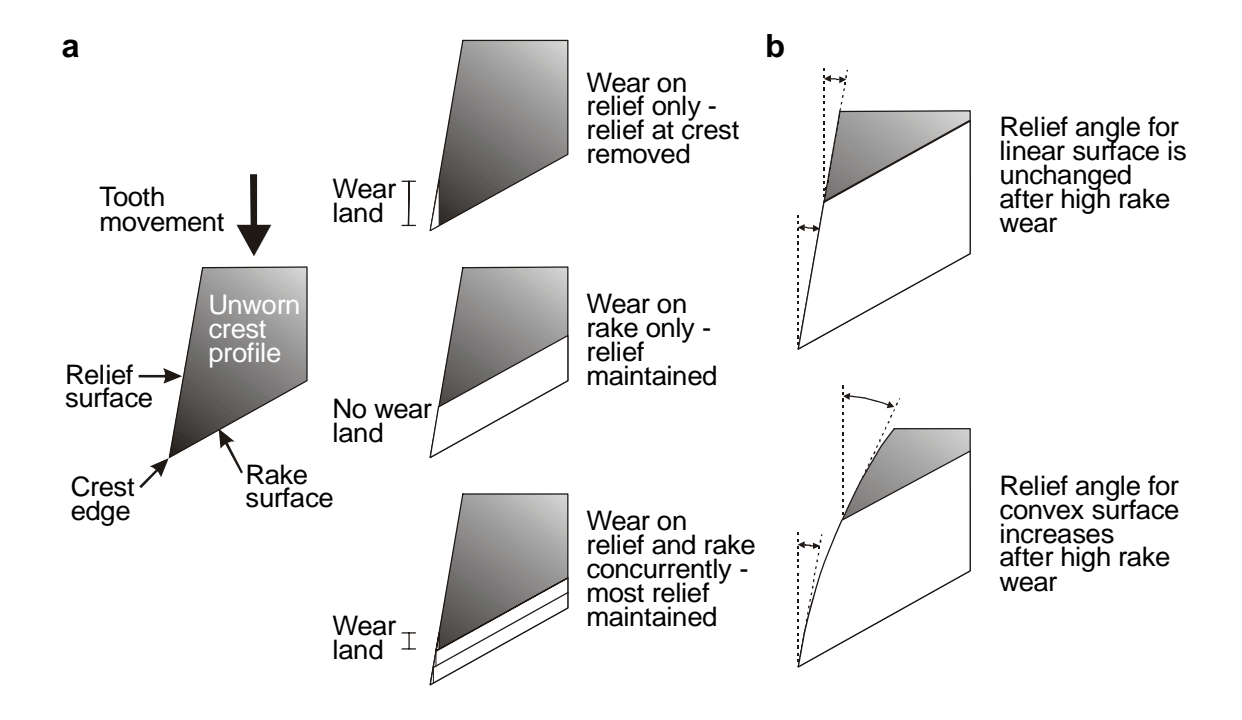


**Fig. 5.7.** a) The effect on the relief behind a crest of relative wear on the rake and relief surfaces. If wear only occurs on the relief surface, then relief behind the crest is removed (as represented by a large wear land). If wear only occurs on the rake surface, relief is maintained. For the more realistic situation where wear occurs on both the rake and relief surfaces concurrently, substantial relief (indicated by small wear land) is maintained. b) Relief angle is maintained after wear on rake surface for a linear relief surface but increases if relief surface is convexly curved. Tooth profile is represented by shaded areas; unshaded areas represent tooth removed by wear.

#### 5.5. Discussion

# **5.5.1. Functional parameters**

The nine functional parameters of crests and cusps measured in this study have a predictable influence on the function of teeth, therefore the changes in tooth shape that result from wear can be assessed, most often directly in terms of force or energy required for a component to function. Changes that occurred following heavy wear that would lead to an increase in the force and/or energy required are: larger radius of curvature for cusp tips and crest edges (tip and edge sharpnesses); larger volume of a cusp for a given distance from the tip (cusp sharpness); diminished relief behind cusp occlusion points (cusp occlusion relief); decreased rake angle (from positive to negative); increased wear land behind three crests; decreased volume behind crests; and decreased flow of material off rake surfaces (fragment clearance). The effect will perhaps be largest for rake angle, which changed by approximately 60° in all of the crests examined – a significant difference in the forces required to fracture plant material occurs between blades with rake angles of 0° and 30° (N. Aranwela, *personal communication*). Individuals of the same wear state clustered in the NMDS plots (Fig. 5.6b), and significant differences between lightly, moderately and heavily worn molars were found in the ANOSIM analysis.

In contrast to this, a decrease in the force to function would result from the larger approach angle of three of the four crests due to increased mechanical advantage of the crests. There was no significant change in wear land for postparacrista, relief angle for all crests and approach angle for premetacrista. Change in capture area is not as straightforward to interpret: the removal of the entire area of capture would diminish function, but a large increase in capture area will require greater forces and not necessarily improve overall function. There was no significant change in capture area for three of four crests.

Overall, it would be expected that the function of these teeth would deteriorate significantly with wear, requiring more force and energy to divide food. There are two independent lines of evidence that support the prediction that increased force and energy will be required. Insectivorous shrews increase the efficiency of the jaw mechanics with age, increasing the available bite force (Carraway *et al.* 1996; Verts *et al.* 1999a). It was only presumed in these studies that worn teeth were less effective at dividing food. Wear scratches on the enamel relief surface of crests appear to be deeper or wider at higher wear states of *C. gouldii* (*unpublished data*). Deeper or wider scratches may require a greater force to produce (Teaford 1988; Ungar and Spencer 1999; although see Maas 1994 for an

alternative view), supporting the proposal that greater force is necessary for worn teeth. Other possible explanations for deeper scratches include a change in enamel structure that makes it easier to scratch at greater depths into the tooth or further down the relief surface (e.g. different hardness or structure at various enamel depths; Ferreira *et al.* 1985; Maas 1993).

There are some important implications of decreased tooth efficacy with wear. Greater energy and possibly time (in number of chews) must be expended in dividing food, leaving less time and energy for other important biological processes, including food searching and gathering, and social interactions (Lanyon and Sanson 1986; Logan and Sanson 2002; McArthur and Sanson 1988). Carraway *et al.* (1996) concluded that older animals must switch to a diet of softer food. Their search for such a dietary shift assumes that the worn teeth have retained the ability to divide 'soft' food; however, worn teeth may be equally ineffective in dividing 'soft' and 'hard' foods. Increases in efficiency of jaw mechanics would then be more important, as were found to occur in shrews (Verts *et al.* 1999a).

The majority of the parameters used in this study have been at least alluded to in the functional dental literature. Lucas (1982) clearly explained the significance of tip sharpness to cusp function and measured it on human cusps by fitting conic sections to cusp profiles. It has since been measured in bat canines (Freeman and Weins 1997) and lemur molars (Yamashita 1998). Both tip sharpness and cusp sharpness were shown to be significantly related to the force and energy for a cusp to function (Evans and Sanson 1998). Rake and relief are common terms in the literature of engineering tool design. They have previously been briefly outlined or described by some authors (e.g. Osborn and Lumsden 1978), but apparently no attempt has been made to measure these parameters. The concept of approach angle has been discussed previously in terms of mechanical advantage (Abler 1992; Evans and Sanson 1998) and its functional significance demonstrated for model teeth (Worley and Sanson 2000), but the term was not used (and has been indirectly referred to elsewhere in the form of 'point cutting'). The importance of capture in bladed systems has been recognised for a long time (e.g. Abler 1992; Freeman 1979; Van Valen 1969) but attempts have rarely been made to quantify it in the various tooth forms in which it occurs. Popowics and Fortelius (1997) measured edge sharpness of crest profiles from a variety of mammals by fitting a circle to the curved part of the profile (see Chapter 8 for further discussion). Fragment clearance has been included previously in analyses of tooth function (Frazzetta 1988; Sanson 1980; Seligsohn 1977). No reference to relief behind points of cusp occlusion has been found in the dental literature, but this can be considered merely a specific instance of relief.

Crompton *et al.* (1994:330) were under the impression that the angle between the 'vertical shearing surfaces and horizontal occlusal surfaces' (the relief and rake surfaces respectively) of a crest are almost always a right angle. In fact, more efficient cutting will be produced if this angle is minimised, which will increase the rake angle of the crest. They also conclude that cutting efficiency will be decreased if the cutting edges are rounded, due to the lack of the right angle between the rake and relief surfaces. It is true that the efficiency of the crest will be decreased, but it is more correctly because such rounding will decrease edge sharpness (increase the radius of curvature of the crest edge) and create negative rake on the crest, which will tend to force crests apart when food is between them.

#### 5.5.2. Crest size

Crest size or length has been used as an indicator of crest function in previous studies, and it is therefore useful to compare any change in crest length due to wear with alterations in the functional parameters discussed above. In general, 3-D length of crests has been used as a surrogate for function. The 3-D length of crests did not significantly change with heavy wear (sum of 3-D lengths of all ectoloph crests: light wear 3080.3  $\pm$  88.0  $\mu$ m; moderate 3141.7  $\pm$  136.6  $\mu$ m; heavy 3136.2  $\pm$  109.3  $\mu$ m; Kruskal-Wallis test statistic = 0.509; p = 0.775).

The length of a cut made by a crest is another good representation of the size of a crest, i.e. the two-dimensional length of the crest when projected onto a plane perpendicular to the occlusal vector (see Fig. 2.6, p. 46). A shorter 2-D crest length indicates that the effective size of the crest has decreased, as it will now divide less food with one stroke. 2-D crest length did on average decrease by about 10% (light 2335.4  $\pm$  81.7  $\mu$ m; moderate 2346.2  $\pm$  89.4  $\mu$ m; heavy 2039.9  $\pm$  123.4  $\mu$ m) but this was not significant (Kruskal-Wallis test statistic = 4.669; p = 0.097). Results were very similar if crest length was standardised according to tooth length.

Therefore, a comparison of function based solely on crest length would detect no change in shape or function with the extreme alteration in molar shape with wear that occurs in *C. gouldii*. This substantial change is displayed very clearly, though, by the decrease in effectiveness in the majority of the tooth components according to the nine functional parameters.

# 5.5.3. Shape and function maintenance during wear

Despite the noticeable change in tooth shape that occurs with wear, several of the features retain good functional aspects even after heavy wear, or even verge upon improvement. The design means that the teeth will retain many aspects of good functional shape longer than may be expected.

**Food capture.** A concave crest is able to maintain its shape to some degree merely through its use. If the entire crest cavity is filled with food and all of the food is divided, then the middle of a concave crest will divide more material than the ends, and may be under greater pressure (or certainly under pressure for a longer time) from the food. Wear on the rake surface of a crest by food abrasion is at least partly determined by the amount of material it divides and by the pressure exerted on the surface, so greater wear will occur in the middle compared to the ends. The thickness of enamel along the length of a crest will influence how it wears. Thinner enamel on the middle of crests compared to the ends will cause the middle to wear more rapidly compared to the ends. Enamel thickness along a crest does not appear to have been quantified before, but in the specimens of C. gouldii examined it appears thicker towards the cusp ends of the crests (the lingual end of ectoloph crests; also found in several other microchiropteran species, e.g. Hipposideros diadema, and appears to be the case from micro-CT scans of Eptesicus sp. molars; personal observation). The greater amount of dentine that must be worn at the buccal end of the crests would have the same effect as the thicker enamel on the other end, reducing the rate at which the height of the crest is decreased. Both of these parameters will preserve or possibly even increase the concavity of the crest, as was found in the worn crests of C. gouldii.

**Cusp sharpness.** Wear in the centre of the crests on two-crested cusps (such as the paracone and metacone) also maintains higher cusp sharpness to some extent. Thicker enamel on the rounded, lingual faces of the cusps will mean the height of the cusp is maintained, and greater wear on the rake surface of the adjoining crests will maintain high cusp sharpness. To a limited extent, this occurs on the upper molar cusps, where in some instances a highly worn cusp has higher cusp sharpness than moderately worn cusps.

**Relief**. The incidence and ratio of wear on the rake and relief surfaces will influence the amount of relief of a crest, particularly the size of the wear land (Fig. 5.7a). Wear on only the relief surface would cause the majority of the relief to be removed, increasing the wear land. If the rake surface were also worn, then no wear land would be produced, and relief would be preserved. If sufficient wear occurs on both the rake and the relief surfaces, then relief will be maintained. *Chalinolobus gouldii* molars have a high

degree of wear on the rake surface relative to wear on the relief surface, reducing the wear land on the relief surface and maintaining relief.

From this, it appears that some abrasive wear is beneficial in maintaining relief of the tooth. There is substantially more wear on the rake surface than the relief surface of these teeth. This may be due to a greater force being applied to the rake surface, or that the applied force is perpendicular to the rake surface compared to almost parallel to the relief surface. The component of the force directed into the tooth is therefore smaller on the relief surface, resulting in the removal of less dental material. The relative enamel thicknesses (thin on the rake surface and thick on the relief) would also contribute, so that enamel on the rake surface is rapidly removed, particularly for areas close to the crests. Once the enamel is breached, the differential hardness of dentine and enamel, along with the microstructure arrangement of enamel prisms (where they are perpendicular to the force on the relief surface and so resist wear to a greater extent; Stern *et al.* 1989) would also play a part.

A non-zero relief angle can be maintained during wear when the relief surface is straight, and will even increase given a convex curvature of the relief surface (Fig. 5.7b). Relief surfaces, particularly those on the lingual side of upper molar cusps, are either straight or slightly concave, so that relief is maintained as tooth wear progresses.

**Edge sharpness**. The edge sharpness of crests was found to significantly decrease with wear. The substantial change in other parameters of crest shape (such as rake angle) may have been expected to produce a major change in edge sharpness, but the small increase in radius of curvature (from 14 to 24 μm) suggests that there are characteristics preventing major change in edge sharpness. These are likely to include enamel microstructure. An enamel edge will wear more slowly than the surrounding dentine, resulting in a ridge of enamel higher than the dentine (Rensberger 1973). This will produce a sharper cutting edge compared to a crest of dentine only. Enamel prisms in the relief surface of crests are arranged parallel to the rake surface, so that when prisms are removed by wear a sharp edge is retained (as has been found in the opossum; Stern *et al.* 1989).

All of these features point to controlled wear in tribosphenic-like molars. Wear cannot be avoided, but teeth can be shaped to influence which regions of the tooth wear more than others. Proportions of cusps and crests, and distribution and structure of enamel, can encourage wear in particular areas during use, allowing function to be maintained.

# 5.5.4. Functional relationships of attrition and abrasion of crests

Two types of wear surfaces result from tooth wear (Every and Kühne 1971; Kay and Hiiemae 1974; Osborn and Lumsden 1978): abrasion wear surfaces, which are

relatively rough and rounded with non-parallel scratches; and attrition wear surfaces, which are essentially planar, with a polished appearance and largely parallel scratches. Abrasive wear is thought to be the result of tooth-food contact, and attrition chiefly due to tooth-tooth contact, with the scratches caused by hard particles between the tooth surfaces (Teaford and Walker 1983a, b).

When these two types of wear are related to the dental surfaces on which they occur, we find that there is a constant relationship between the function of a crest surface and the type of wear that occurs on it (Figs 5.3 and 5.7). When two crests occlude, no tooth-tooth contact occurs on the rake surface of the ectoloph crests: all wear must be due to tooth-food contact, producing a rough 'abrasion' wear surface. Conversely, where relief surfaces contact the relief surfaces of opposing crests, wear due to tooth-tooth contact occurs and the result is planar 'attrition' wear surfaces. It may be that a small amount of dental material is removed from the relief surface through abrasion. However, due to the very clear attrition facet just behind the crest edge, and the observation that there is very little evidence of wear (either by tooth-food or tooth-tooth contact) on the relief surface beyond the attrition facet, we can conclude that abrasion wear on the relief surface is probably inconsequential to any change in tooth shape with wear.

The disparity in the form of wear is due to the differences in function of the surfaces on which they occur. Therefore, the function of a surface can be determined by the type of wear that is found on it. Attrition wear can only occur on the relief surface of a crest, so a crest surface with attrition wear must be a relief surface. One without attrition wear and with an abrasion wear surface will almost certainly be a rake surface. This has been implicit in previous reconstructions of tooth occlusion (e.g. Butler 1952; Crompton 1971; Crompton and Hiiemae 1970; Greaves 1973; Mills 1966, 1967), but the specific correlation with the functional rake and relief surfaces has apparently not been made.

The situation is slightly different in herbivorous forms, such as selenodont artiodactyls. These forms differ from the tribosphenic type considered here in that the relief surface is composed of both enamel (at the crest edge) and dentine (further away from the crest edge; see Chapters 8 and 9). The dentine basin behind the enamel attrition facet on the relief surface will only be worn by abrasion of food, as tooth-tooth contact is not possible due to the shape of the crests. However, any attrition wear will only occur on a relief surface and so can allow the identification of the relief surface. In addition, the relief surface of one crest is often contiguous with the rake surface of the adjacent crest. However, there will still be no attrition wear on this rake surface, which is usually the lateral surface of an enamel crest, either on the side of the tooth or next to a dentine basin.

The identification of relief surfaces according to this definition will be more difficult in some herbivorous teeth where the attrition facet may be removed by large amounts of abrasion (Popowics and Fortelius 1997).

#### **5.6.** Conclusions

Previous comparative measures of function (such as those based on crest length) do not incorporate differences in function according to tooth shape, and are not particularly useful for comparing worn teeth. Other more recently developed methods also lack ability to explain the function of individual cusps and crests. The powerful functional measures elaborated and measured in this study allow the determination of changes in function with the change in shape resulting from wear in tribosphenic-like teeth.

Wear is a significant process that must be taken into consideration when examining tooth form and function. It must have been a highly influential selective force in shaping teeth. Wear is an additional constraint on tooth shape that may not be inherent in unworn tooth function, and should be considered when discussing the apparent function of unworn teeth. Although not as adapted as other tooth forms to cope with high wear and maintain function (e.g. selenodont molars), there are significant features of the teeth that mean that some functional features are retained with wear. Tooth shape may be maintained through geometrical relations of wear or through specific morphological adaptations.

Attrition and abrasion can be considered as wear on the relief and rake surfaces of tribosphenic-like crests respectively. The differences in function of these two surfaces account for the differences in wear patterns.

# Chapter 6. The Material Properties of Insects in Relation to Insectivory: Cuticle Thickness as an Indicator of Insect 'Hardness' and 'Intractability'

## 6.1. Introduction

Invertebrates, like all organisms, are faced with various mechanical challenges that they must meet throughout their lives. Activities such as locomotion (including flight), feeding and burrowing exert a diversity of stresses and strains on the organism, and this is reflected in the variety of materials that have evolved to cope with these functions (e.g. the abdominal membrane of Rhodnius larvae that undergoes plasticisation: Reynolds 1975; extreme extensibility in the locust intersegmental membrane due to stress softening: Vincent 1975; increases in mandible hardness by incorporation of manganese and zinc: Quicke et al. 1998). It is possible that predation by large animals has been influential in the mechanical design of some insects, particularly in life forms such as some beetles that forage on exposed surfaces (e.g. some bats are unable to bite into 'hard' beetles; Goldman and Henson 1977). Regardless of whether that is the case, small mammalian insectivores, such as microbats and shrews, chew their food very finely and in order to do so must deal with the biomechanical properties of the invertebrate. In this thesis, insectivores are considered to consume any invertebrates, not just insects. It is firmly established with a strong theoretical foundation that the biomechanical properties of foods influence the morphology and function of the feeding apparatus of an extremely wide range of organisms (e.g. fish: Wainwright 1996; mammals in general: Turnbull 1970; ungulates: Radinsky 1985; primates: Lucas 1979; Rosenberger and Kinzey 1976; kangaroos: Sanson 1980; insectivores: Freeman 1979; insects: Acorn and Ball 1991; Peeters 2002). Of particular interest to this study are the differences in skull and dental morphology that correlate with dietary 'hardness' found among insectivores (Dumont 1995; Freeman 1979; Strait 1993c).

The biomechanical properties of the bodies of invertebrates have been examined using the concepts of materials engineering. Fundamental to the understanding of materials are the concepts of stress and strain: stress is the load per unit area of the material, and strain is the amount of extension under load per unit length (Gordon 1976). Derived from these are the material properties of strength, which is the resistance of a material to crack initiation (materials with high resistance are strong, those with low resistance are weak), and toughness, the resistance to crack propagation (with tough or fragile as the extremes;

Sanson *et al.* 2001). Stiffness is the resistance to deformation of a material in its elastic range where there is non-permanent deformation (stiff or pliant as the extremes), while ductility (or plasticity) is the resistance to deformation in its plastic range where there is permanent deformation (brittle or ductile as the extremes; Strait and Vincent 1998). Diversity is apparent in all of these quantities in invertebrates. On the whole, biological materials are also viscoelastic, so that their biomechanical properties depend in part on a temporal component, such as the speed of loading (Vincent 1990). Therefore, measurements and characterisations of biological materials in terms of strength, toughness, stiffness and plasticity are complicated by the viscoelastic element of their properties.

Measurements of the material properties of insects are rather limited, and tend to focus on unusual adaptations rather than the more general properties of insects as a whole (Hillerton 1984). This is because the topic is normally addressed from the insect's perspective rather than how the biomechanical properties affect a predator. Fracture of all components of an invertebrate, including internal organs and the cuticle, must be considered if we are to assess the mechanical challenges of insectivores.

Components of invertebrates such as internal organs and intersegmental membranes are pliant, ductile and relatively weak, whereas sclerotised exoskeletons, including mandibles, are stiff and strong (Hepburn and Chandler 1976; Hillerton 1984; Vincent 1980). The material properties of a component will reflect the mechanical demands placed upon it, so that we might expect tendons and muscles will be strong in tension compared with mandibles that are strong in compression, and many exoskeletal parts to be stiff for support and effective transfer of muscular force.

Most of the work on the material properties of insects has focussed on the cuticle. The insect procuticle, the portion of the cuticle containing chitin, comprises the exocuticle and endocuticle. Two principal mechanical forms are stiff cuticle and pliant cuticle (Hillerton 1984). The exocuticle of stiff cuticle is sclerotised to some extent and has a lower chitin content. Pliant cuticles usually have very little or no exocuticle, and they contain greater amounts of chitin. Pliant cuticles with only endocuticle and sclerotised cuticles with brittle matrices comprise only ~20% of the cuticles surveyed by Hepburn and Joffe (1976); the remainder are more complex. The mechanisms causing sclerotisation are only partly understood, and most likely involve dehydration and increased cross-linking of the protein (Andersen *et al.* 1995), but are not important for this discussion.

## 6.1.1. 'Hardness'

The use of the term 'hardness' to describe the properties of diets, including insects, appears to have an inherent appeal, and it has been used for many years (Dumont 1995,

1999; Freeman 1979, 1981a; Grine 1986; Jolly 1970; Kay 1981; Mohsenin 1970; Strait 1993c; Teaford 1985). In engineering, hardness is quantified by scratch or indentation tests (such as Mohs, Vickers, Brinell and Rockwell; Askeland and Phulé 2003). The results of hardness tests are complex; they may be related to the strength of the material and its resistance to plastic deformation (Hillerton 1984), as is the case for some metals, but on the whole can be considered a surface property rather than a property of the entire structure.

When used in dietary studies, there is rarely, if ever, any explicit correlation between the use of the term 'hardness' and any particular physical property or component. However, there have been several efforts to estimate and correlate the hardness of the diet with various aspects of the biology of insectivores. Freeman (1981a) recognised the importance of biomechanical properties of invertebrates and estimated the hardness of various taxa according to an arbitrary scale from 1 to 5, e.g. Trichoptera and Diptera have a score of 1, Araneida and Lepidoptera 2, Orthoptera and Scorpionida 3, Hemiptera and Hymenoptera 4, and Coleoptera 5. An estimate of the hardness of an insectivore's diet was obtained by multiplying the frequency of each taxon estimated in dietary studies by its hardness score (Freeman 1981a; Rodríguez-Durán et al. 1993). However, hardness was not defined, and the hardness scale was not empirically derived or tested. Also, this method does not allow for heterogeneity of 'hardness' within each taxon, and assumes that the insectivore consumes all components of the invertebrate. Frequently, insectivores such as microbats will cull the hardest fragments from the insect before consumption (e.g. elytra or head capsules). These parts should not be counted in the hardness score of the diet, particularly when molar function is being considered, where only the components that are masticated are relevant. This approach also relies on published estimations of frequencies or relative volumes of invertebrates in the diet, the methods of which have been criticised (e.g. Robinson and Stebbings 1993).

Strait (1993c) considered that hard foods, such as adult beetles, are those that are relatively tough, stiff, strong and brittle, and soft foods, such as moths and larvae, are relatively fragile, pliant, weak and ductile. Hardness was said to 'succinctly characterize the multitude of physical properties described above' (Strait 1993c:392). This conception of hardness is probably more biologically useful and intuitive than the definition used in materials engineering. However, it does not give criteria for quantifying or classifying insects as 'hard' or 'soft' and therefore it is difficult to assess the hardness of a diet, compared to Freeman's (1981a) scheme.

Hillerton (1984) considered that the property of some cuticles that had been described as 'hardness' was actually stiffness. In other instances, strength appears to be

closer to the intention (Jolly 1970; Kay 1981). In normal conversational usage, the closest definition is most probably the resistance to deformation, regardless of whether it is elastic or plastic deformation – any material or structure that deforms easily to an applied force is considered 'soft', and one that does not is 'hard'.

A common technique for the assessment of dietary 'hardness' is the use of durometer-type devices. Several studies have used such tests to measure the force necessary to puncture food items using a manual or spring-loaded punch (Dumont 1999; Kinzey and Norconk 1990; Yamashita 1996). Fisher and Dickman (1993) measured hardness as the force to puncture beetles with a sharp metal cone (following Hill 1985). In the very recently-published paper by Aguirre *et al.* (2003), hardness was measured as the force required to 'crush' food items, indicated by mechanical failure.

From the large number of studies using the term 'hardness' and the immense variety of uses to which it is put, it is easy to agree with Boyer (1987:Preface) when he said that 'There is probably no word in the English language for which so many definitions from so many sources have been offered as the term "hardness". This issue needs to be addressed, and so we will now examine the factors that influence the biomechanical properties of insect biomaterials.

#### **6.1.2.** Materials and Structures

At this point it is useful to consider the distinction between a material and a structure, as this influences how we analyse the mechanical properties of an object. In engineering, a material is either a pure substance or an alloy that can be considered essentially homogeneous in composition (Niklas 1992), and a structure is often defined as something that supports a load or resists a force (Francis 1980; Gordon 1978; Megson 1996). The importance of the distinction between material and structure has been recognised for a long time (Jeronimidis 1980; Strait 1993c; Vincent 1980; Wainwright *et al.* 1976), but it has often not been specified clearly what a structure has that a material does not.

A significant portion of engineering involves dealing with the 'essential design problem' (Felbeck and Atkins 1984). For instance, a load-bearing part must be designed with the ability to transmit a load *P* between two points that are *L* distance apart, and the part cannot be higher or thicker than *H*. In terms of performance, there will be particular requirements of the part, such as the maximum deflection that can be tolerated. Rather than test all possible materials and designs for such a part, the most economical method is often to use 'material' properties such as strength and stiffness in the design process. Material properties describe the behaviour of the isolated material standardised to cross-sectional

area, length and shape, and are dictated by the properties and arrangements (including imperfections and movement) of its constituent atoms, ions and molecules (Askeland and Phulé 2003). The part can then be modelled given these properties, and predictions on the thickness required to sustain the load and the amount of deformation that will occur can be made.

The process of designing a part is essentially the designation of its size and shape. Once this is done, the behaviour of the part is a result of the material properties and its particular size and shape. The size and shape of the object can be considered to be structural properties of the object. In this thesis, a 'material' is considered to be dimensionless (without size or shape), and merely the abstracted properties of its constituents. It does not have structural properties and therefore is not a structure. Steel, glass and polyethylene can be considered 'materials', but once the dimensions and shape of an object are defined, a part constructed of steel or ceramic has structural properties, and the load at which it fails and the amount of deflection it incurs under a load are in part dependent on those structural properties.

Structural properties are largely the geometric or morphological components of the structure, including the thickness and distribution of material within a structure, which may be quantified as the second moment of area. In engineering, structural properties can often be successfully analysed in terms of beams, columns, shafts, struts, cables, arches and trusses, using concepts such as beam theory (Megson 1996; Niklas 1992). The ultimate mechanical performance of an object can only be understood through consideration of both the material and structural properties (see Niklas 1992 for an equivalent view). A prime example of this is flexural stiffness, which takes into account the stiffness (elastic modulus) and shape (second moment of area) in quantifying the resistance of a part to bending (Niklas 1992).

Where strength, stiffness and toughness are parameters that are used to summarise the properties of materials, for simplicity, we can think of the structural strength, stiffness and toughness as being the properties that describe structures. What we actually mean is the amount of force required to cause the structure to fail, the extent to which it deforms, and the amount of energy required to do so. This differs slightly from the usual engineering terminology, where the force required for a structure to fail is often called its breaking load (Gordon 1978; Niklas 1992). Resilience is used in engineering to describe the ability of a structure to store strain energy and deflect elastically under a load without breaking (Gordon 1978). However, in many instances we are interested in a structure's ability to resist any deformation, either elastic or plastic, which we may loosely call its structural

'stiffness', which of course is not strictly correct. For the final structural measure, there is very little difference between the concepts of 'toughness' and 'structural toughness' as they both quantify energy to fracture, although material toughness is standardised by the area of new surface.

The most significant aspect of structures compared to materials is that their behaviour can be abundantly more complex than isolated materials due to the addition of structural properties and the potential of combining more than one material. Pure materials cannot be strong, stiff and tough – there is a trade-off between these properties, as a material that is stiff and strong more easily transfers the stress onto fewer bonds and so requires little energy to fracture it (Atkins and Mai 1985; Gordon 1978). A material is therefore unable to achieve this Holy Trinity of materials engineering of high strength, stiffness and toughness, but it can be achieved in a structure as high structural strength, stiffness and toughness. Of course, in biology, the materials and loads under consideration differ from those of modern engineering; stiffness may not always be as important, as a pliant material may be more appropriate or applicable to certain situations than a stiff one (Vincent 1998).

Most considerations of the biomechanical properties of foods, particularly invertebrates, attempt to understand diets in terms of concepts that are specifically applicable to describing materials, e.g. the material properties of strength, stiffness, toughness, yield strength and Poisson's ratio (Vincent 1990). However, the far more complex structures a biologist must deal with often do not yield easily to an analysis based on these material definitions. It is necessary to attempt a more complete biomechanical description of these foods as structures, which must include the description and consideration of their structural properties.

As an example of this, an insectivore obtaining and trying to consume prey is not just dealing with the intrinsic strength (N m<sup>-2</sup>) and toughness (J m<sup>-2</sup>) of the materials of which the prey is constructed, but the composite of these properties with the shape, size and arrangement of the constituent materials. That is, it is the absolute force and energy that must be supplied by the predator to initiate and propagate cracks through the structure that are important. This means that a prey defended by a thin wall of strong, tough material may be equivalent to one with a thick wall of weak, fragile material with regard to a predator: the stress and work to fracture the food could be the same for the two scenarios (Sanson *et al.* 2001). In this instance, the strength and toughness (as standardised for cross-sectional area and elongation, or new surface area created respectively) may tell a different and misleading story compared to the structural strength and toughness. It may be

predicted that 'strength' and 'structural strength' would be correlated, because selection for increased resistance to high force may lead to a change in the material properties (strength) as well as the amount of material present (thickness), but this is not necessarily the case.

# **6.1.3.** Cuticle Structural Properties

Foods previously considered 'hard' can really be considered 'strong' and 'stiff' in the structural sense that a great deal of force and energy is required to deform or fracture the object. 'Hard' invertebrates such as beetles contain components composed of materials that are relatively strong, stiff and tough, but structural mechanisms (such as a thickening of the structure) may be the main cause for the large force required. The behaviour of the cuticle, and also the entire insect, is a result of the structural mechanisms operating at both the cuticle and whole organism level.

As a description of the behaviour of a structure, 'hard' is inadequate. For metals at least, hardness may be directly proportional to yield strength ( $\sigma_y$ ) or tensile strength ( $\sigma$ ) (Ashby and Jones 1996; Askeland and Phulé 2003; Lowrison 1974), and does not really take into account stiffness or toughness. 'Hardness' as measured by materials engineers can be considered to be partially a structural property, as the extent of deformation in an indentation test will be influenced by the material and structure lying underneath and next to the indenter (Ashby and Jones 1996). Due to the baggage of past usage to describe materials, the term 'hard' fails to sufficiently encompass the complex behaviour of structures.

Therefore, structures that require large forces for crack initiation, large amounts of energy to propagate cracks and large forces to create deformation (either elastic or plastic) and eventual fracture can be said to be 'intractable' (difficult to manage or handle, the negative of tractable, from Latin *tractare*, to handle, manage). Intractability is introduced here to describe the extent to which a structure has achieved high structural strength, stiffness and toughness.

To aid in the characterisation of dietary items as tractable or intractable, a distinction is made between 'strength' (defined as the 'maximum stress at fracture', which is standardised for the cross-sectional area of the material) and 'contact stress to fracture' (which is force divided by the area over which the force is applied, i.e. area of contact between tooth and food). Therefore, intractable foods can be said to have a high contact stress and work to fracture, rather than a high 'strength' or 'toughness', compared to tractable foods. These are measures of the structural strength and toughness of the food, respectively. From measurements of the properties of various insect components (Hepburn and Chandler 1976; Hepburn and Joffe 1976; Hillerton 1984; Vincent 1980, 1990), it is

most likely that the main difference in the intractability of invertebrates is due to differences in the cuticle. More specifically, I hypothesise that the stress and work to fracture are proportional to the thickness of the cuticle. This assumes that the biomechanical properties of the internal organs of intractable and tractable invertebrates are relatively similar.

To some extent, this correlation can be inferred directly from the structure of the cuticle. For a material of a given strength, increasing the thickness of the material will increase the stress required for fracture. The cross-sectional area of material over which the force is applied is increased, thereby decreasing the average stress in the material. Increased cuticle thickness is most probably achieved by the addition of layers of chitin, with the chitin fibres in adjacent layers differing in orientation. The greater number of layers and weak interfaces or boundaries allowing controlled debonding of adjacent layers will also increase the work to fracture and hence toughness of the cuticle.

This hypothesis will be tested by measuring the contact stress and work required to fracture in punch tests for invertebrate cuticles of varying thickness. Punch tests have been criticised because the precise mode of failure is not known and they do not examine a specific material property (such as strength, stiffness or toughness) (Vincent 1992a, b). However, this is exactly why this technique is advantageous for examining the combined effect of the material and structural properties. Aranwela *et al.* (1999:382) compared a number of biomechanical tests and concluded that punching correlated well with biomechanical aspects of leaf biology, and that such tests 'may be detecting ecologically significant variation in the fracture properties of leaves'. Punch tests have also been found to be useful in examining the biomechanical basis of sclerophylly in plants (Edwards *et al.* 2000). The concept of 'dietary hardness' as previously used may be considered akin to measures of sclerophylly in plants – an ill-defined concept that has been imprecisely used in describing the biomechanical properties of complex biological materials (Edwards *et al.* 2000). This study aims to achieve a more comprehensive and mechanically meaningful understanding of the diversity of the biomechanical properties of insects.

Punch tests measure the punch strength (force/area of punch; N m<sup>-2</sup>) and work to punch (force × displacement/area of punch; J m<sup>-2</sup>). These are the stress and the work required to initiate and propagate fracture through the cuticle, and are therefore measures of the intractability ('hardness') of the cuticle. The above hypothesis can then be restated as punch strength and work to punch will be positively correlated with cuticle thickness, and these estimate different aspects of intractability. The objective is not to measure the

intrinsic strength or fracture toughness of the insect cuticle, but the absolute stress and work required to fracture cuticle of different thickness.

It is fortunate that the cuticle, which most probably displays the greatest diversity in intractability within invertebrates, survives the passage through the gut of a living insectivore. Although chitin digestion has been shown in some insectivores (Jeuniaux 1961; Jeuniaux and Cornelius 1978; Sheine and Kay 1977), a large proportion of insectivore faeces is composed of cuticular fragments from ingested insects, and so is available for analysis. Therefore, if the first hypothesis is supported, a measurement of the cuticle thickness in insectivore faeces can be used as an estimate of the quantitative intractability of the diet. Differences in cuticle thickness among samples of bats' faeces will distinguish those species whose prey is largely intractable from those with primarily tractable prey.

The hypothesis of a correlation between cuticle thickness and measures of intractability (punch strength and work to punch) will be tested by punch tests of fresh cuticle of varying thickness. To illustrate the practicality and value of the use of cuticle thickness to quantify the biomechanical properties, the thickness of cuticle in faecal samples of several insectivorous microbat species will be measured.

#### **6.2.** Methods

# **6.2.1.** Biomechanical properties of cuticle

Adult beetles (Coleoptera) and moths (Lepidoptera) were trapped using light traps or picked from an illuminated white sheet by hand in March 2002. They were killed immediately before the experiment using a killing jar containing acetone and weighed ( $\pm$  0.1 mg) with a Mettler AE 166 electronic balance. The use of acetone killing jars has been found to not significantly affect the mechanical properties of insects (Evans and Sanson 1998). Sections of relatively flat cuticle at least 2 × 2 mm were dissected from the insects in the following regions: thorax, abdomen (ventral and dorsal) and elytron (beetles only). All components of the insects that were of sufficient size were tested. Muscle attached to the cuticle was removed using a small paintbrush (Hepburn and Chandler 1980), taking care to avoid scratching the cuticle surface. Cuticle thickness ( $\pm$  1  $\mu$ m) was measured with a Mitutoyo digital micrometer with hemispherical attachments to the micrometer anvils (diameter 1 mm) for measurement of thickness over a small area. Fragments were force-tested immediately after dissection to reduce the effect of dehydration.

Punch tests were carried out on 190 fragments from 17 beetles and 15 moths. Each cuticle fragment was punched using a 0.5 mm sharp flat-ended punch (area 0.196 mm²) with clearance of 0.05 mm with the die on a Chatillon UTSE-2 Universal force tester. Force was applied to the specimen by moving the stage up towards the punch at a constant velocity (~0.3 mm s¹), and the force was measured by a load cell of 25 kg. Force and displacement of the punch were captured at 100 Hz using DT Access v. 6.02 (Peter Fell, Monash University). The resulting force-displacement data were analysed using Leaf v. 3.7 (Murray Logan, Monash University) which subtracted a blank run every 10 punches to remove the effect of friction in the machine. The software was also used to obtain the force to punch (N), punch strength (N m²), specific punch strength (N m² m³), work to punch (J m²) and specific work to punch (J m² m³) following Sanson *et al.* 2001) required to punch cuticle fragments.

Multiple fragments from the same insect were force-tested as limited samples were available in March, and so the fragments from the same insect may not strictly be considered independent from one another. However, each fragment was punched and its thickness measured and therefore each represents a separate determination of the relationship between thickness and punch parameters. To see if this had any effect on the conclusions, all statistical tests were carried out for random samples of one fragment per insect (giving a total of 32). No difference was found in the conclusions, and so the total sample of 190 fragments was used.

Data from the force-testing experiments (force to punch, punch strength, specific punch strength, work to punch and specific work to punch) and cuticle thickness were logged to base 10. Simple linear regression was carried out using Systat for Windows v. 10.0 (SPSS, Inc.). Force-testing data were regressed against cuticle thickness for all cuticle samples, and separately according to insect type (beetle and moth), sclerotisation (unsclerotised or sclerotised) and both insect type and sclerotisation (e.g. unsclerotised beetle cuticle). Significant difference of the regression slope from zero was tested with t-tests, with a p = 0.05 significance level.

## **6.2.2.** Cuticle thickness in bat faeces

The microbat species *Chalinolobus gouldii*, *C. morio*, *Miniopterus schreibersii*, *Nyctophilus geoffroyi*, *Vespadelus darlingtoni*, *V. regulus* and *V. vulturnus* were trapped in harp traps at Rotamah Island, Victoria, Australia on 5-7 February 2000. The bats were kept in a cloth bag for up to six hours after trapping, and faecal samples were collected from the bag. Trapping was carried out under *Wildlife Act* 1975 and *National Parks Act* 1975 Research Permit No. 10000763.

A single faecal pellet was randomly chosen from the faecal sample of each individual animal. A 1-2 mg portion of each pellet was weighed ( $\pm$  0.1 mg) with the Mettler balance, placed in distilled water and teased apart with fine forceps. All fragments of sclerotised cuticle larger than approximately 0.25  $\times$  0.25 mm were separated. Only relatively flat cuticle fragments that were approximately of uniform thickness were used, and so limb segments, head capsules or irregularly shaped fragments were excluded. Wing segments were also excluded.

The cuticle fragments were dried and counted. The thickness of 20 fragments randomly selected from each portion of pellet were measured using the micrometer set-up described in 6.2.1. The median and maximum cuticle thicknesses were calculated.

These fragments may not be considered as strictly independent, as many are likely to be from the same insect. However, if chewing resulted in the cuticle being broken into equal-sized pieces (or if all thicknesses are broken into randomly-sized pieces) then a random selection of the fragments will represent a weighted average of the thickness according to the amount of cuticle of that thickness in the diet. In an attempt to reduce the affect of any bias due to this, the median rather than the average cuticle thickness was calculated for each individual, but this will have no effect on the maximum thickness.

## 6.3. Results

The punch strength, specific punch strength, work to punch and specific work to punch cuticle plates of varying thickness are shown in Fig. 6.1. Punch strength and work to punch were significantly positively correlated with cuticle thickness except for unsclerotised beetle cuticle (Table 6.1; Fig. 6.1). The specific measures were significantly correlated with thickness for the total sample, the full sample of sclerotised cuticle and only beetle sclerotised cuticle, but not for all categories of non-sclerotised cuticle or sclerotised moth cuticle (Table 6.1; Fig. 6.1). The region of the insect that the sample was taken from is categorised with the punch parameters in Fig. 6.2. The median and maximum thicknesses of all cuticle fragments taken from the one insect are plotted against insect mass in Fig. 6.3.

The thickness of cuticle fragments found in the faeces of several microbat species is given in Table 6.2. Published reports of the diet of these same species are given in Table 6.3.

**Table 6.1.** Results of regression analyses for logged values of cuticle thickness vs punch strength, specific punch strength, work to punch and specific work to punch according to insect (beetle or moth) and sclerotisation (sclerotised or unsclerotised). n, number of samples; R, correlation coefficient; t, Student's t-test.

		P	unch stren	gth	Specific punch strength		strength
	n	R	t	p	R	t	p
All samples	190	0.919	31.854	< 0.001	0.305	4.399	< 0.001
Sclerotised cuticle	142	0.892	23.315	< 0.001	0.393	5.056	< 0.001
Unsclerotised cuticle	48	0.712	6.880	< 0.001	0.229	-1.596	0.117
Beetle sclerotised	120	0.922	25.927	< 0.001	0.332	3.824	< 0.001
Moth sclerotised	22	0.760	5.231	< 0.001	0.090	0.404	0.691
Beetle unsclerotised	13	0.653	2.858	0.016	0.344	-1.215	0.250
Moth unsclerotised	35	0.732	6.180	< 0.001	0.195	-1.145	0.261

		V	Vork to pu	nch	Specific work to punch		
	n	R	t	p	R	t	p
All samples	190	0.873	24.521	< 0.001	0.223	3.130	0.002
Sclerotised cuticle	142	0.885	22.513	< 0.001	0.462	6.169	< 0.001
Unsclerotised cuticle	48	0.598	5.055	< 0.001	0.012	-0.079	0.937
Beetle sclerotised	120	0.913	24.328	< 0.001	0.451	5.494	< 0.001
Moth sclerotised	22	0.676	4.105	0.001	0.047	0.208	0.837
Beetle unsclerotised	13	0.360	1.278	0.228	0.202	-0.684	0.508
Moth unsclerotised	35	0.689	5.455	< 0.001	0.071	0.411	0.684

**Table 6.2.** Species means ( $\pm$  SE) of median and maximum thickness of cuticle fragments in the faeces of microbats, and number of fragments/mg. n, number of individuals. Cuticle fragments/mg was not measured for *C. gouldii* or *C. morio*.

	n	Median cuticle	Maximum cuticle	Cuticle	
		thickness $(\mu m) \pm SE$	thickness $(\mu m) \pm SE$	fragments/mg	
C. gouldii	4	$12.25 \pm 1.87$	$24.00 \pm 3.52$	-	
C. morio	4	$5.75 \pm 0.32$	$17.75 \pm 1.26$	-	
M. schreibersi	3	$5.12 \pm 0.40$	$11.67 \pm 0.69$	$24.23 \pm 2.99$	
N. geoffroyi	2	$8.35 \pm 2.62$	$19.50 \pm 7.42$	$15.91 \pm 2.89$	
V. darlingtoni	2	$9.95 \pm 0.57$	$26.50 \pm 4.60$	$19.36 \pm 2.38$	
V. regulus	2	$8.00 \pm 2.02$	$28.00 \pm 12.73$	$27.48 \pm 2.72$	

**Table 6.3.** Published reports of diets for species in Table 6.2 that were investigated using the cuticle thickness measurement technique.

Species	Diet	Reference	
C. gouldii	Moths predominant food; moths and bugs in Victoria, Australia	(Churchill 1998)	
	Mainly moths and beetles	(Dixon 1995)	
	Winged reproductive ants taken in large numbers; beetles heavily taken	(Fullard <i>et al.</i> 1991)	
	Wide range of insects; mainly Lepidoptera and Coleoptera	(Lumsden and Bennett 1995b)	
	Large proportion of Coleoptera	(O'Neill and Taylor 1989)	
	Moths important dietary item	(Vestjens and Hall 1977)	
C. morio	Moths main dietary item	(Churchill 1998)	
	Particularly high incidence of Lepidoptera	(Fullard et al. 1991)	
	Moths appear to be main food item	(Lumsden and Bennett 1995a)	
	Mostly Lepidoptera, also Coleoptera	(O'Neill and Taylor 1989)	
M. schreibersii	Moths main dietary item	(Churchill 1998)	
	Feeds principally on moths	(Menkhorst and Lumsden 1995)	
	Mainly moths	(Vestjens and Hall 1977)	
N. geoffroyi	Mainly moths, also wingless insects	(Churchill 1998)	
	Winged reproductive ants taken in large numbers; beetles heavily taken	(Fullard <i>et al.</i> 1991)	
	Moths majority of diet	(Lumsden and Bennett 1995d)	
	Wide variety of flying and non-flying invertebrates	(Maddock and Tidemann 1995)	
	Moths most common food	(Vestjens and Hall 1977)	
V. darlingtoni	Mainly moths, as well as ants, bugs and beetles	(Churchill 1998)	
	Coleoptera, Diptera, Hemiptera and Hymenoptera approximately equal (N. Victoria, Australia)	(Lumsden and Bennett 1995c)	
V. regulus	Moths, flies and beetles	(Churchill 1998)	
	Considerable variety in diet; high proportions of beetles and moths	(Fullard <i>et al.</i> 1991)	
	Predominantly moths	(Lumsden and Bennett 1995e)	
	Favours moths	(Tidemann 1995)	

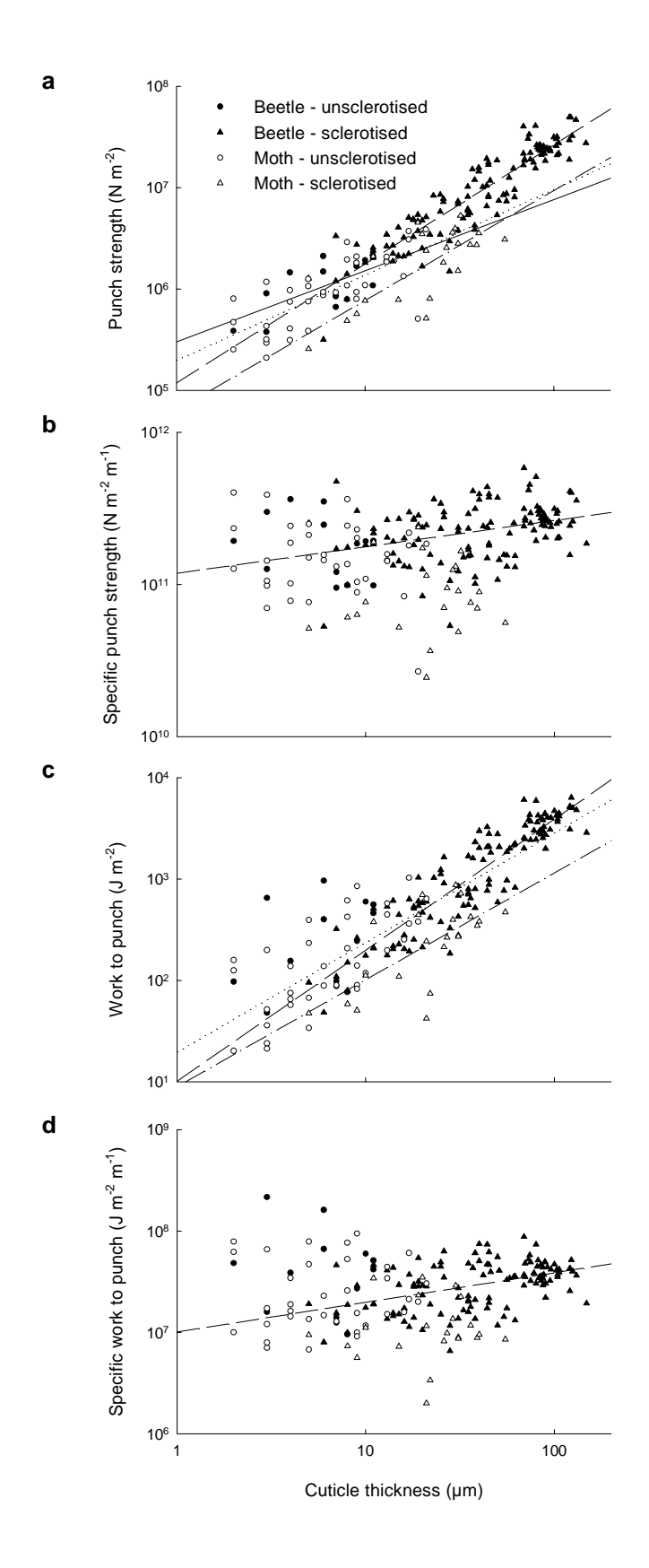


**Fig. 6.1.** Cuticle thickness (μm) vs punch strength (a), specific punch strength (b), work to punch (c) and specific work to punch (d) from punch tests of fresh cuticle according to insect type and level of sclerotisation. Beetle unsclerotised, solid regression line; beetle sclerotised, dashed; moth unsclerotised, dotted; moth sclerotised, dot-dash.

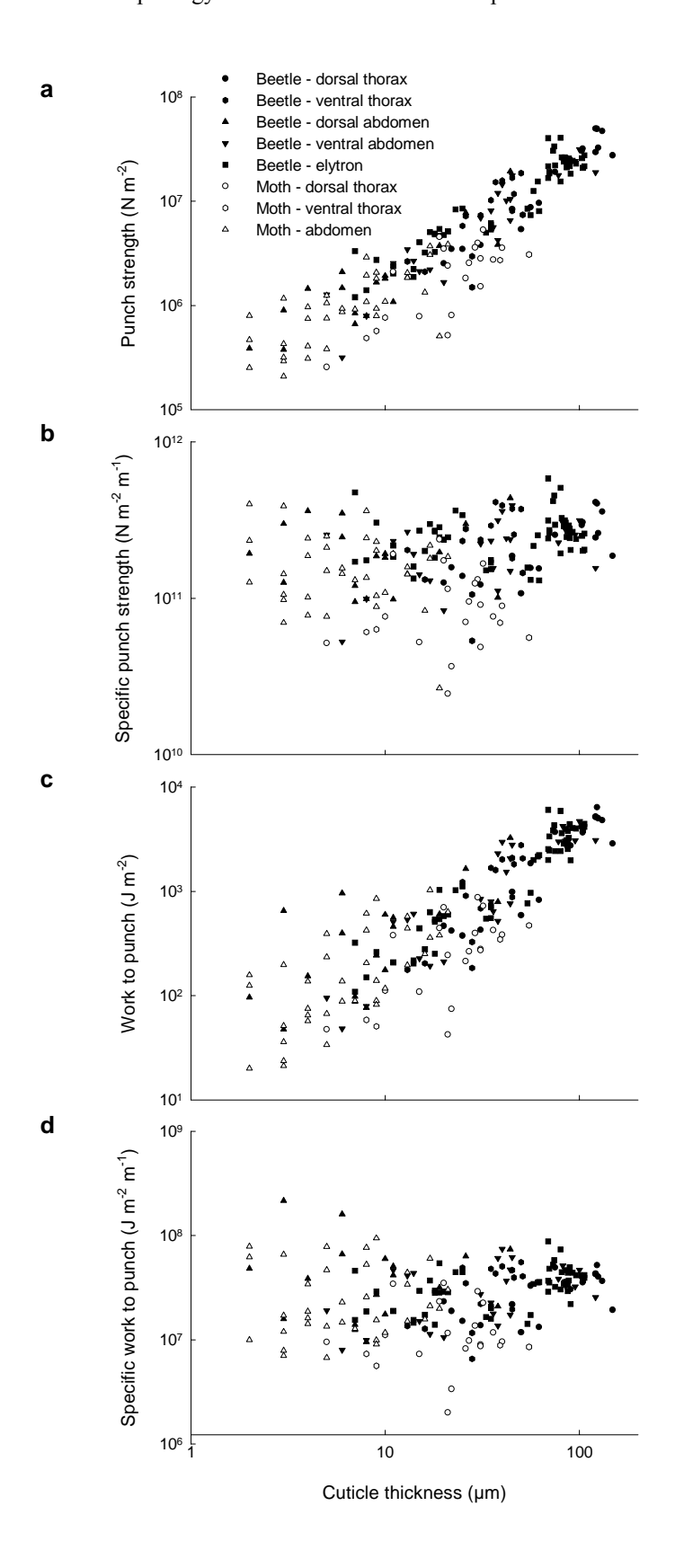


**Fig. 6.2.** Cuticle thickness ( $\mu$ m) vs punch strength (a), specific punch strength (b), work to punch (c) and specific work to punch (d) from punch tests of fresh cuticle according to the region of the body from which the sample was taken.

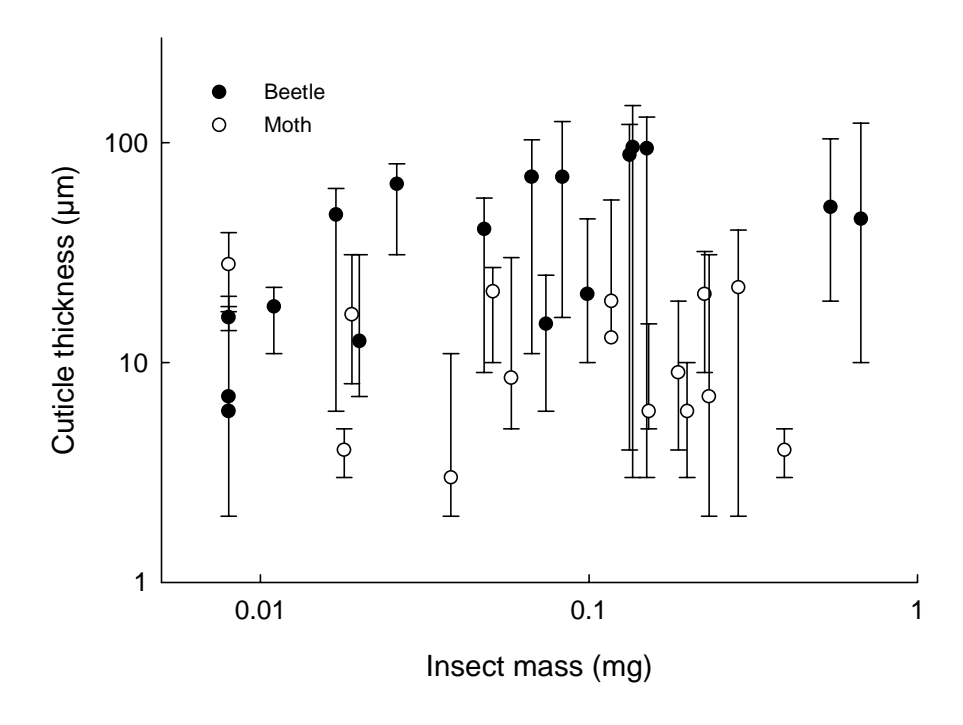


Fig. 6.3. Insect body mass (mg) vs median (circle), minimum (lower bar) and maximum (upper bar) thickness ( $\mu$ m) of cuticle fragments used in punch testing.

## 6.4. Discussion

# **6.4.1.** Cuticle thickness as a measure of biomechanical properties

The strong positive correlation between both punch strength and work to punch for sclerotised cuticle thickness supports the hypothesis that these punch measures would be correlated with cuticle thickness and justifies the use of cuticle thickness as a measure of invertebrate intractability. This was the case for the Coleoptera and Lepidoptera tested here, and the conclusion merits detailed confirmation with a wider range of invertebrates.

The assumption that sclerotised cuticle is a more discriminating measure of intractability compared to unsclerotised cuticle is justified as it showed a greater range of punch strength and work to punch, and the majority of sclerotised cuticle fragments were thicker than unsclerotised for both beetles and moths (lower and upper quartile ranges for unsclerotised beetle and moth: 4-9.5 and 4-9  $\mu$ m; sclerotised beetle and moth: 20-82.25 and 16-31  $\mu$ m respectively).

The force-testing experiments reveal further details about the structural properties of cuticle. The main mechanism of increasing cuticle thickness appears to be the addition of extra layers of chitinous cuticle. If the cuticle were a homogenous material, the force and energy required to punch the cuticle would be likely to linearly increase with thickness, or perhaps tail off with increasing thickness. This is measured as specific punch strength and specific work to punch. Additional strengthening or toughening mechanisms in thick cuticle that are absent in thin cuticle would increase the specific punch measures for thick cuticle. Unsclerotised cuticles of beetles and moths, and the combined sample, did not show a significant correlation of these measures with thickness (Table 6.1). There was a significant correlation for sclerotised beetle cuticles, however, indicating that there is some increase in structural strength and toughness above a simple additive effect of increased thickness. This was not the case for sclerotised moth cuticles, but this may be due to the smaller range of cuticle thicknesses that were tested.

The correlation between cuticle thickness and intractability is not the only significant advantage in using cuticle thickness in faeces as a measure of dietary properties. The method gives a quantitative measure of the proportions of diets of particular degrees of intractability according to the mean and maximum cuticle thickness ingested within an individual or the species. Cuticle fragments that appear in faeces represent only those components of the insect that were ingested and masticated. Therefore, the results are not influenced by parts of insects that are culled and not ingested, such as head capsules and elytra. These components may be among the most intractable of the insect, but should not

be taken into account when considering masticatory or dental adaptations to feeding on intractable foods. They may give an inflated impression of the intractability of the diet. The results will be particularly applicable to an analysis of molar function with respect to intractability, as they show the intractability of food that was actually processed by the molars.

Measurement of cuticle thickness is also significantly easier than conventional faecal analysis of insect diets. Dietary investigation normally requires the taxonomic identification (usually to order or family level) of the fragments. This is a labour-intensive and skilled activity that makes use of invertebrate keys and sample collections of local invertebrates. It also may require a large number of faecal pellets as many do not contain identifiable fragments (Gould 1955; Hamilton 1933). Measuring only the thickness of the cuticle avoids many of these drawbacks, as the taxonomy of the prey is not as relevant to the masticatory adaptations as its biomechanical properties. A greater number of samples can be processed by workers without great experience in identification of insect fragments and the need for reference samples is eliminated. These advantages mainly apply where it is the biomechanical properties of the diet that is the most important factor under consideration.

Previous estimates of dietary 'hardness' also largely rely on estimates of the volume of invertebrate taxa in faeces, the merits of which have been debated (Dickman and Huang 1988; Kunz and Whitaker 1983; Robinson and Stebbings 1993). If there were very little digestion of cuticle, then soft, unsclerotised cuticles would still be present in the faeces (and were found in some samples examined in this study; *personal observation*). However, even if there were extensive digestion of thin or unsclerotised cuticle and little of thick or sclerotised cuticle (which is most probably more likely than the converse), the maximum cuticle thickness would not be affected. As long as the cuticle was not completely digested, the median cuticle thickness would not be greatly affected. Thick cuticle would still be present in the faeces of intractable feeders and absent from tractable feeders, indicating intractable and tractable diets respectively. This means that problems with underestimation of tractable taxa are reduced, as these problems chiefly stem from the lack of identifiable parts of tractable insects.

Another significant advantage of this technique is that both the determination of cuticle thickness of fragments and any conventional quantification of frequency and volume of various taxa can be carried out on the same faecal pellet. Once any taxonomically-identifiable fragments have been classified and used to estimate the proportional volume of the sample that it comprises, the thickness of the cuticle fragments

can be measured, achieving both a conventional assessment of diet according to taxa present and a biomechanical measure of the intractability of the diet.

The principle of quantifying the intractability of an insect according to cuticle thickness has potential even if only published reports of the diet, rather than faecal samples, are available. The intractability of the relevant invertebrate taxa could be measured by force testing a range of body parts of a broad size and phylogenetic range to give a mean and standard deviation of intractabilities to be used as a measure of dietary mechanical properties, rather than using the qualitative scale of Freeman (1981a).

The measurement of cuticle thickness of faecal fragments is in reasonable agreement with previous dietary determinations (Table 6.3). *Chalinolobus gouldii* and *Vespadelus regulus* have been found to consume large numbers of beetles and had a high maximum cuticle thickness measurements (Table 6.2). *Miniopterus schreibersii* was found to feed principally on moths and had the lowest maximum cuticle thickness. It is more difficult to show a correlation between the published diet and this study's results for the species with the second largest maximum cuticle thickness, *V. darlingtoni* – it has been found to feed on small insects, mainly moths, and so would not be expected to have thick cuticle in its faeces. However, the small sample sizes of this study may be the main reason for the discrepancy, but the preliminary findings for the other species show promise, and in theory should give a more accurate depiction of the biomechanical properties of their diets.

From the assumption that the biomechanical properties of the diet are one of the most important indicators of the feeding decisions of the consumer, it is very important to be able to measure the properties of the foods actually eaten. For most feeding guilds, it is largely impossible to directly assess the properties of the material that an animal has consumed, and so we must find an indirect method of predicting the biomechanical properties. The utility of the method of determining invertebrate dietary properties outlined in this thesis can be compared to those of other dietary groups.

A typical method for estimating the types and proportions of items in the diet of an animal is through observations of feeding, taking note of the plants, fruits and animal components that are ingested (e.g. Van Valkenburgh 1996; Yamashita 1996). The foods must be categorised in some way that correlates with their biomechanical properties. However, this assumes that the observer can accurately determine the type of object being eaten. An alternative is to examine the stomach contents or faeces and categorise the fragments found, e.g. as monocotyledonous and dicotyledonous plants. One difficulty with this is that many foods are extensively digested, e.g. fruits and vertebrate flesh, and limit the usefulness of faecal analysis for these groups.

Even if these obstacles are overcome or not relevant, it is very likely that there is fine-level variation in the biomechanical properties of these foods within dietary categories (e.g. ripeness of fruits, age of leaves, size and type of beetles) that may be used by the animal to discriminate between foods. This variation may be indistinguishable either by the observer or from the examination of digestive contents. The measurement of biomechanical properties on discarded fragments of partially-consumed fruit, such as by Kinzey and Norconk (1990), is almost certainly the best measure of such properties of fruits that can be made, but the level of variation within a piece of fruit is unknown, and it cannot consider fruit that is completely ingested. The use of cuticle thickness in the faeces of insectivores appears, on the basis of this limited survey, to have the potential to be the best indirect method for the measurement of biomechanical properties of diet for any dietary type. The good correlation between thickness of cuticle and its biomechanical properties observed in this study, and the persistence of the cuticle in the faeces, largely overcomes the limitations of other methods. However, it must be acknowledged that a more comprehensive survey would be necessary to confirm the potential of the method.

It is now appropriate to compare the use of cuticle thickness to assess the biomechanical properties of insects with techniques currently employed. The use of durometers, which measure the force to penetrate foods with a manual or spring-loaded punch (Dumont 1999; Kinzey and Norconk 1990; Yamashita 1996), are reasonable measures of the structural strength of the diet, and are in several respects similar to the tests carried out here. The tests used by Fisher and Dickman (1993) and Aguirre *et al.* (2003) essentially measure the structural strength of the insects and fruit. However, for all of these studies except Fisher and Dickman (1993), the speed of loading during the mechanical test is not constant, which will affect the force readings obtained due to the viscoelasticity of foods (Vincent 1990). It would need to be assessed to what extent this influences the results, as it may only be a minor effect.

Aguirre *et al.* (2003) were able to show that the structural strength of insects, particularly beetles, increased with size (mass, length and width). From estimates of the dimensions of prey in faeces, they were able to give an estimation of the 'hardness' of the diet. Substantial testing of the methods of the current study and Aguirre *et al.* (2003) would be required to establish their comparative value and significance of correlation with morphological and behavioural characteristics of the insectivores.

# 6.4.2. Biomechanical properties of beetles and moths

Although the punch variables correlated with cuticle thickness for all insects tested (Table 6.1), there were significant differences between beetles and moths. Firstly, there are

large differences in the regression slopes for both sclerotised and unsclerotised cuticle in the two groups (Fig. 6.1), indicating that in general beetle cuticle requires more force and energy to fracture than moth cuticle for a given thickness. Also, the amount and thickness of cuticle varies; beetles have thicker cuticle (maximum and median; Fig. 6.3) and a greater number of sclerotised plate components (measured as the number of sclerotised fragments available for force testing) for a given mass.

For both beetles and moths, the maximum cuticle thickness is significantly correlated with insect mass (beetle: R = 0.515, t = 2.324, p = 0.035; moth: R = 0.524, t = 2.219, p = 0.045), but the slope of the log-log plot for both is substantially lower than would be expected from isometry (slopes 0.002 and 0.004 for beetles and moths, respectively, compared to an expected slope of 0.333). The maximum cuticle thickness is approximately equal for beetles of 100-700 mg. Therefore, the thickness of a cuticle fragment is not a good predictor of beetle size. The same is approximately true for moths, even though the number and thickness of cuticle plates are lower. However, the taxonomy of these insects was not determined below order, and so patterns within the two orders are unknown. The finding suggests that above some threshold there is no advantage in increasing thickness with size. This could be for a number of reasons, not all of which relate to defence against predators, such as the cost of manufacture and transport of a thick cuticle, and could be the subject of an interesting study on the scaling of cuticle thickness with body size.

# **6.4.3.** Insect biomechanical properties

Despite the argument that foods should largely be dealt with as structures, and that the behaviour of the final structure will depend on material as well as structural factors, it may still be useful to examine the data that exist on the material properties of invertebrate components. The diversity of the material and structural properties of insects has been considered in many previous studies (e.g. Freeman 1981a; Strait 1993c), but it seems appropriate to examine the question of what can be considered the typical biomechanical properties of insects: i.e. what properties do all insects have in common, and in what ways do they differ? Specifically, in what ways do they differ that will be important with respect to an insectivore consuming the invertebrate? We will examine toughness, brittleness, stiffness and strength of insects, as the majority of work on the biomechanical properties of invertebrates has considered insects.

Insects have been said to range from tough to fragile. In some respects this is true, in that there is variation among insects in the energy required to fracture them. However, most insect components, and whole insects, are relatively tough in that a fair amount of

energy is required to fracture them and the majority (or all) of the parts of the body resist self-sustained crack propagation. On the whole, biomaterials are designed to resist fracture, although there are exceptions (e.g. crack generation in a probably very stiff and brittle cuticle in the process of autotomy in crickets; Vincent 1998), and we would expect catastrophic failure of components to be avoided as much as possible (Alexander 1981). This is also apparent in engineering, as the history of engineering is almost the history of attempts to prevent cracks spreading (Gordon 1976). Pliant cuticles, such as a maggot cuticle, have a toughness of 1000 J m<sup>-2</sup>, which is as tough as mammalian arteries (Purslow 1980; cited in Hillerton 1984). The toughness of a whole beetle (2770 J m<sup>-2</sup>) is greater than that of a whole caterpillar (390 J m<sup>-2</sup>) (Strait and Vincent 1998), illustrating that toughness does vary between insects, but the relatively high toughness of insect pliant cuticles indicates that no insects can really be considered 'fragile'.

The mechanisms by which insects achieve high toughness are varied. Pliant materials do this by ineffectively transmitting force between components and so can undergo greater strain. Many pliant biomaterials exhibit J-shaped stress-strain curves, where the material can be loaded under great strain before there is any significant increase in the stress (Vincent 1990). In stiff materials, the stress is applied to only a few bonds, and so fracture occurs under lower strain. The result is a trade-off between the strength, stiffness and toughness of materials, as discussed above.

However, toughness can be increased in structures while maintaining high strength and stiffness, as has been achieved in wood (Jeronimidis 1980) and sclerotised insect cuticle (Vincent 1992a). Insect cuticle is a fibre composite constructed of chitin fibres in a protein matrix. In the stiff exocuticle of a beetle, the force is transmitted through the stiff protein matrix to the chitin fibres. The fibres prevent the propagation of cracks, so that fracture of the material requires either fracture of the fibres or fibre pullout, both of which can require significant amounts of energy and so increase toughness. Cuticles are also layered with different orientations of chitin in successive layers (such as helicoidal or parallel; Neville 1984). Cracks may be stopped by the weak interface between the layers by Cook-Gordon debonding (Atkins and Mai 1985). Another mechanism of toughening employed in insect cuticle is case-hardening, where the cuticle is a bilayer with an external stiff, sclerotised cuticle and internal pliant, unsclerotised endocuticle (Vincent 1980). This shifts the neutral axis in the structure so that a greater amount of the stiff material is in compression and the pliant material in tension, which represents the optimum loading regimes for these materials. The layer of pliant endocuticle below the more brittle exocuticle will also reduce the propagation of cracks (Vincent 1980). The resulting

structure of procuticle is structurally stiff, strong and tough, coming close to defeating the obstacles of structural mechanics in achieving the Holy Trinity of materials engineering.

Beetles have been described as brittle (Strait 1993c). This implies that either the invertebrate as a whole or each of its components separately undergo brittle fracture (see fig. 1 in Strait 1993c). The assertion that 'hard' invertebrates like beetles display brittle fracture appears to be an exaggeration. Sclerotised beetle exocuticle exhibits some brittle fracture (Hepburn and Joffe 1976), as does locust tendon (Vincent 1990), and limited brittle fracture in the fracture of a whole beetle can be discerned as rapid decreases in a force-deflection graph (Strait and Vincent 1998). Crack-stopping mechanisms, particularly the ductile endocuticle below the exocuticle, reduce the extent of free-running cracks in the cuticle. Whole insects certainly do not show brittle fracture, and require continual application of force to sequentially initiate and propagate cracks through the insect. In addition, none of the internal organs or the pliant cuticles can be considered brittle.

Stiffness is probably the most extensively examined property of insect components (Hepburn and Joffe 1976; Hillerton 1984; Vincent 1980), with values ranging from 10<sup>3</sup> to 10<sup>10</sup> N m<sup>-2</sup> for pliant and stiff cuticles respectively (Vincent 1980). Information on the strength of insect cuticle appears to be sparse, but using the data on specific punch strength gathered in this study as an estimate of material strength shows there is considerable variability among insect regions and between moths and beetles (Fig. 6.2).

The main differences among insects lie in the strength and stiffness of various components of the invertebrates, but not whole invertebrates. Therefore, an intractable insect is one that has significant amounts of intractable (structurally strong, stiff and tough) cuticle rather than the whole insect being 'hard'. However, we may consider that toughness is an overriding property of insects in two respects. First, a large proportion of the remaining components of insects (e.g. internal organs, certain cuticle components) are relatively tough (which is probably largely related to their low stiffness and plasticity). Second, the fracture of whole invertebrates requires significant amounts of energy, and they do not fail in a brittle manner like some nuts, fruits, bone or shells.

The definition of intractability used in this study may not be as applicable to other food categories such as fruits and bone. These foods may exhibit more brittle fracture and have lower toughness, differing from a relatively high degree of toughness in all insects. However, this supposition remains to be tested.

The definition of structural mechanisms given above includes aspects such as size and shape of the object. We can extend this to consider two basic forms of mechanisms for modifying the properties of structures. The structural strength, stiffness and toughness of a structure can be increased by specific arrangements of a single material in threedimensional space, for example, by increasing thickness, or by creating beams, trusses or folds. These might be termed homostructural mechanisms. Conversely, heterostructural mechanisms involve the use of two or more materials in the construction of the structure, such as the layering of different materials, or placing different materials in tension and compression.

The scale of examination is relevant to the consideration of materials compared to homostructural and heterostructural mechanisms. Strictly, cuticle is a composite of chitin and proteins (where a composite is the combination of more than one material with some internal structural heterogeneity; Niklas 1992), the arrangements of which constitute heterostructural mechanisms of modifying structural properties. However, if this composite is considered as a material from which the cuticle is constructed, we can also examine the arrangement and distribution of this 'cuticular composite material' in terms of homostructural effects. A larger or thicker structure can incorporate additional homostructural mechanisms that increase resistance to stress. These include grooves (sulci) on the outside and ridges on the inside of the cuticle (Chapman 1998), which will essentially form supporting beams along the cuticular plate, increasing stiffness for only a relatively small increase in material. High arching of a beetle's dorsal surface will also constitute a homostructural mechanism (Gordon 1978; Hill 1985), but this will likely not be detected in the punch tests.

If each of the sclerotised exocuticle and unsclerotised endocuticle are considered 'materials' then heterostructural mechanisms include the layering of stiff, strong exocuticle on top of pliant, ductile endocuticle. However, if there is no major change in the structure of the cuticle with increased thickness, then we can consider that the increases in the specific punch measures are due to homostructural mechanisms.

### **6.5.** Conclusions

This chapter challenges previous categorisations of insects according to the ill-defined concept of 'hardness' by erecting a new classification according to 'intractability'. The basis for a new method for assessing the biomechanical properties of insects that appears better than methods currently in use is also established. The thickness of cuticle fragments in the faeces of insectivores can be used as a measure of the intractability of the invertebrates in their diet. For correlations of the biomechanical properties of insects with morphological characters, this procedure is greatly preferable due to its sound biomechanical basis and quantitative nature.

# Chapter 7. Dental Specialisation in Insectivorous Microchiropterans Consuming 'Intractable' and 'Tractable' Invertebrates

## 7.1. Introduction

Until recently, mammalian insectivores were generally treated has a homogeneous group with respect to dietary habits. This misconception, that the diet of all insectivores can be treated as equivalent, has largely been repudiated, and we can consider there to be two aspects to this dietary heterogeneity.

First, insectivores do not feed randomly on the invertebrate community available to them. Many species of insectivores have been found to take invertebrates in different proportions to their measured frequency in the habitat (e.g. Anthony and Kunz 1977; Brigham and Saunders 1990; Buchler 1976; Fenton *et al.* 1998a; Menzel *et al.* 2000; Pavey and Burwell 1998; Swift and Racey 1983) or appear to specialise on particular invertebrates, including beetles, moths and spiders (the diet of an 'insectivore' here includes any invertebrates, including spiders and earthworms; Black 1972; Black 1974; Ross 1967; Schulz 2000; Vaughan 1977; Warner 1985; Whitaker and Black 1976; though see Arlettaz and Perrin 1995; Fenton 1995; Findley 1993 for arguments against selectivity and competition in bats; and Kunz 1988 with regard to difficulty in insect sampling).

Second, the animals eaten by insectivores are diverse in their biomechanical properties. There has been found to be substantial variability both among the components within a single invertebrate and among different types of invertebrates in terms of the material properties of strength, toughness, stiffness and 'hardness', as defined and discussed in Chapter 6. Previous studies that have investigated the feeding adaptations of insectivores have most often used 'hardness' as a criterion for differentiation of the diet (Dumont 1995; Freeman 1979, 1981a; Strait 1993c). However, due to the difficulty in defining and measuring 'hardness' in insects, I have advocated the use of 'intractability' in Chapter 6, which is the degree to which the structural properties of structural strength, toughness and stiffness are increased. The punch strength and work to punch are higher in intractable invertebrates compared to tractable ones.

Both of these aspects of heterogeneity, the diversity of invertebrates eaten by insectivores and the diversity of biomechanical properties of the invertebrates, are presumed to contribute to the differences in many morphological aspects of the feeding apparatus in insectivores that specialise on prey with particular biomechanical properties.

This is to be expected, following selection for anatomical features that are able to deal with the physical demands of acquiring and comminuting food. 'Hard' feeding in insectivores has been found to correlate with skull morphology (thick jaws, well-developed sagittal crests, higher condyles and coronoid processes, wide skull widths relative to skull length; Freeman 1979, 1981a, 1988, 1984; Rodríguez-Durán *et al.* 1993; Jacobs 1996), relative molar size (larger M¹ and M² but smaller M³; Freeman 1979; Rodríguez-Durán *et al.* 1993), gross molar morphology (lower 'shear ratio' of lower molars; Strait 1991, 1993c), molar microwear (greater pitting on occlusal surfaces; Strait 1993b) and molar enamel thickness (thicker enamel; Dumont 1995) compared to soft feeding. To a large extent these epitomise differences found between other dietary groups that vary in hardness (Andrews 1981; Grine 1986; Jolly 1970; Kay 1981; Kinzey 1974; Ravosa 2000; Rosenberger and Kinzey 1976; Teaford 1985). 'Hardness' in these studies is most likely to be referring to foods with high structural strength and stiffness (and perhaps toughness; see Chapter 6), but in the majority of these studies a specific definition for dietary hardness was not given.

Although the use of crests will be advantageous in fracturing tough foods due to the necessity to propagate cracks through them (Lucas and Luke 1984), the precise form and arrangement of both the crest edge and the surrounding tooth surface will have an immense influence on the function and effectiveness of any crest. For the most part, previous studies have not attempted to examine or explain differences in such fine-scale molar morphology between these two guilds. This study will use engineering principles that relate the various aspects of insectivore molar shape to function in order to provide a sounder basis for relating tooth shape to function, as detailed in Chapters 2, 3 and 5. The functional parameters relate the shapes of cusps and crests to the force or energy required for penetration or forced crack propagation of tough foods.

A brief description of the parameters follows – tip sharpness: radius of curvature at the tip of a cusp; cusp sharpness: volume of a cusp to a given distance from the tip; cusp occlusion relief: space behind a point at which a cusp occludes; edge sharpness: radius of curvature of a crest; rake angle: angle of leading face of a crest to a line perpendicular to the direction of movement; crest relief: space behind the edge of a crest; approach angle: angle of the long axis of a crest to a line perpendicular to the direction of movement; capture area: area enclosed by a crest for capturing food; fragment clearance: the ability of a cusp-crest structure to direct food off the rake surface (see Fig. 7.3a for a schematic representation of the functional parameters).

The null hypothesis examined in this study is that there is no difference in tooth shape and function, as indicated by the functional dental parameters, between intractable and tractable insectivores. There are three main hypotheses to explain any difference between the intractable and tractable insectivores: 1) that the optimal functional form of the dentition for comminuting intractable and tractable insects differs, and so there has been selection for different functional shapes in the two groups; 2) that there is a substantial difference in the risk of fracture between insectivores eating intractable and tractable diets that has led to an increased robustness in the dentition in intractable feeders; and 3) that there is a substantial difference in the amount of wear that occurs in intractable and tractable insectivores that has selected for increased dental material to resist wear. These three hypotheses are not mutually exclusive and will be elucidated in the discussion.

The relationships between tooth form and insectivory of invertebrates with varying biomechanical properties will be examined in intractable-tractable species pairs in three families of Microchiroptera. Differences between tooth forms will indicate a functional and/or adaptive response to the biomechanical properties of foods (Lucas 1979; Vinyard *et al.* 2003). Convergence of species with comparable dietary specialisation onto a similar dental form supports the contention that there is a functional relationship between the tooth form and diet (Ridley 1983; Harvey and Pagel 1991; Strait 1993c; Dumont 1995).

#### 7.2. Methods

## 7.2.1. Study species

Three pairs of confamilial species were examined (*Molossus ater* and *Nyctinomops macrotis* – Molossidae; *Eptesicus fuscus* and *Plecotus townsendii* – Vespertilionidae; *Hipposideros diadema* and *Rhinolophus blasii* – Rhinolophidae, following Simmons (1998) with regard to subfamily status of Rhinolophinae and Hipposiderinae), and each pair has a species with an intractable diet (defined as having a diet with a high proportion of beetles or other invertebrates with an intractable, highly sclerotised exoskeleton) and a tractable diet (low proportion of invertebrates with intractable exoskeletons and high proportion of tractable invertebrates, e.g. moths, caterpillars, earthworms). Table 7.1 shows the reported diets of the six species. Intractable species may also consume a reasonable number of moths, and are usually considered more 'generalist' compared to tractable feeders (Freeman 1981a, 1984; Warner 1985; Strait 1993c). Five specimens of each species were examined. Only unworn or very lightly worn specimens were used, apart from three of the *H. diadema* specimens that were slightly more worn due to limited availability of unworn specimens.

Specimens examined were: *M. ater*: AMNH 92565, 92566, 92567, 92573, 92574; *N. macrotis*: AMNH 132773, 169546, 173661, 176096, 6740; *E. fuscus*: AMNH 139509,

258269, 258270, MVZ 99527, 112487; *P. townsendii*: AMNH 170802, 170803, 170806, MVZ 103873, 106001; *R. blasii*: AMNH 54413, 239591, 239592, MVZ 99994, 101000; *H. diadema*: AM 3497, 15201, 20077, 20090, 20102. Institution abbreviations: AMNH, American Museum of Natural History, New York; MVZ, Museum of Vertebrate Zoology, University of California, Berkeley; AM, Australian Museum, Sydney.

### 7.2.2. Functional parameters

Procedures for moulding, casting and confocal imaging of teeth and for measurement of the nine functional parameters follow Chapters 4 and 5. Measurements were made on the upper second molar of five individuals of each of the six species.

The following measurements were taken for the four ectoloph crests on the upper molar (pre- and postparacrista, pre- and postmetacrista): rake angle, crest relief (wear land area, relief volume and relief angle), approach angle and capture area. Cusp sharpness was measured for the paracone and metacone, fragment clearance for the paracone and metacone basins, and cusp occlusion relief for the mesostyle/trigon groove. Tip sharpness and edge sharpness were measured for the metacone and postmetacrista respectively.

Tooth length was measured as the distance from the anterior end of the preparacrista to the posterior point of the postmetacrista. SV3, which equals (skull volume) $^{1/3}$ , was used as a measure of body size, where skull volume was estimated as (condylocanine length × occipital height × zygomatic breadth).

Any measurement of cusp sharpness will greatly vary depending on the distance from the tip from which the volume is measured, i.e. the cusp volume to the same absolute distance from the tip for large and small teeth of isometric shape will differ. However, if the distance from the tip is scaled according to a measure of size then this situation can be avoided. Therefore, three different methods for defining the distance from the tip were used in the calculation of cusp sharpness, with a smaller and larger for each method: constant distance from cusp tip (100 and 400  $\mu$ m); fraction of the tooth length (3/50 and 1/5 × tooth length); and multiple of SV3 (10 and 30 × SV3). Other measurements that used a constant (such as 100  $\mu$ m along rake surface for rake angle) were found to vary much less than cusp volume if the distance over which the parameter was measured was scaled with size. Tip and edge sharpnesses were measured for constant tooth area (400  $\mu$ m<sup>2</sup>) and crest length (100  $\mu$ m) respectively.

#### 7.2.3. Statistical methods and size correction

Differences between intractable and tractable feeders in each family for the quantitative features were tested using Mann-Whitney *U*-tests in Systat for Windows

Version 10.0 (SPSS, Inc.) using raw values of rake and approach angles, and for other quantitative measures divided by SV3 or tooth length (tip, cusp and edge sharpnesses, capture area and cusp occlusion relief). Qualitative features (relief wear land, volume and angle, and fragment clearance) were tested with Fisher's Exact tests using SPSS for Windows Version 10.0 (SPSS, Inc.). Significance level for all tests was p = 0.05.

Recently, there have been debates in the literature as to the best practice for size correction when examining hypotheses correlating morphological features with particular feeding behaviours (e.g. Dumont 1997; Vinyard et al. 2003). Dumont (1997) advocated the use of geometric mean of all variables to standardise for size, but Vinyard et al. (2003) defended the use of ratios with a biomechanically-relevant dimenson such as jaw length rather than geometric mean techniques. Their opposing methods led to conflicting conclusions regarding morphological adaptations for nectar feeding by gouging. Comparing eleven statistical techniques for size-adjustment, Jungers et al. (1995) found that the only measures that correctly grouped geometrically identical animals together were members of the Mosimann family of shape ratios, which make use of the geometric mean (Mosimann 1970; Mosimann and James 1979). However, we are not sure of the applicability of these methods when using a mixed data set (linear, area, volume and angular measurements, and qualitative data). Therefore, it was decided to use principal components analysis on the logged data.

Principal components analyses were carried out using Systat. Volume (mm³) and area (mm²) measures were reduced to linear measures by cube and square root respectively, and then all quantitative values were logged. Analyses were undertaken for functional parameters relating to the following three groups of variables: 1) the entire data set (including SV3 and tooth length, which was included in all analyses, and the three methods for calculating cusp sharpness); 2) all parameters, except for cusp sharpness, where only the cusp sharpness measurements based on SV3 were used (i.e. excluding the constant and tooth length measurements); 3) all parameters, except for cusp sharpness, where only the cusp sharpness measurements based on tooth length were used (i.e. excluding the constant and SV3 measurements). Relief angle and wear land were omitted from the PCAs when there was no variation in these parameters among species.

#### 7.3. Results

The measurements for the nine functional parameters are given in Tables 7.2-7.4. There were no consistent differences in the tooth functional parameters between intractable and tractable feeders within families (Table 7.5). No significant difference within families

was found for tip and edge sharpnesses (divided by either SV3 or tooth length) or any of the qualitative variables (relief parameters and fragment clearance). The molossid and rhinolophid intractable feeders tended to have larger rake angles compared to the tractable feeders, but this was not the case for the vespertilionids. Also, there were significant differences within the vespertilionids and rhinolophids for most measures of cusp sharpness, but not within the molossids. Approach angle, cusp occlusion relief and capture area were significantly different in only some of the intrafamilial comparisons. The low number of families prevents a sign test from being used, as was done by Dumont (1995), although for all measurements of rake angle, the species mean of the tractable feeder was higher than that of the intractable feeder.

The three PCA plots all showed very similar distribution of the species, so only the plot including all variables will be discussed (Fig. 7.2). Factor 1 correlated with cusp sharpness measurements based on SV3 and tooth length (r = 0.963 to 0.981), tooth length (0.953), SV3 (0.948), constant cusp sharpness (0.876 to 0.913), rake angles (preparacrista -0.832; postmetacrista -0.721), capture areas (0.676 to 0.813) and fragment clearance (-0.724). Factor 1 separated the intractable and tractable feeders – this may be largely due to body size differences, as some of these variables represent size (SV3 and tooth length), and so it may in part be considered a size factor. Factor 2 in general separated the intractable and tractable feeders within each family; however, the molossid and vespertilionid intractable feeders generally had lower Factor 2 scores, but the rhinolophid intractable feeder (*H. diadema*) had a higher Factor 2 score than the tractable feeder (*R. blasii*). Approach angles were the only parameters highly correlated with Factor 2 (r = -0.765 to -0.905). Factors 1 and 2 explained 52.99% and 15.31% of the variance respectively.

**Table 7.1.** Diets of the intractable (I) and tractable (T) feeding species examined in this study. % occurrence = proportion of samples containing insect; % volume = proportion of volume of insect in sample; % individuals = proportion of individual insects in sample; % fragments = proportion of culled fragments. Abbreviations: D, digestive system contents; F, faecal analysis; C, culled fragments of prey (e.g. wings). n, number of individuals sampled; np, number of faecal pellets sampled; nf, number of culled fragments.

Family	Diet class	Diet	Reference
Molossidae			
Molossus ater	I	11.5% individuals Coleoptera; n = 1, D	(Pine 1969)
		Coleoptera, Orthoptera, Hymenoptera; n = 1, F	(Howell and Burch 1974)
		Mostly Coleoptera, few moth scales; $n = 4$ , F	(Freeman 1981b)
		37.5% occurrence Coleoptera; n = 8, D	(Marques 1986)
		97.5% volume Coleoptera; n = 2, D	(Bowles et al. 1990)
		74.0% volume Coleoptera; n = 18, F	(Fenton et al. 1998b)
Nyctinomops macrotis	T	100% volume Lepidoptera; n = 1, D	(Ross 1967)
		98% occurrence, 86.1% volume Lepidoptera; n = 49, D	(Easterla and Whitaker 1972)
		100% volume Lepidoptera; n = 4, F	(Freeman 1981b)
Vespertilionidae			
Eptesicus fuscus	I	36.1% fragments Coleoptera; nf ≈ 300, C	(Hamilton 1933)
		80% volume Coleoptera; n = 10, D	(Phillips 1966)
		≥25% occurrence Coleoptera; n = 12, D	(Ross 1967)
		49.6% volume Coleoptera; n = 184, D	(Whitaker 1972)
		84% occurrence Coleoptera; n = 165, F	(Black 1974)
		34.4% volume Coleoptera; n = 30, D	(Whitaker et al. 1977)
		72% occurrence Coleoptera; n = 25, D	(Silva-Taboada 1979; cited in Rodríguez-Durán <i>et al.</i> 1993)
		52.6% volume Coleoptera; n = 60, D; 37.7% volume Coleoptera; n = 177, F	(Whitaker et al. 1981)
		90.5% occurrence Coleoptera; n = 21, D, F	(Griffith and Gates 1985)
		89% occurrence Coleoptera; n = 18, D, F	(Warner 1985)
		5.0% individuals Coleoptera; np = 395, F	(Brigham 1990)
		66.6% occurrence, 54.5% volume Coleoptera; n = 14, F	(Brigham and Saunders 1990)
		100% occurrence Coleoptera; n = 3, F	(Rodríguez-Durán et al. 1993)

Table 7.1 cont.

Family	Diet class	Diet	Reference
Eptesicus fuscus (cont.)		73.7% volume Coleoptera; np = 546, F; 57.9% volume Coleoptera; np = 1300, F	(Whitaker 1995)
		100% occurrence, 78% volume Coleoptera; n = 3, F	(Carter et al. 1998)
		57.0% volume Coleoptera; n = 181, F	(Hamilton and Barclay 1998)
		17.7% volume Coleoptera; np = 75, F	(Verts et al. 1999b)
		81.0% volume Coleoptera; np = 120, F	(Menzel et al. 2000)
Plecotus townsendii	T	92.1% occurrence Lepidoptera; n = 38, D, F	(Ross 1967)
		100% occurrence, 99.7% volume Lepidoptera; n = 16, D	(Whitaker et al. 1977)
		100% occurrence and volume Lepidoptera; $n = 1$ , $D$	(Whitaker et al. 1981)
		97.1% volume Lepidoptera; np = 1222, F	(Dalton et al. 1986)
		95.6% volume, 100% occurrence Lepidoptera; np = 447, F; 90.9% fragments, C	(Sample and Whitmore 1993
Rhinolophidae			
Hipposideros diadema	I	≥58.3% occurrence Coleoptera; n = 12, D	(Vestjens and Hall 1977)
		100% occurrence Coleoptera; n = 1, D	(Nabhitabhata 1986)
		97.2% occurrence Coleoptera; np = 140; 37.7% prey remains	(Pavey and Burwell 1997)
Rhinolophus blasii	T	100% occurrence and volume Lepidoptera (winter); n = 4, D; 100% occurrence, 96.5% volume Lepidoptera (summer); n = 30, D	(Whitaker and Black 1976)

**Table 7.2.** Functional parameters relating to cusps (mean  $\pm$  SE) for paracone and metacone for six species of intractable and tractable feeding bats. n = 5 for all species (except for tip sharpness measurements of M. ater and N. macrotis where n = 4). me, metacone; pa, paracone; tl, tooth length.

		Species					
	Cusp	M. ater	N. macrotis	E. fuscus	P. townsendii	H. diadema	R. blasii
Tooth length (μm)		1938.88 ± 12.44	$1751.07 \pm 6.77$	1511.20 ± 15.65	$1091.89 \pm 4.82$	$2139.33 \pm 29.87$	$1228.60 \pm 8.84$
SV3 (μm)		$13.18 \pm 0.03$	$12.34 \pm 0.07$	$10.90 \pm 0.07$	$8.95 \pm 0.04$	$14.36 \pm 0.26$	$9.68 \pm 0.03$
Tip sharpness (μm)	me	$40.08 \pm 2.72$	$33.36 \pm 1.70$	$24.97 \pm 1.15$	$16.56 \pm 0.34$	$26.50 \pm 1.56$	$15.89 \pm 0.49$
Cusp sharpness to	pa	$1420.53 \pm 54.50$	$1313.58 \pm 53.33$	$1559.52 \pm 76.09$	$750.04 \pm 14.94$	$1629.04 \pm 67.63$	853.09 ± 18.19
$100~\mu m~(10^3~\mu m^3)$	me	$1312.44 \pm 57.02$	$1259.88 \pm 78.04$	$1474.96 \pm 87.04$	$620.21 \pm 25.38$	$1682.09 \pm 50.57$	$811.96 \pm 13.67$
Cusp sharpness to	pa	$27.84 \pm 1.18$	$21.11 \pm 0.62$	$28.43 \pm 1.41$	$12.09 \pm 0.41$	$39.43 \pm 1.25$	$15.46 \pm 0.56$
$400~\mu m~(10^6~\mu m^3)$	me	$24.62 \pm 0.63$	$19.64 \pm 0.63$	$24.66 \pm 1.09$	$9.77 \pm 0.34$	$39.13 \pm 0.93$	$14.64 \pm 0.45$
Cusp sharpness to	pa	1965.10 ± 93.26	$1453.92 \pm 65.04$	$1297.30 \pm 81.80$	$329.26 \pm 7.76$	2946.64 ± 160.95	$459.25 \pm 13.85$
3/50 tl (10 <sup>3</sup> µm <sup>3</sup> )	me	$1849.73 \pm 91.08$	$1395.91 \pm 85.84$	$1224.57 \pm 85.23$	$257.11 \pm 13.14$	$3017.75 \pm 134.61$	$434.99 \pm 12.33$
Cusp sharpness to	pa	$26.04 \pm 1.28$	$16.03 \pm 0.51$	$15.45 \pm 0.89$	$3.33 \pm 0.07$	$47.10 \pm 2.27$	$5.20 \pm 0.19$
1/5 tl (10 <sup>6</sup> µm <sup>3</sup> )	me	$23.19 \pm 0.82$	$15.17 \pm 0.52$	$13.97 \pm 0.76$	$2.86 \pm 0.10$	$46.05 \pm 1.82$	$4.97 \pm 0.14$
Cusp sharpness to	pa	2540.36 ± 88.36	2025.11 ± 100.52	1879.50 ± 107.48	$607.77 \pm 14.50$	$3899.63 \pm 291.02$	$800.63 \pm 21.20$
$10 \times SV3 \ (10^3 \ \mu m^3)$	me	$2420.71 \pm 76.46$	$1950.81 \pm 122.25$	$1759.12 \pm 102.38$	$495.63 \pm 23.33$	$3992.06 \pm 267.15$	$760.94 \pm 16.27$
Cusp sharpness to	pa	$27.07 \pm 1.07$	$18.06 \pm 0.71$	$18.18 \pm 0.94$	$5.07 \pm 0.16$	$48.93 \pm 3.35$	$7.40 \pm 0.28$
$30 \times SV3 \ (10^6 \ \mu m^3)$	me	$24.02 \pm 0.55$	$16.96 \pm 0.67$	$16.28 \pm 0.74$	$4.33 \pm 0.16$	$47.46 \pm 2.79$	$7.14 \pm 0.23$

**Table 7.3.** Functional parameters relating to upper molar ectoloph crests (mean  $\pm$  SE, or median (minimum, maximum) for qualitative data) for six species of intractable and tractable feeding bats. n = 5 for all species. Crests: prpac, preparacrista; popac, postparacrista; prmec, premetacrista; pomec, postmetacrista. Wear land: 1, small wear land; 2, moderate; 3, large. Volume of space behind crest: 1, small volume; 2, moderate; 3, large. Relief angle: 1,  $0^{\circ}$  relief angle; 2, small relief angle; 3, large.

		Species					
	Crest	M. ater	N. macrotis	E. fuscus	P. townsendii	H. diadema	R. blasii
Edge sharpness (µm)	pomec	$19.45 \pm 1.2$	$12.35 \pm 0.71$	$15.63 \pm 0.89$	$9.61 \pm 0.79$	$13.52 \pm 1.28$	16.11 ± 1.44
Rake angle (°)	prpac	$-7.35 \pm 0.46$	$11.56 \pm 2.43$	$18.02 \pm 3.99$	$37.65 \pm 1.23$	$8.69 \pm 4.58$	$40.21 \pm 0.89$
	popac	$-7.00 \pm 1.24$	$11.62 \pm 1.20$	$8.73 \pm 3.04$	$22.25 \pm 0.57$	$23.25 \pm 3.97$	$30.69 \pm 3.19$
	prmec	$-1.03 \pm 1.26$	$15.24 \pm 1.80$	$13.78\pm2.96$	$25.61 \pm 1.66$	$15.92 \pm 2.70$	$35.45 \pm 2.86$
	pomec	-11.20 ± 1.64	$8.07 \pm 2.58$	$10.36 \pm 3.57$	$23.59 \pm 3.19$	$9.55 \pm 2.28$	$40.94 \pm 1.31$
Relief – wear	prpac	2 (1, 2)	1 (1, 1)	2 (1, 2)	1 (1, 1)	1 (1, 1)	1 (1, 1)
land (qual)	popac	1 (1, 2)	1 (1, 1)	1 (1, 3)	1 (1, 1)	1 (1, 1)	1 (1, 1)
	prmec	1 (1, 1)	1 (1, 1)	1 (1, 2)	1 (1, 1)	1 (1, 1)	1 (1, 1)
	pomec	1 (1, 1)	1 (1, 2)	1 (1, 1)	1 (1, 1)	1 (1, 1)	1 (1, 1)
Relief - volume	prpac	3 (3, 3)	3 (3, 3)	3 (3, 3)	3 (3, 3)	3 (3, 3)	3 (3, 3)
behind crest	popac	3 (3, 3)	3 (3, 3)	3 (3, 3)	3 (3, 3)	3 (3, 3)	3 (3, 3)
(qual)	prmec	3 (3, 3)	3 (3, 3)	3 (3, 3)	3 (3, 3)	3 (3, 3)	3 (3, 3)
	pomec	3 (3, 3)	3 (3, 3)	3 (3, 3)	3 (3, 3)	3 (3, 3)	3 (3, 3)
Relief – angle	prpac	2 (2, 2)	2 (2, 2)	2 (2, 2)	2 (2, 2)	2 (2, 2)	2 (2, 2)
(qual)	popac	2 (2, 2)	2 (2, 2)	2 (1, 2)	2 (2, 2)	2 (2, 2)	2 (2, 2)
	prmec	2 (2, 2)	2 (2, 2)	2 (2, 2)	2 (2, 2)	2 (2, 2)	2 (2, 2)
	pomec	2 (2, 2)	2 (2, 2)	2 (2, 2)	2 (2, 2)	2 (2, 2)	2 (2, 2)
Approach angle (°)	prpac	$39.12 \pm 0.65$	$32.47 \pm 0.92$	$41.49 \pm 0.74$	$33.27 \pm 0.34$	$26.70 \pm 0.47$	$25.20 \pm 1.04$
	popac	$37.02 \pm 0.67$	$37.29 \pm 0.51$	$42.27 \pm 0.52$	$41.52 \pm 0.35$	$30.11 \pm 0.44$	$36.67 \pm 0.37$
	prmec	$36.23 \pm 0.66$	$27.55 \pm 0.47$	$35.96 \pm 0.68$	$30.35 \pm 0.59$	$24.35 \pm 0.47$	$29.81 \pm 0.78$
	pomec	$36.30 \pm 0.63$	$32.14 \pm 0.35$	$37.03 \pm 0.91$	$37.21 \pm 0.68$	$25.30 \pm 0.77$	$26.86 \pm 0.64$
Capture area	prpac	$43.15 \pm 1.58$	$67.22 \pm 3.75$	$43.05 \pm 1.79$	$23.41 \pm 0.80$	$61.67 \pm 2.66$	$20.84 \pm 1.65$
$(10^3\mu m^2)$	popac	$134.38 \pm 5.13$	$136.06 \pm 4.45$	$93.19 \pm 3.88$	$50.37 \pm 1.45$	$134.50 \pm 5.86$	$83.77 \pm 2.13$
	prmec	$68.01 \pm 2.68$	$74.16 \pm 2.02$	$57.73 \pm 2.96$	$32.66 \pm 1.77$	$47.02 \pm 1.97$	$30.48 \pm 1.13$
	pomec	$105.04 \pm 4.69$	$99.04 \pm 1.00$	$91.24 \pm 4.51$	$60.44 \pm 0.99$	$115.55 \pm 5.63$	$64.02 \pm 2.23$

**Table 7.4.** Cusp occlusion relief (mean  $\pm$  SE) and fragment clearance (median, with minimum and maximum in parentheses) for paracone and metacone basins and trigon groove for six intractable and tractable feeding species. n = 5 for all species. mesost, mesostyle; paba, paracone basin; meba, metacone basin.

			Species					
	Feature	M. ater	N. macrotis	E. fuscus	P. townsendii	H. diadema	R. blasii	
Cusp occlusion relief (µm)	mesost	$108.29 \pm 2.39$	$76.88 \pm 4.19$	$164.92 \pm 4.26$	$47.54 \pm 3.63$	87.18 ± 14.19	$71.76 \pm 3.17$	
Fragment	paba	2 (2, 2)	2 (2, 2)	2 (2, 3)	3 (3, 3)	3 (2, 3)	3 (3, 3)	
clearance (qual)	meba	2 (2, 2)	2 (2, 2)	2 (2, 3)	3 (3, 3)	3 (2, 3)	3 (3, 3)	

**Table 7.5.** Results of statistical comparisons of functional parameters within three microchiropteran families given as p values. a) Angle data; b) parameters divided by SV3; c) parameters divided by tooth length (tl). a)-c) Mann-Whitney U-test; d) Fisher's Exact test. Abbreviations as in Tables 7.2-7.4. Significance level: \*\*\*  $p \le 0.001$ ; \*\* p < 0.01; \* p < 0.05; NS, not significant.

			Family				
	Feature	Molossi	dae	Vespertili	onidae	Rhinolo	phidae
a) Angles							
Rake angle	prpac	0.016	*	0.117	NS	0.028	*
	popac	0.009	**	0.175	NS	0.917	NS
	prmec	0.028	*	0.076	NS	0.028	*
	pomec	0.028	*	0.175	NS	0.009	**
Approach angle	prpac	0.028	*	0.009	**	0.465	NS
	popac	0.917	NS	0.917	NS	0.009	**
	prmec	0.009	**	0.009	**	0.076	NS
	pomec	0.028	*	0.917	NS	0.917	NS
b) Divided by SV3							
Tip sharpness	me	0.248	NS	0.175	NS	0.602	NS
Cusp sharpness to	pa	0.602	NS	0.028	*	0.009	**
10×SV3	me	0.754	NS	0.009	**	0.009	**
Cusp sharpness to	pa	0.117	NS	0.009	**	0.009	**
30×SV3	me	0.251	NS	0.009	**	0.009	**
Cusp occlusion relief	mesost	0.028	*	0.009	**	0.347	NS
Edge sharpness	pomec	0.076	NS	0.175	NS	0.117	NS
Capture area	prpac	0.009	**	0.117	NS	0.347	NS
	popac	0.251	NS	0.117	NS	0.028	*
	prmec	0.117	NS	0.251	NS	0.028	*
	pomec	0.465	NS	0.917	NS	0.175	NS
c) Divided by tooth length							
Tip sharpness	me	0.248	NS	0.465	NS	0.917	NS
Cusp sharpness to	pa	0.917	NS	0.047	*	0.117	NS
3/50 tl	me	0.917	NS	0.016	*	0.047	*
Cusp sharpness to	pa	0.175	NS	0.016	*	0.009	**
1/5 tl	me	0.465	NS	0.009	**	0.009	**

Table 7.5 cont.

				Fami	ly		
	Feature	Molossi	dae	Vespertili	onidae	Rhinolo	phidae
Cusp occlusion relief	mesost	0.175	NS	0.009	**	0.175	NS
Edge sharpness	pomec	0.117	NS	0.465	NS	0.076	NS
Capture area	prpac	0.175	NS	0.754	NS	0.009	**
	popac	0.009	**	0.602	NS	0.754	NS
	prmec	0.009	**	0.465	NS	0.009	**
	pomec	0.602	NS	0.047	*	0.016	*
d) Qualitative data							
Relief – wear land	prpac	1.000	NS	0.444	NS	1.000	NS
	popac	1.000	NS	1.000	NS	1.000	NS
	prmec	1.000	NS	1.000	NS	1.000	NS
	pomec	1.000	NS	1.000	NS	1.000	NS
Relief – volume	prpac	1.000	NS	1.000	NS	1.000	NS
behind crest	popac	1.000	NS	1.000	NS	1.000	NS
	prmec	1.000	NS	1.000	NS	1.000	NS
	pomec	1.000	NS	1.000	NS	1.000	NS
Relief – angle	prpac	1.000	NS	1.000	NS	1.000	NS
	popac	1.000	NS	1.000	NS	1.000	NS
	prmec	0.167	NS	0.167	NS	1.000	NS
	pomec	1.000	NS	1.000	NS	1.000	NS
Fragment clearance	paba	1.000	NS	0.167	NS	0.444	NS
	meba	1.000	NS	0.167	NS	0.444	NS

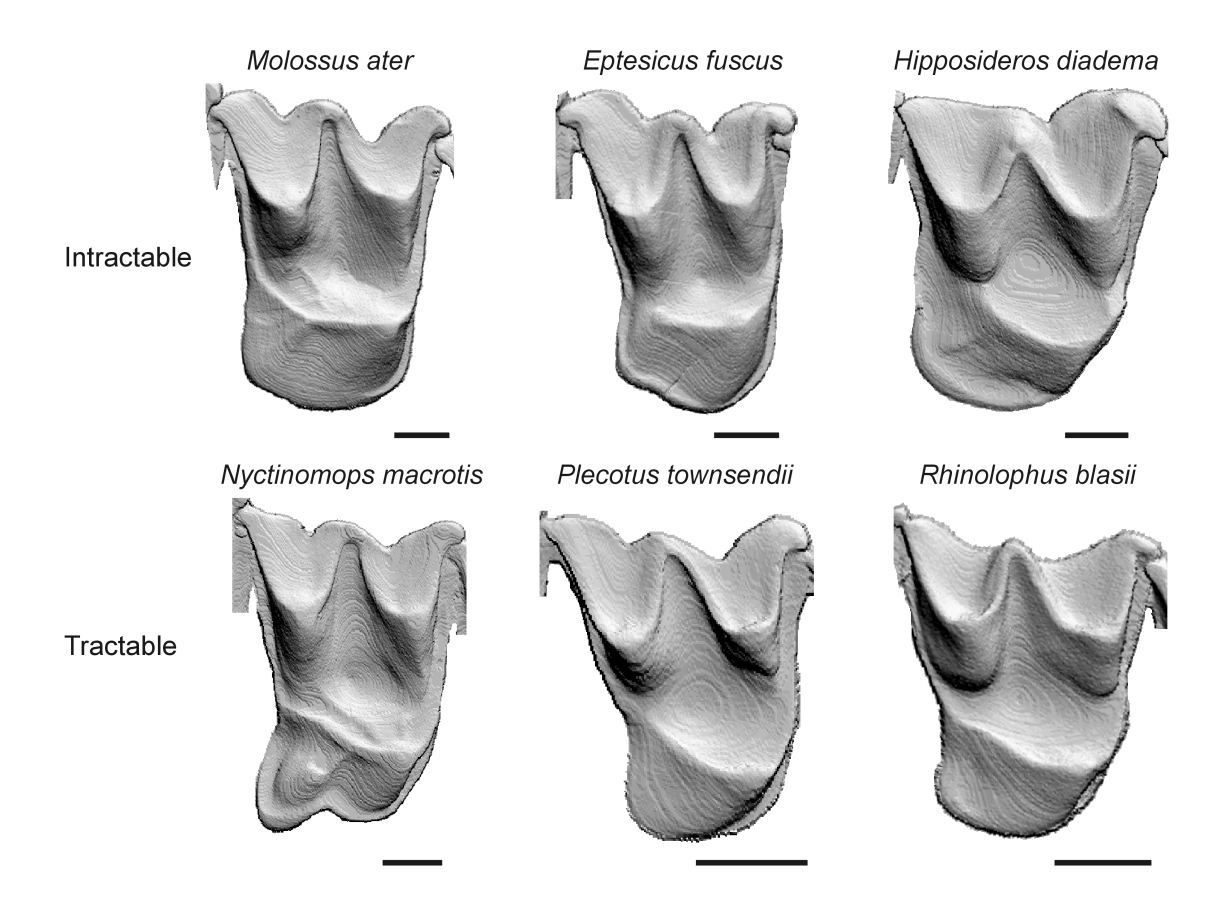
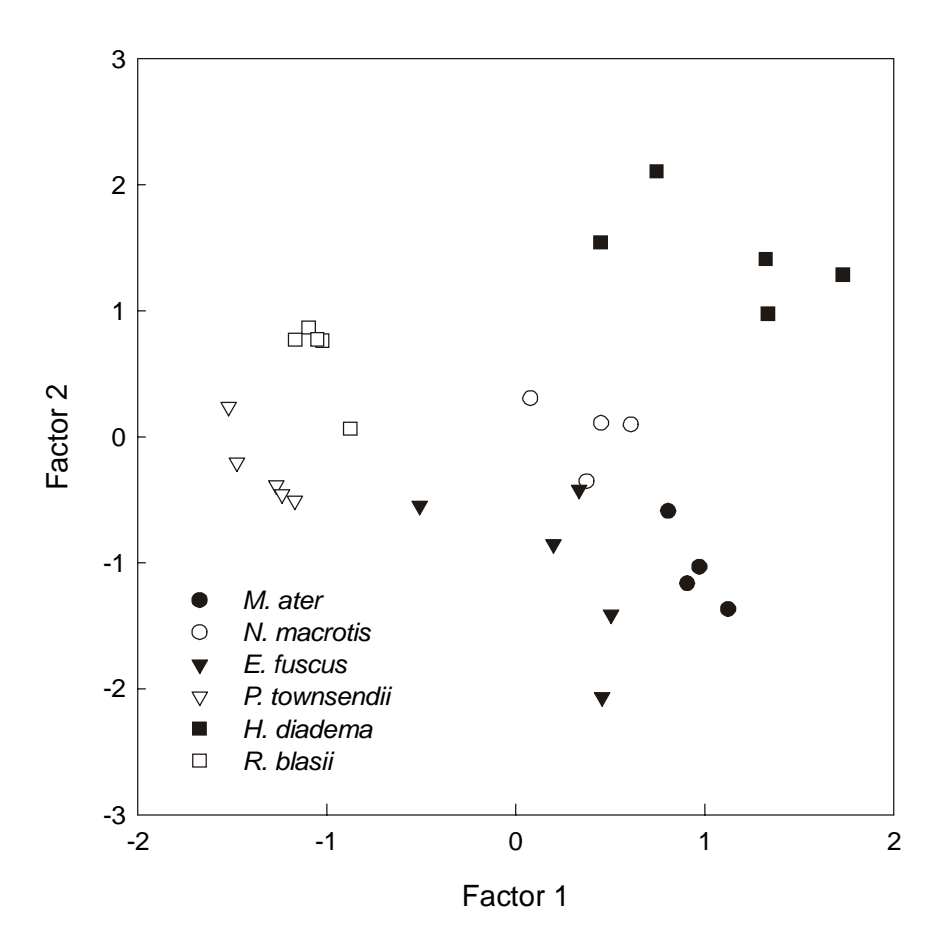
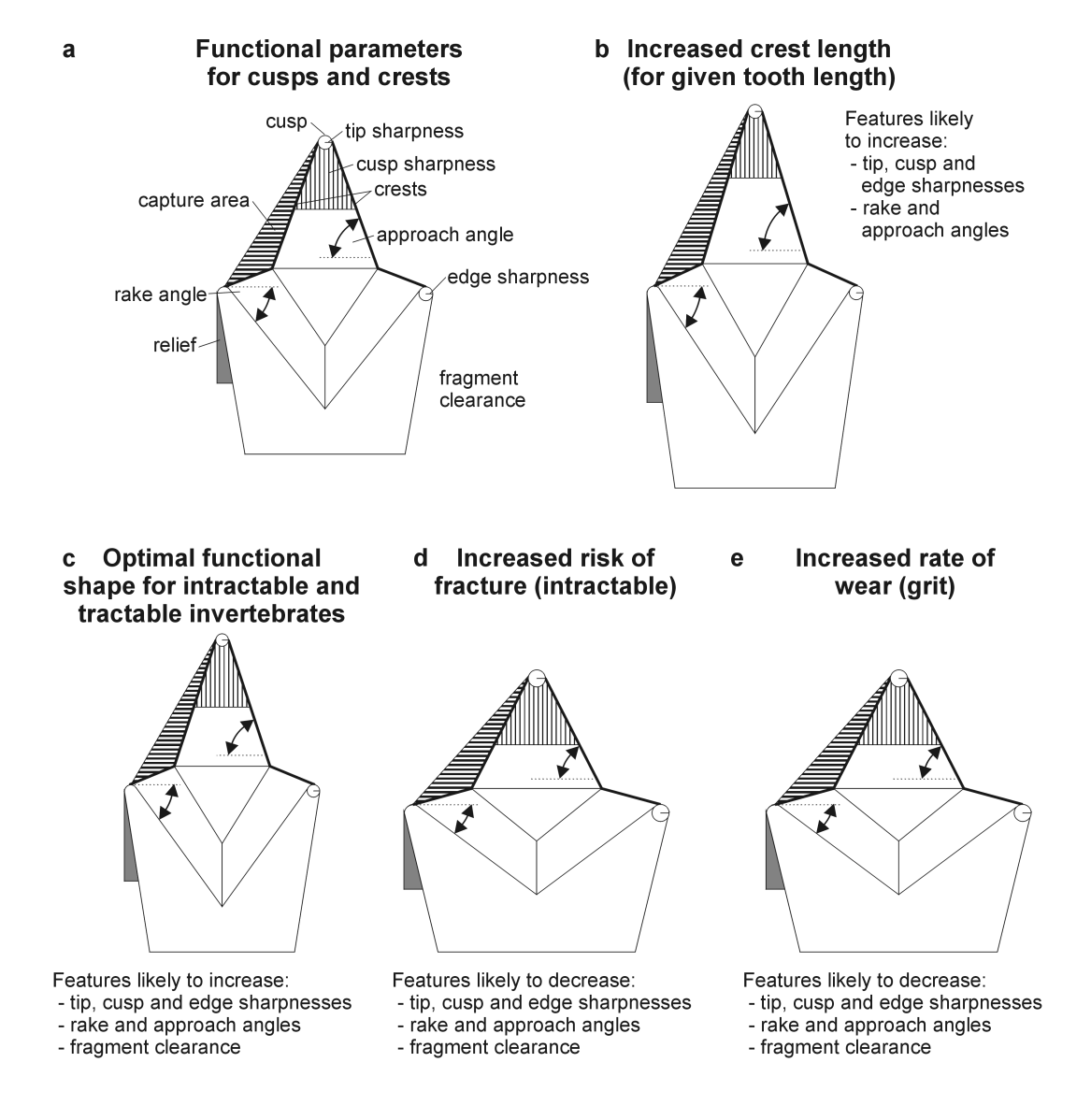


Fig. 7.1. Shaded relief reconstructions of upper second molars of six microchiropteran species. Scale bars =  $500 \, \mu m$ .



**Fig. 7.2.** PCA (Factor 1 vs Factor 2) plot for all functional parameters for three intractable (black symbols) and three tractable (white) feeding species of microchiropterans.



**Fig. 7.3.** a) Eight functional parameters are depicted schematically for a cusp/crest structure, such as the paracone with pre- and postparacristae. b) An increase in the length of the crest (for a given tooth basal area or tooth length) is likely to lead to increases in several of the functional parameters. c)-e) Comparison of the expected tooth shapes for the three hypotheses discussed in the text: the optimal tooth shape for comminuting intractable and tractable invertebrates (c); increased resistance to tooth fracture when feeding on intractable invertebrates (d); increased tooth wear for a diet with high levels of grit (e). Differences between the models and features such tip and edge sharpnesses are exaggerated. The diagram does not purport to represent the exact method of measurement for the parameters.

#### 7.4. Discussion

## 7.4.1. Three hypotheses

Three possible reasons were postulated for any differences found between the tooth form of the intractable and tractable insectivores. The first hypothesis is that the optimal functional form may differ for an intractable and tractable invertebrate diet. Where there are extensive differences in the biomechanical properties of foods, the optimal tools to divide them are predicted to differ dramatically (Lucas 1979; Lucas and Luke 1984; Osborn and Lumsden 1978). The diversity of biomechanical properties among invertebrates is low compared to the great range of all mammalian diets (including bone, meat, skin, grass, leaves, stems, fruit, nectar and blood), but still contains considerable variety. In Chapter 6 it was concluded that the cuticle of intractable insects is structurally tougher than that of tractable insects. However, both types require reasonable amounts of energy to fracture, either because of crack-stopping mechanisms in the stiff cuticle so that there is very little brittle fracture, or due to their ductility. A significant commonality of both types is that their internal organs are generally ductile and relatively tough. In addition, the complex structural nature of an invertebrate means that multiple initiations of fracture are required to completely divide it - cracks do not self-propagate through the whole animal. Therefore, both intractable and tractable types of invertebrates will require cusps to initiate crack propagation and crests to force the propagation of cracks through the entire animal, and we can argue that dealing with toughness is probably the principal objective of insectivore teeth. Invertebrates would not be efficiently divided by a mortar and pestle, as this would require large amounts of force. Such excess force may be available to large-bodied animals that eat insects but not to small insectivores.

Intractable and tractable insects have been found to be substantially different in the structural strength and stiffness of the cuticle (see Chapter 6). In terms of tooth function, this will probably only be relevant to tip and edge sharpnesses. If strength were increased, it would be further advantageous to increase tip and edge sharpnesses to enhance the stress induced in the food. However, Lucas (1982) argued that if stiffness were also increased, the area of contact between tooth and food would not be greatly increased, maintaining higher stress in the food. This does not negate the inference that tip sharpness should still be as high as possible (demonstrated by applications such as emergency hammers with extremely sharp points for breaking glass in the case of an accident), only that the risk of fracture may be increased (which is dealt with in the next hypothesis). An increase in

stiffness may change the ease with which food is captured by concave crests, but it is difficult to predict whether this would encourage a larger or smaller capture area.

Therefore, for both foods, the optimal cusp will have low tip and cusp sharpnesses, which will minimise the force and energy required to penetrate and drive through the food (Fig. 7.3c), as demonstrated for both intractable and tractable invertebrates (Evans and Sanson 1998). There should be relief behind points of cusp occlusion. For crests, edge sharpness, rake and approach angles and fragment clearance should be maximised, and crest relief and capture should be present (Fig. 7.3c). Therefore, no substantial difference in the optimal shapes for comminuting both intractable and tractable insects would be expected, and so would not lead to any difference in dental form. Note that the result of this analysis would differ if the hard food was also significantly brittle for a large proportion of the food, where a mortar and pestle arrangement would be advantageous (Lucas and Luke 1984).

Our prediction for similar optimal tooth shapes for intractable and tractable insectivores differs from that of Strait (1993c). Strait (1993c) predicted that the optimal tooth shape for 'hard' eaters will have short crests to minimise the area of contact between the crest and food. She also reasoned that 'soft' feeders could manage with longer crests because a 'soft' diet is weaker, and critical fracture stress could still be achieved with a higher contact area. However, crests are not oriented parallel to the food (Evans and Sanson 1998); in fact, longer crests (for a given basal area and tooth length) require an increase in the height of the cusp and will tend to give higher tip, cusp and edge sharpnesses and approach and rake angles (Fig. 7.3b). These functional features would be selected for in both intractable and tractable feeders, and may be particularly important for tractable feeders, where the high ductility of the food makes penetration and cutting difficult. The presence of other constraints, particularly on the intractable feeder tooth form, is likely to be responsible for any reduction in these parameters and so for a less effective tooth.

The second hypothesis is that the greater force required to fracture intractable insects increases the risk of tooth fracture. The greater structural strength of intractable foods would require greater bite forces in intractable feeders. Stress in the tooth could be reduced by increasing the structural integrity and robustness of the dental components. A decrease in the height and/or an increase in the width or length of the tooth or individual cusps would achieve this. In terms of functional parameters, this would most likely lead to decreased tip, edge and cusp sharpnesses, and rake and approach angles (Fig. 7.3d). Capture area and fragment clearance may be reduced. Cusp occlusion relief and crest relief

may be diminished, as these features would tend to reduce tooth strength, but perhaps only marginally. Selection for increased resistance to higher bite forces is likely to result in differences in enamel thickness, which is greater in intractable feeders compared to congeners (e.g. Dumont 1995), and in enamel structure (e.g. Koenigswald *et al.* 1987).

Bats are reasonably likely to incur tooth fracture and loss during their lifetime (7.7% of individuals have at least one broken tooth, 19.9% at least one missing or broken tooth; Fenton *et al.* 1998c). Extreme differences in the strength and hardness of the diet can have an effect on the risk of fracture, as was found between bone-feeding and meat-feeding carnivores (Van Valkenburgh 1988). In the case of intractable and tractable insectivores, the increased risk may be very slight, or easily overcome by an increase (possibly only minor) in sturdiness. However, it is unlikely to be great enough to cause a significantly higher rate of tooth fracture, given the lack of significant effect of differences in broad dietary categories among bats (animal, blood, fruit and nectar) on tooth fracture. This differs from the situation in large carnivores, which appear to have reached a structural limit in strengthening the canines (Van Valkenburgh 1988).

The third hypothesis posits that differences in tooth form may result from differential wear from intractable and tractable diets. It has apparently been assumed that the hard exoskeleton of beetles is more likely to cause wear than the softer exoskeleton of other invertebrates, such as moths, larvae and the like (Strait 1993c). 'Hardness' can be defined as the ability of one material to scratch or penetrate another (see Chapter 6; Lowrison 1974). Hardness values for invertebrate skeletons are substantially below those of enamel and dentine. This is supported by some comparative values for hardness from Vickers (V), microvickers (mv) and Knoops (K) tests, the results of which are not directly comparable (Lowrison 1974); invertebrates: tibia 8.3 kg mm<sup>-2</sup>, abdominal tergite 23.9 kg mm<sup>-2</sup>, mandible 36.4 kg mm<sup>-2</sup> (V; Hillerton et al. 1982); leaf-cutting ant 52.1 kg mm<sup>-2</sup> (V; Edwards et al. 1993) and ~100 kg mm<sup>-2</sup> (microindentation and atomic force spectroscopy; Schofield et al. 2002); teeth: human dentine and enamel, 74 and 393 kg mm<sup>-2</sup> respectively (K; Waters 1980); macropodine enamel, 270-379 kg mm<sup>-2</sup> (mv; Palamara et al. 1984); koala dentine and enamel, 122 and 410 kg mm<sup>-2</sup> respectively (K; Young et al. 1990). From this, it seems unlikely that the increase in hardness from tractable to intractable invertebrates would greatly increase wear (even though softer materials can cause wear given sufficient force; Bayer 1994; Puech et al. 1981).

A more likely cause of wear in insectivores is siliceous grit, which may be on the outer surface of the invertebrate or in its gut. Several factors that would influence the amount of grit can be considered: the habitat (terrestrial or aerial) and diet of the

invertebrate, and the intractability of the cuticle. An invertebrate that lives in soil (e.g. burrowing beetle or cricket) will have greater dirt in and on its body than one that lives its life in the air, only occasionally alighting on a surface (e.g. moth or trichopteran). A herbivore or detritivore (e.g. beetle or earthworm) may also ingest large amounts of soil, or phytoliths from plant leaves, that firstly wear the beetle's mandibles, and when ingested and masticated by a bat, subsequently wear the bat's teeth. This contrasts with the non-abrasive diet of a fluid feeder (e.g. moth). The intractability of the exoskeleton is also likely to be influential: a beetle with intractable mandibles will almost certainly consume harder and more abrasive foods than a fluid feeder.

These factors indicate that a beetle is more likely to be associated with a greater amount of grit than a moth. Coupled with the greater bite force of intractable insectivores, this may also increase the rate of wear. The result is that beetle-eaters may experience more dental wear than moth-feeders, but not for the simple reason that a beetle's exoskeleton is harder or more intractable. It is interesting to note that those insectivores that have the least exposure to wear-causing grit (due to their aerial habitat) are also the most long-lived, suggesting that increased longevity may be caused (or at least enabled) by lower tooth wear rates in microchiropterans compared to terrestrial insectivorans and marsupial insectivores (Jürgens and Prothero 1987), but this would need to be examined using data on the influence of tooth wear on longevity in these groups.

Increased wear would select for features that improve wear resistance, such as a greater amount of dental material available for wear. This may have a similar appearance to increased robustness, and have the functional parameter characteristics described above (Fig. 7.3e). Thicker enamel would also be advantageous in this situation due to its greater resistance to wear compared to dentine. It is geometrically possible for robust teeth that resist wear (with large dental volume and low cusp sharpness) to have high tip and edge sharpnesses. This means that 'sharp' and 'robust' are not necessarily mutually exclusive for some functional parameters, as has been assumed (hard-eating 'should be associated with robust rather than sharp teeth because hard, brittle items would rapidly dull a sharp blade'; Freeman 1988:268). Greater wear may blunt cusps and crests, reducing tip and edge sharpnesses, but lower tip and edge sharpnesses in the unworn state will not necessarily be selected for. Sharpness in the unworn state could be as high as possible (without increasing the risk fracture), regardless of whether the sharp edge would later be dulled by wear.

This study shows that there are no general trends in the differences in the functional parameters of teeth for the families Molossidae, Vespertilionidae and Rhinolophidae.

There is a large amount of variability in many of the characters that, compounded by the small sample size, may disguise any broad patterns between species. For instance, there is a great deal of variability in rake angle in the vespertilionid specimens that may account for the lack of significant difference in that parameter. The qualitative measurements of some of the characters may be too imprecise to reveal differences, as no significant differences were found in these parameters. For instance, it may be expected that fragment clearance would be correlated with rake angle (as a larger rake angle will tend to improve the flow of food off the rake surface), but this was not apparent. Also, a different suite of functional parameters may vary between intractable and tractable feeders within each family.

Body size is most probably a confounding factor here, in that the scaling of these features is not isometric and perhaps differs to some extent among the families. The first factor of the PCA highly correlates with SV3 and tooth size. The second differentiates the intractable and tractable feeders in each family according to approach angle: the tractable feeder in Molossidae and Vespertilionidae and the intractable feeder in Rhinolophidae have higher approach angles. This means that approach angle does not necessarily follow changes in other parameters as closely as implied by Fig. 7.3. This shows that various features of the teeth can to some extent be varied independently (as was discussed in Chapter 2), and the situation is not as simple as that modelled in Fig. 7.3.

Strait (1993c) and Dumont (1995) found that there was no consistent value of shear ratio or enamel thickness that will distinguish all intractable feeders from tractable feeders regardless of the phylogenetic relationships. The same appears to be true for the functional parameters measured in this study.

The differences that are apparent within families will tend to decrease the functional effectiveness of the intractable feeder (e.g. smaller rake angle, but was not significantly different in vespertilionids). Variance in tooth form is not expected from Hypothesis 1, and so the lack of difference in many of the functional parameters may be due to the similar function of intractable and tractable invertebrate dentitions. The differences that do exist can be interpreted as being due to an increase in the robustness of the dentition. This robustness may be due to either increased risk of fracture (Hypothesis 2) or increased wear (Hypothesis 3). The result, though, is overall decreased effectiveness of the molars of intractable feeders, meaning that greater force and/or energy would be required for the teeth to function. However, the increased bite force of intractable feeders will allow them to compensate for this decreased effectiveness.

Therefore, tractable feeders are better able to maintain an efficient tooth form due to the fewer constraints placed upon them; intractable feeders build a more robust tooth to cope with additional demands (tooth fracture and wear). The greater jaw musculature that was already required by feeding on intractable foods (Freeman 1979) means that they can generate sufficient bite force for their teeth to function, but this in turn is likely to produce greater wear and to some extent compound the effect.

The extreme changes in function with wear that were apparent following wear in *C. gouldii* (Chapter 5) are much greater than any among different species in this study. It seems, then, that to some extent wear is a more influential factor in tooth form biomechanical properties *per se*, at least within insectivores. This may mean that the rate of wear is not dramatically different between the two feeding types considered here (at least in comparison to herbivorous tooth forms; see Chapter 9), but an increase in wear may still have an effect on tooth form.

The main difference induced by the greater intractability of the diet is likely to be increased bite force and the consequences that flow from this. This has been supported by other studies investigating 'hardness' (Aguirre *et al.* 2003; Dumont 1999; Freeman 1979). The diets of insectivores may be largely limited by the bite force they can generate (see further discussion in Chapter 9). A larger bite force is likely to increase the risk of fracture and tooth wear.

### 7.4.2. Biomechanical properties and tooth form in previous studies

Freeman (1979, 1981a) found a significant difference in the sizes of the molars in 'hard' and 'soft' feeders. In 'hard' feeders, the first and second molars were larger and the third molar smaller, often lacking the premetacrista that was present in the soft feeders, creating a 'V' ectoloph instead of a 'W' or 'N'. The length of the premetacrista of the M<sup>3</sup> was the most significant molar determinant of dietary hardness found by Rodríguez-Durán *et al.* (1993). These differences by themselves do not reveal a lot about the comparative function of the molars. Later studies by Freeman (1984, 1988, 1998) found that hard-feeding bats were more wide-faced than soft-feeding bats. These bats were distinct from soft-feeding insectivorous and carnivorous bats, which form a continuous group. The reduction in the size of the M<sup>3</sup> and the wide faces brings the teeth closer to the fulcrum, increasing leverage (Freeman 1995).

There is a suite of possible explanations for the difference in relative size of the molars. Firstly, it may be related to the number of contact points along the molar row. When penetrating intractable foods, function is aided by minimising contact area between the food and teeth. This can be done by either reducing the overall number or increasing

the spacing between them, ensuring fewer cusps will contact an object of a given size. This has been achieved in the intractable feeders by reducing the number of cusps on the third molar (where the metacone is now absent) and spacing the remaining cusps out along the tooth row. However, the effect of decreasing the number of cusps in contact may only be minor.

Likewise, the greater number of cusps in tractable feeders may be an advantage. Although more cusps will distribute the force over a larger area and thereby reduce the effective stress, the lower structural strength of tractable invertebrates should mean that this does not considerably impede the insectivore. The initiation and propagation of cracks through a ductile material will be aided by an increase in the number of penetration points and therefore locations at which cracks are initiated.

Concurrent with the reduction in cusp number is an increase in the size of the first and second molars. If the increase in tooth size were isometric, then the tip sharpness would be decreased in absolute terms due to a larger radius of curvature. However, if the elastic modulus of the food is increased and animals have a diet that is stiffer (higher intractability), the contact area between tooth and food is not greatly enlarged (as discussed above; Lucas 1982). Therefore, an animal eating foods of higher intractability could afford to have blunter teeth.

The use of a relative measure of crest length, such as shear quotient and shear ratio, is an often-used method in dietary inference, particularly in primates (Anthony and Kay 1993; Benefit and McCrossin 1990; Covert 1986; Dumont *et al.* 2000; Kay and Hylander 1978; Kay *et al.* 1978; Kirk and Simons 2001; Strait 1991, 1993a, c, 2001; Ungar and Kay 1995; Williams and Covert 1994). However, such measures do not reveal a great deal about comparative function with regards to the shape or orientation of the crest and its associated rake and relief surfaces.

As tractable invertebrates are still relatively tough, greater crest lengths will be advantageous for tractable feeders, as this will tend to increase tip, edge and cusp sharpnesses, and rake and approach angles (Fig. 7.3b). The decrease in crest length in intractable feeders found by Strait (1993c) is most likely related to increased probability of fracture and wear. The difference in shear ratio between folivores/insectivores and frugivores is probably due to the importance of crests for fracturing the aforesaid food types and will increase the quantity of food processed by crests. It is very likely that there are also associated improvements in the mechanical efficiency of the crests (e.g. increased rake angles, capture areas, approach angles) that are not as important in a frugivorous dentition.

A potential source of discrepancy between Strait's (1993c) study and the current investigation is that shear ratio was measured for the lower molars in the former and the functional parameters were measured on the upper in the latter. It is unlikely that there would be significantly greater difference between intractable and tractable feeders in the lower molars than the upper, as occlusion must still be maintained, but it could be envisaged that the protoconid of the lower tooth (see Fig. 3.7, p. 66) may show a greater variation in height and therefore crest length than the upper ectoloph crests.

Two-dimensional and three-dimensional crest lengths were measured for the ectoloph crests. The total crest length was standardised for either SV3 (CL/SV3) or tooth length (CL/TL). Total crest length was only significantly different for 2D and 3D CL/TL and 2D CL/SV3 for molossids (Kruskal-Wallis (KW) test statistic = 1, p = 0.016; KW = 3, p = 0.047; KW = 1, p = 0.016, respectively) and for 3D CL/SV3 for vespertilionids (KW = 25, p = 0.009); all other tests showed p > 0.05. From this, crest length of the upper ectoloph crests also does not reveal consistent differences between intractable and tractable feeders.

An extremely interesting investigation on the correlations between several biomechanical properties of the diet and tooth form in five lemur species was carried out by Yamashita (1998). Two of the hypotheses that were tested were: 1) crest length would be positively correlated with shear strength – 'longer crests would be able to drive crack propagation in tougher leaves' (Yamashita 1998:178); and 2) radius of curvature would be positively correlated with food hardness. These two hypotheses and the findings in that paper will be examined in light of the above discussions.

1) The mechanical test used to measure 'shear strength' was a punch test, the results of which have been interpreted in this thesis as a measure of structural strength. Yamashita (1996:357) has a similar interpretation: 'Shear strength is not a substitute for fracture toughness, which measures the work of fracture. It is simply a measure of the breaking stress of a material placed under a shearing load'. Therefore, we cannot test a hypothesis regarding the toughness of leaves from this test. If strength is measured by these tests, we may expect that there would be a negative rather than positive correlation between shear strength and crest length due to increased robustness of the tooth form related to risk of tooth fracture and increased wear.

Despite the punch test measuring structural strength, if the foods measured by Yamashita (1996, 1998) can be considered intractable, structural toughness would also be higher in those foods with high structural strength. This still does not mean that a correlation between dietary toughness and crest length would be expected. If a food were

sufficiently tough that crests are required to drive a crack through it (i.e. it is not fragile or brittle), increasing the toughness further would not encourage longer crests. A longer crest (all other functional parameters being the same) would not help to propagate cracks in a tougher food; it would only increase the amount of food divided, which in itself may be an advantage but it is not what was advocated.

In addition, if the structural strength were also increased along with toughness, greater force would be required to drive the crest through the food for the original crest length. A longer crest would hinder this further, as the stress induced in the food by the crest driving through it will be lower for a given applied force. If sufficient food to maintain the animal's metabolism is divided by a given crest length and the toughness of the food were further increased (as is the situation envisaged by Yamashita 1998), then we may expect that the crest length would not be increased.

The findings of Yamashita (1998) did not support this hypothesis, finding a negative correlation between shear strength and crest length. This is more expected given the alternatives discussed above, such as increased robustness due to the higher strength of foods.

2) The prediction that radius of curvature would be correlated with food hardness is in accord with the approach in this thesis. However, the method by which radius of curvature was measured in Yamashita's (1998) study is suspect. Pilot studies for this thesis showed that the measurement of radius of curvature depends greatly on the resolution at which it is measured (*unpublished data*). The measure of radius of curvature used by Yamashita (1998) does not specify the resolution at which the radius of curvature was measured, i.e. how far B and C are from A in fig. 3 of Yamashita (1998). This is crucial to the answer that is obtained. This issue is why tip and edge sharpness measurements in this study were carried out at the highest possible resolution (1 µm) for the confocal microscope set-up.

In addition to the points raised above regarding the specific hypotheses, the results of the mechanical tests of Yamashita (1996, 1998) should be viewed with caution, as they were not carried out under a constant loading speed, and so will potentially vary due to the viscoelasticity of foodstuffs.

#### 7.4.3. Additional differences in tooth form

The tractable feeders display further differences from the intractable feeders that were not quantified by the nine functional parameters. Some of these can be interpreted as adaptations for improved fracture of tough, ductile foods. In *N. macrotis*, the rake surface of the protocone crests is concave (Fig. 7.1). This would improve the rake angle of these

crests (which was not quantified in the current study). The buccal edges of these grooves meet the lingual faces of the base of the paracone and metacone. This would direct flow of some food cut on the protocone crests into the embrasure between teeth rather than into the talon basin. Fracture of tough, ductile food is unlikely to be efficiently accomplished through the mortar and pestle action of the talon basin (Lucas and Luke 1984), and may impede centric occlusion of the molars when the food is largely incompressible. This grooved rake surface is not found in the other molossid *M. ater* or any of the other species.

The lower molars of *R. blasii* have distinct sharp notches in the paracristid (and sometimes protocristid). This notching improves the approach angle of the crests and the efficiency of cutting at the end of a stroke (similar to a carnassial notch in carnivores). In intractable feeders, this notch is not as emphasised.

In several of the tractable feeders, the relief surface consisted of a thin wear land (attrition facet) along the crest edge, behind which the relief surface was slightly concave. This was particularly noticeable for the postmetacrista and preparacrista. Such an arrangement will improve relief behind a crest, as was noted in *Chalinolobus gouldii* (Chapter 5). However, once a moderate amount of wear has occurred, the thin band along the crest edge is removed, leading to an increase in the width of the wear land and a slight decrease in the amount of relief. This suggests that teeth that undergo significant wear would be less likely to have such a feature, as it would create large wear lands at higher wear states. Since this feature only occurs in tractable feeders, this may indicate that they are less prone to tooth wear than intractable feeders, but this is not conclusive.

Three of the *H. diadema* specimens had undergone more wear than the other two. The enamel on the rake surface was worn away to approximately 100 µm from the crest edge along the length of the ectoloph crests. In general, the five specimens of *H. diadema* group together on PCA plots (Fig. 7.2), so it appears that on the whole this small amount of wear does not affect the shape of the teeth. The two unworn specimens have higher Factor 2 values, giving greater separation from the *R. blasii* specimens. There is a profound difference in rake angle between these specimens, though, which indicates that this is probably the main variable affected by wear at this early stage.

### 7.5. Conclusions

Consistent significant differences between intractable and tractable feeders in three microchiropteran families were not found. However, the differences that were found within families indicated that the effectiveness of teeth of intractable feeders tended to be lower.

This may be due to an increased risk of fracture or rate of tooth wear in intractable feeders, but not due to any predicted difference in the ideal tooth form of these two dietary groups.

It appears that increased structural strength is the main difference in intractable diets, which probably leads to increased bite force by increased musculature, and increased risk of fracture and wear, and so greater robustness of the teeth which reduces the functionality of the tooth. These conflicting forces are not as apparent in tractable feeders, which in general had more advantageous functional characteristics compared to intractable feeders.

# **Chapter 8.** The Scaling of Tooth Sharpness

## 8.1. Introduction

There has been significant interest and debate surrounding the scaling of mammalian teeth in the zoological and palaeontological literature (Fortelius 1985; Gingerich and Smith 1985; Gould 1975; Janis 1988; Kay 1975; Legendre and Roth 1988; Pilbeam and Gould 1974). In some cases, isometry of tooth size (usually molar area) with body mass has been identified, and it has been argued that isometric scaling of tooth planar area would result in isometric scaling with metabolic rate (Fortelius 1985, 1988, 1990). This would coincide with findings of isometric scaling of particular aspects of the mammalian masticatory system with body size (e.g. Fortelius 1985). However, one aspect that requires further investigation is the scaling of particular functional features of teeth with body size, and specifically how this would affect tooth function. It is not sufficiently known to what extent functional features, such as those examined in this thesis, are independent of tooth length or crown area, nor how they scale with body mass.

One important instance of the scaling of dental features is tooth sharpness, and whether isometric scaling of tooth sharpness would be expected. Three aspects of this will be considered: 1) whether geometrically similar teeth will function in the same way in a masticatory system that scales isometrically; 2) the functional consequences of different scaling regimes of sharpness; and 3) the effect of various aspects of teeth (including development and wear) on the scaling of tooth sharpness. Each of these will affect whether isometric scaling of tooth sharpness would be found in mammals. The published information on the scaling of tooth sharpness will be reviewed, and combined with data collected in this thesis to extend the size range over which sharpness has been examined.

## **8.2.** Functional Scaling of Tooth Sharpness

In order to investigate the function of teeth in geometrically-scaled masticatory systems, we will devise two identically-shaped organisms, animal A with a body length l, and B with body length 2l (Table 8.1). The body mass of A is  $M_A$ , which is proportional to  $l^3$ ; similarly, the body mass of B will be  $M_B = 2^3 M_A = 8 M_A$ . Tooth sharpness measured as the radius of curvature at the tip or edge (tip and edge sharpnesses respectively) of the teeth of A will be  $r_A \propto l$ ; for B,  $r_B = 2r_A$ ; the volume (cusp sharpness) of the tooth will be  $v_A \propto l^3$ ; or  $v_B = 8v_A$ . The maximum bite force of animals is typically proportional to the cross-sectional area of the muscle mass, and so for A will be  $b_A \propto l^2$ ; for B,  $b_B = 4b_A$ .

**Table 8.1.** Two isometric animals, A and B, of length l and 2l, respectively, and their proportions for features that relate to tooth function.

	Animal A	Animal B
Length (l)	l	21
Features proportional to length, e.g. radius of curvature (r)	$r_{\rm A} \propto l$	$r_{\rm B} = 2r_{\rm A}$
Area (a)	$a_{\rm A} \propto l^2$	$a_{\rm B} \propto (2l)^2 = 4l^2$
Features proportional to area, e.g. bite force (b)	$b_{ m A} \propto l^2$	$b_{ m B} = 4b_{ m A}$
Volume (V)	$V_{\rm A} \propto l^3$	$V_{\rm B} \propto (2l)^3 = 8l^3$
Features proportional to volume, e.g. body mass (M) and tooth volume (v)	$M_{\rm A} \propto l^3$ $v_{\rm A} \propto l^3$	$M_{\rm B} = 8M_{\rm A}$ $\nu_{\rm B} = 8\nu_{\rm A}$

In this example, we will assume that the application of force onto food is a major factor in tooth function. This assumption is supported by previous findings and discussions on the influence of the functional parameters on tooth function and the absolute strength of structures. Factors such as tooth sharpness will affect the minimum force required for a tooth to function, f. For instance, a blunter tooth will require greater force to penetrate or drive through food (Evans and Sanson 1998). It should be true that an animal cannot make use of a tooth that requires greater force to function than it can generate with its musculature, i.e. if f > b. This may be so in the literal sense (in that the animal physically cannot generate a large enough bite force) or in terms of efficiency (the animal expends substantially greater energy in processing the food than it obtains from consuming it). There will undoubtedly be some degree of plasticity in the forces that can be produced by the musculature, but there must be an upper limit to the bite force. In the present example, we will assume that, for the small animal A, the force required for the tooth to function,  $f_A$ , equals the bite force,  $b_A$ .

The principal question to be answered is: how does the scaling of sharpness affect the force required for the tooth to function? That is, how does f scale with regard to body size? For the example above, if it takes A (with a tooth of radius of curvature  $r_A$  and volume  $v_A$ ) a force of f (=  $b_A$ ) to penetrate or divide food of thickness t, what force does B with radius of curvature  $2r_A$  and volume  $8v_A$  require to act on the same foodstuff of

thickness 2t (also isometrically scaled)? For a tooth to maintain the equivalent function in an isometric system, the answer must be 4f ( $b_B = 4b_A = 4f$ ; i.e.  $f \propto l^2$ ), because this is the bite force generated by the larger animal. Therefore, it must be determined if the force to reduce food scales with  $l^2$  for the same tooth design.

The scaling of force will depend on whether the radius of curvature of the tooth (linear) or the volume of the tooth (cubic) has the greater influence on the force required for the tooth to function. In all likelihood, both of these features will have an effect, along with other factors such as the biomechanical properties of the food (particularly structural properties). However, the determination of the relationship between size and force will require some degree of empirical testing; it will also vary with the exact mode of function of the tooth and for different dental systems (such as protoconoid, carnassial and selenodont; the 'protoconoid-based' tooth form includes zalambdodont, dilambdodont and tribosphenic – see Chapter 9). In one respect, the forces that larger animals can generate with their muscles are lower than those of small animals relative to body size: for example, the force of a muscle will scale with  $l^2$  but the mass of a limb by  $l^3$ , so at some body size an isometric animal will not be able to lift its own limbs.

In light of this, there will most probably be a discrepancy between the scaling of bite force that an animal can generate and the force required for the dentition to function (e.g. in penetrating or fracturing food). In this case, the function of the tooth will in some way be limited or constrained by the bite force that an animal can generate. Specifically, if the force required scales at a greater rate than bite force (i.e. x > 2 for  $f \propto l^x$ ), at some body size the bite force will be less than the force required and so the tooth will either not function at all, or with greatly reduced efficiency.

## 8.3. Processes that Influence Tooth Sharpness

We will first examine two regimes of scaling of tooth sharpness (measured as radius of curvature) and the possible functional consequences of these regimes. The forces that potentially influence scaling will then be considered, and how the relative strengths of these constraints vary with body mass.

The first situation is the isometric (or positively allometric) scaling of tooth sharpness with regard to body mass (Fig. 8.1a). There is likely to be a body size above which the decreased absolute tooth sharpness (higher radius of curvature) means that the force required exceeds the bite force.

Second, if sharpness is constant for all body sizes (Fig. 8.1b), it is likely that below a certain body mass, bite force will be insufficient for the tooth to function. At the other

end of the size scale, as bite force increases and tooth sharpness remains the same, the risk of fracture of the cusp or crest will be prone to increase at some large body size.

The processes of tooth development may have an important influence on tooth sharpness. Isometric scaling (the first situation considered above) may be caused by developmental constraints on tooth form. This would be the case if the minimum radius of curvature that can be produced in development increases with body size. It is conceivable that development could bring about scale-independence of sharpness (the second situation), but it seems less likely than an allometric relationship given the strong relationship between overall tooth size and body mass.

A very significant determinant of sharpness scaling is likely to be post-developmental modification of the tooth that occurs in the animal, i.e. wear. Developmental processes may indeed manufacture teeth with radii of curvature that scale isometrically, but the use of the tooth will reshape its surface. The amount and distribution of wear on a tooth will be influenced by many factors: gross tooth form, bite force, enamel thickness and microstructure, the biomechanical properties and absolute size of foods, and the relative contributions of attrition and abrasion (generally, wear on the relief and rake surfaces respectively; see Chapter 5). The aspects that contribute to wear, and the degree to which they scale with body size, will be the ultimate determinants of tooth sharpness in the living and chewing animal.

The ratio of attrition to abrasion will be a significant factor in tooth sharpness (Popowics and Fortelius 1997). Attrition is tooth-tooth contact of relief surfaces, and will tend to sharpen an edge through the removal of dental material from the relief surface (Fig. 8.2). Wear on the rake surface by food (abrasion) will more likely blunt the edge. Foods that require large bite force (i.e. high structural strength) are likely to result in high degrees of attrition; low attrition will probably result where only a small bite force is needed. Abrasive diets will cause greater amounts of abrasion, rounding the crest edge. Many other factors will affect the degree to which each of these types of wear occur, including the precision of occlusion, the crown shape, the biomechanical properties of the foods (see fig. 12 in Popowics and Fortelius 1997) and the bite force. To a large extent these factors will be closely related to the diet, and so it might be expected that dietary type would affect sharpness to a greater extent than body size.

If the factors that dictate the amount of wear on teeth are largely independent of the size of the tooth, then you may expect there to be no scaling of tooth size. If the amount of attrition and abrasion were the primary dictates of sharpness, it would seem that the maximum sharpness that can be produced through wear is likely to be relatively scale-

independent. Also, there is likely to be an approximate scale-independence of the effects of the biomechanical properties of foods on the wear process that may be another cause of scale-independence of sharpness.

Wear is more likely to even out sharpness in small and large animals: wear in small animals is more likely to blunt a tooth (given the decrease in edge sharpness with moderate to high wear in *C. gouldii*; see Chapter 5) compared to a large animal (where the worn enamel edge is likely to be substantially sharper than the rounded unworn state of herbivores; see Fig. 8.2).

The one main factor that may cause allometric scaling of tooth wear with size is bite force. Larger animals generate higher bite forces on (approximately) equivalent dental materials, which is likely to increase the wear rate and may change the proportion of attrition: abrasion, leading to a roughening of the attritial face. However, the extent to which this is the case is unknown.

Even though high attrition is likely to sharpen a tooth to some extent, there is presumably a maximum sharpness that can be produced through this method. Tooth-on-tooth wear will indiscriminately remove enamel from the relief surface, such that the resulting cutting edge may be fragmented and chipped rather than sharp and precisely angled. Such an effect may be exacerbated by large bite force, resulting in a rougher or more rounded edge.

Given these possible scaling regimes and caveats, we can try to integrate them and speculate on how their relative influence will differ with body size. We will presume that the teeth of an animal will be as sharp as possible, accounting for the increased risk of fracture at high sharpness and bite force. If there is a minimum radius of curvature that can be produced in small animals, which cannot be significantly increased by wear, then the sharpness of the teeth of small animals is dictated by overall tooth shape and is the product of development (perhaps followed by minimal wear, which may slightly increase sharpness compared to the unworn state). Tooth sharpness would increase with body size in small animals (Fig. 8.1c). At intermediate body sizes, the sharpness that can be produced by wear is probably greater than that formed in development, increasing sharpness relative to the unworn state. The sculpting of the edge by wear will produce tooth sharpness that is more scale-independent. This also ameliorates the effect of teeth being too blunt at large body sizes. However, the additional constraint of risk of tooth fracture in larger animals will prevent tooth sharpness from being too high (Fig. 8.1c).

From this, we expect that maintaining high tooth sharpness is more important in small animals than large ones. Tooth sharpness may then be relatively constant in large

animals. This gives larger animals relatively sharper teeth than small animals. It is not known which of developmental or wear processes could produce the sharper crest.

It is not expected that the full predictions of the above discussion will be borne out, but it should set the stage for the types of patterns and data that are required to fully dissect the final influences on the scaling of tooth sharpness.

## **8.4.** Empirical Data on Tooth Sharpness

The only substantial measurement of tooth crest sharpness has been carried out by Popowics and Fortelius (1997). They argued for an isometric scaling of wear-derived tooth sharpness with body size among mammals. The minimum radius of curvature of transverse cross-sections through tooth crests of a wide range of faunivorous and herbivorous mammals was measured; when regressed against body mass, no significant relationship was found. If animals with 'low attrition' were excluded (mostly animals of small body mass with blunter teeth, including Vulpes, Lutra, Alouatta and Colobus, and the large Ceratotherium), then there was a significant relationship with a slope of 0.075. Popowics and Fortelius (1997) also plotted body mass vs radius of curvature multiplied by tooth area (length  $\times$  width), which gave an exponent of 0.679  $\pm$  0.064 SE. However, it was actually intended to regress an estimate of 'blade area' (radius × tooth length), for which the expected slope for isometric scaling would be 0.667 (an area to a volume; M. Fortelius, personal communication). From the similarity between this empirical and the expected slopes, it was erroneously concluded that there was an isometric relationship between body size and blade sharpness, and that body size was the main determinant of blade sharpness. As isometric scaling would be revealed by a slope of 0.33 for the first regression and 1.00 for the second, this in fact suggests that radius of curvature increases at a slower rate than body mass. Therefore, animals of a large body mass and high attrition have relatively sharper teeth (smaller radii of curvature) than smaller animals (Fig. 8.3).

However, for the range of body masses investigated by Popowics and Fortelius (1997), it appears that wear regime is more important than body size in determining tooth sharpness, as the regression of tooth sharpness and body size 'was significant only for those taxa that shape their blades through high attrition' (Popowics and Fortelius 1997:79). This is also indicated by the lack of significant differences in comparisons of blade sharpness, such as between small, medium and large artiodactyls. The sharpest teeth were found in the smallest animals, and the bluntest in the largest, but small animals that eat 'less tough foods' have the bluntest teeth apart from the large *Equus* and *Ceratotherium* (Fig. 8.3).

This suggests that the amount of attrition is the primary determinant of tooth sharpness in these animals. For animals with high attrition, this generates a very slight increase in tooth sharpness with body size, but significantly lower than isometry. This indicates that the sharpness produced by wear is relatively size-independent. However, it is not known to what extent increased bite force in large animals contributes to the slight decrease in tooth sharpness with size, which may cause greater rounding of the attrition surface, or increased risk of fracture (which to some extent can be considered part of the same process). It was hypothesised that increased risk of tooth fracture may cause a decrease in the tooth sharpness at larger body sizes. Sharper edges would then be more likely to be removed, resulting in a decrease in sharpness.

The influences that were considered by Popowics and Fortelius (1997) to be 'secondary', including amounts of attrition and abrasion, are more likely to be primary determinants of sharpness for animals of the size range examined. Wear modifies or obliterates to a large extent any effect that body size *per se* has on tooth size. The absolute amount of wear is therefore not 'irrelevant' to sharpness, as was suspected by Popowics and Fortelius (1997:76) – a critical amount of wear would be necessary to generate sufficient attrition to sharpen crests, as shown by the blunt teeth of animals eating weak foods which only require lower bite forces.

We can use the data on edge sharpness from Chapters 5 and 7 to further investigate this relationship. Within the microchiropterans, there is not a very good relationship between body size and sharpness (Fig. 8.3). This does not appear to be due to the differences in diet (Chapter 7), and to some extent may be attributable to the relatively high variability of edge sharpness within species (particularly *R. blasii*).

If these data are added to the dataset of Popowics and Fortelius (1997), the relationship between sharpness and body size can be examined at a broader scale, as the body size of the microchiropterans measured in this thesis is substantially less than the smallest included in the previous study (0.008-0.040 kg vs 2-2500 kg). Edge sharpness of these species is significantly lower than that of the larger species (Fig. 8.3). This supports several of the points raised earlier: that constant sharpness for all animals is unlikely, as high tooth sharpness is probably more important for function in smaller animals. The higher sharpness in small animals is more likely to be due to a scaling of the maximum tooth sharpness that can be produced through developmental processes compared to increased tooth sharpness from wear, as it is significantly reduced with wear.

However, for the entire dataset there is an approximation to isometry, as a line with a slope of 1/3 passes through *Equus*, *Ceratotherium*, and groups A and B (Fig. 8.3). This

would not be expected from the above discussion. However, the expected pattern of a slower increase in radius of curvature at larger sizes (Fig. 8.1c) is still apparent.

The occlusal morphologies of mammalian teeth have been categorised as primary (the tooth shape is functional upon eruption) and secondary (significant wear is required for the shape to be functional, and the functional form is substantially different from the unworn state; Fortelius 1985). This distinction is apparent in the degree of difference between the unworn and worn states of the forms shown in Fig. 8.2. The protoconoid and carnassial forms can be considered primary, and herbivore lophodont forms are secondary. However, substantial wear does occur in these primary forms, and the resulting morphology differs to some extent from the unworn state (Fig. 8.2). These worn forms can be considered as primary-derived occlusal morphologies, and have their own distinctive patterns (such as the position of enamel on the rake or relief surfaces).

All of the taxa examined in Popowics and Fortelius (1997) have primary-derived (carnassial) or secondary occlusal morphologies. This differs from the microchiropterans of this thesis, which were in a very light state of wear and so have a primary occlusal morphology (other than the *C. gouldii* specimens that were moderately to heavily worn and can be considered primary-derived). Therefore, the primary tooth shape, which is the result of developmental processes, has a greater influence on the sharpness of the microchiropteran form than on the larger carnivores and herbivores. The tooth form of large animals with primary occlusal morphologies (e.g. bears, humans, pigs) is basically rounded cusps and usually lacking in crests (either primary or secondary crests), and the importance of crest sharpness is lower. Therefore, we would expect that the erupted tooth form (resulting from development) has a greater influence in the microchiropterans compared to herbivores, and so any patterns that are apparent in the erupted occlusal morphology (such as allometric scaling of sharpness for unworn cusps) will have a greater influence. This would be expressed as a scaling in sharpness in these forms but not in the secondary crest edges.

These patterns must, however, be examined when sharpness data for small mammals with secondary occlusal morphologies such as rodents are included. If wear were a scale-independent process, then we may expect rodent sharpness to lie along the 'High attrition' trend line in Fig. 8.3. However, there would very likely be strong selection pressure for sharp crest edges in these small mammals, and factors such as specialised enamel microstructure, thin enamel ridges and lower bite force (reducing the risk of fracture) may allow a decrease in the radius of curvature in comparison to the larger animals.

The extent to which major differences in the methodologies of the current work and Popowics and Fortelius (1997) affect the results (such as an approximation to isometry) is not known. Pilot studies showed that the measured radius of curvature was highly correlated with the resolution at which the surface was digitised (unpublished data). This would be expected for a surface that has a fractal nature to some extent. Cusp tips and crest edges were digitised at the highest resolution achievable for the confocal microscope with a dry lens (1 µm for ×40) and then smoothed by a fixed amount to obtain a digitised surface that should represent the contours of the surface at a very fine level but still removing extremely high sharpness values due to the small amount of noise present. It is very likely that radius of curvature values obtained through this method would be higher than those of sectioned profiles for the same specimen. The smallest radius of curvature quantified in this thesis was 4.7 µm, which is probably well below that obtainable from profiles viewed at ×30 magnification. The calculation of surface curvature from splines fit to the three-dimensional surface, which is the method used by the Surfer software, is more objective than fitting by eye. If Popowics and Fortelius' (1997) method tended to underestimate the sharpness compared to the values in this thesis, the approximation of isometry would be removed and the levelling out of sharpness at high body mass would be more apparent.

In conclusion, the data on edge sharpness compiled here largely support the predictions made above: that at small body sizes (<1 kg) sharpness will be more closely correlated with body size as developmental processes may have a greater influence on the final tooth sharpness and there is a lesser risk of tooth fracture. For larger animals (1-2500 kg), the degree of attrition appears to be the main factor in determining sharpness: for animals of high attrition, tooth sharpness is close to constant, and when there is lower attrition, tooth sharpness is lower for the same body size.

However, there is certainly not enough data to confirm these suppositions. Significantly more information is needed for these topics: unworn tooth sharpness and the scaling of the maximum sharpness produced by development; the maximum sharpness that can be produced by attrition; the effects of body size (bite force) on attritial sharpness; the effects of the biomechanical properties of diet on wear; scaling patterns within dietary types; the influence of enamel microstructure on sharpness and how this varies with diet; and data on small mammals with secondary occlusal morphology.

It must be certain that, whatever constraints each body size and dietary type faces, there will be strong selection for a tooth shape that wears in such a way as to maintain function (according to Fig. 8.1), and there may be very many ways of achieving this.

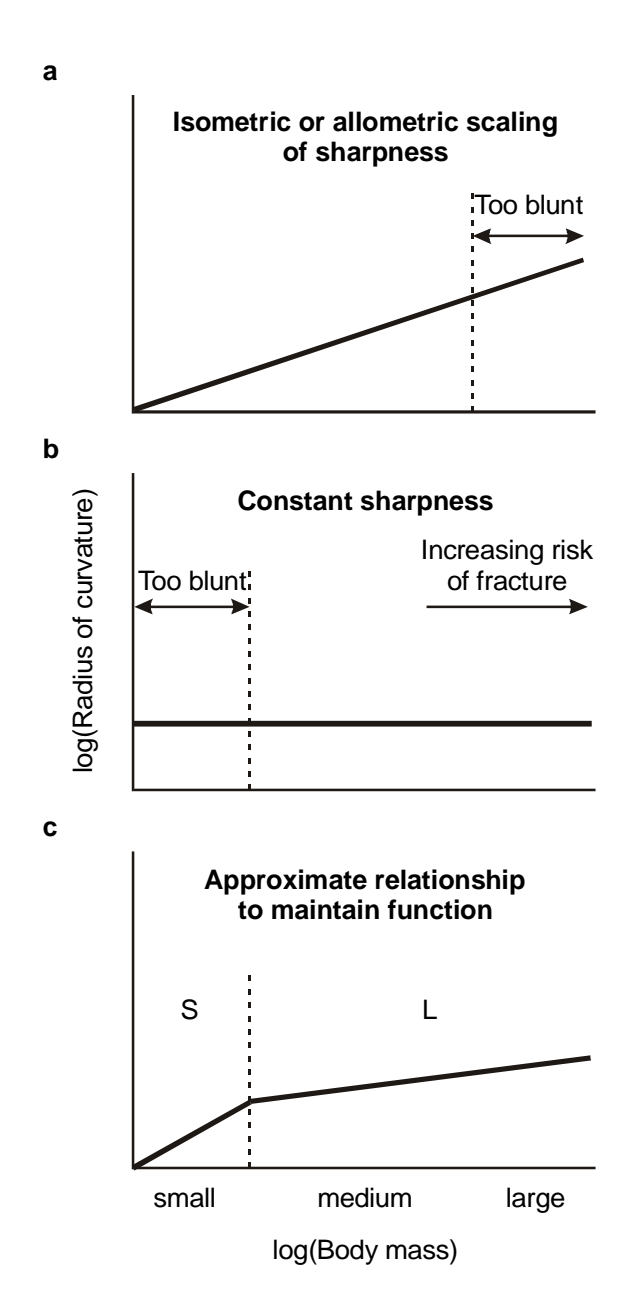


**Fig. 8.1.** Possible scaling regimes for tooth sharpness (measured as radius of curvature) vs body mass. a) Isometric (slope 1/3) or allometric relationship; b) sharpness independent of body size (slope 0). For a), there is likely to be a body size above which the teeth are too blunt and require a greater bite force than can be produced, and for b), a body size below which the teeth are too blunt. The risk of fracture increases at large body sizes in b). c) In order for teeth to maintain function at each body size, we may expect that tooth sharpness scales for small body size (S), and scales at a much lower rate in larger animals (L) due to the effect of wear and the risk of fracture.

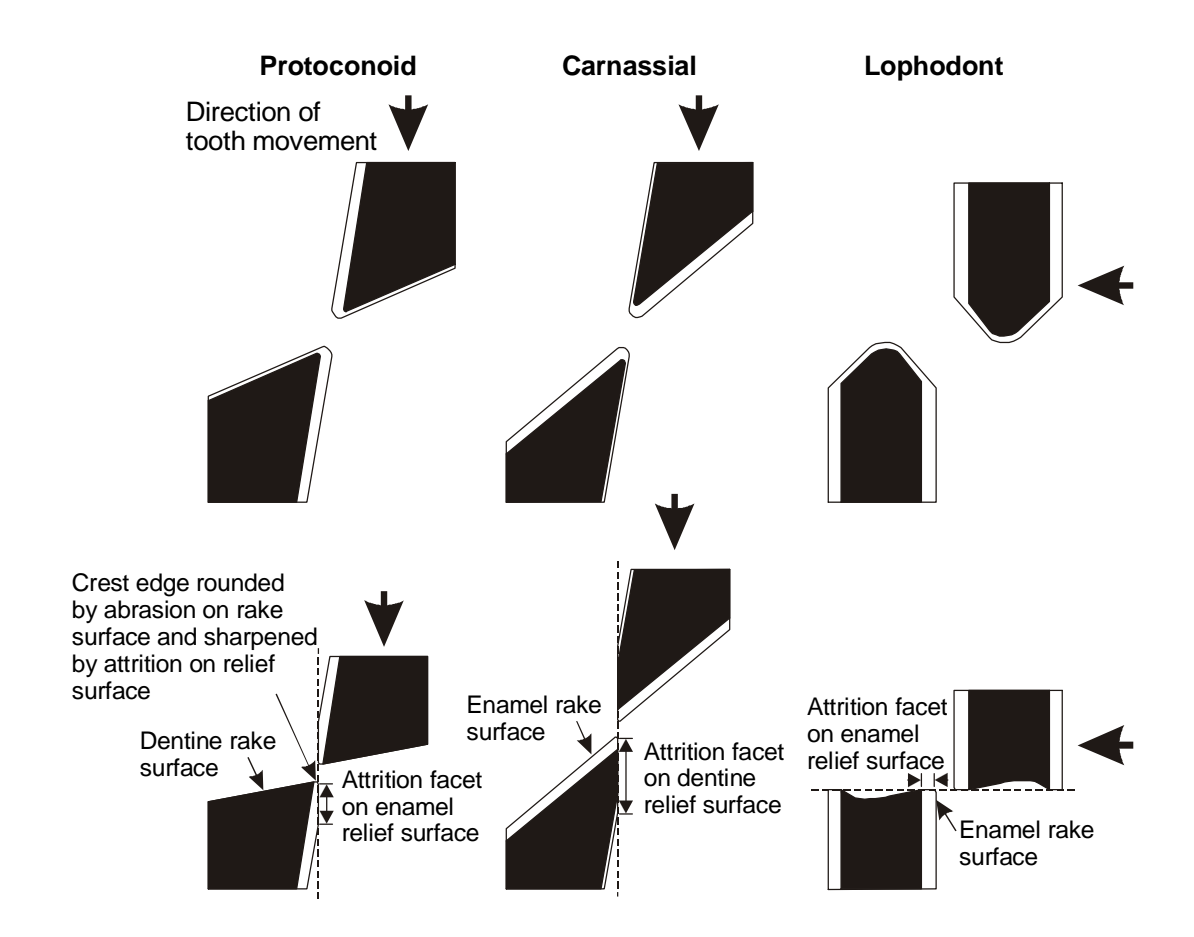


**Fig. 8.2.** Wear and enamel distribution in protoconoid, carnassial and lophodont forms. After wear, the protoconoid crest typically has an attrition facet on the relief surface that is enamel, and the rake surface is dentine. In contrast, the relief surface of the carnassial crest is mostly dentine and the rake surface is enamel. The arrangement of enamel is very different in lophodont forms, with horizontal movement.

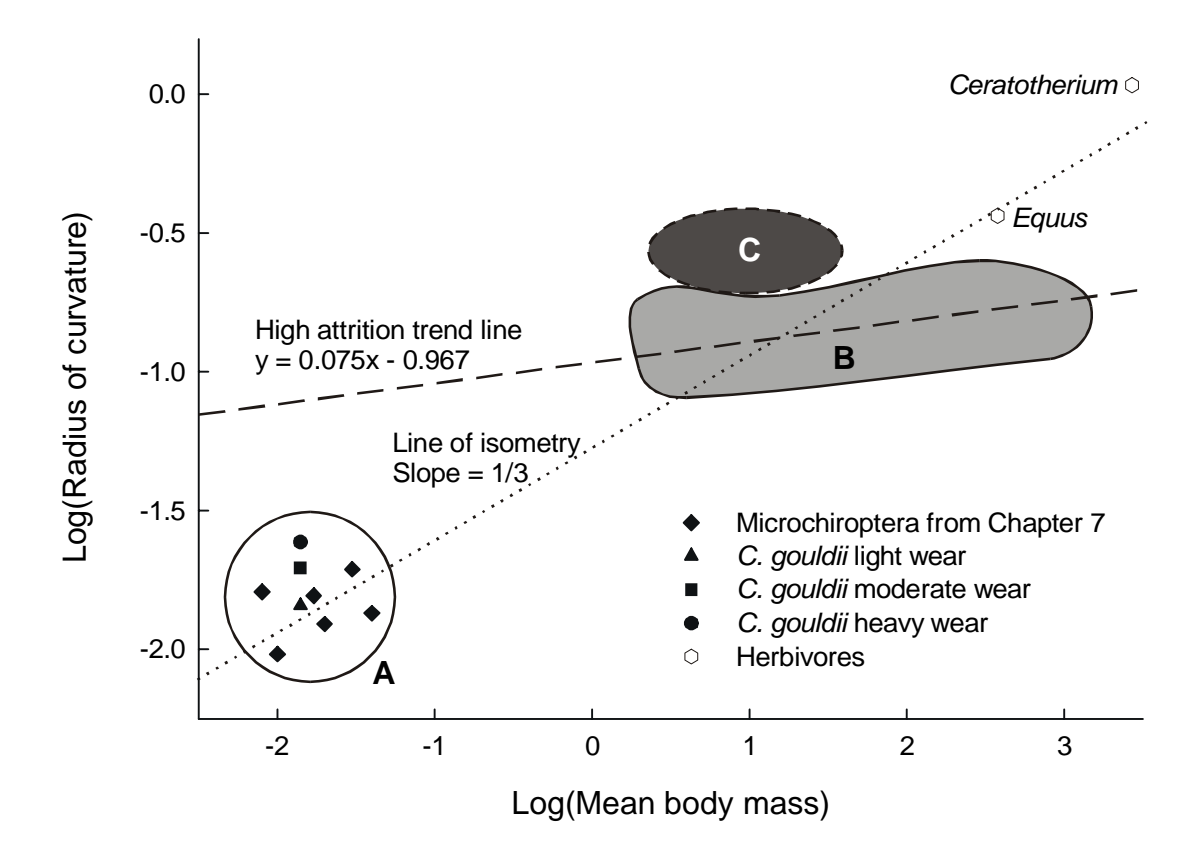


**Fig. 8.3.** Edge sharpnesses of a wide range of body masses and dietary types. A, small insectivorous microchiropterans; B, high attrition medium to large body masses; C, low attrition medium body masses. High attrition trend line for data in B and *Equus*; line of isometry of slope 1/3 shown passing through the middle of microchiropterans. A, data from this thesis; B, C and herbivores, data from Popowics and Fortelius (1997).

# **Chapter 9.** Discussion

A general theme of this thesis has been the examination of factors that affect the function of teeth, and the factors that are most responsible for the tooth form of insectivores. We will now give this consideration a broader scope and examine aspects of comparative function in several tooth forms and speculate on some of the factors that control the large-scale patterns of tooth shape in a wide variety of mammals.

### 9.1. Comparative Function of Protoconoid Tooth Forms

The dental modelling in Chapters 2 and 3 revealed some of the general morphological and functional similarities between the zalambdodont, dilambdodont and tribosphenic tooth forms. These three forms (and slight variations and intermediates) contain the protoconoid structure as either single or multiple copies. The shape of these tooth forms is dominated by this functional complex, and so we can consider these to be protoconoid-based tooth forms – the protoconoid is the unifying morphological and functional feature of these teeth.

Protoconoids are morphologies that combine good functional characteristics for forced crack propagation by a cusp and forced crack propagation by a crest. The main central cusp (apex A; Fig. 2.3, p. 40; protoconid in the lower and paracone and metacone in the upper; Fig. 3.7, p. 66 and Fig. 5.2, p. 107) is well developed, as are the lateral cusps in some cases. These cusps are well suited for the initiation and subsequent continued penetration of foods (according to tip and cusp sharpnesses because their tip and cusp sharpnesses are high). Another characteristic of the protoconoid is the presence of crests with advantageous functional features (e.g. good rake, relief, capture and fragment clearance). We can argue, then, that a greater development of the protoconoid structure in a tooth form can be interpreted as selection for a tooth form for both initial penetration and forced crack propagation or 'cutting'.

However, teeth may perform other functions such as 'crushing' and 'grinding' in addition to the penetration and cutting discussed above. These functions can be idealised as zero (cusp contact and penetration), one (crest contact and penetration) or two (area contact) dimensional contacts, in a similar manner to the definitions of cusps (points) and crests (blades) in Chapter 2. Both 'crushing' and 'grinding' involve the trapping of food between relatively flat, opposable surfaces, but grinding includes some translational

movement parallel to the surface. The protoconoid has no inherent capacity for crushing or grinding, only penetration and cutting, as it does not have flat, opposable surfaces. A reduction in the emphasis on the protoconoid structure along with an increase in relatively flat, opposable surfaces implies increased importance of crushing and grinding.

We can speculate briefly on the differences in the comparative function of the protoconoid tooth forms (Table 9.1). Zalambdodont teeth are essentially single protoconoids; there is no protocone to speak of. This means that the zalambdodont tooth is adapted to puncturing and cutting. This has been assumed in previous descriptions of the form but the principles and models developed in this thesis expound the theoretical basis. There is no apportionment of tooth space to a 'crushing' function.

In contrast, the dilambdodont tooth has duplicated the protoconoid form on each tooth, increasing the number of cusps and crests per tooth. A protocone is also well developed, which expands the number of cutting edges to six. In comparison to the zalambdodont, the number of cutting edges per tooth has been tripled, which will increase the amount of food divided per stroke. However, the efficiency of these crests will be compromised compared to the zalambdodont form. The addition of the protocone reduces the height of the hypoconid, reduces the rake of the crests and impedes fragment clearance from the trigon and talonid basins. It also imposes additional constraints on the occlusal relationships influencing aspects of tooth form such as the relative size of the paracone protoconoid. One effect will be shorter cutting crests (less food cut) and perhaps reduced rake angle (decreased efficiency). An important additional consequence is that it now has opposable surfaces, which can promote crushing or grinding to some extent.

It is arguable that the dilambdodont form is more effective overall than the zalambdodont condition due to the summed action of a greater number of crests. However, the amount of food processed and the overall effectiveness will depend on the number of molars in the tooth row. A form intermediate between the zalambdodont and dilambdodont conditions, with one and a half protoconoids (the 'N'-shaped M<sup>3</sup> of several insectivores, including some of those discussed in Chapter 7), is likely to be less effective, because the complete protoconoid is the ideal functional shape (Chapter 2). Therefore, the zalambdodont and dilambdodont can be seen as local functional maxima in the morphospace of tooth shapes. Therefore, the 'N'-shaped molar can be viewed as an adaptive trough between these two shapes. At first glance this may seem to impede the evolution of a tribosphenic or dilambdodont-type molar from a symmetrodont-type (with a zalambdodont-type pattern); however, forms such as *Amphitherium*, *Peramus* and *Pappotherium* (discussed briefly in Chapter 3; see Bown and Kraus 1979; Butler 1972;

Crompton 1971) show a succession through an alternative route in morphospace in which the second protoconoid of the upper tooth appears gradually (the actual relationships between these forms is not relevant to this discussion, only that the functional morphologies exist and have evolved at some stage). Each stage in this sequence is functional, and is presumably better in some respects than the previous stage for its diet (such as by increasing the total crest length of the tooth).

An extremely interesting study would involve the comparison of the functional parameters in these early therian forms to examine at what stage and rate many of the important functional characteristics of the tooth form developed. I suspect that features such as relief and autocclusion were developed later than features such as food capture and good rake angles, because illustrations of these forms often show very large attrition facets indicating lack of relief and the absence of crest arrangements that reduce contact between opposing relief surfaces (e.g. Bown and Kraus 1979; Butler 1972; Crompton 1971). The occurrence of the intermediate 'N' form at the end of the tooth row in insectivores does not pose a problem for the idea that it is inferior to the 'V' and 'W' shapes, as there is a finite limit to the length of the tooth row and the progression of protoconoids must finish at some point. In addition, the last molar is probably a lot less functionally important than the first two and a reduction in its function may be relatively inconsequential.

An important difference between the tribosphenic and dilambdodont forms is the distance of the mesostyle from the buccal edge of the tooth (Fig. 3.5, p. 64). This affects the size and shape of the centrocrista crests and the occluding crests of the hypoconid. The centrocrista crests of the dilambdodont form (postparacrista and premetacrista) and the lower tooth crests (cristid obliqua and hypocristid) are concave and allow capture between them (Fig. 3.5d, p. 64). However, this is not the case for tribosphenic teeth, where capture is much reduced, and only occurs with the centrocrista crests acting as one concave crest (Fig. 3.5e, p. 64). The tip of the hypoconid occludes after its associated crests (Butler 1996). The protoconoids of the upper tribosphenic form are further from the adaptive peak of protoconoids, and have a less distinctive triangular shape. However, the 'crushing' area that is present in a minor way in the dilambdodont form is often greater in the tribosphenic form. As the hypoconid meets the mesostyle after the entire length of its associated crests have occluded, the space present may represent an exit structure for food trapped between the trigon and talonid basins. If the food is relatively incompressible, completely enclosing the food and then applying force is not likely to result in particle size reduction. However, as the teeth approach one another, food in this interdental space will be extruded out of this gap and sheared by the centrocrista crests when they meet. This may reduce the amount of food trapped in the interdental space and allow the remaining food to be more efficiently reduced. This may then represent an enhancement of crushing and grinding, which are presumably important functions of basins.

Compared to the highly developed shearing of the zalambdodont and dilambdodont forms, there has been a compromising of the protoconoid structure, and therefore the puncture-cutting function, for a greater emphasis on 'crushing' in the tribosphenic form. Dilambdodonty has evolved many times in Mammalia (Butler 1982, 1996), and zalambdodonty at least twice (McDowell 1958) within insectivores. It would be interesting to see how zalambdodonty, dilambdodonty and tribospheny relate to differences in diet, body size and phylogeny, and one may predict zalambdodonty to be associated with tractable insects. Such differences may reveal additional details about the comparative function of these forms. The dilambdodont form may be the more efficient for small insectivores compared to the tribosphenic form, but the absence of the former type from some lineages may be more related to phylogenetic constraints than function.

**Table 9.1.** Comparison of functional features in upper protoconoid-based tooth forms. The number of crests per tooth is also counted in terms of the number of crests that are very close to the shape of crests in the 'ideal' protoconoid.

	Zalambdodont	Dilambdodont	Tribosphenic
No. protoconoids per tooth	One 'ideal'	Two 'ideal', one modified	Three modified
No. crests per tooth	2 (2 'ideal')	6 (4 'ideal')	6 (2 'ideal')
Total crest length per tooth	High	Very high	Moderate
Hypoconid occlusion	n/a	Hypoconid occludes before associated crests	Hypoconid occludes after associated crests

# 9.2. Comparative Function in Protoconoid and Carnassial Tooth Forms

The differences in form between the protoconoid and carnassial forms are significantly greater than those discussed in the previous section. Chapters 2 and 3 illustrated that all of these forms have specific adaptations for cutting, with the main difference being the number and arrangement of the crests.

The functional differences between the carnassial and protoconoid forms can be considered in the same way that was done for the protoconoid forms (Table 9.2). The necessity of insectivores to greatly reduce the size of food fragments is most probably less severe in carnivores as the food is easily digested, and the body size of carnivores is much greater, with consequently lower mass-specific metabolic rates. Therefore, carnivores may not need as many crests as insectivores. Instead, the majority of the cutting potential is concentrated in a single crest per tooth. Carnassial teeth, with essentially one long crest, evolved from the multiple-crested protoconoid-based forms. For example, in recent carnivores, all crests but the postmetacrista on PM<sup>4</sup> and the paracristid on M<sub>1</sub> were reduced, and these became greatly elongated (Butler 1946). The alignment of the crests changed from many crests largely perpendicular to the jaw in the protoconoid forms to the single, long crest parallel to the jaw in carnassials. The re-orientation of the crest allows a longer crest. The function of this single crest is improved compared to those of the protoconoid in terms of rake angle, and perhaps approach angle and food capture, as the shape of each crest is not as impeded by the proximity of adjacent crests of protoconoids. The smaller number of crests, and their improved function, minimises the force required for the tooth to function. The converse advantage of the protoconoid in having multiple crests is the increase in the selection function used by Lucas and Luke (1983b).

Another difference is the apparent capacity to maintain function with wear. It appears that the carnassial form is able to cope with wear better than protoconoid forms in that the worn carnassial probably works comparatively better than a worn protoconoid. Although measurements of the functional parameters for carnassials in various states of wear have not been made, it is likely that at least the rake angle is maintained more effectively in carnassials compared to protoconoids. There is also a greater amount of dental material that can be removed while only making minor changes to the shape of the carnassial, whereas significant change in most of the functional parameters occurs with moderate wear in the protoconoid teeth of *C. gouldii* (Chapter 5). Other aspects of this topic are addressed in section 9.3.

The capability of the carnassial to initiate cracks appears to be reduced compared to the protoconoid. The former tooth shape has two cusps that most probably have lower tip and cusp sharpnesses than the latter. This may be related to differences in the structural properties of the diet, in that invertebrates more often have an intractable covering that requires a greater concentration of force to initiate a crack. This issue is discussed further in section 9.3.

The mechanism and the degree to which relief is maintained in the two forms also differs. Relief in protoconoid forms is present because the crests are arranged so that there is minimal contact between opposing relief surfaces. Single-crested carnassial forms can also be constructed with relief, as shown in models in Chapters 2 and 3 and Mellett's (1981) model. However, when the carnassial wears and relief is removed (such as shown in Fig. 5.7a, p. 112), relief can in principle be restored through the rotation of the upper and lower teeth relative to one another (Osborn and Lumsden 1978), either through rotation of the lower jaw during occlusion, or of the upper and/or lower teeth in their alveoli. Carnassials have been found to rotate in the alveoli throughout the wear process (Mellett 1969; Bryant and Russell 1995). This rotation may not be related to the maintenance of relief but instead to extend the life of the functional tooth by ensuring that as much dental material is used as possible. This should be examined by assessing the amount of relief that does occur in unworn and worn carnassials. It could be predicted from the geometry of the crest edges that rotation will be much easier in a carnassial compared to a protoconoid form, which will be restricted in movement due to the requirement of maintaining occlusion of its additional crests.

There are also differences in the effect of wear on tooth shape. The majority of wear in the protoconoid tooth forms occurs on the rake surface (Fig. 5.3, p. 108), removing the thin layer of enamel on the rake surface and leaving the rake surface as exposed dentine and the relief surface as enamel (Fig. 8.2, p. 185). In the carnassial form, however, significantly more wear occurs on the relief surface, resulting in the opposite situation of thick enamel on the rake surface and dentine on the relief. These differences are very likely to be revealed in differences in enamel microstructure in the two types of crests, and perhaps have implications with regard to the maximum tooth sharpness that can be achieved. The shift from enamel on the rake surface instead of the relief may be a mechanism for resisting wear in the carnassial form if it is most important to resist wear on the rake surface in both the protoconoid and carnassial forms. Substantially greater wear on the relief surface in protoconoid forms may result in a greater change of the occlusal shape (in the sense of occlusal diagrams in Fig. 3.4, p. 63) and make more difficult the maintenance of occlusion between the large number of crests of the upper and lower teeth. The option of thicker enamel on the rake surface would therefore not be available to the protoconoid forms, but it is available to the carnassial form due to its simpler occlusion. There may be other explanations for this pattern.

**Table 9.2.** Comparison of features that function in carnassial and protoconoid-based tooth forms

Carnassial		Protoconoid		
No. crests per tooth	Single crest	Multiple crests		
Crest orientation	Crest parallel to jaw	Crests perpendicular or at angle to jaw		
Rake	Good rake	Fairly good rake		
Enamel arrangement	Enamel on rake surface	Enamel on relief surface		
Resistance to wear (shape)	Does not substantially affect shape	Affects shape substantially after smaller amount of wear		
Type of wear	Most wear by attrition on relief surface	Most wear by abrasion on rake surface		
Effect of wear on relief	Relief removed by wear	Relief generally maintained through wear		

## 9.3. Effect of Size and Diet on Gross Morphology

Several broad-scale patterns in the general morphology of teeth have been noted, such as the increased crest development in both insectivorous and folivorous forms (e.g. Kay 1975). This example has been hypothesised as being due to the similarities in the biomechanical properties of insects and plants. The main two structural polymers in these two groups, chitin and cellulose, have many properties in common (Kay 1975; Sanson 1985). However, tooth forms of much larger animals with similar diets differ qualitatively from those of smaller animals. For instance, small insectivores and carnivores have protoconoid tooth forms, while larger carnivores have often evolved a carnassial form. In the case of herbivores, many smaller herbivores such as primates have derived protoconoid and quadritubercular forms and all large herbivores have more lophodont teeth. Can any generalisations about the general form of teeth and the size and diet of the animal be made?

Cusps are areas of the tooth surface that have sufficiently high tip and cusp sharpnesses, and are important for concentrating force for crack initiation. Cusps can therefore be seen as an adaptation to limited bite force generation by maximising stress and therefore crack initiation. We would expect a greater development of cusps in animals for which the bite force they can generate is close to the structural strength of the food. This is

more likely to be an issue in animals of smaller body mass, as their bite forces are absolutely lower.

Forced crack propagation is required where the food is tough, and this is more effectively achieved by crests (Lucas and Luke 1984). Crests are an adaptation to high toughness, maximising crack propagation. The amount of force required will depend on the biomechanical properties of the food (particularly its structural strength) and the number and length of crests in the tooth and along the tooth row (as increasing the number and/or length of crests will mean that additional force is required for the entire tooth row to operate). If a small animal has sufficient force to drive a certain length of crest through a food with a given structural strength, a larger animal could have a longer crest as it has a greater absolute bite force that is used to overcome the same strength of the food. From this, we would expect both large and small animals consuming tough foods to have crests.

If we examine a small insectivore in the light of the previous two paragraphs, we would expect it to have well-developed cusps, as its lower absolute bite force means that achieving sufficient force for crack initiation is important. In comparison to a larger animal, a small animal is more force-limited in penetrating foods. Its diet has significant structural toughness, and so would require well-developed crests for crack propagation. The tooth form of insectivores matches these requirements well, in the form of the protoconoid.

As the protoconoid is well-adapted to penetration and cutting, we can say that the main function of teeth in which the protoconoid is well-developed is 'puncture-cutting', which is penetration of food by a cusp followed by cutting along crests. This is at variance with the usual view of tribosphenic teeth which follows the work of Crompton and Hiiemae (1970), who describe the action of *Didelphis* teeth as 'puncture-crush' followed by shear. *Didelphis* can be considered more omnivorous than insectivorous, and so has different demands placed on the function of its teeth. The term 'puncture-crush' is therefore probably not very applicable to most insectivores.

Consider instead an animal of larger body mass such as a herbivore or carnivore. The bite force of such an animal may easily overcome the stress required to initiate fracture, and therefore have a lesser requirement for cusps, the main purpose of which is crack initiation. However, since the food is tough, crests are still required to propagate cracks in the food. Cracks can be initiated by the crests but at lower efficiency compared to cusps, and this is possible if there is an excess bite force in relation to the structural strength of the food. The amount of force for crack initiation may not be as limiting in large herbivores. One may expect, then, a greater emphasis on crests in large animals

relative to cusps compared to small animals. This is generally true: large herbivores tend to have substantial batteries of lophs on the molars and are missing the well-developed cusps of small insectivores. Large herbivores are therefore less efficient at crack initiation, but can compensate due to their absolutely larger bite force. The emphasis of cusps in the carnassials of large carnivores is also reduced compared to insectivores: the cusps at the ends of the carnassial would have lower cusp sharpness than the apex A of protoconoids, and the number of cusps per tooth has been reduced.

Two other main reasons for the reduced emphasis of cusps in larger animals are apparent. First, the larger bite forces of such animals may increase the risk to any cusp to the point that cusps are not possible. Second, the necessity for bulk processing in herbivores may mitigate against the incorporation of cusps: if the amount of food processed depends on crest length, then it must scale with positive allometry to keep up with metabolic scaling (Rensberger 1973, 2000). This may lead to very few cusps on the teeth due to spatial constraints on the existence of cusps on teeth with a very large number of crests. On the whole, it is probable that cusps are more incompatible in a secondary occlusal morphology than a primary or primary-derived one, and large herbivores most often have the former.

Rensberger (1988) put forward a view that is not incompatible with that expressed here, that the evolution of herbivory from insectivory involved first an increase in the compressive mode of surface interaction and then the subsequent development of shearing of a different form to that of insectivores. A significant effect in this evolution is likely to have been the increase in body size alone, although the increase in cusp size may not have initially been in order of resist tooth fracture (Rensberger 1988). However, this does not avoid the possibility that it is only by having absolutely greater bite forces that large animals can avoid the necessity of cusps.

A possible exception to this generalisation of greater cusp development in small animals occurs in the rodents, which have lophodont teeth. It may be that rodents have special adaptations for increased jaw force compared to other mammals of similar size (insectivores such as microchiropterans and insectivorans) by adaptations such as the posterior position of the molars and the loss of canines, propalinal jaw movement and large jaw muscle mass that may extend onto the maxilla. These may have allowed the rodents to escape the limitations of small body size and removed the need for largely cuspidate teeth. The biomechanical properties of the diet may be more important, though, judging by the tooth form of the unusual rodent *Deomys ferrugineus* with tall, sharp cusps and an insectivorous diet (Lemire 1966).

It can be expected that, although large carnivores and herbivores will both emphasise crests, the form and number of crests will differ. As great reduction in the particle size of food is not required in carnivores, a large number of crests are not required. This means that it is likely that food particles will be bigger, and a crest that has a substantial capture area and therefore has a long occlusal stroke will be best for dividing a large particle. It is more difficult to fit a large number of such high crests in a tooth row. In contrast, herbivores usually must divide their food more finely. It will be necessary to fracture small particles, and so a crested system that makes it easy to align small particles on the crests is required. A large number of crests will also be advantageous, and the crests do not need to be high. The system of alternating enamel ridges and dentine basins of lophodont teeth provides just such a mechanism, where food is trapped in the basins and forced onto the enamel ridges during the occlusal stroke.

The bite force of large animals is not only relatively greater than the absolute strength of food but also the absolute strength of the materials from which teeth are made. This will be reflected in the risk of fracture and the amount of wear that will occur and will have the opposite effect compared to the development of cusps. The teeth of large animals will be relatively weak compared to their bite force, with resulting large stresses in their teeth. This is particularly apparent in large herbivores, which have specialised enamel structures that enabled the development of greater bite forces in the evolution of herbivores (e.g. prism decussation, including Hunter-Schreger bands; Koenigswald et al. 1987; Rensberger 2000). Large animals also more often have special adaptations for resisting wear and maintaining tooth function after significant wear (Janis and Fortelius 1988). In contrast, the stresses in small insectivore teeth would be lower. This is supported by the relatively unspecialised nature of insectivore enamel microstructure (Dumont 1996). Small insectivores also have fewer adaptations for resisting wear compared to herbivores, as detailed in Chapter 5. As was the case for the presence of cusps, the rodents present an exception with respect to enamel microstructure (Koenigswald et al. 1987), as many have some degree of development of Hunter-Schreger bands. Overall, small animals appear to be bite force-limited with respect to foods compared to large animals, and large animals are strength-limited with respect to the dental materials.

#### 9.4. Thesis Conclusions

This thesis set out to validate the application of concepts and principles from engineering to the realm of functional dental morphology. Functional parameters that can be used to predict change in the function of cusps and crests were established or modified from current engineering and dental knowledge. These parameters were applied in several contexts: they were used to show that several fundamental dental shapes in mammals are essentially ideal functional shapes that conform to spatial and functional constraints; the intraspecific variability of these parameters was measured for an insectivorous microchiropteran, and they enabled a prediction of a decrease in the efficacy of function with wear; and they were used to investigate the effect of the biomechanical properties of the diet on tooth form.

A consistent theme through this work has been the investigation of the forces that shape insectivore teeth, and to a limited extent, those of all mammals. It is unlikely that developmental or phylogenetic constraints have a great influence on the functional form of insectivores and carnivores because the molar and premolar forms of these guilds match ideal functional shapes with only minor changes. These small variations from the ideal forms can be interpreted in terms of decreased the risk of fracture and increased resistance to wear. The biomechanical properties of the diet undoubtedly have an influence on the tooth form of insectivores: the structural toughness of all insects, and the intractability (high structural strength, toughness and stiffness/ductility) of certain components of some insects dictates that blades are required. Small body size also probably influences the cuspidate nature of the insectivore dentition. Among insectivores with diets of varying intractability, increases in the structural strength of the teeth and resistance to wear are probably the main factors that lead to a compromise in certain functional parameters. This matches the general increase in adaptations of skull morphology for increased force generation. However, the small body size is also likely to mean that no special adaptations of the dental materials (e.g. in terms of enamel microstructure) are required for insectivores as a whole. Resistance to wear does not seem to be a significant selection pressure for microbat teeth: there are some adaptations that improve the maintenance of shape with wear, but it is likely that such features are not required to the same extent as animals with highly abrasive diets.

From the discussion on the invertebrate biomechanical properties, it appears that the concept of 'hardness', although very attractive as an easily understood term, is liable to confusion and misinterpretation. For this reason, it is hoped that 'intractability', or some similar concept, can be constructively used in describing the biomechanical properties of mammalian diets. In the guild of insectivores, cuticle thickness has great potential to be a very revealing indicator of dietary properties, and its utility can only be established by further investigation of both the invertebrates themselves and the ways in which insectivores deal with them.

#### 9.5. References

- **Abler WL (1992)** The serrated teeth of tyrannosaurid dinosaurs, and biting structures in other animals. *Paleobiology* **18**: 161-183.
- **Acorn JH and Ball GE (1991)** The mandibles of some adult ground beetles: structure, function, and the evolution of herbivory (Coleoptera: Carabidae). *Canadian Journal of Zoology* **69**: 638-650.
- **Aguirre LF, Herrel A, Van Damme R and Matthysen E (2003)** The implications of food hardness for diet in bats. *Functional Ecology* **17**: 201-212.
- **Alexander RM (1981)** Factors of safety in the structure of animals. *Science Progress* **67**: 109-130.
- Alexander RM (1983) Animal Mechanics. 2nd ed. (Blackwell: Oxford)
- Alexander RM ed. (1992) Mechanics of Animal Locomotion: Advances in Comparative and Environmental Physiology 11. (Springer-Verlag: Berlin)
- Andersen SO, Højrup P and Roepstorff P (1995) Insect cuticular proteins. *Insect Biochemistry & Molecular Biology* 25: 153-176.
- **Andrews P (1981)** Species diversity and diet in monkeys and apes during the Miocene. In: *Aspects of Human Evolution*. pp. 25-61. CB Stringer, ed. (Taylor & Francis: London)
- **Anthony ELP and Kunz TH (1977)** Feeding strategies of the little brown bat, *Myotis lucifugus*, in southern New Hampshire. *Ecology* **58**: 775-786.
- **Anthony MRL and Kay RF (1993)** Tooth form and diet in ateline and alouattine primates: reflections on the comparative method. *American Journal of Science* **293**-**A**: 356-382.
- **Aranwela N, Sanson G and Read J (1999)** Methods of assessing leaf-fracture properties. *New Phytologist* **144**: 369-383.
- Arlettaz R and Perrin N (1995) The trophic niches of sympatric sibling *Myotis myotis* and *M. blythii*: do mouse-eared bats select prey? *Symposia of the Zoological Society of London* 67: 361-376.
- **Ashby MF and Jones DRH (1996)** Engineering Materials 1: an Introduction to Their Properties and Applications. 2nd ed. (Butterworth-Heinemann: Oxford)
- **Askeland DR and Phulé PP (2003)** *The Science and Engineering of Materials.* 4th ed. (Brooks/Cole: Pacific Grove, California)
- Atkins AG and Mai YW (1985) Elastic and Plastic Fracture. (Ellis Horwood: Chichester)
- Atkins AG and Vincent JFV (1984) An instrumented microtome for improved histological sections and the measurement of fracture toughness. *Journal of Materials Science Letters* 3: 310-312.
- **Barlow KE, Jones G and Barratt EM (1997)** Can skull morphology be used to predict ecological relationships between bat species? A test using two cryptic species of pipistrelle. *Proceedings of the Royal Society of London, Series B* **264**: 1695-1700.
- **Bayer RG (1994)** *Mechanical Wear Prediction and Prevention.* (Marcel Dekker, Inc: New York)
- Bels VL, Chardon M and Vandewalle P eds (1994) Biomechanics of Feeding in Vertebrates: Advances in Comparative and Environmental Physiology 18. (Springer-Verlag: Berlin)
- **Benefit BR and McCrossin ML (1990)** Diet, species diversity and distribution of African fossil baboons. *Kroeber Anthropological Society Papers* **71-72**: 77-93.
- **Black HL** (1972) Differential exploitation of moths by the bats *Eptesicus fuscus* and *Lasiurus cinereus. Journal of Mammalogy* 53: 598-601.

- **Black HL** (1974) A north temperate bat community: structure and prey populations. *Journal of Mammalogy* 55: 138-157.
- **Bowles JB, Heideman PD and Erickson KR (1990)** Observations on six species of Freetailed Bats (Molossidae) from Yucatan, Mexico. *Southwestern Naturalist* **35**: 151-157.
- **Bown TM and Kraus MJ (1979)** Origin of the tribosphenic molar and metatherian and eutherian dental formulae. In: *Mesozoic Mammals: the First Two-thirds of Mammalian History*. pp. 172-181. JA Lillegraven, Z Kielan-Jaworoska and WA Clemens, eds. (University of California Press: Berkeley)
- **Boyde A and Fortelius M (1991)** New confocal LM method for studying local relative microrelief with special reference to wear studies. *Scanning* **13**: 429-430.
- **Boyde A and Jones SJ (1995)** Mapping and measuring surfaces using reflection confocal microscopy. In: *Handbook of Biological Confocal Microscopy*. pp. 255-266. JB Pawley, ed. (Plenum Press: New York)
- **Boyer HE ed. (1987)** *Hardness Testing.* (ASM International: Metals Park, Ohio)
- **Brigham RM** (1990) Prey selection by Big Brown Bats *Eptesicus fuscus* and Common Nighthawks *Chordeiles minor*. *American Midland Naturalist* 124: 73-80.
- **Brigham RM and Saunders MB (1990)** The diet of big brown bats (*Eptesicus fuscus*) in relation to insect availability in southern Alberta, Canada. *Northwest Science* **64**: 7-10
- **Bryant HN and Russell AP (1995)** Carnassial functioning in nimravid and felid sabertooths: theoretical basis and robustness of inferences. In: *Functional Morphology in Vertebrate Paleontology*. pp. 116-135. J Thomason, ed. (Cambridge University Press: Cambridge)
- **Buchler ER (1976)** Prey selection by *Myotis lucifugus* (Chiroptera: Vespertilionidae). *American Naturalist* **110**: 619-628.
- **Butler PM (1937)** Studies of the mammalian dentition: I. The teeth of *Centetes ecaudatus* and its allies. *Proceedings of the Zoological Society of London, Series B* **107**: 103-132.
- **Butler PM** (1939) Studies of the mammalian dentition. Differentiation of the post-canine dentition. *Proceedings of the Zoological Society of London, Series B* 109: 1-36.
- **Butler PM (1941)** A theory of the evolution of mammalian molar teeth. *American Journal of Science* **239**: 421-450.
- **Butler PM (1946)** The evolution of carnassial dentitions in the Mammalia. *Proceedings of the Zoological Society of London, Series B* **116**: 198-220.
- **Butler PM** (1952) The milk-molars of Perissodactyla, with remarks on molar occlusion. *Proceedings of the Zoological Society of London* 121: 777-817.
- **Butler PM (1961)** Relationships between upper and lower molar patterns. In: *International Colloquium on the Evolution of Lower and Non-Specialised Mammals*. Brussels, 1960, pp. 117-126. G Vandebroek, ed.
- Butler PM (1972) Some functional aspects of molar evolution. Evolution 26: 474-483.
- **Butler PM** (1981) Dentition in function. In: *Dental Anatomy and Embryology*. pp. 329-356. JW Osborn, ed. (Blackwell Scientific Publications: Oxford)
- **Butler PM** (1982) Directions of evolution in the mammalian dentition. In: *Problems of Phylogenetic Reconstruction*. pp. 235-244. KA Joysey and AE Friday, eds. (Academic Press: London)
- **Butler PM (1990)** Early trends in the evolution of tribosphenic molars. *Biological Reviews* **65**: 529-552.
- **Butler PM** (1995) Ontogenetic aspects of dental evolution. *International Journal of Developmental Biology* 39: 25-34.
- **Butler PM (1996)** Dilambdodont molars: a functional interpretation of their evolution. *Palaeovertebrata* **25**: 205-213.

- **Butler PM (2001)** Evolutionary transformations of the mammalian dentition. *Mitt. Mus Nat. kd. Berl.*, *Zool. Reihe* **77**: 167-174.
- Carraway LN, Verts BJ, Jones ML and Whitaker JO, Jr (1996) A search for agerelated changes in bite force and diet in shrews. *American Midland Naturalist* 135: 231-240.
- Carroll RL (1988) Vertebrate Paleontology and Evolution. (WH Freeman and Company: New York)
- Carter TC, Menzel MA, Krishon DM and Laerm J (1998) Prey selection by five species of vespertilionid bats on Sapelo Island, Georgia. *Brimleyana* 25: 158-170.
- **Chapman BR (1998)** *The Insects: Structure and Function*. 4th ed. (Cambridge University Press: Cambridge)
- Cheng PC and Kriete A (1995) Image contrast in confocal light microscopy. In: Handbook of Biological Confocal Microscopy. pp. 281-310. JB Pawley, ed. (Plenum Press: New York)
- Chow M and Rich THV (1982) Shuotherium dongi, n. gen. and sp., a therian with pseudo-tribosphenic molars from the Jurassic of Sichuan, China. Australian Mammalogy 5: 127-142.
- **Churchill S (1998)** *Australian Bats.* (Reed New Holland: Sydney)
- Covert HH (1986) Biology of early Cenozoic primates. In: Comparative Primate Biology, Volume 1: Systematics, Evolution, and Anatomy. pp. 335-359. DR Swindler and J Erwin, eds. (Alan R. Liss: New York)
- **Crompton AW (1971)** The origin of the tribosphenic molar. In: *Early Mammals*. pp. 65-87. DM Kermack and KA Kermack, eds. (Academic Press: London)
- Crompton AW and Hiiemae K (1970) Molar occlusion and mandibular movements during occlusion in the American opossum, *Didelphis marsupialis* L. *Zoological Journal of the Linnean Society* 49: 21-47.
- **Crompton AW and Sita-Lumsden A (1970)** Functional significance of the therian molar pattern. *Nature* **227**: 197-199.
- Crompton AW, Wood CB and Stern DN (1994) Differential wear of enamel: a mechanism for maintaining sharp cutting edges. In: *Biomechanics of Feeding in Vertebrates: Advances in Comparative and Environmental Physiology 18.* pp. 321-346. VL Bels, M Chardon and P Vandewalle, eds. (Springer-Verlag: Berlin)
- Crompton RH, Savage R and Spears IR (1998) The mechanics of food reduction in *Tarsius bancanus*: hard-object feeder, soft-object feeder or both? *Folia Primatologica* 69 (suppl 1): 41-59.
- **Cubberly WH ed. (1989)** *Tool and Manufacturing Engineers Handbook.* (Society of Manufacturing Engineers: Dearborn)
- Czarnecki RT and Kallen FC (1980) Craniofacial, occlusal and masticatory anatomy in bats. *Anatomical Record* 198: 87-106.
- **Dalton VM, Brack V, Jr and McTeer PM (1986)** Food habits of the big-eared bat, *Plecotus townsendii virginianus*, in Virginia. *Virginia Journal of Science* **37**: 248-254.
- **Dawkins R (1986)** The Blind Watchmaker. (Longman Scientific & Technical: Harlow)
- **Delorme R, Benchaib M, Bryon PA and Souchier C** (1996) Measurement accuracy in confocal microscopy. *Journal of Microscopy* 192: 151-162.
- **Dickman CR and Huang C (1988)** The reliability of fecal analysis as a method for determining the diet of insectivorous mammals. *Journal of Mammalogy* **69**: 108-113.
- **Dixon JM (1995)** Gould's Wattled Bat. In: *The Mammals of Australia*. 2nd ed. pp. 512-513. R Strahan, ed. (Australian Museum/Reed Books: Sydney)
- **Dumont ER (1995)** Enamel thickness and dietary adaptation among extant primates and chiropterans. *Journal of Mammalogy* **76**: 1127-1136.

- **Dumont ER (1996)** Enamel prism morphology in molar teeth of small eutherian mammals. *Scanning Microscopy* **10**: 349-370.
- **Dumont ER (1997)** Cranial shape in fruit, nectar, and exudate feeders: implications for interpreting the fossil record. *American Journal of Physical Anthropology* **102**: 187-202.
- **Dumont ER (1999)** The effect of food hardness on feeding behaviour in frugivorous bats (Phyllostomidae): an experimental study. *Journal of Zoology* **248**: 219-229.
- **Dumont ER, Strait SG and Friscia AR (2000)** Abderitid marsupials from the Miocene of Patagonia: an assessment of form, function, and evolution. *Journal of Paleontology* **74**: 1161-1172.
- Easterla DA and Whitaker JO, Jr (1972) Food habits of some bats from Big Bend National Park, Texas. *Journal of Mammalogy* 53: 887-890.
- Edwards AJ, Fawke JD, McClements JG, Smith SA and Wyeth P (1993) Correlation of zinc distribution and enhanced hardness in the mandibular cuticle of the leaf-cutting ant Atta sexdens rubropilosa. Cell Biology International 17: 697-698.
- Edwards C, Read J and Sanson G (2000) Characterising sclerophylly: some mechanical properties of leaves from heath and forest. *Oecologia* 123: 158-167.
- **Evans AR (2000)** Applications of confocal microscopy to functional morphology: the effect of diet and wear on tooth sharpness and function in two microchiropterans *Chalinolobus gouldii* and *C. morio*. Abstracts of the 9th Australasian Bat Conference, Tocal, Australia, 25-28 April 2001. *Bat Research News* **41**: 44.
- **Evans AR** (*in press*) Quantifying the relationship between form and function and the geometry of the wear process in bat molars. In: *Functional and Evolutionary Ecology of Bats: Proceedings of the 12th International Bat Research Conference*. Z Akbar, GF McCracken and TH Kunz, eds. (Oxford University Press: New York)
- Evans AR, Harper IS and Sanson GD (2001) Confocal imaging, visualization and 3-D surface measurement of small mammalian teeth. *Journal of Microscopy* 204: 108-118
- **Evans AR and Sanson GD (1998)** The effect of tooth shape on the breakdown of insects. *Journal of Zoology* **246**: 391-400.
- **Every RG and Kühne WG (1971)** Bimodal wear of mammalian teeth. In: *Early Mammals*. pp. 23-26. DM Kermack and KA Kermack, eds. (Academic Press: London)
- **Farlow JO, Brinkman DL, Abler WL and Currie PJ (1991)** Size, shape, and serration density of theropod dinosaur lateral teeth. *Modern Geology* **16**: 161-198.
- Felbeck DK and Atkins AG (1984) Strength and Fracture of Engineering Solids. (Prentice-Hall: Englewood Cliffs, NJ)
- **Fenton MB (1995)** Constraint and flexibility bats as predators, bats as prey. *Symposia of the Zoological Society of London* **67**: 277-289.
- Fenton MB, Cumming DHM, Rautenbach IL, Cumming GS, Cumming MS, Ford G, Taylor RD, Dunlop J, Hovorka MD, Johnston DS, Portfors CV, Kalcounis MC and Mahlanga Z (1998a) Bats and the loss of tree canopy in African woodlands. *Conservation Biology* 12: 399-407.
- Fenton MB, Rautenbach IL, Rydell J, Arita HT, Ortega J, Bouchard S, Hovorka MD, Lim B, Odgren E, Portfors CV, Scully WM, Syme DM and Vonhof MJ (1998b) Emergence, echolocation, diet and foraging behavior of *Molossus ater* (Chiroptera: Molossidae). *Biotropica* 30: 314-320.
- Fenton MB, Waterman JM, Roth JD, Lopez E and Fienberg SE (1998c) Tooth breakage and diet: a comparison of bats and carnivorans. *Journal of Zoology* 246: 83-88.

- Ferreira JM, Phakey PP, Rachinger WA, Palamara J and Orams HJ (1985) A microscopic investigation of enamel in wombat (*Vombatus ursinus*). Cell & Tissue Research 242: 349-355.
- **Findley JS** (1993) *Bats: a Community Perspective.* (Cambridge University Press: Cambridge)
- **Fisher DO and Dickman CR (1993)** Diets of insectivorous marsupials in arid Australia: selection for prey type, size or hardness? *Journal of Arid Environments* **25**: 397-410
- **Fortelius M (1985)** Ungulate cheek teeth: developmental, functional, and evolutionary interrelations. *Acta Zoologica Fennica* **180**: 1-76.
- **Fortelius M** (1988) Isometric scaling in mammalian cheek teeth is also true metabolic scaling. In: *Teeth Revisited: Proceedings of the VIIth International Symposium on Dental Morphology*. Paris, 1986, pp. 459-462. DE Russell, J-P Santoro and D Sigogneau-Russell, eds.
- **Fortelius M (1990)** Problems with using fossil teeth to estimate body sizes of extinct mammals. In: *Body Size in Mammalian Paleobiology: Estimation and Biological Implications*. pp. 207-228. J Damuth and BJ MacFadden, eds. (Cambridge University Press: Cambridge)
- Francis AJ (1980) Introducing Structures. (Pergamon Press: Oxford)
- **Frazzetta TH** (1988) The mechanics of cutting and the form of shark teeth (Chondrichthyes, Elasmobranchii). *Zoomorphology* 108: 93-107.
- **Freeman PW (1979)** Specialized insectivory: beetle-eating and moth-eating molossid bats. *Journal of Mammalogy* **60**: 467-479.
- **Freeman PW** (1981a) Correspondence of food habits and morphology in insectivorous bats. *Journal of Mammalogy* **62**: 166-173.
- **Freeman PW** (1981b) A multivariate study of the family Molossidae (Mammalia, Chiroptera): morphology, ecology, evolution. *Fieldiana Zoology* 7: 1-173.
- **Freeman PW** (1984) Functional cranial analysis of large animalivorous bats (Microchiroptera). *Biological Journal of the Linnean Society* 21: 387-408.
- **Freeman PW** (1988) Frugivorous and animalivorous bats (Microchiroptera): dental and cranial adaptations. *Biological Journal of the Linnean Society* 33: 249-272.
- **Freeman PW** (1992) Canine teeth of bats (Microchiroptera): size, shape and role in crack propagation. *Biological Journal of the Linnean Society* **45**: 97-115.
- **Freeman PW** (1995) Nectarivorous feeding mechanisms in bats. *Biological Journal of the Linnean Society* 56: 439-463.
- **Freeman PW** (1998) Form, function, and evolution in skulls and teeth of bats. In: *Bat Biology and Conservation*. pp. 140-156. TH Kunz and PA Racey, eds. (Smithsonian Institution Press: Washington)
- **Freeman PW (2000)** Macroevolution in Microchiroptera: recoupling morphology and ecology with phylogeny. *Evolutionary Ecology Research* **2**: 317-335.
- **Freeman PW and Weins WN (1997)** Puncturing ability of bat canine teeth: the tip. In: *Life Among the Muses: Papers in Honor of James S. Findley.* pp. 225-232. TL Yates, WL Gannon and DE Wilson, eds. (The Museum of Southwestern Biology: Albuquerque)
- Fullard JH, Koehler C, Surlykke A and McKenzie NL (1991) Echolocation ecology and flight morphology of insectivorous bats (Chiroptera) in south-western Australia. *Australian Journal of Zoology* 39: 427-438.
- **Gingerich PD and Smith BH (1985)** Allometric scaling in the dentition of primates and insectivores. In: *Size and Scaling in Primate Biology*. pp. 257-272. WJ Jungers, ed. (Plenum Press: New York)

- **Goldman LJ and Henson OW** (1977) Prey recognition and selection by the constant frequency bat, *Pteronotus p. parnellii. Behavioral Ecology and Sociobiology* 2: 411-419.
- Gordon JE (1976) The New Science of Strong Materials, or Why You Don't Fall Through the Floor. 2nd ed. (Penguin: Harmondsworth)
- Gordon JE (1978) Structures, or Why Things Don't Fall Down. (Penguin: London)
- **Gordon KD** (1982) A study of microwear on chimpanzee molars: implications for dental microwear analysis. *American Journal of Physical Anthropology* **59**: 195-216.
- **Gordon KD** (1984) Pitting and bubbling artefacts in surface replicas made with silicone elastomers. *Journal of Microscopy* 134: 183-188.
- **Gould E (1955)** The feeding efficiency of insectivorous bats. *Journal of Mammalogy* **36**: 399-407.
- **Gould SJ (1975)** On the scaling of tooth size in mammals. *American Zoologist* **15**: 351-362.
- **Gould SJ (1989)** A development constraint in *Cerion* with comments on the definition and interpretation of constraint in evolution. *Evolution* **43**: 516-539.
- Gould SJ and Lewontin RC (1979) The spandrels of San Marco and the Panglossian paradigm: a critique of the adaptationist programme. *Proceedings of the Zoological Society of London, Series B* 205: 581-598.
- **Greaves WS** (1972) Evolution of the merycoidodont masticatory apparatus (Mammalia, Artiodactyla). *Evolution* 26: 659-667.
- **Greaves WS (1973)** The inference of jaw motion from tooth wear facets. *Journal of Paleontology* **74**: 1000-1001.
- **Gregory WK** (1916) Studies on the evolution of the primates. I. The Cope-Osborn 'Theory of Trituberculy' and the ancestral molar patterns of the primates. *Bulletin of the American Museum of Natural History* 35: 239-355.
- **Gregory WK (1920)** On the structure and relations of *Notharctus*, an American Eocene primate. *Memoirs of the American Museum of Natural History, New Series* **3**: 49-243.
- **Griffith LA and Gates JE (1985)** Food habits of cave-dwelling bats in the central Appalachians. *Journal of Mammalogy* **66**: 451-460.
- **Grine FE** (1986) Dental evidence for dietary differences in *Australopithecus* and *Paranthropus*: a quantitative analysis of permanent molar microwear. *Journal of Human Evolution* 15: 783-822.
- **Hamilton IM and Barclay RMR (1998)** Diets of juvenile, yearling, and adult big brown bats (*Eptesicus fuscus*) in southeastern Alberta. *Journal of Mammalogy* **79**: 764-771.
- **Hamilton WJ** (1933) The insect food of the big brown bat. *Journal of Mammalogy* 14: 155-156.
- **Harvey PH and Pagel MD (1991)** The Comparative Method in Evolutionary Biology. (Oxford University Press: Oxford)
- **Hepburn HR and Chandler HD (1976)** Material properties of arthropod cuticles: the arthrodial membranes. *Journal of Comparative Physiology B* **109**: 177-198.
- **Hepburn HR and Chandler HD (1980)** Materials testing of arthropod cuticle preparations. In: *Cuticle Techniques in Arthropods*. pp. 1-44. TA Miller, ed. (Springer-Verlag: New York)
- **Hepburn HR and Joffe I (1976)** On the material properties of insect exoskeletons. In: *The Insect Integument*. pp. 207-235. HR Hepburn, ed. (Elsevier: Amsterdam)
- **Hill D (1985)** Functional Dental Morphology in Some Small Dasyurids. BSc (Hons) thesis. Department of Zoology. Monash University, Melbourne.

- **Hillerton JE** (1984) Cuticle: mechanical properties. In: *Biology of the Integument, Vol 1, Invertebrates.* pp. 626-637. J Bereiter-Hahn, AG Matoltsy and KS Richards, eds. (Springer-Verlag: Berlin)
- **Hillerton JE, Reynolds SE and Vincent JFV (1982)** On the indentation hardness of insect cuticle. *Journal of Experimental Biology* **96**: 45-52.
- **Howell DJ and Burch D (1974)** Food habits of some Costa Rican bats. *Revista de Biologia Tropical* **21**: 281-294.
- **Hunter JP and Jernvall J (1998)** Decomposing early morphological diversity in ungulates: analysis of early Paleocene arctocyonid teeth. *Journal of Vertebrate Paleontology* **18**: 52A-53A.
- **Jacobs DS** (1996) Morphological divergence in an insular bat, *Lasiurus cinereus semotus*. *Functional Ecology* 10: 622-630.
- **Janis CM (1988)** An estimation of tooth volume and hypsodonty indices in ungulate mammals, and the correlation of these factors with dietary preference. In: *Teeth Revisited: Proceedings of the VIIth International Symposium on Dental Morphology*. Paris, 1986, pp. 367-387. DE Russell, J-P Santoro and D Sigogneau-Russell, eds.
- **Janis CM and Fortelius M (1988)** The means whereby mammals achieve increased functional durability of their dentitions, with special reference to limiting factors. *Biological Reviews* **63**: 197-230.
- **Jernvall J** (1995) Mammalian molar cusp patterns: developmental mechanisms of diversity. *Acta Zoologica Fennica* 198: 1-61.
- **Jernvall J and Selänne L (1999)** Laser confocal microscopy and geographic information systems in the study of dental morphology. *Palaeontologia Electronica* 1: 12 pp., 219 kb. http://palaeo-electronica.org/1999 1/confocal/issue1 99.htm.
- **Jeronimidis G (1980)** Wood, one of nature's challenging composites. In: *The Mechanical Properties of Biological Materials (34th Symposium of the Society for Experimental Biology)*. pp. 169-182. JFV Vincent and JD Currey, eds. (Cambridge University Press: Cambridge)
- **Jeuniaux C** (1961) Chitinase: an addition to the list of hydrolases in the digestive tract of vertebrates. *Nature* 192: 135-136.
- **Jeuniaux C and Cornelius C (1978)** Distribution and activity of chitinolytic enzymes in the digestive tract of birds and mammals. In: *Proceedings of the First International Conference on Chitin/Chitosan*, pp. 542-549.
- **Johanson Z** (1996) Revision of the Late Cretaceous North American marsupial genus *Alphadon. Palaeontographica Abt. A* 242: 127-184.
- **Jolly CJ** (1970) The seed-eaters: a new model of hominid differentiation based on a baboon analogy. *Man* 5: 5-26.
- **Jungers WL, Falsetti AB and Wall CE (1995)** Shape, relative size, and size-adjustments in morphometrics. *Yearbook of Physical Anthropology* **38**: 137-161.
- **Jürgens KD and Prothero J (1987)** Scaling of maximal lifespan in bats. *Comparative Biochemistry & Physiology, Part A* **88A**: 361-367.
- **Kallen KC and Gans C (1972)** Mastication in the Little Brown Bat, *Myotis lucifugus*. *Journal of Morphology* **136**: 385-420.
- **Kay RF (1975)** The functional adaptations of primate molar teeth. *American Journal of Physical Anthropology* **43**: 195-216.
- **Kay RF** (1978) Molar structure and diet in extant Cercopithecidae. In: *Development, Function and Evolution of Teeth.* pp. 309-339. PM Butler and KA Joysey, eds. (Academic Press: London)
- **Kay RF (1981)** The nut-crackers a new theory of the adaptations of the Ramapithecinae. *American Journal of Physical Anthropology* **55**: 141-151.

- **Kay RF (1984)** On the use of anatomical features to infer foraging behavior in extinct primates. In: *Adaptations for Foraging in Non-human Primates: Contributions to an Organismal Biology of Prosimians, Monkeys and Apes.* pp. 21-53. PS Rodman and JGH Cant, eds. (Columbia University Press: New York)
- **Kay RF and Covert HH (1984)** Anatomy and behaviour of extinct primates. In: *Food Acquisition and Processing in Primates*. pp. 467-508. DJ Chivers, BA Wood and A Bilsborough, eds. (Plenum Press: New York)
- **Kay RF and Hiiemae KM (1974)** Jaw movement and tooth use in recent and fossil primates. *American Journal of Physical Anthropology* **40**: 227-256.
- **Kay RF and Hylander WL (1978)** The dental structure of mammalian folivores with special reference to Primates and Phalangeroidea (Marsupialia). In: *The Ecology of Arboreal Folivores*. pp. 173-191. GG Montgomery, ed. (Smithsonian Institution Press: Washington DC)
- **Kay RF, Sussman RW and Tattersall I (1978)** Dietary and dental variations in the genus *Lemur*, with comments concerning dietary-dental correlations among Malagasy primates. *American Journal of Physical Anthropology* **49**: 119-128.
- **Kinzey WG (1974)** Ceboid models for the evolution of hominoid dentition. *Journal of Human Evolution* **3**: 193-203.
- **Kinzey WG and Norconk MA (1990)** Hardness as a basis of fruit choice in two sympatric primates. *American Journal of Physical Anthropology* **81**: 5-15.
- **Kirk EC and Simons EL (2001)** Diets of fossil primates from the Fayum Depression of Egypt: a quantitative analysis of molar shearing. *Journal of Human Evolution* **40**: 203-229.
- Knowles JR and Albery WJ (1977) Perfection in enzyme catalysis: the energetics of triosephosphate isomerase. *Accounts of Chemical Research* 10: 105-111.
- **Koenigswald Wv and Clemens WA (1992)** Levels of complexity in the microstructure of mammalian enamel and their application in studies of systematics. *Scanning Microscopy* **6**: 195-218.
- **Koenigswald Wv, Rensberger JM and Pretzschner HU (1987)** Changes in the tooth enamel of early Paleocene mammals allowing increased diet diversity. *Nature* **328**: 150-152.
- **Kunz TH** (1988) Methods of assessing the availability of prey to insectivorous bats. In: *Ecological and Behavioral Methods for the Study of Bats*. pp. 191-210. TH Kunz, ed. (Smithsonian Institution Press: Washington D.C.)
- **Kunz TH and Whitaker JO** (1983) An evaluation of fecal analysis for determing food habits of insectivorous bats. *Canadian Journal of Zoology* 61: 1317-1321.
- **Lanyon JM and Sanson GD (1986)** Koala (*Phascolarctos cinereus*) dentition and nutrition. II. Implications of tooth wear in nutrition. *Journal of Zoology* **209**: 169-181.
- **Legendre S and Roth C (1988)** Correlation of carnassial tooth size and body weight in recent carnivores. *Historical Biology* 1: 85-98.
- **Lemire M** (1966) Particularites de l'appareil masticateur d'un rongeur insectivore *Deomys ferrugineus* (Cricetidae, Dendromurinae). *Mammalia* 30: 454-494.
- **Lessa EP and Stein BR (1992)** Morphological constraints in the digging apparatus of pocket gophers (Mammalia: Geomyidae). *Biological Journal of the Linnean Society* **47**: 439-453.
- **Logan M and Sanson GD (2002)** The effects of tooth wear on the activity patterns of free-ranging koalas (*Phascolarctos cinereus* Goldfuss). *Australian Journal of Zoology* **50**: 281-292.
- **Lowrison GC (1974)** *Crushing and Grinding: the Size Reduction of Solid Materials.* (Butterworths: London)

- **Lucas PW** (1979) The dental-dietary adaptations of mammals. *Neues Jahrbuch für Geologie und Paläontologie Monatshefte* 1979: 486-512.
- **Lucas PW** (1982) Basic principles of tooth design. In: *Teeth: Form, Function and Evolution*. pp. 154-162. B Kurtén, ed. (Columbia University Press: New York)
- **Lucas PW and Luke DA (1983a)** Computer simulation of the breakdown of carrot particles during human mastication. *Archives of Oral Biology* **28**: 821-826.
- **Lucas PW and Luke DA (1983b)** Methods for analysing the breakdown of food in human mastication. *Archives of Oral Biology* **28**: 813-819.
- **Lucas PW and Luke DA (1984)** Chewing it over: basic principles of food breakdown. In: *Food Acquisition and Processing in Primates*. pp. 283-301. DJ Chivers, BA Wood and A Bilsborough, eds. (Plenum Press: New York)
- **Lucas PW and Teaford MF (1994)** Functional morphology of colobine teeth. In: *Colobine Monkeys: their Ecology, Behaviour and Evolution.* pp. 173-203. AG Davies and JF Oates, eds. (Cambridge University Press: Cambridge)
- **Luke DA and Lucas PW (1983)** The significance of cusps. *Journal of Oral Rehabilitation* **10**: 197-206.
- **Lumsden LF and Bennett AF (1995a)** Chocolate Wattled Bat. In: *Mammals of Victoria: Distribution, Ecology and Conservation*. pp. 176-177. PW Menkhorst, ed. (Oxford University Press: Melbourne)
- **Lumsden LF and Bennett AF (1995b)** Gould's Wattled Bat. In: *Mammals of Victoria: Distribution, Ecology and Conservation*. pp. 174-175. PW Menkhorst, ed. (Oxford University Press: Melbourne)
- **Lumsden LF and Bennett AF (1995c)** Large Forest Bat. In: *Mammals of Victoria: Distribution, Ecology and Conservation*. pp. 195-196. PW Menkhorst, ed. (Oxford University Press: Melbourne)
- **Lumsden LF and Bennett AF (1995d)** Lesser Long-eared Bat. In: *Mammals of Victoria: Distribution, Ecology and Conservation*. pp. 184-186. PW Menkhorst, ed. (Oxford University Press: Melbourne)
- **Lumsden LF and Bennett AF (1995e)** Southern Forest Bat. In: *Mammals of Victoria: Distribution, Ecology and Conservation*. pp. 196-198. PW Menkhorst, ed. (Oxford University Press: Melbourne)
- Maas MC (1993) Enamel microstructure and molar wear in the Greater Galago, *Otolemur crassicaudatus* (Mammalia, Primates). *American Journal of Physical Anthropology* 92: 217-233.
- **Maas** MC (1994) A scanning electron-microscope study of *in vitro* abrasion of mammalian tooth enamel under compressive loads. *Archives of Oral Biology* 39: 1-11.
- **Macho GA and Spears IR (1999)** Effects of loading on the biomechanical behavior of molars of *Homo*, *Pan*, and *Pongo*. *American Journal of Physical Anthropology* **109**: 211-227.
- **Maddock TH and Tidemann CR (1995)** Lesser Long-eared Bat. In: *The Mammals of Australia*. 2nd ed. pp. 502-503. R Strahan, ed. (Australian Museum/Reed Books: Sydney)
- Marques SA (1986) Activity cycle, feeding and reproduction of *Molossus ater* (Chiroptera: Molossidae) in Brazil. *Boletim do Museu Paraense Emilio Goeldi Serie Zoologia* 2: 157-179.
- Maynard Smith J, Burian R, Kauffman S, Alberch P, Campbell J, Goodwin B, Lande R, Raup D and Wolpert L (1985) Developmental constraints and evolution. *Quarterly Review of Biology* 60: 265-287.
- McArthur C and Sanson GD (1988) Tooth wear in eastern grey kangaroos (*Macropus giganteus*) and western grey kangaroos (*Macropus fuliginosus*), and its potential

- influence on diet selection, digestion and population parameters. *Journal of Zoology* **215**: 491-504.
- McDowell SB, Jr. (1958) The Greater Antillean insectivores. Bulletin of the American Museum of Natural History 115: 113-214.
- McGeer T (1992) Principles of walking and running. In: *Mechanics of Animal Locomotion: Advances in Comparative and Environmental Physiology 11*. pp. 113-139. RM Alexander, ed. (Springer-Verlag: Berlin)
- Megson THG (1996) Structural and Stress Analysis. (Arnold: London)
- **Meldrum DJ and Kay RF (1997)** *Nuciruptor rubricae*, a new pitheciin seed predator from the Miocene of Colombia. *American Journal of Physical Anthropology* **102**: 407-427.
- **Mellett JS (1969)** Carnassial rotation in a fossil carnivore. *American Midland Naturalist* **82**: 287-289.
- **Mellett JS** (1981) Mammalian carnassial function and the 'Every Effect'. *Journal of Mammalogy* 62: 164-166.
- **Mellett JS** (1985) Autocclusal mechanisms in the carnivore dentition. *Australian Mammalogy* 8: 233-238.
- Menkhorst PW and Lumsden LF (1995) Common Bent-wing Bat. In: *Mammals of Victoria: Distribution, Ecology and Conservation*. pp. 180-181. PW Menkhorst, ed. (Oxford University Press: Melbourne)
- Menzel MA, Carter TC, Mitchell BL, Lablonowski LR, Chapman BR and Laerm J (2000) Prey selection by a maternity colony of big brown bats (*Eptesicus fuscus*) in the southeastern United States. *Florida Scientist* 63: 232-241.
- Mills JRE (1966) The functional occlusion of the teeth of Insectivora. *Journal of the Linnean Society (Zoology)* 46: 1-25.
- **Mills JRE** (1967) A comparison of lateral jaw movements in some mammals from wear facets on the teeth. *Archives of Oral Biology* 12: 645-661.
- **Mohsenin NN (1970)** *Physical Properties of Plant and Animal Materials.* (Gordon and Breach: New York)
- **Moore SJ and Sanson GD (1995)** A comparison of the molar efficiency of two insecteating mammals. *Journal of Zoology* **235**: 175-192.
- **Mosimann JE (1970)** Size allometry: size and shape variables with characterizations of the lognormal and generalized gamma distributions. *Journal of the American Statistical Association* **65**: 930-945.
- **Mosimann JE and James FC (1979)** New statistical methods for allometry with application to Florida red-winged blackbirds. *Evolution* **33**: 444-459.
- Nabhitabhata J (1986) Food of Thai bats: preliminary study of the food habits of insectivorous bats from Thailand. *Courier Forschunginstitut Senckenberg* 87: 55-71.
- **Nee JG** (1998) Fundamentals of Tool Design. 4th ed. (Society of Manufacturing Engineers: Dearborn)
- **Neville AC** (1984) Cuticle: organization. In: *Biology of the Integument, Vol 1, Invertebrates*. pp. 611-625. J Bereiter-Hahn, AG Matoltsy and KS Richards, eds. (Springer-Verlag: Berlin)
- **Niklas KJ** (1992) Plant Biomechanics: an Engineering Approach to Plant Form and Function. (University of Chicago Press: Chicago)
- Norberg UM (1990) Vertebrate Flight: Mechanics, Physiology, Morphology, Ecology and Evolution. (Springer-Verlag: Berlin)
- **O'Neill MG and Taylor RJ (1989)** Feeding ecology of Tasmanian bat assemblages. *Australian Journal of Ecology* **14**: 19-31.
- **Oberg E, Jones FD, Horton HL and Ryffell HH (2000)** *Machinery's Handbook.* 26th ed. (Industrial Press: New York)

- **Osborn HF (1888)** The evolution of mammalian molars to and from the tritubercular type. *American Naturalist* **22**: 1067-1079.
- **Osborn HF (1897)** Trituberculy: a review dedicated to the late Professor Cope. *American Naturalist* **31**: 993-1016.
- **Osborn JW and Lumsden AGS (1978)** An alternative to "thegosis" and a re-examination of the ways in which mammalian molars work. *Neues Jahrbuch für Geologie und Paläontologie Abhandlungen* **156**: 371-392.
- Ostwald PF and Muñoz J (1997) Manufacturing Processes and Systems. 9th ed. (John Wiley & Sons: New York)
- Palamara J, Phakey PP, Rachinger WA, Sanson GD and Orams HJ (1984) The nature of the opaque and translucent enamel regions of some Macropodinae (*Macropus giganteus*, Wallabia bicolor and Peradorcas concinna). Cell & Tissue Research 238: 329-338.
- **Patterson B (1956)** Early Cretaceous mammals and the evolution of mammalian molar teeth. *Fieldiana Geology* **13**: 1-105.
- **Pavey CR and Burwell CJ (1997)** The diet of the diadem leaf-nosed bat *Hipposideros diadema*: confirmation of a morphologically-based prediction of carnivory. *Journal of Zoology* **243**: 295-303.
- Pavey CR and Burwell CJ (1998) Bat predation on eared moths: a test of the allotonic frequency hypothesis. *Oikos* 81: 143-151.
- **Peeters PJ (2002)** Correlations between leaf structural traits and the densities of herbivorous insect guilds. *Biological Journal of the Linnean Society* **77**: 43-55.
- **Pérez-Barbería FJ and Gordon IJ (1998)** The influence of molar occlusal surface area on the voluntary intake, digestion, chewing behaviour and diet selection of red deer (*Cervus elaphus*). *Journal of Zoology* **245**: 307-316.
- **Phillips GL** (1966) Ecology of the Big Brown Bat (Chiroptera: Vespertilionidae) in northeastern Kansas. *American Midland Naturalist* 75: 168-198.
- **Pigliucci M and Kaplan J (2000)** The fall and rise of Dr Pangloss: adaptationism and the *Spandrels* paper 20 years later. *Trends in Ecology and Evolution* **15**: 66-70.
- **Pilbeam D and Gould SJ (1974)** Size and scaling in human evolution. *Science* **186**: 892-901.
- Pine RH (1969) Stomach contents of a free-tailed bat, Molossus ater. Journal of Mammalogy 50: 162.
- **Pollack HW** (1976) *Tool Design*. (Reston Publishing Company, Inc. Reston)
- **Popowics TE and Fortelius M (1997)** On the cutting edge: tooth blade sharpness in herbivorous and faunivorous mammals. *Annales Zoologici Fennici* **34**: 73-88.
- **Popowics TE, Rensberger JM and Herring SW (2001)** The fracture behaviour of human and pig molar cusps. *Archives of Oral Biology* **46**: 1-12.
- **Puech P-F, Prone A and Albertini H (1981)** Mechanical process of dental surface alteration by nonabrasive and nonadhesive friction, reproduced by experimentation and applied to the diet of early man. *Comptes Rendus des Seances de L'Academie des Sciences Serie III Sciences de la Vie* **294**: 497-502.
- **Purslow PP (1980)** Toughness of Extensible Connective Tissues. Thesis. Reading University, UK.
- Quicke DLJ, Wyeth P, Fawke JD, Basibuyuk HH and Vincent JFV (1998) Manganese and zinc in the ovipositors and mandibles of hymenopterous insects. *Zoological Journal of the Linnean Society* 124: 387-396.
- **Radinsky L** (1985) Patterns in the evolution of ungulate jaw shape. *American Zoologist* 25: 303-314.
- **Ravosa MJ** (2000) Size and scaling in the mandible of living and extinct apes. *Folia Primatologica* 71: 305-322.

- **Reduker DW** (1983) Functional analysis of the masticatory apparatus in two species of *Myotis. Journal of Mammalogy* 64: 277-286.
- **Reed DNO (1997)** Contour mapping as a new method for interpreting diet from tooth morphology. *American Journal of Physical Anthropology* **Suppl 24**: 194.
- **Rensberger JM (1973)** An occlusal model for mastication and dental wear in herbivorous mammals. *Journal of Paleontology* **47**: 515-528.
- **Rensberger JM** (1975) Function in the cheek tooth evolution of some hypsodont geomyoid rodents. *Journal of Paleontology* 49: 10-22.
- **Rensberger JM** (1978) Scanning electron microscopy of wear and occlusal events in some small herbivores. In: *Development, Function and Evolution of Teeth.* pp. 415-438. PM Butler and KA Joysey, eds. (Academic Press: London)
- **Rensberger JM** (1986) Early chewing mechanisms in mammalian herbivores. *Paleobiology* 12: 474-494.
- **Rensberger JM** (1988) The transition from insectivory to herbivory in mammalian teeth. In: *Teeth Revisited: Proceedings of the VIIth International Symposium on Dental Morphology*. Paris, 1986, pp. 351-365. DE Russell, J-P Santoro and D Sigogneau-Russell, eds.
- **Rensberger JM** (1995) Determination of stresses in mammalian dental enamel and their relevance to the interpretation of feeding behaviors in extinct taxa. In: *Functional Morphology in Vertebrate Paleontology*. pp. 151-172. JJ Thomason, ed. (Cambridge University Press: Cambridge)
- **Rensberger JM** (2000) Dental constraints in the early evolution of mammalian herbivory. In: *Evolution of Herbivory in Terrestrial Vertebrates*. pp. 144-167. H-D Sues, ed. (Cambridge University Press: Cambridge)
- **Rensberger JM and Koenigswald Wv (1980)** Functional and phylogenetic interpretation of enamel microstructure in rhinoceroses. *Paleobiology* **6**: 477-495.
- **Rensberger JM and Pfretzschner HU (1992)** Enamel structure in astrapotheres and its functional implications. *Scanning Microscopy* **6**: 495-508.
- **Reynolds SE (1975)** The mechanism of plasticization of the abdominal cuticle in *Rhodnius. Journal of Experimental Biology* **62**: 81-98.
- **Ridley M** (1983) The Explanation of Organic Diversity: the Comparative Method and Adaptations for Mating. (Clarendon Press: Oxford)
- **Robinson MF and Stebbings RE (1993)** Food of the serotine bat, *Eptesicus serotinus* is faecal analysis a valid qualitative and quantitative technique? *Journal of Zoology* **231**: 239-248.
- Rodríguez-Durán A, Lewis AR and Montes Y (1993) Skull morphology and diet of antillean bat species. *Caribbean Journal of Science* 29: 258-261.
- **Rosenberger AL and Kinzey WG (1976)** Functional patterns of molar occlusion in platyrrhine primates. *American Journal of Physical Anthropology* **45**: 281-298.
- **Ross A (1967)** Ecological aspects of the food habits of insectivorous bats. Western Foundation of Vertebrate Zoology 1: 203-263.
- Russell ES (1916) Form and Function: a Contribution to the History of Animal Morphology. (University of Chicago Press: Chicago)
- **Ryan AS (1979)** Wear striation direction on primate teeth: a scanning electron microscope examination. *American Journal of Physical Anthropology* **50**: 155-168.
- **Ryder JA** (1878) On the mechanical genesis of tooth-forms. *Proceedings of the Academy of Natural Sciences of Philadelphia* 79: 45-80.
- **Sample BE and Whitmore RC** (1993) Food habits of the endangered Virginia big-eared bat in West Virginia. *Journal of Mammalogy* 74: 428-435.
- Sanson G, Read J, Aranwela N, Clissold F and Peeters P (2001) Measurement of leaf biomechanical properties in studies of herbivory: opportunities, problems and procedures. *Austral Ecology* 26: 535-546.

- **Sanson GD (1980)** The morphology and occlusion of the molariform cheek teeth in some Macropodinae (Marsupialia: Macropodidae). *Australian Journal of Zoology* **28**: 341-365.
- **Sanson GD** (1985) Functional dental morphology and diet selection in dasyurids (Marsupialia: Dasyuridae). *Australian Mammalogy* 8: 239-247.
- Savage RJG (1977) Evolution in carnivorous mammals. *Palaeontology* 20: 237-271.
- **Schofield RMS, Nesson MH and Richardson KA (2002)** Tooth hardness increases with zinc-content in mandibles of young adult leaf-cutter ants. *Naturwissenschaften* **89**: 579-583.
- **Schulz M** (2000) Diet and foraging behavior of the golden-tipped bat, *Kerivoula papuensis*: a spider specialist? *Journal of Mammalogy* 81: 948-957.
- **Seligsohn D** (1977) Analysis of species-specific molar adaptations in strepsirhine primates. In: *Contributions to Primatology, Volume 11*. pp. 1-116. FS Szalay, ed. (S. Karger: Basel)
- **Sheine WS and Kay RF (1977)** An analysis of chewed food particle size and its relationship to molar structure in the primates *Cheirogaleus medius* and *Galago senegalensis* and the insectivoran *Tupaia glis. American Journal of Physical Anthropology* **47**: 15-20.
- **Sigogneau-Russell D, Hooker JJ and Ensom PC (2001)** The oldest tribosphenic mammal from Laurasia (Purbeck Limestone Group, Berriasian, Cretaceous, UK) and its bearing on the 'dual origin' of Tribosphenida. *Comptes Rendus de L'Academie des Sciences Serie II Sciences de la Terre et des Planetes* **333**: 141-147.
- **Silva M and Downing JA (1995)** *CRC Handbook of Mammalian Body Masses.* (CRC Press, Inc: Boca Raton)
- Silva-Taboada G (1979) Los murciélagos de Cuba. (Editorial Academia: La Habana)
- **Simmons NB** (1998) A reappraisal of interfamilial relationships of bats. In: *Bat Biology and Conservation*. pp. 3-26. TH Kunz and PA Racey, eds. (Smithsonian Institution Press: Washington)
- **Skogland T (1988)** Tooth wear by food limitation and its life history consequences in wild reindeer. *Oikos* **51**: 238-242.
- **Slaughter BH (1970)** Evolutionary trends of chiropteran dentitions. In: *About Bats: A Chiropteran Biology Symposium*. pp. 51-83. BH Slaughter and DW Walton, eds. (Southern Methodist University Press: Dallas)
- **Spears IR** (1997) A three-dimensional finite element model of prismatic enamel: a reappraisal of the data on the Young's modulus of enamel. *Journal of Dental Research* 76: 1690-1697.
- **Spears IR and Crompton RH (1996)** The mechanical significance of the occlusal geometry of great ape molars in food breakdown. *Journal of Human Evolution* **31**: 517-535.
- **Spears IR and Macho GA (1998)** Biomechanical behaviour of modern human molars: implications for interpreting the fossil record. *American Journal of Physical Anthropology* **106**: 467-482.
- Spears IR, van Noort R, Crompton RH, Cardew GE and Howard IC (1993) The effects of enamel anisotropy on the distribution of stress in a tooth. *Journal of Dental Research* 72: 1526-1531.
- **Stern D, Crompton AW and Skobe Z (1989)** Enamel ultrastructure and masticatory function in molars of the American opossum, *Didelphis virginiana*. *Zoological Journal of the Linnean Society* **95**: 311-334.
- **Stevens PS (1974)** *Patterns in Nature.* (Atlantic Monthly Press: Boston)
- **Strait SG** (1991) *Dietary Reconstruction in Small-bodied Fossil Primates*. PhD dissertation. Anthropology. State University of New York, Stony Brook.

- **Strait SG** (1993a) Differences in occlusal morphology and molar size in frugivores and faunivores. *Journal of Human Evolution* 25: 471-484.
- **Strait SG** (1993b) Molar microwear in extant small-bodied faunivorous mammals: An analysis of feature density and pit frequency. *American Journal of Physical Anthropology* 92: 63-79.
- **Strait SG (1993c)** Molar morphology and food texture among small-bodied insectivorous mammals. *Journal of Mammalogy* **74**: 391-402.
- **Strait SG (2001)** Dietary reconstruction of small-bodied omomyoid primates. *Journal of Vertebrate Paleontology* **21**: 322-334.
- **Strait SG and Vincent JFV (1998)** Primate faunivores: physical properties of prey items. *International Journal of Primatology* **19**: 867-878.
- **Swift SM and Racey PA (1983)** Resource partitioning in two species of vespertilionid bats (Chiroptera) occupying the same roost. *Journal of Zoology* **200**: 249-259.
- **Teaford MF (1985)** Molar microwear and diet in the genus *Cebus. American Journal of Physical Anthropology* **66**: 363-370.
- **Teaford MF (1988)** A review of dental microwear and diet in modern mammals. *Scanning Microscopy* **2**: 1149-1166.
- **Teaford MF and Oyen OJ (1989)** Live primates and dental replication: new problems and new techniques. *American Journal of Physical Anthropology* **80**: 73-81.
- **Teaford MF and Walker A (1983a)** Dental microwear in adult and still-born guinea pigs (*Cavia porcellus*). Archives of Oral Biology **28**: 1077-1081.
- **Teaford MF and Walker A (1983b)** Prenatal jaw movements in the guinea pig, *Cavia porcellus*: evidence from patterns of tooth wear. *Journal of Mammalogy* **64**: 534-536.
- **Thompson DAW** (1942) *On Growth and Form.* 2nd ed. (Cambridge University Press: Cambridge)
- **Tidemann CR** (1995) Southern Forest Bat. In: *The Mammals of Australia*. 2nd ed. pp. 543-544. R Strahan, ed. (Australian Museum/Reed Books: Sydney)
- **Turnbull WD (1970)** Mammalian masticatory apparatus. Fieldiana Geology **18**: 147-356.
- Ungar P and Williamson M (2000) Exploring the effects of tooth wear on functional morphology: a preliminary study using dental topographic analysis. *Palaeontologia Electronica* 3: 18 pp., 752 kb. <a href="http://palaeo-electronica.org/2000\_1/gorilla/issue1">http://palaeo-electronica.org/2000\_1/gorilla/issue1</a> 00.htm.
- **Ungar PS and Kay RF (1995)** The dietary adaptations of European Miocene catarrhines. *Proceedings of the National Academy of Sciences of the United States of America* **92**: 5479-5481.
- **Ungar PS and Spencer MA (1999)** Incisor microwear, diet, and tooth use in three Amerindian populations. *American Journal of Physical Anthropology* **109**: 387-396.
- Valeri CJ, Cole TMI, Lele S and Richtsmeier JT (1998) Capturing data from threedimensional surfaces using fuzzy landmarks. *American Journal of Physical Anthropology* 107: 113-124.
- Van Valen L (1966) Deltatheridia, a new order of mammals. *Bulletin of the American Museum of Natural History* 132: 1-126.
- **Van Valen L** (1969) Evolution of dental growth and adaptation in mammalian carnivores. *Evolution* 23: 96-117.
- Van Valkenburgh B (1988) Incidence of tooth breakage among large, predatory mammals. *American Naturalist* 131: 291-302.
- **Van Valkenburgh B (1991)** Iterative evolution of hypercarnivory in canids (Mammalia: Carnivora): evolutionary interactions among sympatric predators. *Paleobiology* **17**: 340-362.

- **Van Valkenburgh B** (1996) Feeding behavior in free-ranging, large African carnivores. *Journal of Mammalogy* 77: 240-254.
- Van Valkenburgh B and Ruff CB (1987) Canine tooth strength and killing behaviour in large carnivores. *Journal of Zoology* 212: 379-397.
- **Vaughan TA (1977)** Foraging behaviour of the giant leaf-nosed bat (*Hipposideros commersoni*). East African Wildlife Journal **15**: 237-249.
- **Verts BJ, Carraway LN and Benedict RA (1999a)** Body-size and age-related masticatory relationships in two species of *Blarina*. *Prairie Naturalist* 31: 43-52.
- **Verts BJ, Carraway LN and Whitaker JO, Jr (1999b)** Temporal variation in prey consumed by big brown bats (*Eptesicus fuscus*) in a maternity colony. *Northwest Science* **73**: 114-120.
- **Vestjens WJM and Hall LS (1977)** Stomach contents of forty-two species of bats from the Australasian region. *Australian Wildlife Research* **4**: 25-35.
- **Vincent JFV (1975)** Locust oviposition: stress softening of the extensible intersegmental membranes. *Proceedings of the Royal Society of London, Series B* **188**: 189-201.
- Vincent JFV (1980) Insect cuticle: a paradigm for natural composites. In: *The Mechanical Properties of Biological Materials (34th Symposium of the Society for Experimental Biology)*. pp. 183-210. JFV Vincent and JD Currey, eds. (Cambridge University Press: Cambridge)
- **Vincent JFV (1990)** *Structural Biomaterials*. Revised ed. (Princeton University Press: Princeton)
- **Vincent JFV (1992a)** Composites. In: *Biomechanics Materials: a Practical Approach*. pp. 57-74. JFV Vincent, ed. (Oxford University Press: Oxford)
- **Vincent JFV (1992b)** Plants. In: *Biomechanics Materials: a Practical Approach*. pp. 165-191. JFV Vincent, ed. (Oxford University Press: Oxford)
- Vincent JFV (1998) The cuticle as an exoskeleton. In: *Microscopic Anatomy of Invertebrates, Volume 11A: Insecta.* pp. 139-149. FW Harrison and M Locke, eds. (Wiley-Liss: New York)
- **Vinyard CJ, Wall CE, Williams SH and Hylander WL (2003)** Comparative functional analysis of skull morphology of tree-gouging primates. *American Journal of Physical Anthropology* **120**: 153-170.
- **Wainwright PC (1996)** Ecological explanation through functional morphology: the feeding biology of sunfishes. *Ecology* **77**: 1336-1343.
- Wainwright SA, Biggs WD, Currey JD and Gosline JM (1976) Mechanical Design in Organisms. (Princeton University Press: Princeton)
- Walker A, Hoeck HN and Perez L (1978) Microwear in mammalian teeth as an indicator of diet. *Science* 201: 908-910.
- Warner RM (1985) Interspecific and temporal dietary variation in an Arizona bat community. *Journal of Mammalogy* 66: 45-51.
- Waters NE (1980) Some mechanical and physical properties of teeth. In: *The Mechanical Properties of Biological Materials (34th Symposium of the Society for Experimental Biology)*. pp. 99-135. JFV Vincent and JD Currey, eds. (Cambridge University Press: Cambridge)
- Whitaker JO, Jr (1972) Food habits of bats from Indiana. *Canadian Journal of Zoology* **50**: 877-883.
- Whitaker JO, Jr (1995) Food of the big brown bat *Eptesicus fuscus* from maternity colonies in Indiana and Illinois. *American Midland Naturalist* 134: 346-360.
- Whitaker JO, Jr and Black H (1976) Food habits of cave bats from Zambia, Africa. Journal of Mammalogy 57: 199-204.
- Whitaker JO, Jr, Maser C and Cross SP (1981) Food habits of eastern Oregon bats, based on stomach and scat analyses. *Northwest Science* 55: 281-292.

- Whitaker JO, Jr, Maser C and Keller LE (1977) Food habits of bats of western Oregon. *Northwest Science* 51: 46-55.
- Williams BA and Covert HH (1994) New Early Eocene anaptomorphine primate (Omomyoidae) from the Washakie Basin, Wyoming, with comments on the phylogeny and paleobiology of anaptomorphines. *American Journal of Physical Anthropology* 93: 323-340.
- Worley M and Sanson GD (2000) The effect of tooth wear on grass fracture in grazing kangaroos. In: *Plant Biomechanics 2000: Proceedings of the 3rd Plant Biomechanics Conference*. Freiburg-Badenweiler, pp. 583-589. H-C Spatz and T Speck, eds. Georg Thieme Verlag.
- Wroe S, Ebach M, Ahyong S, Muizon Cd and Muirhead J (2000) Cladistic analysis of dasyuromorphian (Marsupialia) phylogeny using cranial and dental characters. *Journal of Mammalogy* 81: 1008-1024.
- **Yamashita N** (1996) Seasonal and site specificity of mechanical dietary patterns in two Malagasy lemur families (Lemuridae and Indriidae). *International Journal of Primatology* 17: 355-387.
- **Yamashita N** (1998) Functional dental correlates of food properties in five Malagasy lemur species. *American Journal of Physical Anthropology* 106: 169-188.
- Yettram AL, Wright KWJ and Pickard HM (1976) Finite element stress analysis of the crowns of normal and restored teeth. *Journal of Dental Research* 6: 1004-1011.
- **Young WG, Douglas WB and Robson SK** (1990) Differential wear resistance as a function of tooth enamel structure in the koala *Phascolarctos cinereus*. In: *Biology of the Koala*. pp. 145-150. AK Lee, KA Handasyde and GD Sanson, eds. (Surrey Beatty & Sons: Sydney)
- Zar JH (1999) Biostatistical Analysis. (Prentice-Hall, Inc. Upper Saddle River)
- **Zuccotti LF, Williamson MD, Limp WF and Ungar PS** (1998) Modeling primate occlusal topography using geographic information systems technology. *American Journal of Physical Anthropology* 107: 137-142.

**Plates** 

**Plate 1.** (**Top**) Three-dimensional reconstruction of the protoconoid, a fundamental double-bladed tool. Two lower and two upper protoconoids with latero-vertical movement are shown in occlusion.

(Bottom) Comparisons between the models and real mammalian tooth forms. L-R. Model tools: (A) single-bladed tools, symmetrical (2i) and asymmetrical (2ii); (B) double-bladed tools (3i, 3ii, 4ii). Mammalian tooth forms: (C) lower carnassials of *Felis catus* (Carnivora: Felidae) and *Mustela frenata* (Carnivora: Mustelidae); (D) premolar of *F. catus*; (E) lower zalambdodont molar of *Tenrec ecaudatus* (Insectivora: Tenrecidae), lower tribosphenic molar of *Didelphis virginiana* (Didelphimorphia: Didelphidae), lower dilambdodont molar of *Chalinolobus gouldii* (Chiroptera: Vespertilionidae), and upper dilambdodont molar of *Desmana moschata* (Insectivora: Talpidae). Scale bars = 1 mm.

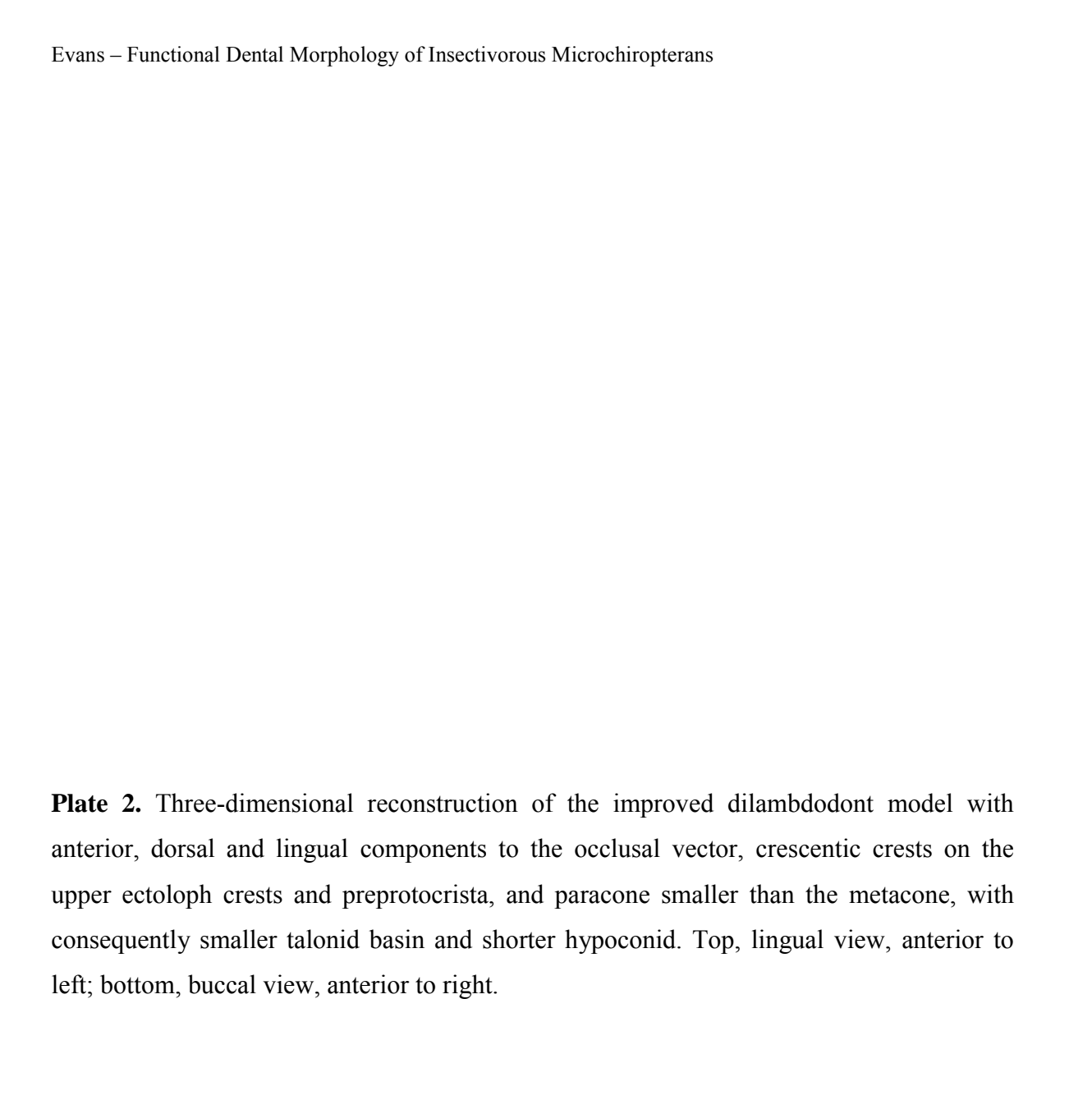


**Plate 3.** Front cover of *Journal of Microscopy*, November 2001 that accompanied the publication of Chapter 4. Caption: Virtual Reality Modelling Language (VRML) reconstruction with glow look-up table overlay of the upper second molar of Gould's Wattled Bat *Chalinolobus gouldii*. The tooth is approximately 1.4 × 1.8 mm. Lingual view, anterior to right. The tooth was cast into urethane, and the cast was dyed with eosin and confocal imaged with rhodamine optics using a ×10 dry objective. Reconstruction of the entire three-dimensional surface of morphological features such as teeth allows accurate quantification of their morphology and assists in relating the three-dimensional shape to their function. These reconstructions can be viewed from any direction or distance on the computer screen, and occluding teeth can be animated in virtual space to illustrate the complex relationships between the components.

# **Appendices**

# **Appendix 1.** Full VRML files for major models constructed in Chapter 2.

```
Fig. 2.2i
#VRML V2.0 utf8
# VRML reconstruction of single-bladed tool
# Evans (2003), Fig. 2.2i
WorldInfo {}
NavigationInfo {
  type [ "EXAMINE", "WALK" ]
Background {
   skyColor 1 1 1
}
Transform {
  translation 0 0 -10
   translation 0 0 -10 rotation 0 1 0 4 children [
DirectionalLight {
    direction 0 0 1 1
           direction 0 0 1 ambientIntensity 1
    ]
Viewpoint {
  description "View A"
  position 2.323 2.255 -2.393
  orientation -0.0716076 0.969793 0.233182
2.51137
Viewpoint {
    description "View B"
    position -2.86793 2.39065 -2.84977
    orientation 0.0808925 0.979127 0.18646 3.95001
    description "View C" position 0.330973 1.30776 5.54706 orientation 0.978918 0.203613 0.0161817
6.08598
Transform {
  translation 2 2 0
  rotation 0 0 1 3.141
  children [
       nlidren [
DEF Upper Transform {
    children [
        Shape {
            geometry DEF UpperFace IndexedFaceSet
{
                        solid FALSE
                       coord Coordinate {
                           point [
0 0 0,
0.9 0 0,
0.9 0 1,
0 0 1,
0 0 1,
                                1 1 0,
                               0 0.4 1,
0 0 0.5,
1 0.6 0.5
                           ]
                       }
                   appearance Appearance {
  material Material {
     diffuseColor 0 0 1
               0, 1, 2, -1
                        coord Coordinate {
                           point [
1 1 0,
1 0.6 0.5,
1 1 1
```

}

```
fappearance DEF AppearLine Appearance {
  material Material {
    emissiveColor 1 0 0
} ] }
 DEF Lower Transform {
     children [
Shape {
             geometry USE UpperFace
appearance Appearance {
material Material {
diffuseColor 1 1 0
         Shape {
    geometry USE Line
    appearance USE AppearLine
     ]
 }
 DEF TS TimeSensor {
  loop TRUE
  cycleInterval 4
 DEF PI1 PositionInterpolator {
      keyValue [
0 -0.1 0,
0 0.9 0,
0 -0.1 0
     key [
0, 0.5, 1
      ]
  ROUTE TS.fraction_changed TO PI1.set_fraction ROUTE PI1.value_changed TO Lower.translation
                  Fig. 2.2ii
  #VRML V2.0 utf8
# VRML reconstruction of single-bladed tool
# Evans (2003), Fig. 2.2ii
 NavigationInfo { type [ "EXAMINE", "WALK" ] }
 Background {
   skyColor 1 1 1
 }
 direction 0 0 1 ambientIntensity 1
    ] }
 }
 Viewpoint {
  description "View A"
  position 2.323 2.255 -2.393
  orientation -0.0716076 0.969793 0.233182
2.51137
}
  Viewpoint
     iewpoint {
description "View B"
position -2.86793 2.39065 -2.84977
orientation 0.0808925 0.979127 0.18646 3.95001
 Viewpoint {
    description "View C"
    position 0.330973 1.30776 5.54706
    orientation 0.978918 0.203613 0.0161817
  6.08598
 Transform {
  translation 2 2 0
  rotation 0 0 1 3.141
  children [
    DEF Upper Transform {
```

children [

```
Shape {
                       geometry DEF UpperFace IndexedFaceSet
                                                                                                                                      Transform {
  translation 0 0 -10
  rotation 0 1 0 4
  children [
{
                             solid FALSE
                            solid FALSE
coordIndex [
0, 1, 2, 3, -1,
0, 1, 5, 4, -1,
1, 5, 9, -1,
2, 6, 9, -1,
2, 3, 7, 6, -1,
0, 8, 4, -1,
3, 7, 8, -1,
4, 5, 9, 8, -1,
6, 7, 8, 9, -1
                                                                                                                                               DirectionalLight {
                                                                                                                                                    direction 0 0 1
ambientIntensity 1
                                                                                                                                      }
                                                                                                                                     Viewpoint {
  description "View A"
  position 2.323 2.255 -2.393
  orientation -0.0716076 0.969793 0.233182
2.51137
                            coord Coordinate {
                                point [ 0 0 0, 0.92 0 0, 0.92 0 0, 0.92 0 1, 0 0 1, 0 0 1, 0 0 1, 0 0.5 1 1 1 1, 0 0 0.5, 1 0 0.3 0.5
                                                                                                                                      Viewpoint {
    description "View B"
    position -2.86793 2.39065 -2.84977
    orientation 0.0808925 0.979127 0.18646 3.95001
                                                                                                                                      Viewpoint {
    description "View C"
    position 0.330973 1.30776 5.54706
    orientation 0.978918 0.203613 0.0161817
6.08598
                                ]
                            }
                       appearance Appearance {
  material Material {
    diffuseColor 0 0 1
                                                                                                                                      Transform {
  translation 2 1.3 0
  rotation 0 0 1 3.141
  children [
                       }
                                                                                                                                               DEF Upper Transform {
    children [
        Shape {
                  geometry DEF UpperFace IndexedFaceSet
                                                                                                                                      {
                                                                                                                                                                  solid FALSE
coordIndex [
    0, 1, 2, 3, -1,
    0, 1, 5, 4, -1,
    2, 1, 5, 9, 6, -1,
    2, 3, 7, 6, -1,
    0, 8, 4, -1,
    0, 3, 8, -1,
    3, 7, 8, -1,
    4, 5, 9, 8, -1,
    6, 7, 8, 9, -1
]
                            coord Coordinate {
                                point [
1 0.6 0,
1 0.3 0.5,
1 1 1
                                ]
                            }
                       fappearance DEF AppearLine Appearance {
   material Material {
     emissiveColor 1 0 0
}
  coord Coordinate {
  point [
    0 0 0,
    0.90 0,
    0.95 0 1,
    0 0 1,
    0 0.7 0,
    110
}
                                                                                                                                                                            1 1 0,
1 0.3 1,
0 0 1,
0 0.1 0.5,
DEF Lower Transform {
    children [
        11Idren ,
    Shape {
    geometry USE UpperFace
    appearance Appearance {
        material Material {
            diffuseColor 1 1 0
        }
}
                                                                                                                                                                            1 0.4 0.5
                                                                                                                                                                       ]
                                                                                                                                                                  }
                                                                                                                                                              appearance Appearance {
  material Material {
    diffuseColor 0 0 1
         Shape {
   geometry USE Line
   appearance USE AppearLine
                                                                                                                                                         Shape {
                                                                                                                                                              geometry DEF Line IndexedLineSet {
  coordIndex [
    0, 1, 2, -1
DEF TS TimeSensor {
                                                                                                                                                                  loop TRUE
cycleInterval 4
DEF PI1 PositionInterpolator {
  keyValue [
    0 -0.1 0,
                                                                                                                                                                       ]
                                                                                                                                                                  }
         0 1.5 0,
0 -0.1 0
                                                                                                                                                              fappearance DEF AppearLine Appearance {
  material Material {
    emissiveColor 1 0 0
    key [
0, 0.5, 1
                                                                                                                                        1 } }
                                                                                                                                                                  }
ROUTE TS.fraction_changed TO PI1.set_fraction ROUTE PI1.value_changed TO Lower.translation
                                                                                                                                      }
                    Fig. 2.2iii
                                                                                                                                      DEF Lower Transform {
                                                                                                                                           children [
                                                                                                                                                  hape {
  geometry DEF LowerFace IndexedFaceSet {
    solid FALSE
    coordIndex [
      0, 1, 2, 3, -1,
      0, 1, 5, 4, -1,
      6, 9, 5, 1, 2, -1,
      2, 3, 7, 6, -1,
      0, 8, 4, -1,
      0, 3, 8, -1,
      3, 7, 8, -1,
      4, 5, 9, 8, -1,
      6, 7, 8, 9, -1
}
#VRML V2.0 utf8
                                                                                                                                               Shape {
# VRML reconstruction of single-bladed tool
# Evans (2003), Fig. 2.2iii
WorldInfo {}
NavigationInfo {
  type [ "EXAMINE", "WALK" ]
Background { skyColor 1 1 1
```

```
0, 2, 5, 6, 3, -1,
1, 2, 5, 7, 4, -1,
5, 6, 9, 7, -1,
3, 6, 9, 8, -1,
4, 7, 9, 8, -1
                coord Coordinate {
                    point [
0 0 0,
0.95 0 0,
0.9 0 1,
0 0 1,
0 0 0,
1 0.3 0,
                                                                                                                                          coord Coordinate {
                                                                                                                                             1 1 1, 0 0.7 1,
                        0 0.1 0.5
                    ]
                }
            appearance Appearance {
  material Material {
    diffuseColor 1 1 0
  }
}
                                                                                                                                                  0.5054 1.1114 0.3163
                                                                                                                                              ]
                                                                                                                                          }
       appearance DEF Appear Appearance {
  material Material {
    diffuseColor 1 1 0
                                                                                                                             ] }
                 coord Coordinate {
                   point [
1 0.3 0,
1 0.4 0.5,
1 1 1
                                                                                                                         }
                                                                                                                                  coord Coordinate {
            appearance USE AppearLine
  ] }
                                                                                                                                     point [
0 1.2 0,
0.25 1.3 0.433,
0.5 2 0.866,
0.75 1.3 0.433,
1 1.2 0
}
DEF TS TimeSensor {
  loop TRUE
  cycleInterval 4
                                                                                                                                 }
                                                                                                                              fappearance DEF AppearLine Appearance {
  material Material {
    emissiveColor 1 0 0
 DEF PI1 PositionInterpolator {
    keyValue [
0 -0.1 0,
0 0.6 0,
                                                                                                                    } }
        0 -0.1 0
    key [
0, 0.5, 1
                                                                                                                  }
    ]
                                                                                                                  Transform {
 translation 0.5 3.2 0.866
 rotation 1 0 0 3.141
 children [
 Transform {
  Transform [
ROUTE TS.fraction_changed TO PI1.set_fraction ROUTE PI1.value_changed TO Lower.translation
                                                                                                                              children
                 Fig. 2.3i
                                                                                                                                 hildren | DEF ShapeTool1 Shape {
    geometry USE GeometryTool appearance {
        material Material {
            diffuseColor 0 0 1
#VRML V2.0 utf8
# VRML reconstruction of double-bladed tool
# Evans (2003), Fig. 2.3i
                                                                                                                                      }
 WorldInfo {}
                                                                                                                                 } '
USE Line
NavigationInfo { type [ "EXAMINE", "WALK" ]
                                                                                                                              ]
                                                                                                                         Transform {
  translation -1 0 0
  children [
   USE ShapeTool1
   USE Line
Background {
   skyColor 1 1 1
}
                                                                                                                             ]
Transform {
 translation 14 0 -10
 rotation 0 1 0 4.183
 children [
                                                                                                                    ] }
                                                                                                                  }
        DirectionalLight {
                                                                                                                  DEF TS TimeSensor {
  loop TRUE
  cycleInterval 4
            direction 0 0 1
ambientIntensity 1
    1
                                                                                                                  DEF LowerMovePI PositionInterpolator {
Viewpoint {
  description "View A"
  position 5.025 2.988 -3.843
  orientation -0.068 0.986 0.153 2.316
                                                                                                                     keyValue [
0 -0.1 0,
0 0.8 0,
0 -0.1 0
                                                                                                                      key [
0, 0.5, 1
Viewpoint {
  description "View B"
  position -0.875 2.650 -5.272
  orientation 0.003 0.995 0.099 3.296 }
                                                                                                                      ]
                                                                                                                  ROUTE TS.fraction_changed TO
LowerMovePI.set_fraction
ROUTE LowerMovePI.value_changed TO
LowerTrans.set_translation
Viewpoint {
  description "View C"
  position -5.482 1.337 -0.726
  orientation 0.023 0.999 0.028 4.521 }
                                                                                                                                   Fig. 2.3ii
DEF LowerTrans Transform {
  translation 0 0 0 0
  children [
   Transform {
    children [
    DEF ShapeTool Shape {
    geometry DEF GeometryTool
IndexedFaceSet {
                                                                                                                   #VRML V2.0 utf8
                                                                                                                   # VRML reconstruction of double-bladed tool
# Evans (2003), Fig. 2.3ii
                                                                                                                  WorldInfo {}
IndexedFaceSet {
    solid FALSE
                                                                                                                  NavigationInfo {
  type [ "EXAMINE", "WALK" ]
                        coordIndex [
    0, 1, 2, -1,
    0, 1, 4, 8, 3, -1,
```

```
Background {
   skyColor 1 1 1
                                                                                                                                                 translation -1 0 0
                                                                                                                                                 children [
                                                                                                                                                      USE ShapeTool1
USE Line
Transform {
  translation 14 0 -10
                                                                                                                                     }
     rotation 0 1 0 4.183
children [
DirectionalLight {
direction 0 0 1
                                                                                                                                   }
                                                                                                                                   DEF TS TimeSensor {
             ambientIntensity 1
                                                                                                                                       loop TRUE
cycleInterval 4
     ]
}
                                                                                                                                   DEF LowerMovePI PositionInterpolator {
Viewpoint {
  description "View A"
  position 5.025 2.988 -3.843
  orientation -0.068 0.986 0.153 2.316
                                                                                                                                       keyValue [
0 -0.1 0,
                                                                                                                                            0 1.3 0,
0 -0.1 0
                                                                                                                                       key [
0, 0.5, 1
Viewpoint {
    description "View B"
    position -0.875 2.650 -5.272
    orientation 0.003 0.995 0.099 3.296 }
                                                                                                                                   ROUTE TS.fraction_changed TO
LowerMovePI.set_fraction
ROUTE LowerMovePI.value_changed TO
LowerTrans.set_translation
Viewpoint {
    description "View C"
    position -5.482 1.337 -0.726
    orientation 0.023 0.999 0.028 4.521 }
                                                                                                                                                       Fig. 2.3iii
DEF LowerTrans Transform {
  translation 0 0 0
  children [
   Transform {
    children [
                                                                                                                                   #VRML V2.0 utf8
# VRML reconstruction of double-bladed tool
# Evans (2003), Fig. 2.3iii
DEF ShapeTool Shape {
    geometry DEF GeometryTool
IndexedFaceSet {
    solid FALSE
                                                                                                                                   WorldInfo {}
                                                                                                                                   NavigationInfo {
  type [ "EXAMINE", "WALK" ]
                            solid FALSE
coordIndex [
    0, 1, 2, -1,
    0, 1, 4, 8, 3, -1,
    0, 2, 5, 6, 3, -1,
    1, 2, 5, 7, 4, -1,
    5, 6, 9, 7, -1,
    3, 6, 9, 8, -1,
    4, 7, 9, 8, -1
                                                                                                                                   Background { skyColor 1 1 1
                                                                                                                                   }
                                                                                                                                   Transform {
 translation 14 0 -10
 rotation 0 1 0 4.183
 children [
 DirectionalLight {
                            coord Coordinate {
                                direction 0 0 1
ambientIntensity 1
                                                                                                                                            }
                                                                                                                                       1
                                                                                                                                   }
                                                                                                                                   Viewpoint {
  description "View A"
  position 5.025 2.988 -3.843
  orientation -0.068 0.986 0.153 2.316
                                     0.5034 0.8741 0.3785
                           }
                                                                                                                                   Viewpoint {
    description "View B"
    position -0.875 2.650 -5.272
    orientation 0.003 0.995 0.099 3.296 }
                       fappearance DEF Appear Appearance {
  material Material {
    diffuseColor 1 1 0
                     }
                                                                                                                                   Viewpoint {
  description "View C"
  position -5.482 1.337 -0.726
  orientation 0.023 0.999 0.028 4.521 }
              ]
         DEF LowerTrans Transform {
  translation 0 0 0
  children [
    Transform {
                   coord Coordinate {
                                                                                                                                                children [
DEF ShapeTool Shape {
geometry DEF GeometryTool
                       point [
0 1.2 0,
0.25 1 0.433,
0.5 2 0.866,
0.75 1 0.433,
1 1.2 0
                                                                                                                                 ]
                  }
              appearance DEF AppearLine Appearance {
  material Material {
    emissiveColor 1 0 0
  } }
                                                                                                                                                                    ]
Transform {
  translation 0.5 3.2 0.866
  rotation 1 0 0 3.141
  children [
  Transform {
                                                                                                                                                               coordIndex [
                                                                                                                                                                   oordIndex [
0, 1, 2, -1,
0, 1, 4, 9, -1,
0, 3, 8, -1,
0, 8, 9, -1,
1, 2, 5, 6, 3, -1,
1, 2, 5, 7, 4, -1,
3, 6, 8, -1,
4, 7, 9, -1,
5, 6, 7, -1,
6, 7, 9, 8, -1
         nildren [
Transform {
    children [
    DEF ShapeTool1 Shape {
        geometry USE GeometryTool
        appearance Appearance {
            material Material {
                diffuseColor 0 0 1
                            }
                                                                                                                                                               ]
                       }
                                                                                                                                                          appearance DEF Appear Appearance {
  material Material {
    diffuseColor 1 1 0
                   ÚSE Line
          Transform {
```

```
}
                                                                                                                                          description "View C"
position -5.482 1.337 -0.726
orientation 0.023 0.999 0.028 4.521 }
           DEF Line Shape {
  geometry IndexedLineSet {
   coord Coordinate {
                                                                                                                                     DEF LowerTrans Transform {
  translation 0 0 0
                        oord Coordinate {
    point [
        0 2 0,
        0.25 1.3 0.433,
        0.5 2 0.866,
        0.75 1.3 0.433,
        1 2 0
    ]
                                                                                                                                           children [
Transform {
    children [
                                                                                                                                      children | DEF ShapeTool Shape {
    geometry DEF GeometryTool
IndexedFaceSet {
    solid_FALSE
  solid FALSE coordindex [
0,1,2,-1,0,1,9,8,-1,
1,4,9,-1,
0,2,5,6,3,-1,
1,2,5,7,4,-1,
3,6,8,-1,
4,7,9,-1,
5,6,10,-1,
5,7,10,-1,
6,8,10,-1,
7,9,10,-1,
8,9,10,-1,
Transform {
  translation 0.5 3.6 0.866
  rotation 1 0 0 3.141
  children [
   Transform {
    children [
    DEF ShapeTool1 Shape {
        geometry USE GeometryTool appearance Appearance {
        material Material {
            diffuseColor 0 0 1
        }
}
                                                                                                                                                                  coord Coordinate {
                                                                                                                                                                      0.25 1.3 0.433,
0.75 1.3 0.433,
0.35 0.8 0,
0.65 0.8 0,
                        }
                                                                                                                                                                           0.5 1 0.5
                    ÚSE Line
                                                                                                                                                                      ]
               ]
                                                                                                                                                                 }
           }
Transform
                                                                                                                                                              appearance DEF Appear Appearance {
  material Material {
    diffuseColor 1 1 0
               ransform {
translation -1 0 0
children [
USE ShapeTool1
USE Line
                                                                                                                                                  ] }
    ] ]
                                                                                                                                               }
DEF Line Shape {
  geometry IndexedLineSet {
    coordIndex [
      0, 1, 2, 3, 4, -1
      ]
  }
  DEF TS TimeSensor {
      loop TRUE
cycleInterval 4
                                                                                                                                                         coord Coordinate {
                                                                                                                                                             point [ 0 2 0,
  DEF LowerMovePI PositionInterpolator {
      keyValue [
0 -0.5 0,
0 1.1 0,
0 -0.5 0
                                                                                                                                                                 0.25 1.3 0.433,
0.5 1.2 0.866,
0.75 1.3 0.433,
1 2 0

}
appearance DEF AppearLine Appearance {
    material Material {
       emissiveColor 1 0 0
    }
}

      key [
0, 0.5, 1
      ]
 ROUTE TS.fraction_changed TO
LowerMovePI.set_fraction
ROUTE LowerMovePI.value_changed TO
LowerTrans.set_translation
                                                                                                                                      }
                    Fig. 2.3iv
                                                                                                                                      #VRML V2.0 utf8
  # VRML reconstruction of double-bladed tool
# Evans (2003), Fig. 2.3iv
                                                                                                                                                       nildren [
DEF ShapeTool1 Shape {
  geometry USE GeometryTool
  appearance Appearance {
   material Material {
      diffuseColor 0 0 1
   }
  }
  WorldInfo {}
  NavigationInfo { type [ "EXAMINE", "WALK" ] }
 Background {
   skyColor 1 1 1
}
                                                                                                                                                             }
                                                                                                                                                         }
USE Line
                                                                                                                                                    ]
      ransform {
translation 14 0 -10
rotation 0 1 0 4.183
children [
DirectionalLight {
  Transform
                                                                                                                                               Transform {
  translation -1 0 0
  children [
   USE ShapeTool1
   USE Line
             direction 0 0 1
ambientIntensity 1
                                                                                                                                         ] }
} ]
                                                                                                                                      }
 Viewpoint {
  description "View A"
  position 5.025 2.988 -3.843
  orientation -0.068 0.986 0.153 2.316
                                                                                                                                      DEF TS TimeSensor {
  loop TRUE
  cycleInterval 4
                                                                                                                                      DEF LowerMovePI PositionInterpolator {
 Viewpoint {
    description "View B"
    position -0.875 2.650 -5.272
    orientation 0.003 0.995 0.099 3.296 }
                                                                                                                                           keyValue [
0 -0.1 0,
0 0.7 0,
0 -0.1 0
  Viewpoint {
```

```
key [
0, 0.5, 1
      ]
                                                                                                                                                         fappearance DEF AppearLine Appearance {
  material Material {
    emissiveColor 1 0 0
                                                                                                                                                             }
ROUTE TS.fraction changed TO
                                                                                                                                             ] }
LowerMovePI.set_fraction
ROUTE LowerMovePI.value_changed TO
LowerTrans.set_translation
                                                                                                                                        Transform {
  translation 0.5 3.2 0.866
  rotation 1 0 0 3.141
  children [
  Transform {
    children [
    DEF ShapeTool1 Shape {
      geometry USE GeometryTool
      appearance Appearance {
      material Material {
         diffuseColor 0 0 1
      }
                     Fig. 2.3v
#VRML V2.0 utf8
# VRML reconstruction of double-bladed tool
# Evans (2003), Fig. 2.3v
WorldInfo {}
NavigationInfo {
  type [ "EXAMINE", "WALK" ]
Background {
   skyColor 1 1 1
                                                                                                                                                                  }
                                                                                                                                                             ÚSE Line
                                                                                                                                                        ]
}
Transform {
  translation -1 0 0
  children [
    USE ShapeTool1
    USE Line
               direction 0 0 1
ambientIntensity 1
                                                                                                                                        } 1
      ]
Viewpoint {
  description "View A"
   position 5.025 2.988 -3.843
  orientation -0.068 0.986 0.153 2.316
                                                                                                                                          DEF TS TimeSensor {
                                                                                                                                               loop TRUE cycleInterval 4
                                                                                                                                          DEF LowerMovePI PositionInterpolator {
                                                                                                                                               keyValue [
0 -0.1 0,
0 0.7 0,
0 -0.1 0
     .ewpoint {
description "View B"
position -0.875 2.650 -5.272
orientation 0.003 0.995 0.099 3.296 }
                                                                                                                                               key [
0, 0.5, 1
      lewpoint {
description "View C"
position -5.482 1.337 -0.726
orientation 0.023 0.999 0.028 4.521 }
                                                                                                                                               ]
                                                                                                                                          }
DEF LowerTrans Transform {
  translation 0 0 0
  children [
   Transform {
    children [
                                                                                                                                          ROUTE TS.fraction_changed TO
LowerMovePI.set_fraction
ROUTE LowerMovePI.value_changed TO
LowerTrans.set_translation
DEF ShapeTool Shape {
    geometry DEF GeometryTool
IndexedFaceSet {
    solid FALSE
                                                                                                                                                              Fig. 2.4i
                                                                                                                                          #VRML V2.0 utf8
# VRML model of single-bladed tool with serial
duplication and lateral movement
# Evans (2003), Fig. 2.4i
                             solid FALSE coordIndex [
0, 1, 2, -1, 0, 1, 9, 8, -1, 0, 3, 8, -1, 1, 4, 9, -1, 0, 2, 5, 6, 3, -1, 1, 2, 5, 7, 4, -1, 3, 6, 8, -1, 4, 7, 9, -1, 5, 6, 10, -1, 5, 7, 10, -1, 6, 8, 10, -1, 7, 9, 10, -1, 8, 9, 10, -1, 1
                                                                                                                                          WorldInfo {}
                                                                                                                                          NavigationInfo {
  type [ "EXAMINE", "WALK" ]
                                                                                                                                          Background { skyColor 1 1 1 1 }
                                                                                                                                         Transform {
  translation 14 0 -10
  rotation 0 1 0 4
  children [
                              coord Coordinate {
                                  DirectionalLight {
                                                                                                                                                       direction 0 0 1
ambientIntensity 1
                                                                                                                                                   }
                                                                                                                                              1
                                       0.25 1 0.433,
0.75 1 0.433,
0.35 0.7 0,
0.65 0.7 0,
0.5 0.9 0.5
                                                                                                                                          }
                                                                                                                                         Viewpoint {
  description "View A"
   position 2.323 2.255 -2.393
   orientation -0.072 0.970 0.233 2.511
                            }
                         fappearance DEF Appear Appearance {
  material Material {
    diffuseColor 1 1 0
                                                                                                                                         Viewpoint {
  description "View B"
  position -2.868 2.391 -2.850
  orientation 0.081 0.979 0.186 3.950
                  }
                                                                                                                                         Viewpoint {
  description "View C"
  position 0.331 1.308 5.547
  orientation 0.979 0.204 0.016 6.086
}
               ]
          JEF Line Shape {
  geometry IndexedLineSet {
    coordIndex [
      0, 1, 2, 3, 4, -1
      1
                                                                                                                                          DEF LowerTrans Transform {
   children [
    Transform {
                    coord Coordinate {
                        point [
0 2 0,
0.25 1 0.433,
0.5 1.2 0.866,
0.75 1 0.433,
1 2 0
                                                                                                                                         Transform {
    children [
        DEF ShapeTool Shape {
        geometry DEF GeometryTool
IndexedFaceSet {
        solid_FALSE
                                                                                                                                                                       coordIndex [
```

```
0, 1, 2, 3, -1,
0, 1, 5, 4, -1,
1, 2, 6, 9, 5, -1,
2, 3, 7, 6, -1,
0, 8, 4, -1,
3, 7, 8, -1,
4, 5, 9, 8, -1,
6, 7, 8, 9, -1
                                                                                                                                   # Evans (2003), Fig. 4ii
                                                                                                                                   WorldInfo {}
                                                                                                                                   NavigationInfo {
  type [ "EXAMINE", "WALK" ]
}
                                                                                                                                   Background {
   skyColor 1 1 1
}
                            coord Coordinate {
                                point [
0 0 0,
1 0 0,
1 0 1,
0 0 1,
0 0.4 0,
0.8 1 0,
                                                                                                                                  Transform {
  translation 14 0 -10
  rotation 0 1 0 4
  children [
    DirectionalLight {
      direction 0 0 1
      ambientIntensity 1
  }
                                     0.8 1 1,
0 0.4 1,
0 0 0.5,
1 0.6 0.5
                                                                                                                                      }
                                ]
                                                                                                                                   }
                           }
                                                                                                                                   Viewpoint {
   description "View A"
   position 5.025 2.988 -3.843
   orientation -0.068 0.986 0.153 2.316
                       fappearance DEF Appear Appearance {
  material Material {
    diffuseColor 1 1 0
                       }
                                                                                                                                   Viewpoint {
  description "View B"
  position -0.875 2.650 -5.272
  orientation 0.003 0.995 0.099 3.296
}
                  }
                            coord Coordinate {
                                                                                                                                   Viewpoint
                                                                                                                                        ewpoint {
  description "View C"
  position -5.482 1.337 -0.726
  orientation 0.0228 0.999 0.028 4.521
                               point [
    0.8 1 0,
    1 0.6 0.5,
    0.8 1 1
                               ]
                                                                                                                                   }
                       }
appearance DEF AppearLine Appearance {
  material Material {
    emissiveColor 1 0 0
                                                                                                                                                children [
DEF ShapeTool Shape {
    geometry DEF GeometryTool
                                                                                                                                  geometry DEF GeometryTool IndexedFaceSet { solid FALSE coordIndex [ 0, 1, 2, -1, 0, 1, 4, 8, 3, -1, 0, 2, 10, 6, 3, -1, 1, 2, 10, 7, 4, -1, 5, 6, 10, -1, 5, 7, 10, -1, 5, 6, 7, -1, 6, 7, 9, -1, 3, 6, 9, 8, -1, 4, 7, 9, 8, -1
       Transform {
translation 0 0 1
children [
USE ShapeTool
USE ShapeLine
  ] ]
}
DEF TopTrans Transform {
    translation 1.80 1.60 rotation 0 0 1 3.14159 children [
Transform {
    children [
                                                                                                                                                               coord Coordinate {
                                                                                                                                                                  hildren [
DEF ShapeTool1 Shape {
   geometry USE GeometryTool appearance Appearance {
   material Material {
      diffuseColor 0 0 1 }
   }
}
                                                                                                                                                                  ]
                  ÚSE ShapeLine
                                                                                                                                                               }
              ]
        Transform {
  translation 0 0 1
  children [
    USE ShapeTool1
    USE ShapeLine
                                                                                                                                                           appearance DEF Appear Appearance {
  material Material {
    diffuseColor 1 1 0
                                                                                                                                                               }
  } }
                                                                                                                                                     }
DEF ShapeLine Shape {
  geometry IndexedLineSet {
    coord Coordinate {
        coint [
                                                                                                                                                                  oord Coordinate {
point [
      0 1.2 0,
      0.25 1.3 0.433,
      0.5 2 0.433,
      1.2 0
DEF TS TimeSensor {
  loop TRUE
  cycleInterval 4
                                                                                                                                                                   ]
DEF LowerMovePI PositionInterpolator {
    coordIndex [ 0, 1, 2, 3, 4, -1
                                                                                                                                                               ]
    key [
0, 0.5, 1
                                                                                                                                                           fappearance DEF AppearLine Appearance {
  material Material {
    emissiveColor 1 0 0
    ]
                                                                                                                                                     }
ROUTE LowerMovePI.value_changed TO
LowerTrans.translation
ROUTE TS.fraction_changed TO
LowerMovePI.set_fraction
                                                                                                                                                 ]
                                                                                                                                            }
Transform {
  translation -1 0 0
  children [
   USE ShapeTool
   USE ShapeLine
                   Fig. 2.4ii
#VRML V2.0 utf8
                                                                                                                                                 ]
# VRML wodel of double-bladed tool with serial duplication and lateral movement
```

# **Appendix 2.** Full VRML files for all models constructed in Chapter 3.

```
Fig. 3.5a

#VRML V2.0 utf8

# Model of carnassial tooth
# Evans (2003), Fig. 3.5a

WorldInfo {}

NavigationInfo {
   type [ "EXAMINE", "WALK" ]
```

Background {
 skyColor 1 1 1

1

Transform {
 translation 0 0 -10
 rotation 0 1 0 4
 children [
 DirectionalLight {
 direction 0 0 1
 ambientIntensity 1

Viewpoint {
 description "Lingual"
 position -3.486 1.14156 -0.949
 orientation 0.049 0.997 0.066 4.406
}
Viewpoint {
 description "Posterior"
 position -0.702 1.031 4.483
 orientation -0.315 -0.948 -0.053 0.336

DEF LowerTrans Transform {
 translation 0 0 0
 children [
 DEF Protol Shape {
 geometry DEF CarnassialFace IndexedFaceSet
 {
}

point [
0.6 0 0,
1.1 0 0,
1.1 0 1,
0.6 0 1,
0.8 1 0,
0.8 1 1,
0.6 0.4 1,
0.6 0 0.5,
1.07 0.46 0.5,
0.96 0.68 0.49,
0.96 0.68 0.51,
0.6 0 0.5,
0.6 0 0.5,
0.6 0 0.5,

```
0.6 0.16 0.7
                 }
             fappearance DEF AppearL Appearance {
  material Material {
    diffuseColor 1 1 0
            }
        }
   ]
DEF TopTrans Transform {
  translation 1.85 1.5 0
  rotation 0 0 1 3.14159
  children [
       Shape {
    geometry USE CarnassialFace
    appearance DEF AppearU Appearance {
        material Material {
            diffuseColor 0 0 1
        }
    }
  }
}
DEF TS TimeSensor {
    loop TRUE
cycleInterval 4
DEF LowerMovePI PositionInterpolator {
    key [
_ 0, 0.5, 1
    keyValue [
-0.36 0.72 0,
0.3 -0.6 0,
-0.36 0.72 0
    1
ROUTE LowerMovePI.value_changed TO
LowerTrans.set_translation
ROUTE TS.fraction_changed TO
LowerMovePI.set_fraction
```

# Fig. 3.5b

```
#VRML V2.0 utf8
# Model of insectivore premolar
# Evans (2003), Fig. 3.5b

WorldInfo {}

NavigationInfo {
   type [ "EXAMINE", "WALK" ]
}

Background {
   skyColor 1 1 1
}

Transform {
   translation 0 0 -10
   rotation 0 1 0 4
   children [
     DirectionalLight {
        direction 0 0 1
        ambientIntensity 1
   }
}

Viewpoint {
   description "Lingual"
   position -3.416 1.695 -0.927
```

```
orientation 0.049 0.997 0.066 4.406
                                                                                                                                                                                                                                                                               }
                                                                                                                                                                                                                                                                               Viewpoint {
  description "Lingual"
  position 0.02 3.47 -6.13
  orientation 0 1 0.13 3.15
  Viewpoint {
  description "Posterior"
  position -0.950 1.540 4.344
  orientation -0.315 -0.948 -0.053 0.336
                                                                                                                                                                                                                                                                               Viewpoint {
  description "Posterior lingual"
  position -3.72 2.58 -4.74
  orientation 0.02 1 0.06 3.86
 Transform {
  translation 0.8 2 0
  rotation 0 0 1 3.141
  children [
    DEF Upper Transform {
    children [
        Shape {
        geometry DEF UpperPremolarFace
    TradsyadFaceSet {
    }
                                                                                                                                                                                                                                                                               DEF Lower Transform {
  translation 0 0 0
  children [
 geometry DEF UpperProperty Jeff 
                                                                                                                                                                                                                                                                               children [
Transform {
    translation 0 0 0 children [
        DEF Proto_Lower Shape {
            geometry DEF Proto_LowerFace
IndexedFaceSet {
            solid FALSE
                                                                                                                                                                                                                                                                                                                                         coordIndex [
                                                                                                                                                                                                                                                                                                                                                 oordIndex [
0, 1, 2, -1,
0, 1, 4, 8, 3, -1,
0, 2, 10, 6, 3, -1,
1, 2, 10, 7, 4, -1,
5, 6, 7, -1,
5, 6, 10, -1,
5, 7, 10, -1,
6, 7, 9, -1,
3, 6, 9, 8, -1,
4, 7, 9, 8, -1
                                                             coord Coordinate {
                                                                    point [
0 0 0,
0.3 0 0,
0.32 0 0.7,
                                                                              0.32 0 0.7,
0 0 0.7,
0 0.2 0,
0.4 1 0,
0.4 0.4 0.7,
0 0.05 0.7,
0 0 0.5,
0.4 0.15 0.5
                                                                                                                                                                                                                                                                                                                                         coord Coordinate {
                                                                                                                                                                                                                                                                                                                                                ]
                                                           }
                                                   appearance DEF AppearL Appearance {
  material Material {
    diffuseColor 0 0 1
       ]
                                                                                                                                                                                                                                                                                                                                        }
                                                                                                                                                                                                                                                                                                                                appearance DEF AppearL Appearance {
  material Material {
     diffuseColor 1 1 0
                                                                                                                                                                                                                                                                                                          ] }
  DEF Lower Transform {
  children {
    Shape {
        geometry USE UpperPremolarFace
        appearance DEF AppearU Appearance {
            material Material {
                diffuseColor 1 1 0
            }
        }
                                                                                                                                                                                                                                                                                                 }
Transform {
  translation -1 0 0
  children [
   USE Proto_Lower
} 1 }
                                        }
                                                                                                                                                                                                                                                                                                           ]
                                                                                                                                                                                                                                                                                     ] }
                                                                                                                                                                                                                                                                               }
                                                                                                                                                                                                                                                                               Transform {
  translation -1 3.2 1
   DEF TS TimeSensor {
  loop TRUE
  cycleInterval 4
                                                                                                                                                                                                                                                                                       DEF PI1 PositionInterpolator {
  keyValue [
    0 -0.1 0,
    0 1.8 0,
    0 -0.1 0
                                                                                                                                                                                                                                                                                                                                      eometry DEF Proto_Uppe:

Set {

    solid FALSE

    coordIndex [

        0, 1, 2, -1,

        0, 1, 4, 8, 3, -1,

        0, 2, 10, 6, 3, -1,

        1, 2, 10, 7, 4, -1,

        5, 6, 7, -1,

        5, 6, 10, -1,

        5, 7, 10, -1,

        6, 7, 9, -1,

        3, 6, 9, 8, -1,

        4, 7, 9, 8, -1
                                                                                                                                                                                                                                                                               IndexedFaceSet
           key [
0, 0.5, 1
   ROUTE TS.fraction_changed TO PI1.set_fraction ROUTE PI1.value_changed TO Lower.translation
                                         Fig. 3.5c
                                                                                                                                                                                                                                                                                                                                       2, /, 9, 8, -1
coord Coordinate {
point [
    0.1 0 0,
    0.9 0 0.9,
    0.1.2 0,
    1 1.2 0,
    1 2 0.7,
    0.5 1.42 0.575,
    1 1.42 0.575,
    0.5 0.9 0,
    0.65 1.1 0.35,
    0.9 1.3 1
]
    #VRML V2.0 utf8
# Model of zalambdodont molars
# Evans (2003), Fig. 3.5c
     WorldInfo {}
   NavigationInfo {
  type [ "EXAMINE", "WALK" ]
}
   Background {
   skyColor 1 1 1
}
                                                                                                                                                                                                                                                                                                                                                 ]
   }
                                                                                                                                                                                                                                                                                                                                appearance DEF AppearU Appearance {
  material Material {
                                                                                                                                                                                                                                                                                                                                                  aterial Material {
diffuseColor 0 0 1
                                 ambientIntensity 1
```

```
Transform {
  translation -1 0 0
  children [
    USE Proto_Upper
]
                                                                                                                                                                fappearance DEF AppearL Appearance {
  material Material {
    diffuseColor 1 1 0
  ] }
                        ]
                                                                                                                                                                }
                                                                                                                                                           Transform {
  translation -1 0 0
  children DEF Proto_LowerPost Shape {
                                                                                                                                        geometry DEF Proto_LowerPostFace
IndexedFaceSet {
DEF TS TimeSensor {
  cycleInterval 4
  loop TRUE
                                                                                                                                                                        Solid FALSE coordIndex [ 0, 1, 2, -1, 0, 1, 8, 12, 3, -1, 1, 7, 11, -1, 1, 7, 10, 2, -1, 0, 2, 10, 6, 3, -1, 5, 6, 7, -1, 5, 6, 10, -1, 5, 7, 10, -1, 6, 7, 9, 11, -1, 7, 9, 11, -1, 7, 9, 11, -1, 8, 9, 12, -1, 6, 9, 12, -1, 3, 6, 12, -1, 1, 4, 13, -1 ]
                                                                                                                                                                          : {
   solid FALSE
DEF LowerMovePI PositionInterpolator {
     keyValue [
0 -0.12 0.15
0 0.6 -0.75
0 -0.12 0.15
     key [
0, 0.5, 1
      ]
ROUTE LowerMovePI.value_changed TO
Lower translation
ROUTE TS.fraction_changed TO
LowerMovePI.set_fraction
                                                                                                                                                                          coord Coordinate {
                                                                                                                                                                             Fig. 3.5d
#VRML V2.0 utf8
# Model of dilambdodont molars
# Evans (2003), Fig. 3.5d
WorldInfo {}
                                                                                                                                                                                  1 0.8 0,
0.35 0.85 0.2,
0.1 1.1 1.2,
1 0.71 .1,
0.25 1.1 0,
NavigationInfo {
  type [ "EXAMINE", "WALK" ]
Background { skyColor 1 1 1
                                                                                                                                                                                   1.1 0 0
                                                                                                                                                                         }
Transform {
  translation 0 0 -10
  rotation 0 1 0 4
  children [
    DirectionalLight {
      direction 0 0 1
      ambientIntensity 1
  }
                                                                                                                                                                    appearance USE AppearL
                                                                                                                                                                }
                                                                                                                                        Transform {
    children Transform {
        translation -1 0 0
        children DEF LowerPlate Shape {
        geometry DEF LowerPlateFace
IndexedFaceSet {
        colid FALSE
     ]
                                                                                                                                                                              solid FALSE
coord Coordinate {
Viewpoint {
  description "Lingual"
  position 1.496 3.309 -6.074
  orientation -0.003 0.992 0.124 3.064
                                                                                                                                                                                   point [
0.1 0 0,
1.9 0 0,
1.1 0 0.9,
                                                                                                                                                                                        0.1 0 0.9
                                                                                                                                                                                   ]
Viewpoint {
    description "Posterior"
    position -5.370 1.168 -1.403
    orientation -0.019 0.999 -0.028 4.326
                                                                                                                                                                              coordIndex [
0, 1, 2, 3, -1
                                                                                                                                                    } }
                                                                                                                                                                          appearance USE AppearL
Viewpoint
     -ewpoint {
  description "Occlusal upper"
  position 0.355 -3.579 5.227
  orientation 0.998 -0.066 -0.017 0.848
                                                                                                                                                 Transform {
  translation 2 0 0
DEF Lower Transform {
  translation 0 0 0
  children [
                                                                                                                                                      children USE LowerTooth
children [
DEF LowerTooth Transform {
    translation 0 0 0
    children [
    DEF Proto_LowerAnt Shape {
        geometry DEF Proto_LowerAntFace
IndexedFaceSet {
        solid FALSE
        geometry DEF Proto_LowerAntFace
                                                                                                                                            ]
                                                                                                                                 }
                             solid FALSE
coordIndex [
    0, 1, 2, -1,
    0, 1, 4, 8, 3, -1,
    0, 2, 10, 6, 3, -1,
    1, 2, 10, 7, 4, -1,
    5, 6, 7, -1,
    5, 7, 10, -1,
    6, 7, 9, -1,
    3, 6, 9, 8, -1,
    4, 7, 9, 8, -1
                              coord Coordinate {
                                 point [
0.1 0 0,
0.9 0 0,
0.9 0 0.9,
0 1.2 0,
                                       0.1 1.3 1
```

```
1 1.2 0,
1 2 0.7,
0.5 1.42 0.575,
1 1.42 0.575,
0.5 0.9 0,
0.65 1.1 0.35,
0.9 1.3 1
                                                                                                                                           DEF LowerMovePI PositionInterpolator {
                                                                                                                                                key [
_ 0, 0.25, 0.5, 0.75, 1
                                                                                                                                                keyValue [
                                                                                                                                                     0 -0.48 0.6,
0 0.4 -0.5,
0 -0.7 -1.2,
0 -1.5 0,
                                              ]
                                          }
                                                                                                                                               0 -1.5 0,
0 -0.48 0.6
                                      appearance DEF AppearU Appearance
    {
                                         material Material {
   diffuseColor 0 0 1
}
                                                                                                                                           }
                                                                                                                                           ROUTE LowerMovePI.value_changed TO Lower.set_translation ROUTE TS.fraction_changed TO
                                Transform {
  translation -1 0 0
  children USE Proto_Upper
                                                                                                                                            LowerMovePI.set_fraction
                                                                                                                                                              Fig. 3.5e
   #VRML V2.0 utf8
# Model of tribosphenic molars
# Evans (2003), Fig. 3.5e
                                                                                                                                           WorldInfo {}
                                                                                                                                           NavigationInfo {
  type [ "EXAMINE", "WALK" ]
}
                                                        oordIndex [
0, 1, 2, -1,
0, 1, 4, 8, 3, -1,
1, 2, 10, 7, 4, -1,
0, 2, 10, 6, 3, -1,
5, 6, 7, -1,
5, 6, 10, -1,
5, 7, 10, -1,
6, 7, 9, -1,
3, 6, 9, 8, -1,
4, 7, 9, 8, -1
                                                                                                                                           Background {
   skyColor 1 1 1
}
                                                                                                                                           Transform {
  translation 0 0 -10
                                                                                                                                                translation 0 0 -10
rotation 0 1 0 4
children [
DirectionalLight {
direction 0 0 1
ambientIntensity 1
                                                    coord Coordinate {
                                                       }
                                                                                                                                               ]
                                                                                                                                           }
                                                                                                                                           Viewpoint {
  description "Lingual"
  position 1.49642 3.30922 -6.07428
  orientation -0.00290564 0.99227 0.124061
                                                                                                                                           3.06403
}
                                                                                                                                           Viewpoint {
    description "Posterior"
    position -5.37006 1.16835 -1.40338
    orientation -0.0187888 0.999434 -0.0279208
                                              appearance USE AppearU
                                                                                                                                            4.3256
                                     ]
   Transform {
    translation -1 0 0
    children DEF UpperPlate Shape {
        geometry DEF UpperPlateFace
IndexedFaceSet {
        colid PALSE
                                                                                                                                           Viewpoint {
    description "Occlusal upper"
    position 0.355386 -3.57943 5.22683
    orientation 0.997709 -0.0656025 -0.0165429
                                               solid FALSE
coord Coordinate {
                                                                                                                                            0.848198
                                                   DEF Lower Transform {
  translation 0 0 0
  children [
  DEF LowerTooth Transform {
    translation 0 0 0
    children [
    DEF Proto_LowerAnt Shape {
    geometry DEF Proto_LowerAntFace
IndexedFaceSet {
}
                                                       1.1 0 0,

1 1.2 0,

1 1.19 0.9,

0.9 1.2 0.9,

0.99 1.05 0,

1.01 1.05 0,

2 1.29 0.9,

1.5 1.09 0.9,

1 0.72 0.6
                                                                                                                                          oordIndex [
0, 1, 2, -1,
0, 1, 4, 8, 3, -1,
0, 2, 10, 6, 3, -1,
1, 2, 10, 7, 4, -1,
5, 6, 7, -1,
5, 6, 10, -1,
5, 7, 10, -1,
6, 7, 9, -1,
3, 6, 9, 8, -1,
4, 7, 9, 8, -1
                                                    ]
                                              }
coordIndex [
    0, 1, 2, 3, 4, -1,
    5, 6, 7, -1,
    3, 4, 9, 8, -1,
    10, 11, 12, 13, -1,
    10, 13, 14, -1,
    8, 13, 9, 14, -1,
    9, 10, 14, -1
} } } } } } 
                                                                                                                                                                        coord Coordinate {
                                                                                                                                                                             point [
0.1 0 0,
0.9 0 0,
0.1 0 0.9,
                                                                                                                                                                                 0 1.2 0, 1 1.2 0,
                                                                                                                                                                                 1 1.2 0,
0 2 0.7,
0 1.42 0.575,
0.5 1.42 0.575,
0.5 0.9 0,
0.35 1.1 0.35,
0.1 1.3 1
                                                                                                                                                                             ]
                                                                                                                                                                        }
   Transform {
  translation 2 0 0
  children USE UpperTooth
                                                                                                                                                                   fappearance DEF AppearL Appearance {
  material Material {
    diffuseColor 1 1 0
   DEF TS TimeSensor {
   cycleInterval 4
   loop TRUE
                                                                                                                                                               fransform {
  translation -1 0 0
  children DEF Proto_LowerPost Shape {
```

#### Evans – Functional Dental Morphology of Insectivorous Microchiropterans

```
geometry DEF Proto_LowerPostFace
IndexedFaceSet {
    solid FALSE
                                                                                                                                                                                             appearance DEF AppearU Appearance
                                      sólid FALSE

coordIndex [

0, 1, 2, -1,

0, 1, 8, 12, 3, -1,

1, 7, 11, -1,

1, 8, 11, -1,

2, 10, 7, 1, -1, #1, 7, 10, 2, -
                                                                                                                                                       {
                                                                                                                                                                                                 material Material {
  diffuseColor 0 0 1
                                                                                                                                                                                      1.
                                          0, 2, 10, 6, 3, -1, 5, 6, 10, -1, 5, 6, 10, -1, 5, 7, 10, -1, 6, 7, 9, -1, 8, 9, 11, -1, 7, 9, 11, -1, 8, 9, 12, -1, 6, 9, 12, -1, 1, 4, 13, -1
                                                                                                                                                       geometry DEF
Proto_UpperPostFace IndexedFaceSet {
    solid FALSE
    coordIndex [
                                                                                                                                                                                                                 pordIndex [
0, 1, 2, -1,
0, 1, 4, 8, 3, -1,
0, 2, 10, 6, 3, -1,
1, 2, 10, 7, 4, -1,
5, 6, 7, -1,
5, 6, 10, -1,
5, 7, 10, -1,
6, 7, 9, -1,
3, 6, 9, 8, -1,
4, 7, 9, 8, -1
                                      coord Coordinate {
                                          point [ 0.1 0 0,
                                               0.1 0 0,

1 0 0,

0.1 0 0.9,

0 1.2 0,

1 1.2 0,

0 1.34 0.65,

0.7 1.11 0.36,

1 0.8 0,

0.35 0.85 0.2,

0.1 0.8 0.9,

1 0.6 0.2,

0.25 1.1 0.
                                                                                                                                                                                                            coord Coordinate {
                                                                                                                                                                                                                0.25 1.1 0,
1.1 0 0
                                     }
                                                                                                                                                                                                         }
                                                                                                                                                                                                                       0.9 1.3 1
                                appearance USE AppearL
                          }
Transform {
    children Transform {
        translation -1 0 0
        children DEF LowerPlate Shape {
            geometry DEF LowerPlateFace
IndexedFaceSet {
            realid PALCE
                                                                                                                                                                                                       áppearance USE AppearU
                                                                                                                                                                                            ]
                                                                                                                                                      solid FALSE
                                          coord Coordinate {
  point [
    0.1 0 0,
    1.9 0 0,
    1.1 0 0.9,
    0.1 0 0.9
                                                                                                                                                                                                                 pordIndex [
0, 1, 2, -1,
0, 1, 4, 8, 3, -1,
1, 2, 10, 7, 4, -1,
0, 2, 10, 6, 3, -1,
5, 6, 7, -1,
5, 6, 10, -1,
6, 7, 9, -1,
3, 6, 9, 8, -1,
4, 7, 9, 8, -1
                                                ]
                                          coordIndex [
0, 1, 2, 3, -1
                                     áppearance USE AppearL
              ] } }
                                                                                                                                                                                                            coord Coordinate {
                                                                                                                                                                                                                oord Coordinate {
point [
    0.1 -0.09 0,
    0.9 -0.09 0,
    0.9 -0.09 0,
    1.2 0,
    1.2 0,
    1.3 0.5,
    0.5 0.8 0,
    0.625 0.9 0.3,
           Transform {
  translation 2 0 0
                children USE LowerTooth
DEF UpperTooth Transform {
   children [
    Transform {
}
                                                                                                                                                                                                                       0.9 1.1 1
                                                                                                                                                                                                       appearance USE AppearU
                                                                                                                                                                                          }
                                                                                                                                                                                      Transform {
  translation -1 0 0
  children DEF UpperPlate Shape {
    geometry DEF UpperPlateFace
                                          solid FALSE coordIndex [ 0, 1, 2, -1, 0, 1, 4, 8, 3, -1, 0, 2, 10, 6, 3, -1, 1, 2, 10, -1, 5, 6, 7, -1, 5, 6, 10, -1, 6, 7, 9, -1, 3, 6, 9, 8, -1, 4, 7, 9, 8, -1 ]
                                                                                                                                                       IndexedFaceSet {
                                                                                                                                                                                                       solid FALSE
coord Coordinate {
                                                                                                                                                                                                           oord Coordinat

point [

0.1 0 0,

1.9 0 0,

1.9 0 1.8,

1.14 0 0.9,

0.9 0 0.9,

0.9 0 0,

1.1 0 0,

1 1.2 0,
                                           coord Coordinate {
                                               oord Coordinate {
    point [
        0.1 0 0,
        0.9 0 0,
        0.9 0 0,
        1.2 0,
        1 1.2 0,
        1 2.0,
        1 1.42 0.6,
        1 1.42 0.575,
        0.5 0.9 0,
        0.65 1.1 0.35,
        0.9 1.3 1
                                                                                                                                                                                                                1 1.2 0,
1 0.89 1,
0.9 0.89 0.96846,
0.99 1.05 0,
1.01 1.05 0,
2 1.29 0.9,
1.5 0.89 0.9,
1 0.72 0.6
                                                                                                                                                                                                            ]
                                                                                                                                                                                                       coordIndex [
  0, 1, 2, 3, 4, -1,
```

```
5, 6, 7, -1,
3, 4, 9, 8, -1,
10, 11, 12, 13, -1,
10, 13, 14, -1,
8, 9, 14, 13, -1,
9, 10, 14, -1
}
                                                                                                                                                                                          } appearance DEF AppearL Appearance {
  material Material {
    diffuseColor 1 1 0
  }
}
 Transform {
  translation 2 0 0
  children USE UpperTooth
                                                                                                                                                             DEF TS TimeSensor {
   cycleInterval 4
   loop TRUE
                                                                                                                                                                                                          {
    solid FALSE
    coordIndex [
        0, 13, 21, 17, 2, -1,
        3, 12, 8, 1, 0, -1,
        2, 10, 15, -1,
        2, 15, 7, 17, -1,
        2, 6, 10, -1,
        3, 16, 6, 2, 0, -1,
        5, 6, 15, -1,
        6, 7, 15, -1,
        5, 6, 10, -1,
        6, 7, 15, -1,
        9, 11, 14, -1,
        7, 9, -1,
        9, 14, -1,
        8, 11, 9, 12, -1,
        3, 9, 16, -1,
        3, 9, 12, -1,
        3, 9, 12, -1,
        3, 9, 14, 17, -1,
        8, 11, 14, 17, -1,
        8, 11, 14, 17, -1,
        8, 4, 13, -1,
        7, 14, 17, -1,
        8, 17, 18, 19, -1,
        21, 20, 19, 18, -1,
        17, 18, 21, -1,
        1
        coord Coordinate {
 DEF LowerMovePI PositionInterpolator {
      key [
0, 0.25, 0.5, 0.75, 1
      ]
keyValue [
0 -0.48 0.6,
0 0.4 -0.5,
0 -0.7 -1.2,
0 -1.5 0,
0 -0.48 0.6
      ]
ROUTE LowerMovePI.value_changed TO Lower.set_translation ROUTE TS.fraction_changed TO LowerMovePI.set_fraction
                        Fig. 3.7
 #VRML V2.0 utf8
# Modified model of dilambdodont molars
# Evans (2003), Fig. 3.7
 WorldInfo {}
                                                                                                                                                                                                              coord Coordinate {
 NavigationInfo { type [ "EXAMINE", "WALK" ]
Background {
   skyColor 1 1 1
}
Transform {
  translation 0 0 -10
  rotation 0 1 0 4
  children [
    DirectionalLight {
      direction 0 0 1
      ambientIntensity 1
    }
 }
Viewpoint {
  description "Lingual"
  position 1.276 2.005 -4.297
  orientation 0.003 0.995 0.101 3.109
                                                                                                                                                                                                               ]
                                                                                                                                                                                                          }
Viewpoint {
  description "Posterior"
  position -3.854 1.104 -0.923
  orientation 0.010 1.000 0.015 4.366
                                                                                                                                                                            } }
                                                                                                                                                                                                    appearance USE AppearL
Viewpoint {
  description "Occlusal upper"
  position -0.165 -3.043 3.945
  orientation 0.999 -0.044 0.000 0.888
                                                                                                                                                                         Transform {
  translation 1.8 0 0
  children USE LowerTooth
DEF UpperTooth Transform {
  children [
    Transform {
                                                                                                                                                                              children
                                                                                                                                                             children |
Transform {
    translation -0.6 2.0 0.6
    rotation 1 0 0 3.141
    children |
    DEF Proto_UpperAnt Shape {
        geometry DEF Proto_UpperAntFace
IndexedFaceSet {
        solid FALSE
                                                                                                                                                                                                            solid FALSE
                                                                                                                                                                                                          solid FALSE
coordIndex [
    0, 1, 2, -1,
    3, 8, 4, 1, 0, -1,
    3, 11, 6, 10, 2, 0, -1,
    4, 14, 7, 10, 2, 1, -1,
    5, 12, 6, 7, 13, -1,
    5, 12, 6, 10, -1,
    5, 13, 7, 10, -1,
                                   coord Coordinate {
```

```
6, 7, 9, -1,
3, 11, 6, 9, 8, -1,
4, 14, 7, 9, 8, -1
                                                                                                                                                                     }
Transform {
  translation -1 0 0
  children [
    DEF UpperPlate Shape {
    geometry DEF UpperPlateFace
                                       coord Coordinate {
                                           IndexedFaceSet {
                                                                                                                                                                                          solid FALSE
                                                                                                                                                                                        solid FALSE
coordIndex [
0, 1, 2, 3, -1,
4, 5, 6, -1,
7, 8, 9, -1,
7, 9, 10, -1,
7, 11, 12, -1,
7, 12, 13, -1,
7, 8, 11, -1,
7, 10, 13, -1
                                                                                                                                                                                        /, 10, 13, -1
coord Coordinate {
  point [
    0.1 0 0,
    1.8 0 0,
    1.8 -0.26 1.3,
    0.9 -0.18 0.9,
    0.9 0 0,
    1.1 0 0,
    1 0.5 0,
    1.125 0 0.375,
    0.84625 0.095 0.87875,
    1.2625 0.050 0.6875,
    1.7805 0.09 0.5935,
    0.95 0.46 0,
    1 0.4 0,
    1.05 0.46 0
]
                                            1
                                       }
                                   appearance DEF AppearU Appearance
 {
                                       material Material {
  diffuseColor 0 0 1
                                  }
                             Transform {
  translation -1 0 0
]
                                                                                                                                                                                        }
                                                                                                                                          1 } 1 }
                                                                                                                                                                                    appearance USE AppearU
                                                     pordIndex | 0, 1, 2, -1, 3, 8, 4, 1, 0, -1, 3, 11, 6, 10, 2, 0, -1, 4, 14, 7, 10, 2, 1, -1, 5, 12, 6, 7, 13, -1, 5, 13, 7, 10, -1, 6, 7, 9, -1, 3, 11, 6, 9, 8, -1, 4, 14, 7, 9, 8, -1
                                                                                                                                         Transform {
  translation 1.8 0 0
  children USE UpperTooth
                                                 coord Coordinate {
                                                     DEF TS TimeSensor {
  cycleInterval 4
  loop TRUE
}
                                                                                                                                         DEF LowerMovePI PositionInterpolator {
                                                                                                                                              key [
0, 0.25, 0.5, 0.75, 1
                                                          0.5 0.1 0,
0.65 0.3 0.35,
                                                                                                                                        keyValue [
-0.0125 -0.05 0.0375
0.3 1.2 -0.9
0.6125 -0.05 -1.8375
0.3 -1.3 -0.9
-0.0125 -0.05 0.0375
                                                          0.9 0.6 1,
0.9 0.6 1,
0.25625 0.525 0.31875,
0.71875 0.775 0.80625,
0.96875 0.775 0.80625,
1.00625 0.525 0.31875,
                                                     1
                                                }
                                            appearance USE AppearU
                                                                                                                                         ROUTE LowerMovePI.value_changed TO Lower.set_translation ROUTE TS.fraction_changed TO LowerMovePI.set_fraction
                                  ]
Fig. 3.8
                                                                                                                                        #VRML V2.0 utf8
# Crompton and Sita-Lumsden (1970) model of
therian molar function
# Evans (2003), Fig. 3.8
                                                     pordIndex [
0, 1, 2, -1,
0, 1, 4, 8, 3, -1,
4, 12, 7, 10, 2, 1, -1,
0, 2, 10, 6, 3, -1,
5, 6, 7, 11, -1,
5, 6, 10, -1,
5, 11, 7, 10, -1,
6, 7, 9, -1,
3, 6, 9, 8, -1,
4, 12, 7, 9, 8, -1
                                                                                                                                         WorldInfo {}
                                                                                                                                         NavigationInfo {
  type [ "EXAMINE", "WALK" ]
                                                                                                                                        Background {
   skyColor 1 1 1
}
                                                 coord Coordinate {
                                                     Transform {
  translation 14 0 -10
  rotation 0 1 0 4
  children [
    DirectionalLight {
     direction 0 0 1
     ambientIntensity 1
  }
                                                                                                                                             ]
                                                                                                                                        DEF ViewA Viewpoint {
description "ViewA"
position -2.00 2.07 -2.03
orientation 0.09 0.97 0.21 3.91
                                                                                                                                        DEF ViewD Viewpoint {
  description "ViewD"
  position 1.29 1.29 4.05
  orientation -0.58 0.81 0.04 0.37
                                            appearance USE AppearU
```

```
}
                                                                                                                                                                                                                                                                                                                                                                                                      DEF CSL_mirror Transform {
translation 0.9 1.08 0.895
rotation 0.708 0 -0.707 3.141
children [
   Transform {
  translation 3.3 -0.69 0.895
  rotation 0 1 0 1.57
  children [
                                                                                                                                                                                                                                                                                                                                                                                                                                  nildren |

DEF CSL_Model_Upper Shape

geometry IndexedFaceSet

solid FALSE

creaseAngle 1
                             nildren [
DEF OVector Viewpoint {
  description "View along occlusal vector"
  position 0 0 0
  orientation 1 0 0 0.5
                                                                                                                                                                                                                                                                                                                                                                                                                                                           }
   DEF Lower Transform {
  translation -0.2 0.05 0
  children [
                         coord Coordinate {
                                                                                                                                                                                                                                                                                                                                                                                                                                                                     oord Coordinate, point [ 0.000 0.000 0.000, 0.000, 0.000, 0.000, 0.000, 0.000, 0.000, 0.000, 0.000, 0.000, 0.000, 0.000, 0.000, 0.000, 0.000, 0.000, 0.000, 0.000, 0.000, 0.000, 0.000, 0.000, 0.000, 0.000, 0.000, 0.000, 0.000, 0.000, 0.000, 0.000, 0.000, 0.000, 0.000, 0.000, 0.000, 0.000, 0.000, 0.000, 0.000, 0.000, 0.000, 0.000, 0.000, 0.000, 0.000, 0.000, 0.000, 0.000, 0.000, 0.000, 0.000, 0.000, 0.000, 0.000, 0.000, 0.000, 0.000, 0.000, 0.000, 0.000, 0.000, 0.000, 0.000, 0.000, 0.000, 0.000, 0.000, 0.000, 0.000, 0.000, 0.000, 0.000, 0.000, 0.000, 0.000, 0.000, 0.000, 0.000, 0.000, 0.000, 0.000, 0.000, 0.000, 0.000, 0.000, 0.000, 0.000, 0.000, 0.000, 0.000, 0.000, 0.000, 0.000, 0.000, 0.000, 0.000, 0.000, 0.000, 0.000, 0.000, 0.000, 0.000, 0.000, 0.000, 0.000, 0.000, 0.000, 0.000, 0.000, 0.000, 0.000, 0.000, 0.000, 0.000, 0.000, 0.000, 0.000, 0.000, 0.000, 0.000, 0.000, 0.000, 0.000, 0.000, 0.000, 0.000, 0.000, 0.000, 0.000, 0.000, 0.000, 0.000, 0.000, 0.000, 0.000, 0.000, 0.000, 0.000, 0.000, 0.000, 0.000, 0.000, 0.000, 0.000, 0.000, 0.000, 0.000, 0.000, 0.000, 0.000, 0.000, 0.000, 0.000, 0.000, 0.000, 0.000, 0.000, 0.000, 0.000, 0.000, 0.000, 0.000, 0.000, 0.000, 0.000, 0.000, 0.000, 0.000, 0.000, 0.000, 0.000, 0.000, 0.000, 0.000, 0.000, 0.000, 0.000, 0.000, 0.000, 0.000, 0.000, 0.000, 0.000, 0.000, 0.000, 0.000, 0.000, 0.000, 0.000, 0.000, 0.000, 0.000, 0.000, 0.000, 0.000, 0.000, 0.000, 0.000, 0.000, 0.000, 0.000, 0.000, 0.000, 0.000, 0.000, 0.000, 0.000, 0.000, 0.000, 0.000, 0.000, 0.000, 0.000, 0.000, 0.000, 0.000, 0.000, 0.000, 0.000, 0.000, 0.000, 0.000, 0.000, 0.000, 0.000, 0.000, 0.000, 0.000, 0.000, 0.000, 0.000, 0.000, 0.000, 0.000, 0.000, 0.000, 0.000, 0.000, 0.000, 0.000, 0.000, 0.000, 0.000, 0.000, 0.000, 0.000, 0.000, 0.000, 0.000, 0.000, 0.000, 0.000, 0.000, 0.000, 0.000, 0.000, 0.000, 0.000, 0.000, 0.000, 0.000, 0.000, 0.000, 0.000, 0.000, 0.000, 0.000, 0.000, 0.000, 0.000, 0.000, 0.000, 0.000, 0.000, 0.000, 0.000, 0.000, 0.000, 0.000, 0.000, 0.000, 0.000, 0.000, 0.000, 0.000, 0.000, 0.000, 
                                                                                                                                                                                                                                                                                                                                                                                                                                                                                         0.298 0.000
0.398 0.000
0.497 0.000
0.597 0.000
0.696 0.000
0.796 0.000
0.895 0.000
0.000 0.127
0.000 0.157
                                                                                    0.000,
                                                                                                                                                                                                                                                                                                                                                                                                                                                                                           0.000
                                                                                                                                                                                                                                                                                                                                                                                                                                                                                                                                   0.234
0.322
0.418
                                                                                                                                                                                                                                                                                                                                                                                                                                                                                                                                                                            0.505,
0.617,
0.702,
                                                                                                                                                                                                                                                                                                                                                                                                                                                                                                                                                                           0.702,
0.767,
0.817,
0.854,
0.880,
0.895,
0.817,
0.767,
0.762,
0.617.
                                                                                                                                                                                                                                                                                                                                                                                                                                                                                                                                0.418
0.518
0.622
0.730
0.840
0.953
0.840
0.730
0.622
                                                                                                                                                                                                                                                                                                                                                                                                                                                                                           0.000
0.000
0.000
0.000
                                                                                                                                                                                                                                                                                                                                                                                                                                                                                           0.000
0.099
0.199
0.298
                                                                                                                                                                                                                                                                                                                                                                                                                                                                                           0.398 0.518 0.767,
0.497 0.418 0.702,
0.597 0.322 0.617,
0.696 0.234 0.505,
                                                                                                                                                                                                                                                                                                                                                                                                                                                                                           0.796 0.157 0.345
0.895 0.127 0.000
                                                                                                                                                                                                                                                                                                                                                                                                                                                                              ]
                                                                                                                                                                                                                                                                                                                                                                                                                                                                 }
                                                                                                                                                                                                                                                                                                                                                                                                                                                 appearance Appearance {
  material Material {
    diffuseColor 0 0 1
                                                                                                               0.895 0.953 0.000, 0.880 0.840 0.099, 0.854 0.730 0.199, 0.817 0.622 0.298, 0.767 0.518 0.398, 0.702 0.418 0.497, 0.617 0.322 0.597, 0.505 0.234 0.696, 0.345 0.157 0.796, 0.000 0.127 0.895
                                                                                                                                                                                                                                                                                                                                                                                                                                                              }
                                                                                                                                                                                                                                                                                                                                                                                                                               }
                                                                                                                                                                                                                                                                                                                                                                                                                    ]
                                                                                                                                                                                                                                                                                                                                                                                                        }
                                                                                                                                                                                                                                                                                                                                                                                                         Shape {
                                                                                                                                                                                                                                                                                                                                                                                                                    hape {
    geometry IndexedFaceSet {
        solid FALSE
        coordIndex [
            0, 1, 11, 10, -1,
            1, 2, 12, 11, -1,
            2, 3, 13, 12, -1,
            3, 4, 14, 13, -1,
            4, 5, 15, 14, -1,
            5, 6, 16, 15, -1,
            6, 7, 17, 16, -1,
            7, 8, 18, 17, -1,
            8, 9, 19, 18, -1,
            20, 21, 22, 23, -1
}
                                                                                    }
                                                                        appearance Appearance {
  material Material {
    diffuseColor 1 1 0
                            }
Transform {
  translation 0 0 0.895
  children [
   USE CSL_Model_Lower
                                                                                                                                                                                                                                                                                                                                                                                                                                    coord Coordinate {
                                                                                                                                                                                                                                                                                                                                                                                                                                                point [
1.3 0.850 0.000,
1.3 0.733 0.099,
1.3 0.617 0.199,
1.3 0.500 0.298,
} ]
```

#### Evans – Functional Dental Morphology of Insectivorous Microchiropterans

```
1.3 0.383 0.398,

1.3 0.267 0.497,

1.3 0.150 0.597,

1.3 0.033 0.696,

1.3 -0.083 0.796,

1.3 -0.200 0.895,

-0.9 1.400 0.000,

-0.9 1.283 0.099,

-0.9 1.167 0.199,

-0.9 0.933 0.398,

-0.9 0.933 0.398,

-0.9 0.935 0.583,

-0.9 0.583 0.696,

-0.9 0.467 0.796,

-0.9 0.467 0.796,

-0.9 0.467 0.796,

-0.9 0.350 0.895,

-0.9 0.895,

-0.9 0.895,

-0.9 0.895,
                                                                                                                                                                                                                                          diffuseColor 1 0 0 specularColor 0.5 0 0
                                                                                                                                                                                                              ] }
                                                                                                                                                                                                      Transform {
  translation 1 1 1.5
  rotation 0 1 0 0
  children [
    Shape {
      geometry Cylinder {
      height 0.5
      radius 0.02
    }
}
                                                                                                                                                                                                                             appearance USE VectorAppear
                                                                                                                                                                                            }
       appearance Appearance {
  material Material {
    diffuseColor 0 0 0
    transparency 0.7
}
                                                                                                                                                                                            DEF TS TimeSensor {
  loop TRUE
  cycleInterval 4
                                                                                                                                                                                            DEF LowerMove PositionInterpolator {
                                                                                                                                                                                                  keyValue [
0.2 -0.05 0,
-0.75 0.1875 0,
0.2 -0.05 0,
}
Transform {
  translation 1 -0.5 0.5
  rotation 0 0 1 1.326
  children [
  Transform {
                                                                                                                                                                                                  key [
0, 0.5, 1
                    cansform {
translation 1 1.25 1.5
children [
Shape {
geometry Cone {
height 0.2
bottomRadius 0.08
}
                                                                                                                                                                                                  ]
                                                                                                                                                                                            ROUTE LowerMove.value_changed TO Lower.translation ROUTE TS.fraction_changed TO LowerMove.set_fraction
                                  appearance DEF VectorAppear Appearance
 {
                                        material Material {
```

### **Appendix 3.** Supporting material.

Commentary in *Nature* on Chapter 2.

Manuscript accepted for publication from the International Bat Research Conference, 2001 (Evans *in press*).

# news and views

correspond directly to the permeability of the olivine matrix to metallic-melt percolation, the separation of a core from silicate mantle could happen very quickly in a planetesimal. The high temperatures required could result from the heat produced by the decay of short-lived isotopes present at the birth of the Solar System. More complete calculations of the thermal evolution of growing planetesimals (which include, for example, latent heat of melting, release of gravitational potential energy and impact kinetic energy) point to many sources of heat in the early Solar System that probably led to core formation and magma oceans in many growing planetesimals<sup>5</sup>.

But heating in a static environment may not be the whole answer. Deforming systems can have higher permeabilities than static systems, and impact-induced melting or differential stress may connect isolated melt pockets and produce pools of metal<sup>6</sup> that may then sink through unmelted material. Each of these processes will tend to shorten the interval between accretion and core formation, so core formation should be ubiquitous once an accreting rocky planetesimal reaches a radius of 50–100 km. But then the existence of large bodies that do not seem to have differentiated (including some large asteroids such as Ceres, and Jupiter's moon

Callisto) is puzzling: is there some mechanism that prevented these bodies heating sufficiently to produce a core?

Building on the success of Yoshino  $et\,al.^1$ , future experiments may be able to determine melt connectivity through conductivity measured  $in\,situ$  and monitor dynamically evolving microstructure, such as during deformation or reactions. Synchrotron X-ray microtomography is another promising technique, which enables three-dimensional imaging with resolution approaching  $1\,\mu\mathrm{m}^3$ . These experimental advances will help us to understand the processes that have shaped the Solar System.

Bill Minarik is in the Department of Geology, University of Maryland, College Park, Maryland 20742, and at the Carnegie Institution of Washington, Washington, DC 20015, USA. e-mail: minarik@geol.umd.edu

- Yoshino, T., Walter, M. J. & Katsura, T. Nature 422, 154–157 (2003).
- 2. Yin, Q. et al. Nature 418, 949-952 (2002).
- Kleine T., Münker, C., Mezger, K. & Palme, H. Nature 418, 952–955 (2002).
- von Bargen, N. & Waff, H. S. J. Geophys. Res. 91, 9261–9276 (1986).
- Ghosh, A. & McSween, H. Y. *Icarus* 134, 187–206 (1998).
   Bruhn, D., Growbner, N. & Kohlstedt, D. L. *Nature* 403, 883–886 (2000)
- Roberts, J. J., Tyburczy, J. A., Locke, D., Minarik, W. & Kinney, J. Eos 83, F400 (2002).

**Evolutionary biology** 

# Teeth as tools

Anne Weil

What determines the shapes of mammalian teeth? When tools are designed to cut to the meat of the question, form follows function rather than developmental or evolutionary constraints.

Very different groups of mammals have teeth of similar shapes. One obvious explanation for this is that the greatest efficiency in chewing similar foods is strongly favoured by natural selection. But other reasons could include the constraints imposed in the process of development, or the historical limitations imposed within mammal lineages, and each of these factors might act against or in concert with the demands of optimizing function.

Writing in the *Biological Journal of the Linnean Society* (**78**, 173–191; 2003), Alistair R. Evans and Gordon D. Sanson describe how they have taken an engineer's approach to this question. They have carried out a computer-modelling exercise, designing tools to cut tough substances, and find that the most efficient tools closely resemble the molars of carnivorous and insectivorous mammals. They conclude that in many cases developmental and evolutionary factors have not strongly influenced molar shape, and that function is indeed the primary determinant.

Most mammals use differentiated cheek

teeth for chewing, to divide food into small pieces that can be swallowed easily and digested efficiently. Mammalian teeth are replaced at most once in an individual's lifetime, so exact positioning of them is possible, allowing the cutting edges and points of upper and lower teeth to meet in a precise way. The hands, tongue and facial muscles are variously used to position food between the teeth. Tough (as opposed to brittle or soft) foods are divided by an initial puncture (or punctures), which is then extended into a longer cut. Chewing tough foods can thus be envisaged as a mechanical task in which the teeth act as simple, edged tools.

Evans and Sanson considered six functional factors used by engineers in tool design: sharpness of points; sharpness of blades; the angle between the blade and the substance cut; the angle between the blade and a line perpendicular to the cut; the entrapment of substance between blades; and the movement of substance away from the blade that prevents the implement from becoming clogged up. They considered these

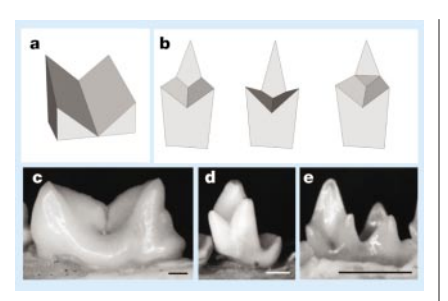


Figure 1 Efficient model cutting tools, and some similarly shaped mammalian cheek teeth. The single-bladed (a) and double-bladed (b) models optimize eight efficiency factors considered by Evans and Sanson. On that evidence, real mammalian molars (c, single-bladed; d, e, double-bladed) may approach a functional ideal. Scale bars, 1 mm.

factors for tools with single blades (which are rectangular in horizontal cross-section, and can resemble a chisel, scissors or a guillotine), as well as for tools with two blades that meet at an angle (which are triangular in cross-section). Not surprisingly, they found that some shapes work better than others. The field of optimal shapes narrowed further when trueto-life criteria were applied: a serial arrangement for the blades, like that of teeth in the jaw, and a degree of lateral as well as vertical movement, as commonly occurs in chewing.

In the case of the single blades, the most efficient is a symmetrical, notched blade (Fig. 1a), strikingly similar to 'carnassial' teeth that have evolved in several mammal lineages (Fig. 1c). The optimal double-bladed models have three points and two high crests (Fig. 1b), forming a 'protoconoid' that closely resembles the trigonid of simple mammalian lower molars (Fig. 1d, e). This notched triangle is a familiar shape to any student of mammalian evolution, because it evolved early and possibly more than once in mammalian history and is present in many living groups, such as opossums and bats.

Evans and Sanson's study did not address the significant role of crushing in chewing. Their modelling therefore did not produce a 'tribosphenic' tooth shape, characterized on the lower molars by a low basin behind the high trigonid (Fig. 1d, e) into which the largest cusp of the upper tooth fits. Tribosphenic molars perform both slicing and crushing functions, and were present in the ancestors of all living mammals. Although Evans and Sanson focused on cutting alone, the superior efficiency of their protoconoid models, and the evident supremacy of function in determining tooth form, may support the arguments of those who believe that tribospheny evolved two or even three times within early mammals.

Anne Weil is in the Department of Biological Anthropology and Anatomy, Duke University, Durham, North Carolina 27708-0383, USA. e-mail: annew@duke.edu

Manuscript accepted for publication in Functional and Evolutionary Ecology of Bats: Proceedings of the 12th International Bat Research Conference. Eds Z. Akbar, G.F. McCracken and T.H. Kunz. New York, Oxford University Press.

# Quantifying Relationships between Form and Function and the Geometry of the Wear Process in Bat Molars

#### Alistair R. Evans

#### **Synopsis**

Despite many important predictive features of the dentition having been described in the literature, many of these have not been given sufficient attention or measured on real teeth. The current study aims to address this by establishing criteria for the choice of useful functional parameters. These are that: 1. they apply to tooth components rather than the entire teeth, where the three main tooth components are cusps, crests and basins; and 2. they have a predictive element, so that changes in the parameter are readily interpretable in terms of changes in function, such as increased force or energy required for the component to function. Parameters that influence the function of cusps and crests in forced crack propagation of tough foods are described in detail: tip and cusp sharpness, cusp occlusion relief, rake angle, crest relief, approach angle, food capture, edge sharpness and fragment clearance. All of the parameters were measured for the upper molars of the microchiropteran *Chalinolobus gouldii*. Many of the parameters did not change significantly with heavy wear, pointing to geometrical and design characteristics for the maintenance of shape with wear in the dilambdodont tooth form.

#### 1.1. Introduction

Molar function as a means of understanding animal diets has received considerable attention in recent years (e.g. Fortelius, 1985; Kay, 1984), and such work aids in the interpretation of the teeth of both extant and fossil animals. This view is supported by demonstrations of the importance of the dentition to the nutritional ecology of an animal (Lanyon and Sanson, 1986; McArthur and Sanson, 1988; Pérez-Barberia and Gordon, 1998).

Examining teeth as tools for the breakdown of food aids in analyzing tooth function (Lucas, 1979). As for any tool, the shape of a tooth is a significant determinant of its function, and its examination should be revealing. The object of functional dental studies should be to comprehend the interaction between tooth shape and function, allowing inferences of dental function and predictive measures of tooth function from morphology.

However, previous analyses have not revealed important factors that relate shape to function, or the quantification of relevant aspects of shape has not been carried out, sometimes because of the difficulty of doing so with traditional methods. The aim of this study is to closely examine tooth shape and function using engineering principles and computer modelling. My particular focus is the dilambdodont tooth form, possessed by most microchiropterans and some insectivorans, but the principles and findings can equally be applied to similar tooth forms (e.g. zalambdodont, tribosphenic).

Past studies of variation in dilambdodont-like (in particular, primate) tooth shape has been quantified by measuring changes in the relative or absolute lengths of the crests (Kay, 1975; Kay *et al.*, 1978), or the sum of all main crest lengths on a tooth standardized for tooth length or area (Strait, 1993). Another approach by Freeman (1988) was to analyze

tooth structure by comparing the relative proportions of the palate or tooth row dedicated to molars, the dilambdodont ectoloph, premolars, canines or incisors. However, none of the characters in these past studies adequately describes the relationship between the complex tooth morphology and the way it works.

Consideration of dental function is complicated by tooth wear. Change in the shape of teeth is likely to have an effect on their function. The common assumption is that the wear on a mammal's tooth results in an alteration of shape, and therefore function, of the tooth. However, wear may or may not change the shape of teeth. The teeth of most herbivores, such as the selenodont molars of bovids, are essentially non-functional when they first erupt. Moderate wear by tooth-tooth or tooth-food contact is required to transform the tooth shape into its functional configuration (Janis and Fortelius, 1988; Luke and Lucas, 1983). Beyond this point, shape, and therefore most probably function, is static despite the large amount of wear that occurs on the teeth during most of the remainder of the animal's life. Eventually these high-crowned teeth stop growing and the functional form rapidly degrades.

For dilambdodont-like teeth, the relationship between wear and shape has been largely neglected. The pre-formed occlusal morphology is presumed to be fully functional, requiring no wear for the tooth to become operational (Luke and Lucas, 1983). It is implicitly assumed that wear adversely affects the function of the teeth; however, little substantive data support this proposition.

Functional occlusion of dilambdodont molars is complex, because precise alignment of the many interlocking crests and cusps is required. The possibility of malocclusion due to wear-induced changes has not been addressed in studies of this tooth form.

There may be design features of dilambdodont teeth that minimize changes in tooth shape during the wear process, thereby maintaining tooth shape and function as well as proper occlusion. Such features are common in herbivore teeth (such as the vertical enamel pillars of the molars; Janis and Fortelius, 1988) but have not been adequately described in dilambdodont teeth. Most functional studies have examined only unworn or slightly worn molars, as the measures of function used are inadequate to describe the changes in function with wear.

Ungar and Williamson (2000), in one of the few studies on the effect of wear on tooth shape, also recognised this issue. Their use of surface reconstruction and topographic software for gorilla teeth shows the potential for such techniques. However, the majority of the quantities in their study relates to changes in the tooth shape as a whole (e.g. slope, surface area of whole tooth, and topographic aspect), and are difficult to explicitly relate to any specific change in function. The teeth also differ from those under consideration here in that precise alignment may not be as important.

#### 1.2. Functional Parameters

#### 1.2.1. Criteria for Functional Parameters

Two different types of dental measurements that have been used as surrogates of function can be distinguished. The first may be seen to relate to the quantity of food processed. For example, shear length measurements (Kay, 1975; Kay *et al.*, 1978; Strait, 1993) and relative areas of talonid/trigonid basins (Kay, 1975) are of this type. They approximate the amount of food processed or the relative allocation of the dentition to distinct types of food processing, such as 'shearing' or 'grinding'. These characteristics largely reflect the size of the features rather than their shape.

The second type of measure specifically relates the shape of tooth components to their function. These are interpretable in terms of differences in function, such as the amount of force or energy required, and describe the shape of the features rather than primarily their size. In lineages showing a decrease in the emphasis on shearing, as shown by decreases in *size* of crests or the trigonid basin, there may be concurrent modifications in the *shape* of the crest. The latter will have an equal if not greater effect on the crest's function.

However, not all measures of shape will be useful in determining function. We can suggest that firstly, the parameter should relate to specific components of the teeth rather than the shape of the whole tooth surface at once. Variables relating to the shape of the entire tooth are difficult, if not impossible, to interpret. Dilambdodont teeth can be seen as combinations of three different types of tools, or tooth components: cusps, crests and basins. These tools may not be independent of one another; for example, cusps often occur at the ends of crests, but it is a useful distinction. Analysis of tooth function is greatly simplified, and arguably more powerful, if the tooth is considered a conglomerate of tool components, each of which can be more successfully analyzed separately.

The parameter must be predictive, so that changes in the parameter are clearly testable in terms of changes in function. Most often, this should be in terms of the force and/or energy that will be required for the component to function. The comparison may be quantitative or qualitative, but the direction of functional change should be clear from the change in the functional parameter.

Parameters that fulfill these aspects will be useful in comparing unworn molars between individuals of the same species, of individuals of species with different diets, and of unworn and worn molars of the same species.

#### 1.2.2. Functional Parameters

Several characters of tooth component shape with a predictive capacity can be found in the literature on engineering tools (e.g. Nee, 1998; Ostwald and Muñoz, 1997) and theoretical discussions of tooth shape and function (e.g. Frazzetta, 1988; Lucas, 1979, 1982; Lucas and Luke, 1984; Osborn and Lumsden, 1978). The function of the cusps and crests of dilambdodont teeth can be analyzed with reference to the following nine functional parameters: tip sharpness, cusp sharpness, cusp occlusion relief, edge sharpness, rake angle, crest relief, approach angle, capture area and fragment clearance. These appear to cover all major aspects of shape as they relate to the function of cusps and crests.

Most of these have not been measured in teeth, in part because of the technical difficulty. Recently developed techniques allow the reconstruction and visualization of occluding three-dimensional tooth surfaces (Evans *et al.*, 2001; Jernvall and Selänne, 1999; Ungar and Williamson, 2000). These techniques permit the three-dimensional measurement of important shape parameters that were previously difficult (e.g. curvature of tooth surface) with accuracy and relative ease, irrespective of wear state.

The third major topographic feature of teeth is basins. Quantification and interpretation of the function of basins is difficult. An increase in the size of a basin will most likely lead to a greater amount of food processed, but the force and energy required for such processing is likely to increase. A greater understanding of the processes of food division carried out in a basin is necessary. Functional parameters for basins will not be dealt with in this paper.

#### Cusps

Cusps are important for initial penetration of food, either alone (in puncture-crushing) or followed by crest-against-crest contact in occlusion. I will examine the effect of cusp and crest shape on the breakdown of tough foods, which are those that resist crack propagation and do not undergo brittle fracture (Strait, 1993).

**Tip Sharpness** – The stress required for a cusp to initiate a crack in food will depend on the surface area of contact between the cusp and food. Tip sharpness of a cusp is measured as the radius of curvature at its tip, so a cusp with higher tip sharpness has a smaller radius of curvature (Evans and Sanson, 1998; Freeman and Weins, 1997). A smaller radius of curvature will give a smaller area of contact (for a given elastic modulus of the food), and so produce a higher stress in the food (Lucas, 1982) and allow crack initiation with lower force.

Tip sharpness has been measured in different ways for human cusps by Lucas (1982), bat canines by Freeman and Weins (1997), and lemur molars by Yamashita (1998). Empirical tests on several foods by Freeman and Weins (1997) and Evans and Sanson (1998) demonstrated that higher tip sharpness decreases the force necessary to penetrate food.

Cusp Sharpness – Once a cusp has initiated a crack in a tough food, it must be continually driven into the food to sustain propagation of the crack. The force and energy required will in part depend on the volume of the tool and the amount of food displaced. This can be quantified as 'cusp sharpness', the volume of the cusp at increasing distances from the tip (Evans and Sanson, 1998). A cusp with higher cusp sharpness has a smaller cusp volume for a given distance from the tip. For a cusp with high cusp sharpness (smaller volume), fewer bonds in the material will be broken or strained when it is driven through a tough food, and so will require a lower force and less energy.

This parameter has only been measured for artificial cusps used in force testing (Evans and Sanson, 1998), where cusps with lower cusp sharpness required lower force and energy to penetrate food.

**Cusp Occlusion Relief** – In occlusion, cusps often move into a valley between two cusps or crests. Friction between the adjacent tooth surfaces, and food caught between the surfaces that push apart occluding teeth, will increase the force required to maintain tooth contact (also see below under 'Relief of Crests'). Relief behind the point at which the cusp occludes (cusp occlusion relief) can reduce the friction and the tendency for occluding teeth to be pushed apart.

#### Crests

Crests are important in dividing food through 'cutting', which can be defined as dividing a tough material using a blade or crest, or 'forced crack propagation using a blade'. Crests can function either singly, such as on the side of a tooth when driving through food (e.g. some bat canines; Freeman, 1992), or in occluding pairs in an analogous manner to a guillotine, the latter particularly during chewing.

**Edge Sharpness** – The edge sharpness of a crest is the radius of curvature of the crest edge. A crest with a smaller radius of curvature will have higher edge sharpness, analogous to the 'tip sharpness' of a point except the maximum curvature is extended in one dimension. Higher edge sharpness will decrease the area of contact and so increase stress in the food.

Edge sharpness has been most extensively discussed by Popowics and Fortelius (1997), where its functional implications were described in some detail and measured for a range of mammals. It was also measured for bat canines by Freeman (1992).

Rake of Crests – The angle between the leading surface of a tool and a line perpendicular to the direction of tool movement is termed the rake angle (Figure 1.1a). A crest with a positive rake angle has its leading face angled away from the material to be divided (Figure 1.1b). Compared to a crest with negative rake, less force is required to fracture food for a number of reasons. First, a negative rake crest must displace more material than one with positive rake, and so requires greater force. Second, the surface area of contact between the food and a crest with negative rake will be greater, and so a positive rake crest will achieve higher stress for a given force. Third, the rake angle affects the force required to keep occluding crests together. When a rake surface contacts food, the crest will tend to be pushed in the direction perpendicular to the surface. Therefore, crests with a negative rake angle will be pushed apart when food is trapped between them, whereas a positive rake angle helps to direct a crest towards its opposing crest.

The importance of rake angle is widely recognized in engineering (e.g. Ostwald and Muñoz, 1997) and has been discussed in regard to teeth (Osborn and Lumsden, 1978). However, rake angle has never been measured for the crests of the multitude of tooth forms in which it is important.

**Relief of Crests** – The space between the direction of tooth movement and the trailing surface of the crest is called relief (Figure 1.1a). Relief behind crests (also called 'clearance' in some engineering texts) reduces the effect of crests being forced apart by material caught between them, which would require greater force to maintain the proximity of the crests. It also reduces crest-against-crest friction and friction attributable to material caught between the crests. Once sufficient relief is attained, no further benefit is achieved by increasing the angle; e.g. between 4° and 7° is best for sharp metal or glass sectioning blades shearing plant material for histology sections (Atkins and Vincent, 1984).

Relief is important in the design of machine cutting tools (e.g. Nee, 1998; Ostwald and Muñoz, 1997), and has been noted by some workers in dental morphology (Osborn and Lumsden, 1978). Nonetheless, measurements of relief of crests have not been taken for real teeth.

A number of different aspects relate to the amount of relief for a crest. The first is that many teeth and tools, either by design or following wear, have an area of no relief immediately behind the cutting edge (Figure 1.1a). This is called the 'wear land' (Nee, 1998; Ostwald and Muñoz, 1997). In teeth, it is the attrition facet – a planar surface where tooth-tooth contact occurs. The size of the wear land in section is then the width of the attrition facet on the crests. Second is the volume of space behind a cusp, which represents the amount of space into which food could be directed, and is estimated by the height of the crest above the adjacent valley. Third is the relief angle behind the wear land, which is the angle between the trailing surface and the direction of tooth movement (Fig. 1a).

Approach Angle – The approach angle of a crest is the angle between the long axis of the crest and a line perpendicular to the direction of movement (Figure 1.1c). The mechanical advantage (MA) of a crest will depend on the approach angle ( $\alpha$ ) of the crest, where MA =  $1/\cos(\alpha)$  (Abler, 1992; Evans and Sanson, 1998), so that a larger approach angle will have a greater mechanical advantage. The approach angle of crests will affect the 'point cutting' of the system, which occurs when the long axes of two occluding crests are not parallel. As a result only one point (or two points if at least one crest is concave) meets at a time rather than the entire length of the crest (Figure 1.1c). Point cutting will decrease the amount of crest surface area in contact at any one time (if there is a wear land or no relief), which will increase pressure and decrease friction between the crests. Point cutting does not imply that the crest only fractures food at one point at a time, as fracture of food will occur along the entire length of the crest in contact with food (Abler, 1992).

This is like a pair of scissors cutting thick rubber: the majority of the material is cut by the crests before the cutting points come into close proximity.

Approach angle has been discussed by a few authors in reference to teeth (Abler, 1992; Evans and Sanson, 1998), and point cutting by others (e.g. Crompton and Sita-Lumsden, 1970; Seligsohn, 1977). Approach angle has not been measured on real teeth but the effect of approach angle on the required occlusal force has been measured for sharp blades (Abler, 1992) and facsimile tooth crests (Worley and Sanson, 2000).

**Food Capture** – It is advantageous to 'trap' the food between crest edges, preventing it from escaping off the ends of the crests and therefore being incompletely divided. Crests can be concave so that the ends meet first, enclosing the food before it is then divided. This is advantageous for foods with a high Poisson's ratio (e.g. over 1.0; Lucas and Luke, 1984) which may be particularly hard to trap between crests. A crest may be notched or curved (a sharp or rounded concavity respectively). The amount of food trapped can be estimated by the area enclosed by one crest. The importance of food capture has been recognized for many teeth (such as carnassial and dilambdodont; Abler, 1992; Freeman, 1979; Savage, 1977).

**Fragment Clearance** – The function of crests will improve if the fractured material is directed away from the crests and off the rake surfaces. If material is trapped on rake surfaces, it may prevent fracture of any remaining food between the crests. Where there is insufficient space into which fractured material can flow, food may be compressed between opposing tooth structures and prevent the occlusion of crests. It is advantageous to create flow channels and exit structures through which food can flow away from the crests.

The movement and clearance of food has been given some attention in the dental literature: food movement was incorporated into Rensberger's (1973) models of herbivore teeth, Seligsohn (1977) discussed it in terms of food escapement, Sanson (1980) as sluiceways and Frazzetta (1988) as clearance provided by 'gullets' between successive teeth.

#### 1.3. Methods

Molars of 20 specimens of an insectivorous microbat, Gould's Wattled Bat *Chalinolobus gouldii*, were examined. This species is common in Australia, is approximately 10-18 g in weight, and its upper second molar is 1.2-1.4 mm in length. The methods for digitization of tooth surfaces follow Evans *et al.* (2001); briefly, casts of the upper second molar were stained with eosin and imaged using fluorescence confocal microscopy. Geographic information systems (GIS) software (Surfer v6.04, Golden Software Inc.) and algorithms written by the author were used to calculate the parameters. The main two cusps (paracone and metacone) and the four ectoloph crests (pre- and postparacrista and pre- and postmetacrista) of these teeth were measured for the nine functional parameters for cusps and crests respectively.

Specimens of three gross wear states (10 unworn or lightly worn, five moderately worn and five heavily worn) were measured. Wear states were determined as follows (see Fig. 2): unworn or lightly worn – only a small amount of wear had occurred along the crests, usually apparent as attrition facets on the relief surfaces; moderate wear — approximately a quarter to a half of the rake surface is exposed dentine; heavy wear — the majority of the rake surface is exposed dentine, and the height of the cusps has been substantially reduced.

Occlusion of the upper and lower molars was simulated using Virtual Reality Modeling Language (VRML) reconstructions of the molar tooth row with the VRML browser CosmoPlayer 2.1 (Computer Associates, Inc.), allowing the occlusion of unworn

and worn molars to be compared (Evans et al., 2001). Examination of the occlusal relations of teeth is only an exploratory study.

# 1.4. Results

The results of measurements of the nine functional parameters for one cusp, the metacone, and one crest, the postmetacrista, for low and high wear states are given in Table 1.1. In terms of capture area and relief angle, there was no significant difference between the unworn and highly worn molars. The only parameter to display a large difference that would decrease the force and/or energy for components to function was approach angle. Moderately increased force and/or energy for function would be required for cusp sharpness, edge sharpness and wear land, and large increases for tip sharpness, cusp occlusion relief, rake angle, relief volume and fragment clearance.

Computer reconstructions of the upper and lower molars in occlusion for several wear states showed that occlusion is maintained between crests despite heavy wear. Where crest shape and arrangement were altered due to wear, corresponding changes in opposing crests meant that proper alignment of crests was retained.

#### 1.5. Discussion

#### 1.5.1. Functional Parameters

Changes in the nine functional parameters of crests and cusps measured in this study have a predictable influence on the function of the tooth components. Only one (approach angle) showed significant improvement, where the increased angle improved the mechanical advantage of the crest. The majority of parameters showed no significant change after heavy wear. However, dramatic change was evident in some. A change of 55° in rake angle is very likely to have a large effect on the force required for the crest to function (where a significant difference in forces required was found between blades with rake angles of 0° and 30°; N. Aranwela, personal communication). It would be expected that the overall effectiveness of these teeth would decrease with wear, requiring more force and energy to divide tough food. This is the first demonstration of changes in measurable tooth features that predict an increase in force or energy for a tooth to function (decreased tooth 'efficiency'). Previously, this had usually only been assumed.

There are some independent lines of evidence that support this prediction. Carraway *et al.* (1996) and Verts *et al.* (1999) showed that insectivorous shrews increase the efficiency of their jaw mechanics with age, increasing the available bite force. It was only presumed in these studies that worn teeth were less effective at dividing food.

Wear scratches on the enamel relief surface of crests appear to be deeper or wider at higher wear states of *C. gouldii*, or are at least more visible (personal observation). Deeper or wider scratches would likely require a greater force to produce, supporting the proposal that greater force is necessary for worn teeth to function (Teaford, 1988; Ungar and Spencer, 1999). Alternative explanations for such a difference, such as change in enamel structure with increased depth, may also account for this observation.

There are some important implications of decreased tooth efficacy. Greater energy and possibly time (in number of chews) must be expended in dividing food, reducing the amount available for other important biological processes, including food searching and gathering, and social interactions. The presumption of Carraway *et al.* (1996) was that older animals must switch to a diet of softer food. Their search for such a dietary shift assumes that the worn teeth have retained the ability to divide 'soft' food; however, worn teeth may be equally ineffective in dividing 'soft' and 'hard' foods. Increases in efficiency

of jaw mechanics would then be more important, as were found to occur in shrews (Verts et al., 1999).

In principle, all of the nine parameters may vary independently, although there is a high dependence between some variables. For example, allowing food capture requires a change in approach angle of the crest to make it concave. It cannot be assumed that a single quantitative measure, taken either individually from teeth or as a complex combination of any of the functional parameters discussed here, can be used to predict or represent the function of the entire tooth. This is compounded by the presence of multiple components on teeth, where their number, arrangement and shape will vary. This should not be seen as a failure of functional morphology, rather as an advance in our ability to comprehend the full complexity of tooth shape and function. However, if it were shown that the majority of the variables alter in synchrony in real teeth, an estimate of the change in effectiveness of the teeth using one or several parameters as surrogates for a given tooth form may be possible.

# 1.5.2. Shape and Function Maintenance During Wear

Despite the noticeable change in tooth shape that occurs due to wear, many of the functional features retain a reasonably advantageous state with wear. The design of certain features of these teeth means that the teeth retain many aspects of good functional shape longer than expected according to the traditional view of dilambdodont teeth as ineffective in coping with wear. This may be either through particular design characteristics of teeth or through the geometry of the wear process.

**Food capture** – A concave crest is able to maintain its shape to some degree merely through its use. If the entire crest cavity is filled with food and all of the food is divided, then the middle of a concave crest will divide more material than the ends, and may be under greater pressure (or certainly under pressure for a longer time) from the food. Wear on the rake surface of a crest by food abrasion will be at least partly determined by the amount of material it divides and by the pressure exerted on the surface, so greater wear will occur in the middle compared to the ends. Relative wear at positions along a crest will also be influenced by the thickness of the enamel along a crest. Thinner enamel on the middle of crests compared to the ends will cause the middle to wear more rapidly compared to the ends. The enamel appears thicker towards the lingual end of each ectoloph crest in the specimens of *C. gouldii* examined (personal observation). The greater amount of dentine that must be worn at the buccal end of the crests would have the same effect as the thicker enamel on the other end, reducing the rate at which the height of the buccal end of the crest is decreased. Both of these parameters will preserve or possibly even increase the concavity of the crest following wear.

Cusp sharpness – Wear in the center of the crests on two-crested cusps (such as the paracone and metacone) maintains higher cusp sharpness to some extent. Thicker enamel on the rounded, lingual faces of the cusps will preserve the height of the cusp, while wear on the rake surface of the adjoining crests will reduce the volume of the cusp, maintaining high cusp sharpness. To a limited extent, this occurs on the upper molar cusps, where in some instances a highly worn cusp has higher cusp sharpness than moderately worn cusps.

**Relief** – The incidence and proportion of wear on the rake and relief surfaces will influence the amount of relief of a crest (Figure 1.3a). Wear on the relief surface only would cause the majority of the relief to be removed, producing a wide wear land. If the rake surface is also worn, then this wear land will be removed and relief retained. If sufficient wear occurs on both the rake and the relief surfaces, then relief will be

maintained. *Chalinolobus gouldii* molars have high degrees of wear on the rake surface relative to wear on relief surface, reducing the wear land on the relief surface and maintaining relief (Figure 1.2).

A non-zero relief angle can be maintained during wear when the relief surface is straight, and will even increase given a convex curvature of the relief surface (Figure 1.3b). Relief surfaces, particularly those on the lingual side of upper molar cusps, are either straight or slightly convex, so that the relief angle is maintained as tooth wear progresses.

**Edge sharpness** – The edge sharpness of crests is also maintained to some extent during wear. This is likely to be attributable to both the enamel thickness and microstructure. A thin enamel edge will wear more slowly than the surrounding dentine, resulting in a ridge of enamel higher than the dentine (as occurs in many herbivore teeth). Enamel prisms in the relief surface of crests are arranged parallel to the rake surface, so that when prisms are removed by wear a sharp edge is retained (Stern *et al.*, 1989).

Capture area and relief can be maintained to some extent purely by geometrical relations of wear, a point that has never been noted when the effect of wear on teeth has been considered. Maintenance of features can be achieved or aided by specific design considerations, such as enamel thickness and prism structure. In addition, these features point to controlled wear. Wear cannot be avoided, but teeth can be shaped to dictate which regions of the tooth wear more than others. The utilization of cusps and crests, and distribution and structure of enamel, can encourage wear of particular areas, allowing function to be maintained.

Molar occlusion – For proper occlusion to be maintained, the shape of the crest edges when viewed along the vector of tooth movement must be the same for the upper and lower molars (Figure 1.4). The shape of the crest profile can be reduced to three features that must correspond between the upper and lower molars: the projected two-dimensional lengths of crests; the angle of the crests; and curvature at the junction between crests. In principle, all of these could be altered to different extents and at various rates during tooth wear. Therefore, it is not guaranteed that worn upper and lower molars maintain occlusion. In occlusal view, the tips of cusps and the junctions of crests of unworn teeth are relatively pointed, approximating a 'W' shape. With wear, the upper molar crests are now closer to the base of the paracone and metacone, where it is slightly wider than in the unworn state. Also, the two-dimensional crest length is reduced (Figure 1.4). Concurrent changes in the occluding features must also occur in the lower molar: if this were not the case, the cusp will not fit into its embrasure, or the crests on both sides of a junction will not meet.

#### 1.6. Conclusions

Functional characteristics elaborated and quantified here allow me to determine changes in function with change in shape resulting from wear in dilambdodont or tribosphenic teeth. This has not been possible before.

Wear is a significant process that must be taken into consideration when examining tooth form and function. It must have been a highly influential selective force in shaping teeth during evolution. Wear is an additional constraint on tooth shape that may not be inherent in unworn tooth function, and should be considered when discussing the apparent function of unworn teeth. Although not as adapted as some other tooth forms to cope with high wear and maintain function, there are significant features of dilambdodont and tribosphenic teeth that mean that some functional features are retained with wear.

Despite their high complexity in shape and relations between features of opposing teeth, dilambdodont teeth are able to maintain functional occlusion through many wear

states. New approaches and technology now make it possible to study the design of teeth in greater detail and how the design ensures the shapes of the upper and lower crests remain in tandem despite wear.

# 1.7. Acknowledgments

I am extremely grateful to Assoc. Prof. Gordon Sanson for discussions on the topics presented here and for advice on drafts of this paper. I also thank Gudrun Arnold, Deb Archer, Nuvan Aranwela and Betsy Dumont for comments on earlier drafts, and to Professor Patricia Freeman and an anonymous reviewer for many helpful suggestions to improve the paper. Thanks to Lina Frigo of Melbourne Museum for loan of specimens.

#### 1.8. Literature Cited

Abler, W. L. 1992. The serrated teeth of tyrannosaurid dinosaurs and biting structures in other animals. Paleobiology, 18: 161-183.

Atkins, A. G., and J. F. V. Vincent. 1984. An instrumented microtome for improved histological sections and the measurement of fracture toughness. Journal of Materials Science Letters, 3: 310-312.

Carraway, L. N., B. J. Verts, M. L. Jones, and J. O. Whitaker, Jr. 1996. A search for age-related changes in bite force and diet in shrews. American Midland Naturalist, 135: 231-240.

Crompton, A. W., and K. Hiiemae. 1970. Molar occlusion and mandibular movements during occlusion in the American opossum, *Didelphis marsupialis* L. Zoological Journal of the Linnean Society, 49: 21-47.

Crompton, A. W., and A. Sita-Lumsden. 1970. Functional significance of the therian molar pattern. Nature, 227: 197-199.

Evans, A. R., I. S. Harper, and G. D. Sanson. 2001. Confocal imaging, visualization and 3-D surface measurement of small mammalian teeth. Journal of Microscopy, 204: 108-119.

Evans, A. R., and G. D. Sanson. 1998. The effect of tooth shape on the breakdown of insects. Journal of Zoology, 246: 391-400.

Fortelius, M. 1985. Ungulate cheek teeth: developmental, functional, and evolutionary interrelations. Acta Zoologica Fennica, 180: 1-76.

Frazzetta, T. H. 1988. The mechanics of cutting and the form of shark teeth (Chondrichthyes, Elasmobranchii). Zoomorphology, 108: 93-107.

Freeman, P. W. 1979. Specialized insectivory: beetle-eating and moth-eating molossid bats. Journal of Mammalogy, 60: 467-479.

Freeman, P. W. 1988. Frugivorous and animalivorous bats (Microchiroptera): dental and cranial adaptations. Biological Journal of the Linnean Society, 33: 249-272.

Freeman, P. W. 1992. Canine teeth of bats (Microchiroptera): size, shape and role in crack propagation. Biological Journal of the Linnean Society, 45: 97-115.

Freeman, P. W. 1998. Form, function and evolution in skulls and teeth of bats. Pp. 140-156, In: Bat Biology and Conservation. (T. H. Kunz, and P. A. Racey, eds.). Smithsonian Institution Press, Washington.

Freeman, P. W., and W. N. Weins. 1997. Puncturing ability of bat canine teeth: the tip. Pp. 225-232, In: Life Among the Muses: Papers in Honor of James S. Findley. (T. L. Yates, W. L. Gannon, and D. E. Wilson, eds.). The Museum of Southwestern Biology, Albuquerque.

- Janis, C. M., and M. Fortelius. 1988. The means whereby mammals achieve increased functional durability of their dentitions, with special reference to limiting factors. Biological Review, 63: 197-230.
- Jernvall, J., and L. Selänne. 1999. Laser confocal microscopy and geographic information systems in the study of dental morphology. Palaeontologia Electronica, 1: 12 pp., 219 kb. http://palaeo-electronica.org/1999 1/confocal/issue1 99.htm.
- Kay, R. F. 1975. The functional adaptations of primate molar teeth. American Journal of Physical Anthropology, 43: 195-216.
- Kay, R. F. 1984. On the use of anatomical features to infer foraging behavior in extinct primates. Pp. 21-53, In: Adaptations for foraging in non-human primates: contributions to an organismal biology of prosimians, monkeys and apes. (P. S. Rodman, and J. G. H. Cant, eds.). Columbia University Press, New York.
- Kay, R. F., R. W. Sussman, and I. Tattersall. 1978. Dietary and dental variations in the Genus *Lemur*, with comments concerning dietary-dental correlations among Malagasy primates. American Journal of Physical Anthropology, 49: 119-128.
- Lanyon, J. M., and G. D. Sanson. 1986. Koala (*Phascolarctos cinereus*) dentition and nutrition. II. Implications of tooth wear in nutrition. Journal of Zoology, 209: 169-181.
- Lucas, P. W. 1979. The dental-dietary adaptations of mammals. N. Jb. Geol. Paläont. Mh., 1979: 486-512.
- Lucas, P. W. 1982. Basic principles of tooth design. Pp. 154-162, In: Teeth: function, form and evolution. (B. Kurtén, ed.). Columbia University Press, New York.
- Lucas, P. W., and D. A. Luke. 1984. Chewing it over: basic principles of food breakdown. Pp. 283-301, In: Food acquisition and processing in primates. (D. J. Chivers, B. A. Wood, and A. Bilsborough, eds.). Plenum Press, New York.
- Luke, D. A., and P. W. Lucas. 1983. The significance of cusps. Journal of Oral Rehabilitation, 10: 197-206.
- McArthur, C., and G. D. Sanson. 1988. Tooth wear in eastern grey kangaroos (*Macropus giganteus*) and western grey kangaroos (*Macropus fuliginosus*), and its potential influence on diet selection, digestion and population parameters. Journal of Zoology, 215: 491-504.
- Mills, J. R. E. 1966. The functional occlusion of the teeth of Insectivora. Journal of the Linnean Society (Zoology), 46: 1-25.
- Nee, J. G. 1998. Fundamentals of Tool Design. Society of Manufacturing Engineers, Dearborn.
- Osborn, J. W., and A. G. S. Lumsden. 1978. An alternative to "thegosis" and a re-examination of the ways in which mammalian molars work. N. Jb. Geol. Paläont. Abh., 156: 371-392.
- Ostwald, P. F., and J. Muñoz. 1997. Manufacturing Processes and Systems. John Wiley & Sons, New York.
- Pérez-Barberia, F. J., and I. J. Gordon. 1998. The influence of molar occlusal surface area on the voluntary intake, digestion, chewing behaviour and diet selection of red deer (*Cervus elaphus*). Journal of Zoology, 245: 307-316.
- Popowics, T. E., and M. Fortelius. 1997. On the cutting edge: tooth blade sharpness in herbivorous and faunivorous mammals. Annales Zoologici Fennici, 34: 73-88.
- Rensberger, J. M. 1973. An occlusal model for mastication and dental wear in herbivorous mammals. Journal of Paleontology, 47: 515-528.
- Sanson, G. D. 1980. The morphology and occlusion of the molariform cheek teeth in some Macropodinae (Marsupialia: Macropodidae). Australian Journal of Zoology, 28: 341-365.

- Savage, R. J. G. 1977. Evolution in carnivorous mammals. Palaeontology, 20: 237-271.
- Seligsohn, D. 1977. Analysis of species-specific molar adaptations in strepsirhine primates. Contributions to Primatology, Volume 11. (F. S. Szalay, ed.). S. Karger, Basel.
- Stern, D., A. W. Crompton, and Z. Skobe. 1989. Enamel ultrastructure and masticatory function in molars of the American opossum, *Didelphis virginiana*. Zoological Journal of the Linnean Society, 95: 311-334.
- Strait, S. G. 1993. Molar morphology and food texture among small-bodied insectivorous mammals. Journal of Mammalogy, 74: 391-402.
- Teaford, M. F. 1988. A review of dental microwear and diet in modern mammals. Scanning Microscopy, 2: 1149-1166.
- Ungar, P., and M. Williamson. 2000. Exploring the effects of tooth wear on functional morphology: a preliminary study using dental topographic analysis. Palaeontologia Electronica, 3: 18 pp., 752 kb. http://palaeo-electronica.org/2000 1/gorilla/issue1 00.htm.
- Ungar, P. S., and M. A. Spencer. 1999. Incisor microwear, diet, and tooth use in three Amerindian populations. American Journal of Physical Anthropology, 109: 387-396.
- Verts, B. J., L. N. Carraway, and R. A. Benedict. 1999. Body-size and age-related masticatory relationships in two species of *Blarina*. Prairie Naturalist, 31: 43-52.
- Worley, M., and G. Sanson. 2000. The effect of tooth wear on grass fracture in grazing kangaroos. Pp. 583-589, In: Proceedings of the Plant Biomechanics Meeting. Freiburg-Badenweiler. (H.-C. Spatz, and T. Speck, eds.). Georg Thieme Verlag.
- Yamashita, N. 1998. Functional dental correlates of food properties in five Malagasy lemur species. American Journal of Physical Anthropology, 106: 169-188.

**Table 1.1.** Measurements for the nine functional parameters for cusp and crest function considered in the current paper for the upper second molar of *Chalinolobus gouldii*. Low wear/High wear: the mean and S.E. (or median for qualitative data; qual) for the metacone and postmetacrista at low and high wear states.

Component	Parameter		Low wear	High wear
Metacone	Tip sharpness (μm)		$25.6 \pm 2.6$	$50.3 \pm 8.0$
	Cusp sharpness to $100 \mu m (10^3 \mu m^3)$		$1084.6 \pm 118.0$	$1067.6 \pm 280.7$
	Cusp occlusion relief of trigon groove		$129.7 \pm 11.5$	$33.2 \pm 5.7$
	(µm)			
Postmetacrista	Edge sharpness (µm)		$14.4 \pm 2.1$	$24.4 \pm 3.0$
	Rake angle (°)		$14.6 \pm 5.4$	$-40.8 \pm 6.0$
	Relief:	Wear land (qual)	Small	Moderate
		Volume (qual)	Large	Moderate
		Angle (qual)	Small	Small
	Approach angle (°) Food capture (10 <sup>3</sup> μm <sup>2</sup> ) Fragment clearance (qual)		$37.8 \pm 0.8$	$50.0 \pm 1.5$
			$63.5 \pm 3.1$	$78.9 \pm 13.5$
			High	Low

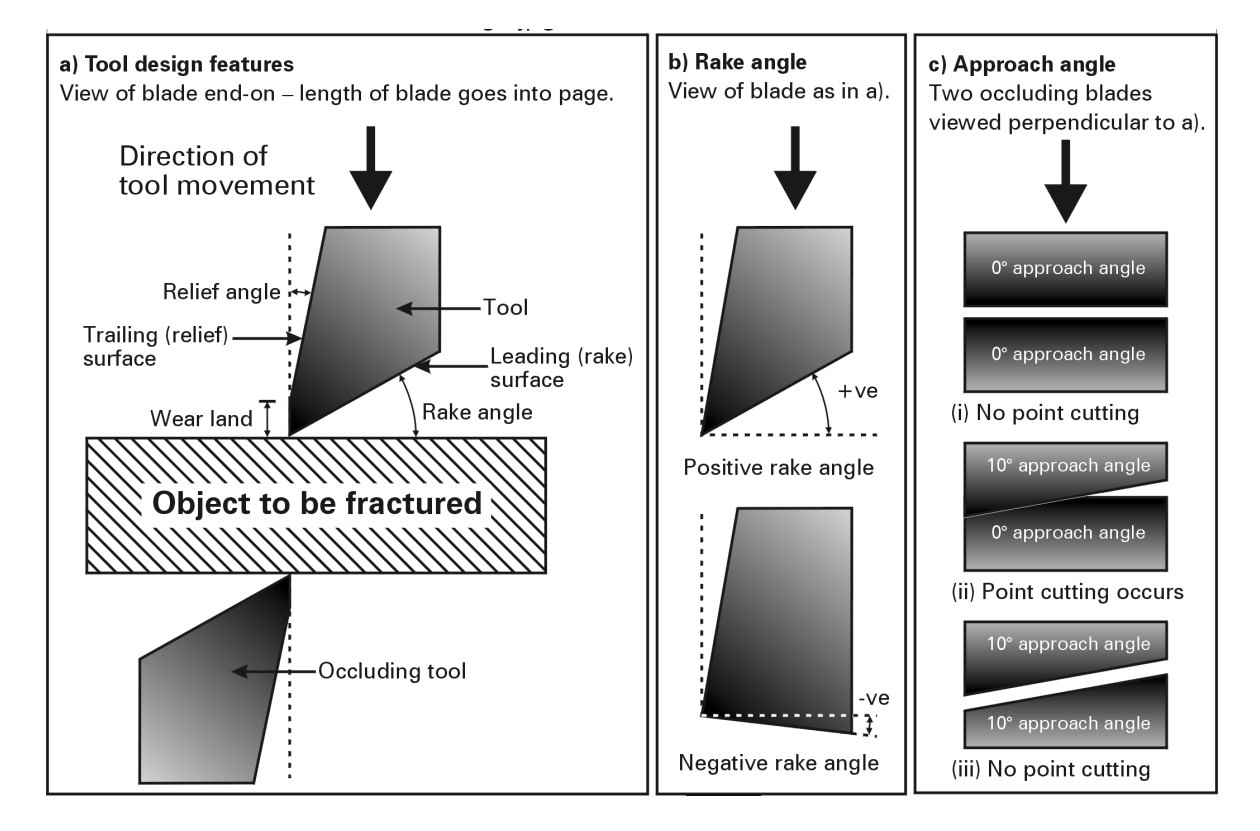


**Figure 1.1.** Tool design features. a) Basic tool design features: leading surface, trailing surface, rake angle, relief angle, wear land; b) positive and negative rake angles; c) different approach angles of two occluding blades and the effect on point cutting.

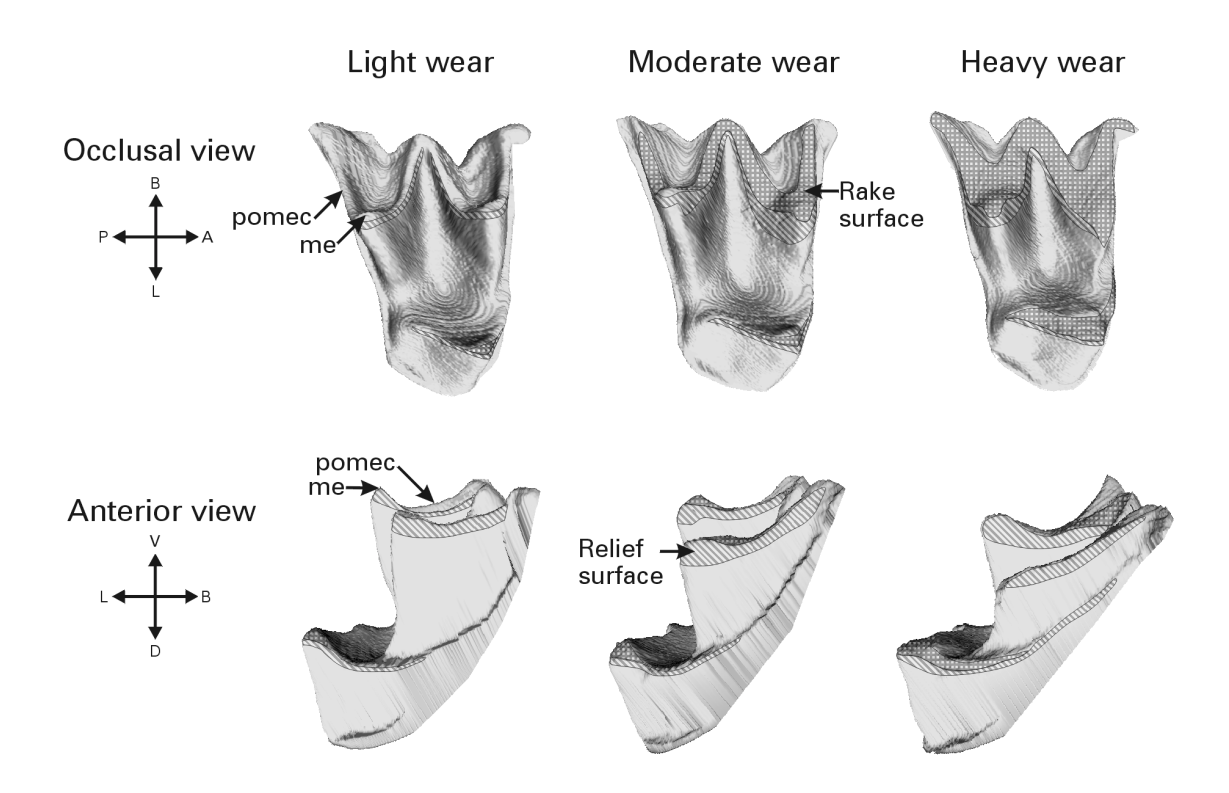


**Figure 1.2.** Occlusal and anterior views of the right upper second molar of *Chalinolobus gouldii*. Three wear states are shown: light, moderate and heavy wear. Wear on rake surface is shown by hatching; wear on relief surface by diagonal lines. Illustrations are generated from VRML reconstructions of confocal scans. A, anterior; B, buccal; D, dorsal; L, lingual; P, posterior; V, ventral; me, metacone; popac, postmetacrista.

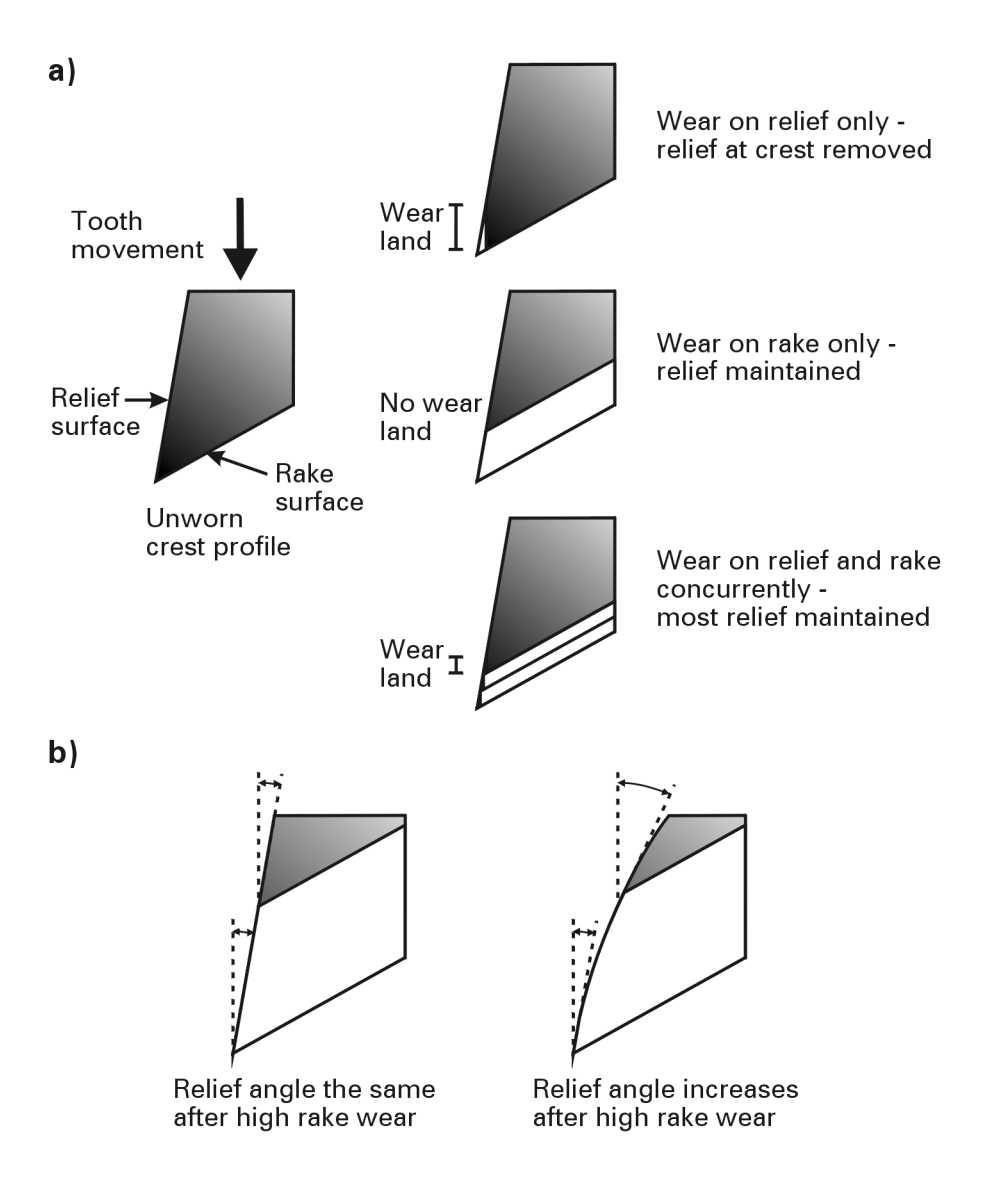


**Figure 1.3.** a) Effect of relative wear on rake and relief surfaces on the relief behind a crest. If wear only occurs on relief surface, then relief behind crest is removed (as represented by a wear land). If wear only occurs on rake surface, relief is maintained. For the more realistic situation, where wear occurs on both the rake and relief surfaces concurrently, substantial relief (indicated by small wear land) is maintained. b) Relief angle is maintained after wear on rake surface for a linear relief surface but increases if relief surface is convexly curved. Tooth profile is represented by shaded areas; unshaded areas represent tooth removed by wear.

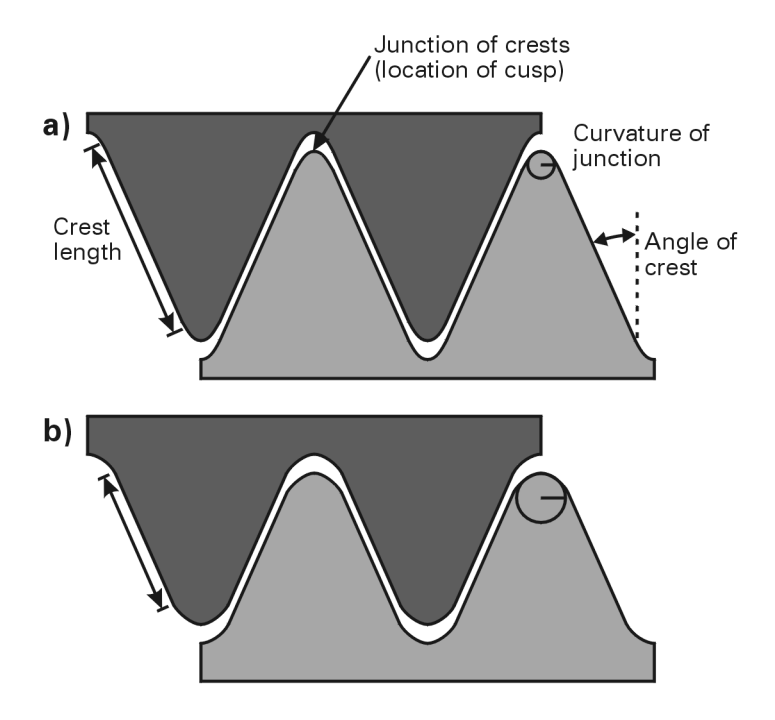


**Figure 1.4.** Changes in shape of molars during wear must be concurrent in upper and lower molars in order for occlusion to be maintained. This shows diagrammatic profiles of the crests of upper (dark) and lower (light) molars as viewed along the direction of tooth movement. Three main elements must correspond between each pair of upper and lower occluding crests: the two-dimensional length of the crest, the angle of the crest and the curvature at cusp points. Two of the three (2-D crest length and curvature) are shown to alter between a light wear state (a) and a heavy wear state (b).